

**BIOREDUCTIVE METABOLISM OF SMALL MOLECULE  
NITROAROMATICS AND *N*-OXIDES IN HYPOXIA**

---

A Dissertation

Presented to

The Faculty of the Graduate School

University of Missouri-Columbia

---

In partial Fulfillment

Of the Requirement of the Degree

Doctor of Philosophy

---

By

ANURUDDHA RAJAPAKSE

Prof. Kent S. Gates, Dissertation Supervisor

December 2012

© Copyright by Anuruddha Rajapakse 2012

All Rights Reserved

The undersigned, appointed by the Dean of the Graduate School, have examined the dissertation entitled

BIOREDUCTIVE METABOLISM OF SMALL MOLECULE NITROAROMATICS  
AND *N*-OXIDES IN HYPOXIA

Presented by **Anuruddha Rajapakse**

A candidate for the degree of Doctor of Philosophy

and hereby certify that in their opinion it is worthy of acceptance

---

Professor Kent S. Gates

---

Professor Timothy Glass

---

Professor Paul S. Sharp

---

Professor Frank Schmidt

## ACKNOWLEDGEMENTS

I would like to take this opportunity to thank everyone who helped me during my graduate studies at MU. First, I thank Professor Kent S. Gates, my advisor, for his dedicated guidance, encouragement and support. From the early stages and throughout my study, his availability to talk and motivation to instruct made my interest in bioorganic research grow immensely. Dr. Gates' outstanding knowledge on fundamentals of chemistry and his research experience have shaped my scientific career. I also want to thank my committee members Prof. Timothy Glass, Professor Paul Sharp and Professor Frank Schmidt for their comments and help along the way of my graduate study.

I would like to thank my parents, especially my mother for her support and my father for his dedicated guidance and I thank also my brothers.

In my graduate studies I have worked with many people from different backgrounds. Specially, I would like to thank all past and current Gates' group members for their intelligence and work ethics that we have shared and passed along. I am grateful to all students and staff members of the scientific community at MU that I have interacted with over the years.

Again I would like to restate my sincerer appreciation and gratitude for Dr. Gates. I would not have reached the current stage without his help.



## TABLE OF CONTENT

ACKNOWLEDGEMENTS.....	ii
LIST OF SCHEMES.....	vii
LIST OF FIGURES.....	x
LIST OF TABLES.....	xiii
TABLE OF COMPOUND STRUCTURE AND NUMBER.....	xiv
ABSTRACT.....	xxv
<b>Chapter 1: Nitroaromatics and <i>N</i>-oxide compounds as radiosensitizers, oxygen sensors and cytotoxic agents in tumor therapy</b>	
1.1. Hypoxia.....	1
1.2. Ionizing radiation therapy.....	1
1.3. Radio sensitizing oxygen mimetic agents.....	4
1.3.1. Nitro aromatic reduction in hypoxic cells.....	6
1.3.2. Elimination of active agent through nitroaromatic reduction.....	8
1.4. <i>N</i> -oxides.....	11
1.5. Summary.....	14
References for chapter 1.....	15

## **Chapter 2: Hypoxia-selective, enzymatic conversion of 6-nitroquinoline into a fluorescent helicene: pyrido[3,2-f]quinolino[6,5-c]cinnoline 3-oxide**

2.1. Hypoxia as a parameter to be determined qualitatively and quantitatively.....	23
2.2. Fluorescent probes to detect hypoxia.....	24
2.3. Reduction of <b>42</b> to Obtain <b>43</b> under anaerobic conditions.....	24
2.4. Identification of products arising from the anaerobic reaction .....	26
2.4. Synthesis and structural characterization of <b>44</b> .....	29
2.5. Conclusion.....	34
2.6. Experimental.....	35
References for chapter 2.....	55

## **Chapter 3: Hypoxia-selective enzymatic conversion of 6-nitroquinoline to the fluorescent product, 6-aminoquinoline**

3.1. Hypoxia is an attractive target to develop fluorescent probes.....	59
3.2. Fluorescent Probes to Detect Hypoxia.....	59
3.3. LC/MS analysis of the reaction mixtures generated by hypoxic metabolism of <b>42</b> by xanthine/xanthine oxidase.....	63
3.4. LC/MS analysis of the reaction mixtures generated by aerobic metabolism of <b>42</b> by xanthine/xanthine oxidase.....	67
3.5. Xanthine oxidase oxidizes aryl carbon, bonded to heteroatom of <b>42</b> to produce 6-nitroquinolone <b>51</b> .....	67

3.6. Hypoxia-selective conversion of hydroxylamine <b>50</b> to amine <b>43</b> .....	69
3.7. Hypoxia-selective conversion of 6-nitroquinolone <b>51</b> to 6-aminoquinolone <b>54</b> .....	72
3.8. Enzymatic conversion of <b>42</b> to 6-nitroquinolone <b>51</b> followed by hypoxia-selective conversion to 6-aminoquinolone <b>54</b> .....	73
3.9. Conclusions.....	74
3.10. Experimental.....	76
References for chapter 3.....	94

## **Chapter 4: Mechanistic Analysis Related to the Oxidative DNA**

### **Damage Caused by 1,2,4-Benzotriazine Dioxide**

4.1. Introduction .....	98
4.2. Mechanistic evidence for the oxidizing radical formation by TPZ.....	99
4.3. Hypothesis and design of experiments.....	100
4.4. Examine the dehydration mechanism in relation to the release of oxidizing species from 1,2,4-benzotriazine-di-oxide.....	102
4.5. Chemical Synthesis of 1,2,4-benzotriazine 1,4-dioxide.....	103
4.6. DNA-damaging properties of TPZ and TPZ analogs.....	103
4.6.1. TPZ analogs perform concentration dependent DNA damage.....	103
4.6.2. DNA damage is decreased by radical scavengers.....	106
4.7. Examining chemical mechanism of bio-reductive metabolism of <b>55</b> and <b>60</b> .....	111
4.8. Metabolic studies of <b>55</b> and <b>60</b> with organic substrate.....	111
4.9 Deuterium incorporation into <b>55</b> .....	115
4.10. Isotope washout from drug <b>60</b> .....	116

4.11. Isotope replacement analysis and dehydration mechanism.....	117
4.12. Conclusion.....	118
4.13. Experimental.....	119
References for chapter 4.....	132
<b>Chapter 5: Synthesis of bioreductively-activated nitroaromatic triggers</b>	
5.1. Qualitative and quantitative determination of hypoxia.....	139
5.2. Goal: Constructing suitable nitroaromatic fluorescent probes for hypoxia.....	140
5.3. Synthesis of 5-nitrothienyl moiety, 2-(5-Nitrothien-2-yl) propan-2-ol <b>73</b> .....	141
5.4. Synthesis of 1-methyl-2-nitro-5-hydroxymethyl imidazole <b>79</b> .....	142
5.5. Synthesis of <b>80</b> and <b>81</b> .....	144
5.6. Synthesis of 3-acetylquinoline-1,2,4-benzotriazine 1,4-dioxide <b>84</b> .....	144
5.7. Experimental.....	145
References for chapter 5.....	164
VITA.....	167

## LIST OF SCHEMES

### Chapter 1

Scheme 1.1 Gamma radiolysis generates radical species.....	1
Scheme 1.2 Hydroxyl radical abstract hydrogen from DNA.....	1
Scheme 1.3 DNA radical on C4' is fixed by oxygen.....	2
Scheme 1.4 Formation of ribonolactone.....	3
Scheme 1.5 Thiols can repair DNA radical damage .....	3
Scheme 1.6 Radiolysis induced nitro-reduction and DNA radical formation.....	4
Scheme 1.7 Oxygen of nitro group is donated to DNA.....	5
Scheme 1.8 Enzyme mediated-Nitro reduction undergo in hypoxia.....	5
Scheme 1.9 Hydroxylamine produces glyoxal-dialdehyde alkylator.....	5
Scheme 1.10 Nitroaromatics reduction in hypoxia produces the active drug .....	7
Scheme 1.11 Nitrophenyl-mustard alkylating agents.....	7
Scheme 1.12 Nitrophenyl-mustard alkylating agents.....	8
Scheme 1.13 Hydroxylamine release the active drug.....	9
Scheme 1.14 Phosphoramidate forms azide upon elimination of leaving group.....	9
Scheme 1.15 Cyclophosphoramide ( <b>18</b> ) metabolism by CYP <sub>450</sub> .....	9
Scheme 1.16 Nitroquinoline phosphoramidate prodrug release.....	10
Scheme 1.17 Nitrophenyl, nitrofuryl and nitrothienyl phosphoramidate conjugates .....	10
Scheme 1.18 Nitrothienyl and nitrophenyl dimethyl pro-drugs.....	11
Scheme 1.19 <i>N</i> -oxide radiosensitising agents.....	12
Scheme 1.20 Enzyme mediated reduction of <b>33</b> in hypoxia.....	12

Scheme 1.21. Enzyme-mediated reduction of **33** in hypoxia abstract proton from DNA, followed by dehydration releases **35** as the major metabolite.....13

Scheme 1.22. The enzyme-mediated reduction of **33** in hypoxia may produce hydroxyl radical or benzotrazine radicals **39**, **40** or **41** as the oxidizing species.....13

## **Chapter 2**

Scheme 2.1. Enzymatic reduction profile of nitroaromatic compound.....24

Scheme 2.2. Hypoxic metabolism of **42** is expected to form fluorescent **43**.....25

Scheme 2.3. Metabolites formed by the reduction of **42** with NADPH/CYP450R.....29

Scheme 2.4. Mechanism for the formation of **44** under anaerobic conditions.....34

## **Chapter 3**

Scheme 3.1. Enzymatic reduction steps of a typical nitroaromatic compound.....60

Scheme 3.2. Hypoxic metabolism of **42** forms fluorescent **43**.....61

Scheme 3.3. CYP450R mediates conversion of **42** into fluorescent metabolites.....61

Scheme 3.4 Hypoxic metabolism of **42** by xanthine and xanthine oxidase.....64

Scheme 3.5 Enzymatic generation of **51** by xanthine and xanthine oxidase.....68

Scheme 3.6 Enzymatic generation of **43** by xanthine and xanthine oxidase.....69

Scheme 3.7 Enzymatic generation of **54** from **51** by xanthine and xanthine oxidase is hypoxia selective.....72

Scheme 3.8 Enzymatic generation of **51** from **42** and production of **54** from **51**.....73

## Chapter 4

Scheme 4.1 Enzymatic reduction of <b>33</b> produces DNA damaging radicals and oxidative stress.....	99
Scheme 4.2 Different mechanisms are proposed to explain enzymatic metabolism of <b>33</b> .....	100
Scheme 4.3 Enzymatic reduction of <b>55</b> under low oxygen concentrations forms major metabolite <b>59</b> .....	101
Scheme 4.4 Isotopic content of major metabolite of <b>55/60</b> determines mechanism.....	102

## Chapter 5

Scheme 5.1. Bio-reducible moieties can be used as oxygen sensors.....	139
Scheme 5.2. Nitro phenyl benzyl phosphoramidite prodrugs.....	140
Scheme 5.3. 1,6-elimination of active drug species.....	140
Scheme 5.4. Synthesis of <b>70</b> .....	141
Scheme 5.5. Synthesis of 2-(5-nitrothien-2-yl) propan-2-ol <b>73</b> .....	142
Scheme 5.6. Synthesis of <b>76</b> from sarcosine ethyl ester <b>74</b> .....	143
Scheme 5.7. Synthesis of 1-methyl-2-nitro-5hydroxymethyl imidazole <b>79</b> .....	143
Scheme 5.8. Fluorescent probes <b>83</b> and <b>84</b> .....	144
Scheme 5.9. Synthesis of <b>84</b> using triphosgene <b>82</b> and <b>43</b> .....	144

## LIST OF FIGURES

### Chapter 2

- Figure 2.1. Enzymatic conversion of **42** into a fluorescent product under hypoxic conditions.....26
- Figure 2.2. LC/MS analysis of the reaction mixture generated by anaerobic metabolism of **42** (0.8 mM) by cytochrome p450 reductase (1.1 U/mL) and NADPH (6.4 mM).....28
- Figure 2.3. In **44**, the 4 and 4'-hydrogens (see numbering system in Scheme 2.2) are close in space.....32
- Figure 2.4. Fluorescence spectrum of authentic **44** (50  $\mu$ M,  $\lambda_{ex}$  307 nm) in sodium phosphate buffer.....33

### Chapter 3

- Figure 3.1. Enzymatic conversions of **42** to a fluorescent product selectively under hypoxic conditions.....62
- Figure 3.2. LC/MS analysis of the reaction mixture generated by anaerobic metabolism of **42** (0.8 mM).....65
- Figure 3.3. LC/MS analysis of authentic compounds.....66
- Figure 3.4. LC/MS analysis of the reaction mixture generated by aerobic metabolism of **42** (0.8 mM).....67
- Figure 3.5. ORTEP diagram of **51**.....68



Figure 3.6. Enzymatic conversion of <b>50</b> into a fluorescent <b>43</b> under hypoxic conditions.....	70
Figure 3.7. LC/MS analysis of the reaction mixture generated by anaerobic metabolism of <b>50</b> (0.8 mM).....	71
Figure 3.8 Enzymatic conversions of <b>51</b> to <b>54</b> under hypoxic conditions.....	72
Figure 3.9 Enzymatic conversion of <b>42</b> to <b>51</b> and reduction to <b>54</b> in hypoxia.....	74
Figure 3.10 Fluorescence spectra of control reactions.....	77

## Chapter 4

Figure 4.1. Cleavage of supercoiled plasmid DNA by <b>33</b> (50-250 $\mu$ M) in the presence of NADPH:cytochrome P450 reductase as an activating system.....	104
Figure 4.2. Cleavage of supercoiled plasmid DNA by <b>55</b> (50-250 $\mu$ M) in the presence of NADPH:cytochrome P450 reductase as an activating system.....	105
Figure 4.3. Cleavage of supercoiled plasmid DNA by <b>60</b> (50-250 $\mu$ M) in the presence of NADPH:cytochrome P450 reductase as an activating system.....	105
Figure 4.4. Comparison of DNA cleavage by reductively activated <b>33</b> , <b>55</b> and <b>60</b> under anaerobic conditions .....	106
Figure 4.5. Cleavage of supercoiled plasmid DNA by <b>33</b> (25 $\mu$ M) in the presence of NADPH:cytochrome P450 reductase as an activating system is reduced by radical scavengers .....	108

Figure 4.6. Cleavage of supercoiled plasmid DNA by <b>55</b> (50 $\mu$ M) in the presence of NADPH:cytochrome P450 reductase as an activating system is reduced by radical scavengers.....	109
Figure 4.7. Cleavage of supercoiled plasmid DNA by <b>60</b> (50 $\mu$ M) in the presence of NADPH:cytochrome P450 reductase as an activating system is reduced by radical scavengers .....	110
Figure 4.8. Comparison of DNA cleavage by reductively activated <b>33</b> , <b>55</b> or <b>60</b> under anaerobic conditions and DNA cleavage is reduced by radical scavengers .....	110
Figure 4.9. LC/MS analysis of anaerobic metabolism of <b>55</b> and <b>60</b> (0.5 mM) by cytochrome p450 reductase (0.4 U/mL)/NADPH (0.5 mM).....	113
Figure 4.10. LC/MS analysis of authentic <b>60</b> , <b>63</b> , <b>55</b> and <b>59</b> .....	114
Figure 4.11. HRMS of the major metabolite 1- <i>N</i> -oxide <b>59</b> arising from metabolism of <b>60</b> under reductively activated conditions in hypoxia .....	116
Figure 4.12. HRMS of the major metabolite 1- <i>N</i> -oxide <b>63</b> arising from metabolism of <b>60</b> under reductively activated conditions in hypoxia .....	117

## LIST OF TABLES

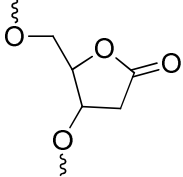
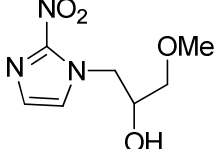
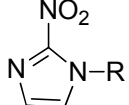
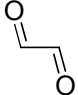
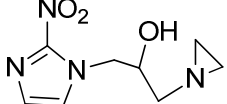
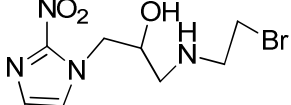
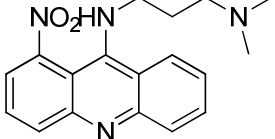
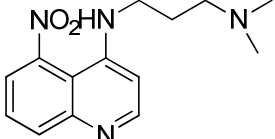
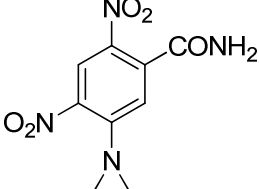
### Chapter 2

Table 2.1. NMR Data (CDCl <sub>3</sub> ) for compound <b>44</b> .....	31
---	----

### Chapter 4

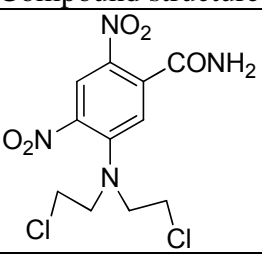
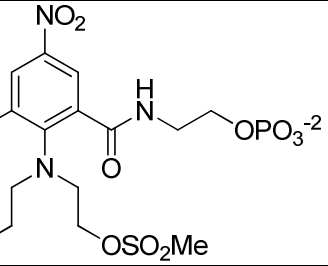
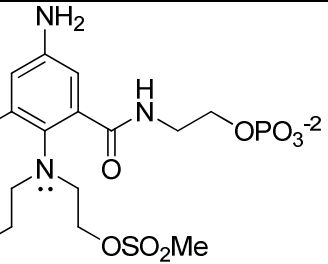
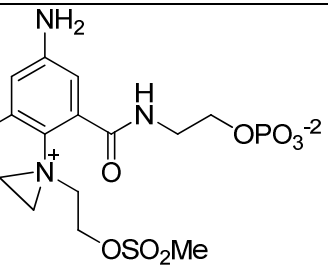
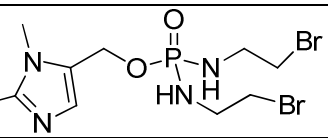
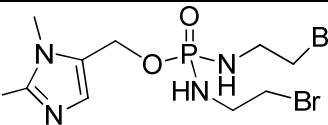
Table 4.1. Cleavage of plasmid DNA in control reactions.....	107
--	-----

**TABLE OF COMPOUND STRUCTURE AND NUMBER**

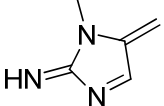
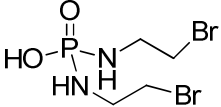
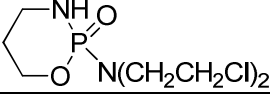
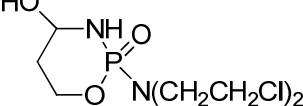
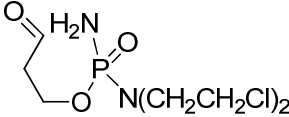
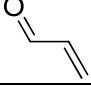
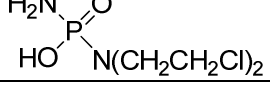
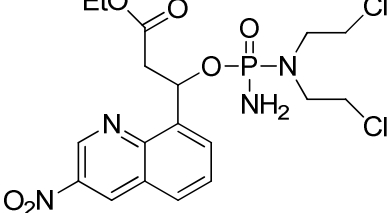
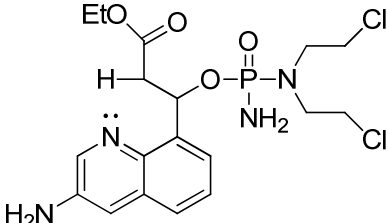
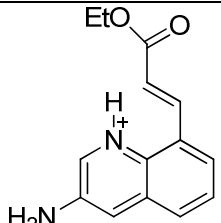
Compound structure	Number
	1
	2
	3
	4
	5
	6
	7
	8
	9



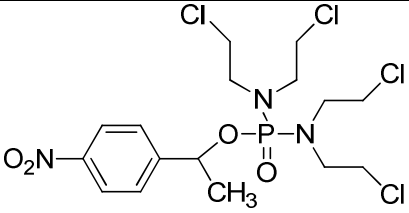
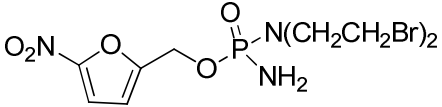
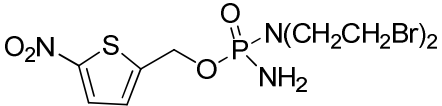
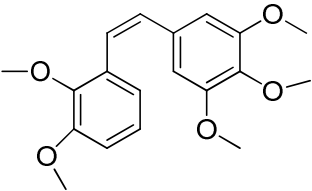
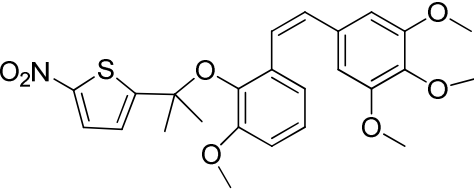
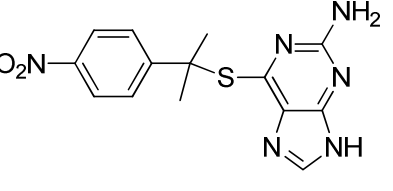
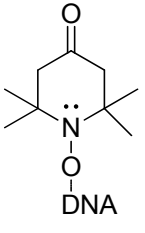
**TABLE OF COMPOUND STRUCTURE AND NUMBER CONT'D.**

Compound structure	Number
	<b>10</b>
	<b>11</b>
	<b>12</b>
	<b>13</b>
	<b>14</b>
	<b>15</b>

**TABLE OF COMPOUND STRUCTURE AND NUMBER CONT'D.**

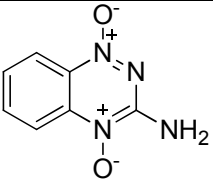
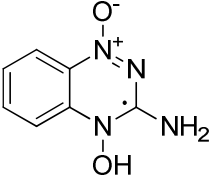
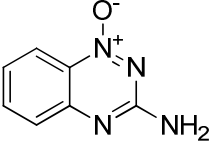
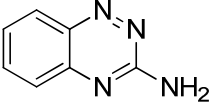
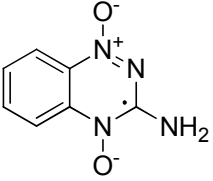
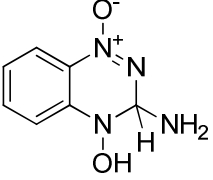
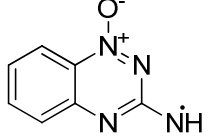
Compound structure	Number
	16
	17
	18
	19
	20
	21
	22
	23
	24
	25

**TABLE OF COMPOUND STRUCTURE AND NUMBER CONT'D.**

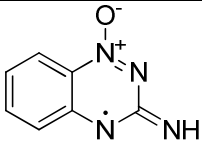
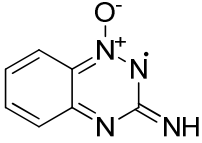
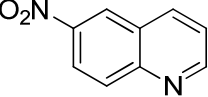
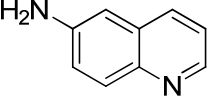
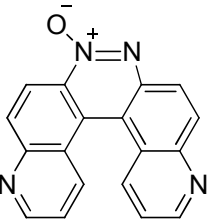
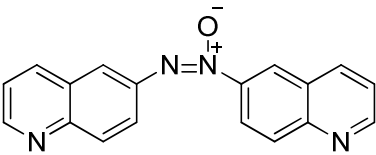
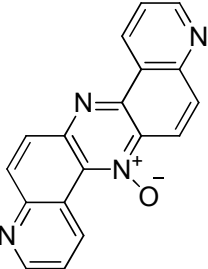
Compound structure	Number
	26
	27
	28
	29
	30
	31
	32



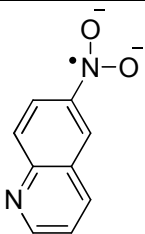
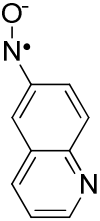
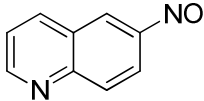
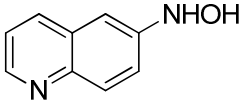
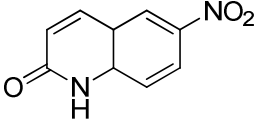
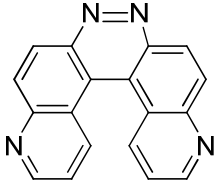
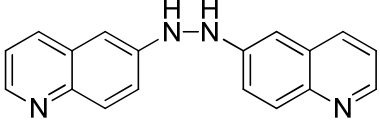
**TABLE OF COMPOUND STRUCTURE AND NUMBER CONT'D.**

Compound structure	Number
	33
	34
	35
	36
	37
	38
	39

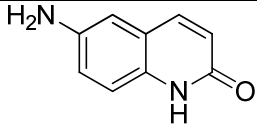
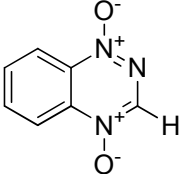
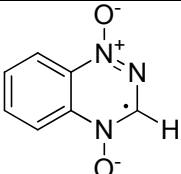
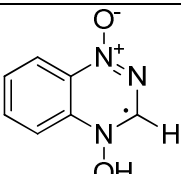
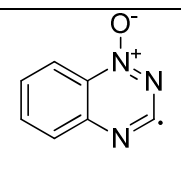
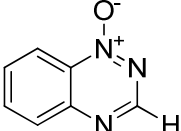
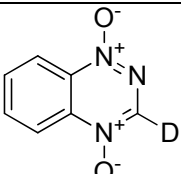
**TABLE OF COMPOUND STRUCTURE AND NUMBER CONT'D.**

Compound structure	Number
	<p><b>40</b></p>
	<p><b>41</b></p>
	<p><b>42</b></p>
	<p><b>43</b></p>
	<p><b>44</b></p>
	<p><b>45</b></p>
	<p><b>46</b></p>

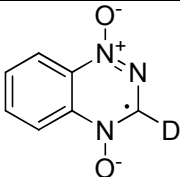

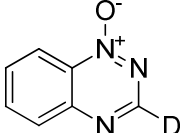
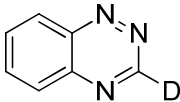
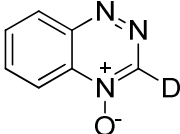
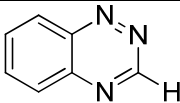
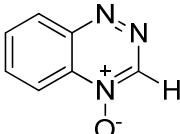
**TABLE OF COMPOUND STRUCTURE AND NUMBER CONT'D.**

Compound structure	Number
	<p style="text-align: center;"><b>47</b></p>
	<p style="text-align: center;"><b>48</b></p>
	<p style="text-align: center;"><b>49</b></p>
	<p style="text-align: center;"><b>50</b></p>
	<p style="text-align: center;"><b>51</b></p>
	<p style="text-align: center;"><b>52</b></p>
	<p style="text-align: center;"><b>53</b></p>

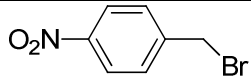
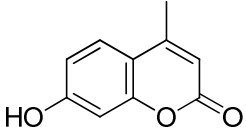
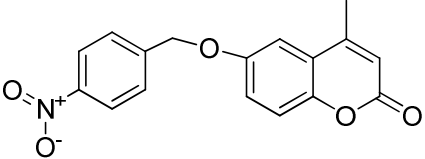
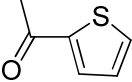
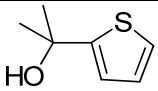
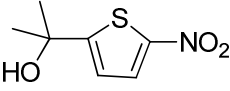
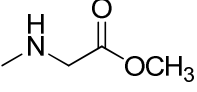
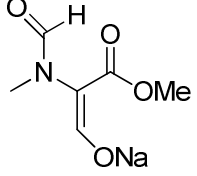
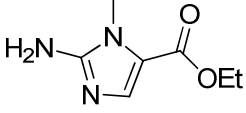
**TABLE OF COMPOUND STRUCTURE AND NUMBER CONT'D.**

Compound structure	Number
	<b>54</b>
	<b>55</b>
	<b>56</b>
	<b>57</b>
	<b>58</b>
	<b>59</b>
	<b>60</b>

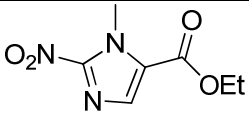
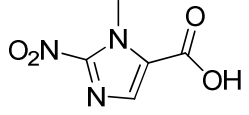
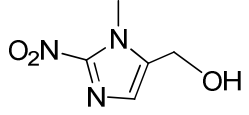
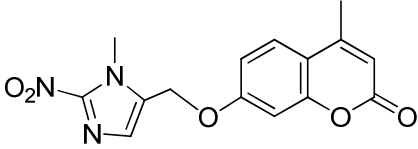
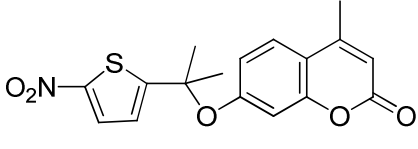
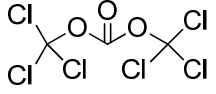
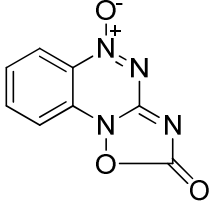
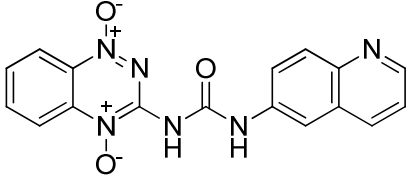
**TABLE OF COMPOUND STRUCTURE AND NUMBER CONT'D.**

Compound structure	Number
 <p>Chemical structure of 2-deuterio-1,2,4-diazaphenyl radical. It consists of a benzene ring fused to a 1,2,4-diazole ring. The nitrogen at position 1 is bonded to an oxygen anion (O<sup>-</sup>). The nitrogen at position 2 is bonded to a deuterium atom (D) and has a radical dot (·) on it.</p>	61
 <p>Chemical structure of 2-deuterio-1,2,4-diazaphenol. It consists of a benzene ring fused to a 1,2,4-diazole ring. The nitrogen at position 1 is bonded to an oxygen anion (O<sup>-</sup>). The nitrogen at position 2 is bonded to a deuterium atom (D) and a hydroxyl group (OH).</p>	62
 <p>Chemical structure of 2-deuterio-1,2,4-diazaphenyl anion. It consists of a benzene ring fused to a 1,2,4-diazole ring. The nitrogen at position 1 is bonded to an oxygen anion (O<sup>-</sup>). The nitrogen at position 2 is bonded to a deuterium atom (D).</p>	63
 <p>Chemical structure of 2-deuterio-1,2,4-diazaphenyl. It consists of a benzene ring fused to a 1,2,4-diazole ring. The nitrogen at position 2 is bonded to a deuterium atom (D).</p>	64
 <p>Chemical structure of 2-deuterio-1,2,4-diazaphenyl cation. It consists of a benzene ring fused to a 1,2,4-diazole ring. The nitrogen at position 1 is bonded to an oxygen anion (O<sup>-</sup>). The nitrogen at position 2 is bonded to a deuterium atom (D) and has a positive charge (+).</p>	65
 <p>Chemical structure of 2,4-diazaphenyl. It consists of a benzene ring fused to a 1,2,4-diazole ring. The nitrogen at position 2 is bonded to a hydrogen atom (H).</p>	66
 <p>Chemical structure of 2,4-diazaphenyl cation. It consists of a benzene ring fused to a 1,2,4-diazole ring. The nitrogen at position 1 is bonded to an oxygen anion (O<sup>-</sup>). The nitrogen at position 2 is bonded to a hydrogen atom (H) and has a positive charge (+).</p>	67

**TABLE OF COMPOUND STRUCTURE AND NUMBER CONT'D.**

Compound structure	Number
	<b>68</b>
	<b>69</b>
	<b>70</b>
	<b>71</b>
	<b>72</b>
	<b>73</b>
	<b>74</b>
	<b>75</b>
	<b>76</b>

**TABLE OF COMPOUND STRUCTURE AND NUMBER CONT'D.**

Compound structure	Number
	77
	78
	79
	80
	81
	82
	83
	84

## ABSTRACT

Hypoxia in tumors causes adverse effects to therapy and negatively impacts on patient prognosis. Identification and quantification of hypoxia is considered to have a strong impact on treatments in tumor therapy. Fluorescent-based detection to mark hypoxia may be vital to be used along with available methods such as radiochemical and immunohistochemical staining.

In this work, the non-fluorescent 6-nitroquinoline (**42**) was used to investigate the production of a fluorescent 6-aminoquinoline (**43**) and other metabolites under bio-reducing hypoxic conditions. In the presence of the enzymatic reducing system NADPH:cytochrome P450 reductase/NADPH, 6-nitroquinoline (**42**) produced the fluorescent helicene (**44**), along with the non-fluorescent azo (**45**). An authentic sample of (**44**) was chemically synthesized and characterized and used to confirm the production of this molecule in the enzymatic process. Interestingly, the expected fluorophore (**43**) is not produced by NADPH:cytochrome P450 reductase/NADPH.

In another study, the enzymatic reducing system xanthine/xanthine oxidase was used to reduce (**42**) under hypoxia to obtain (**43**). In these experiments (**43**) was produced and the yield is increased with xanthine concentration. Metabolic identification revealed that intermediates of typical nitro reduction pathway are present along with 6-nitroquinolone (**51**), which is formed by xanthine oxidase mediated oxidation of (**42**). The absence of (**44**) as a metabolite with xanthine/xanthine oxidase system highlights the complexity of bio-reduction of nitroaromatics under hypoxia.



In our laboratory, bio-activation of di-*N*-oxides such as tirapazamine (TPZ, **42**) has been studied. TPZ undergoes one-electron bio-reduction to produce oxidizing radical, which causes DNA damage under hypoxia. In our laboratory, the mechanism by which TPZ mediated DNA damage has been investigated using TPZ and its analogs.

Our evidence suggests that upon undergoing bio-reduction, TPZ produces hydroxyl radical as the DNA damaging radical species. Others have suggested another mechanism, which proposes the formation benzotriazine radical (**38**) upon dehydration process over the bioreduction step. In the current work, TPZ analog 1,2,4-benzotriazine-1,4-dioxide (**55**) and deuterated (**60**) were used to test the dehydration mechanism. Isotopic content analysis of metabolites, derived from bio-reducing metabolism of (**55**) and its deuterated analog (**60**), using HRMS show evidence against the dehydration mechanism.

## Chapter 1

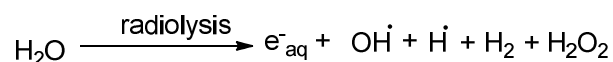
### Nitroaromatics and *N*-oxide compounds as radiosensitizers, oxygen sensors and cytotoxic agents in tumor therapy

#### 1.1 Hypoxia.

Low oxygen levels (hypoxia) is considered as an important physiological factor in tumor biology.<sup>1</sup> The oxygen concentration, found in a normal tissue falls within a range of 20  $\mu\text{M}$  to 90  $\mu\text{M}$ .<sup>2</sup> It is well established that solid tumors contain cell populations having low oxygen concentrations.<sup>3</sup> Hypoxia is the end physiological result, caused by the presence of irregular vasculature in tumors.<sup>4</sup> The inconsistent blood flow in tumors may produce acute or chronic hypoxia.<sup>1</sup> Hypoxic conditions can diminish effects of ionizing radiation mediated tumor therapy.<sup>5</sup> Ionizing radiation is a key method in tumor therapy and hypoxia has drawn attention as a challenge which should be addressed to achieve clinical success.<sup>6</sup>

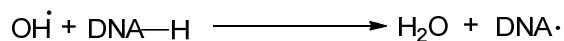
#### 1.2 Ionizing radiation therapy

In the presence of ionizing radiation water molecules break down to form highly reactive, oxidizing hydroxyl radicals (Scheme 1.1).<sup>7</sup>



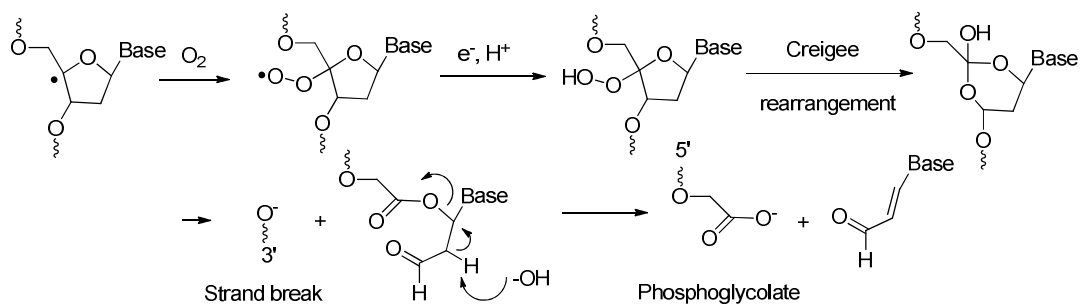
**Scheme 1.1.** Gamma radiolysis generates radical species

The hydroxyl radical is able to abstract hydrogen from organic substrates such as DNA, which can cause cell death (Scheme 1.2).<sup>8</sup>



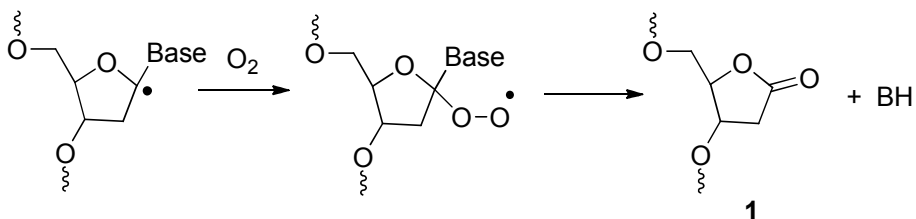
**Scheme 1.2.** Hydroxyl radical abstract hydrogen from DNA

The oxidative abstraction of hydrogen atoms from DNA produces DNA radicals.<sup>9</sup> DNA radicals can be created on the DNA bases or on sugar phosphate backbone. DNA radicals, formed on thymidine or guanine DNA bases would develop into strand breaks.<sup>10</sup> The hydrogen atom abstraction, which occurs on the sugar phosphate backbone produces carbon centered radicals on C1', C2', C3', C4' and C5' carbons and oxygen is required to make the radical damage permanent and induce strand breaks.<sup>9</sup> The radical fixation, which is mediated by oxygen on DNA backbone carbon radicals, produces characteristic DNA lesions.<sup>11</sup> The damage, on C4' and C5' carbons, produces 3'-phosphoglycolate and strand breaks (Scheme 1.3).<sup>12</sup>



**Scheme 1.3.** DNA radical on C4' is fixed by oxygen

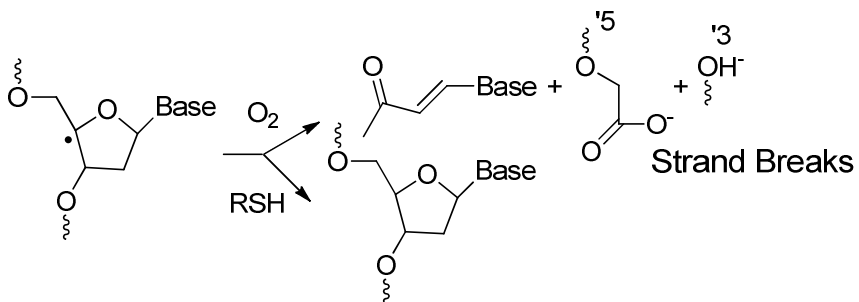
Formation of a ribonolactone occurs when oxygen fixes a C1' DNA radical.<sup>13</sup> Under basic conditions 1, ribonolactone undergo elimination to yield strand breaks. (Scheme 1.4).<sup>8</sup>



**Scheme 1.4.** Formation of ribonolactone

Once the DNA damage, either on backbone or DNA base, is made permanent by producing strand breaks, a cascade of cellular events triggers cell death.<sup>14</sup>

Under hypoxic conditions, the low oxygen levels diminish DNA radical fixation.<sup>3</sup> Hence DNA radical-mediated cell death might not occur in solid tumors.<sup>15</sup> It is noted that the DNA radicals created by ionizing radiation would be trapped by cellular thiols such as glutathione.<sup>7, 16</sup> The chemical repair of DNA damage by thiols under low oxygen levels may cause the tumor cell resistance to radiation therapy.<sup>13</sup> The cellular glutathione levels are present in millimolar levels under physiological conditions (Scheme 1.5).<sup>7</sup>



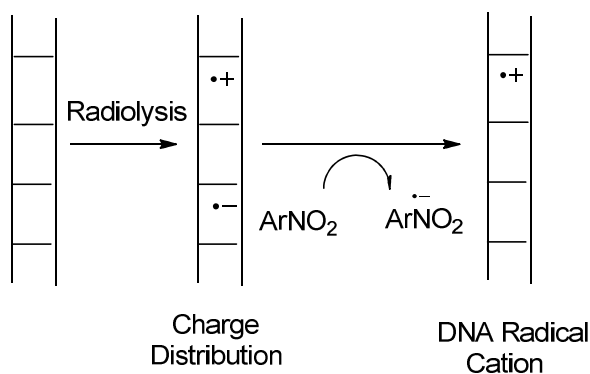
**Scheme 1.5.** Thiols can repair DNA radical damage

Accordingly, the fate of DNA radicals in tumors depends on the oxygen concentration of the cell.<sup>8</sup> The lack of oxygen causes tumor cell to resist radiation therapy.<sup>3</sup> Thus there was a need for alternative agents that can fix DNA radicals under low oxygen concentrations to potentiate radiation therapy.

### 1.3 Radiosensitizing oxygen mimetic agents

In an effort to reduce tumor cell resistance to radiation therapy, investigations have been carried out to find agents that can mimic the behavior of oxygen in radiotherapy.<sup>17</sup> As a part of the search nitro aromatic and *N*-oxide drugs have been tested as radiosensitizing agents to accompany radiotherapy in treatments.<sup>17b</sup>

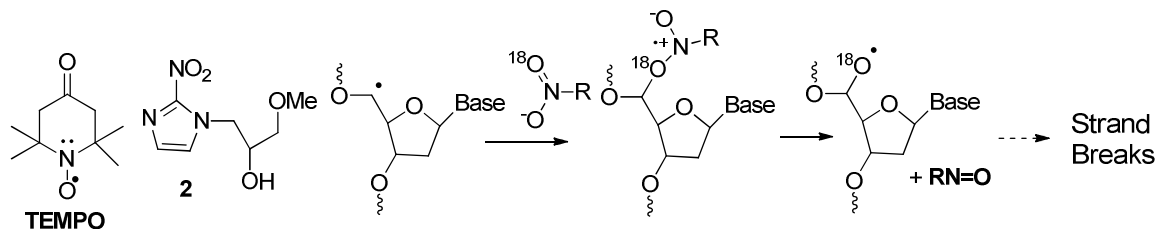
Potential agents such as TEMPO and misonidazole, **2** were tested in cytotoxicity assays with radiation.<sup>18</sup> Nitroaromatics became the leading candidates in the search for radiation sensitizing agent.<sup>17a</sup> The sensitizing capacity of nitroaromatics can be radical fixation which can occur through oxygen mimetic ability of nitro group. Or the ability of nitro group to undergo reduction to form amine can be contribute for the radiation sensitivity.<sup>17a</sup> The higher electron affinity of nitroaromatic compounds can facilitate oxidation of DNA from which the charge distribution has been altered by radiolysis.<sup>19</sup> This can produce DNA radical cations and oxygen sensitive nitroradicals which oxidize back to parent nitro group in the presence of oxygen (Scheme 1.6).<sup>10</sup>



**Scheme 1.6.** Radiolysis induced nitro-reduction and DNA radical formation

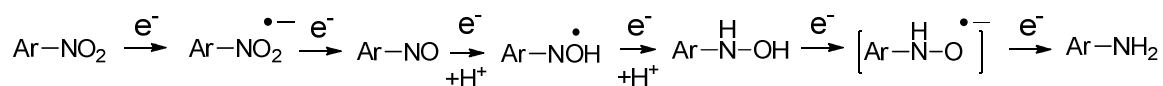
There is evidence for donation of an oxygen atom from a nitro group to a DNA radical.<sup>20</sup> Goldberg and researchers used an <sup>18</sup>O-labeled nitro group containing

misonidazole **2** and DNA radical precursors in his  $^{18}\text{O}$ -incorporation experiments. When misonidazole interacts with C5' DNA radical, nitroxide intermediate forms, followed by fragmentation caused strand breaks (Scheme 1.7).<sup>21</sup>



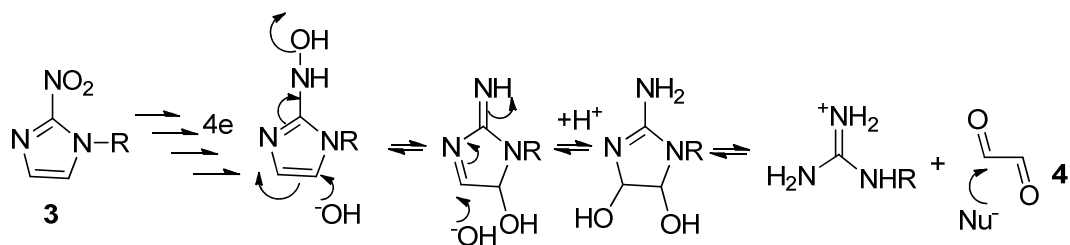
**Scheme 1.7.** Oxygen of nitro group is donated to DNA

Further studies on misonidazole-mediated radiosensitization revealed that **2** causes toxicity without ionizing radiation.<sup>22</sup> The higher electron affinity of nitroaromatic compounds makes them substrate for cellular reductases.<sup>23</sup> It was suggested that cellular reducing systems such as NADPH cytochrome P450 reductase may reduce nitro group to hydroxylamine and to amine groups via six consecutive  $e^-$  reduction steps under hypoxic conditions (Scheme 1.8).<sup>24</sup>



**Scheme 1.8.** Enzyme mediated Nitro reduction undergo in hypoxia

The hydroxylamine intermediate may cause cytotoxicity by forming reactive intermediates.<sup>25</sup> The reduction of 2-nitro-5-alkyl-nitroimidazole **3** would produce the hydroxylamine and then converts to the glyoxal-dialdehyde **4** form which may alkylate nucleophilic sites on DNA (Scheme 1.9).<sup>26</sup>



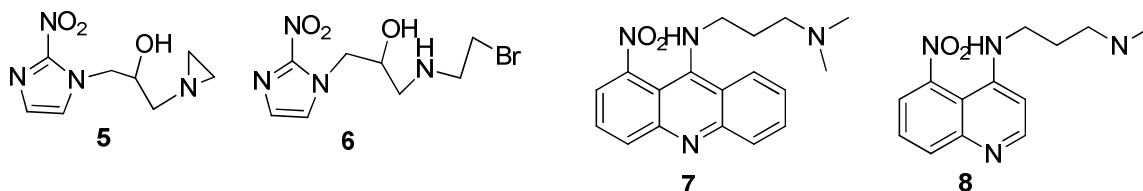
**Scheme 1.9.** Hydroxylamine produces glyoxal-dialdehyde alkylator **4**

The clinical test, carried out using **2** produced neurotoxicity among patients. The observed toxicity may have arisen due to the formation of hydroxylamine intermediate.

### 1.3.1 Nitroaromatic reduction in hypoxic cells

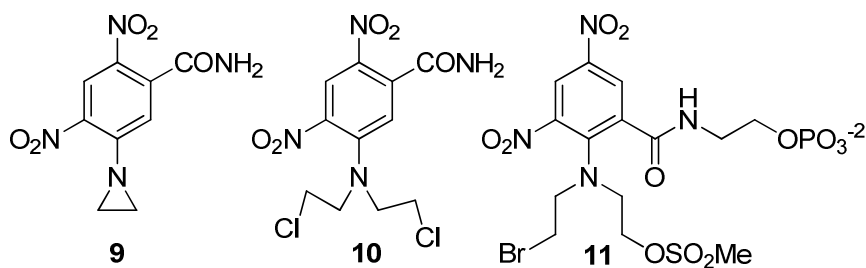
Studies on reduction of nitroaromatic-radiosensitizing drugs established nitro reduction mechanism which may occur in cells.<sup>17a, 27</sup> The stepwise electron addition would produce the hydroxylamine intermediate. Further reduction produces the amino product.<sup>28</sup> The nitro group reduction is mediated by cellular enzymes such as NADPH cytochrome P450 reductase, xanthine oxidase, nitroreductases and DT diaphorase.<sup>17a, 24</sup> These enzymes can be overexpressed or already abundant in tumor environment.<sup>27, 29</sup> The hypoxic conditions in tumors would permit sequential e- reduction to occur and produce reduced metabolites such as hydroxylamine and amine.<sup>30</sup> The enzyme-mediated functional group transition from nitro to hydroxylamine has been considered as an electronic switch.<sup>27</sup> The electron poor nitro group is converted to an electron rich hydroxylamine, and further reduction produces the amine moiety.<sup>31</sup> For some drug candidates electron rich hydroxylamine represents the active form of the drug to be effective in tumor cells.<sup>32</sup> The first nitro imidazole aziridine containing agent RSU1069, **5**, explored hypoxia selective, redox activated generation of an alkylating agent.<sup>33</sup> Similar nitro-imidazole-containing mustards such as RB6145 **6** and **5** were tested in tumor cells.<sup>34</sup> In addition to mustard-type alkylating agents, DNA intercalating moieties such as

acridine **7** and quinoline **8** groups were used as bio reductively activated agents. Upon bio-reduction, the intercalating ability of amine compounds of **7** and **8** is enhanced to cause interferences during DNA replication (Scheme 1.10).<sup>35</sup>



**Scheme 1.10.** Nitro aromatics reduction in hypoxia produces the active drug

Mustard groups have been attached to nitrophenyl moiety, as a continuation of efforts to develop nitroaryl-aziridine conjugates.<sup>36</sup> Nitrobenzene aziridines CB 1954, **9**, SN 23862, **10**, and PR 104, **11** explore nitro reduction as the mean of mustard activation in tumor cells (Scheme 1.11).<sup>37</sup>

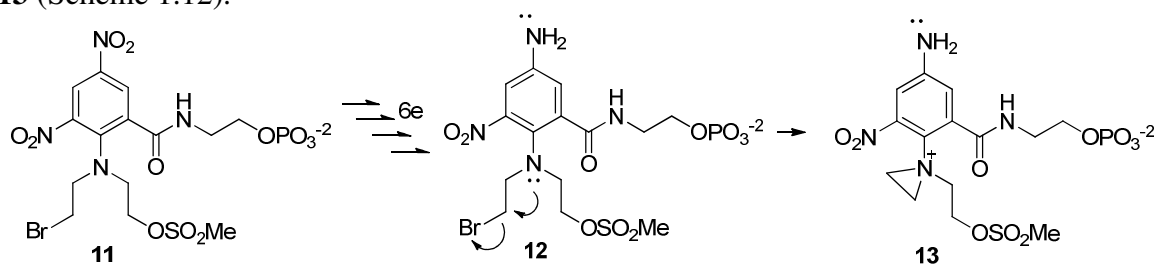


**Scheme 1.11.** Nitrophenyl-mustard alkylating agents

The aziridine alkylating moiety would attain greater activity upon the reduction of nitro group to amine group under hypoxia. Specific enzymes such as *E. coli* nitroreductases has been used as the reducing enzyme under gene directed enzyme pro-drug therapy GDEPT to test nitrobenzyl mustard **9**.<sup>32</sup> In addition, DT diaphorase has been used with nitrophenyl-aziridines and nitrogen mustards to test the enhanced selectivity toward hypoxia and improved cytotoxicity.<sup>38</sup> In the mechanism, of which nitroaryl-mustards attain activity, nitro compound **11** undergoes reduction to produce amine **12**.



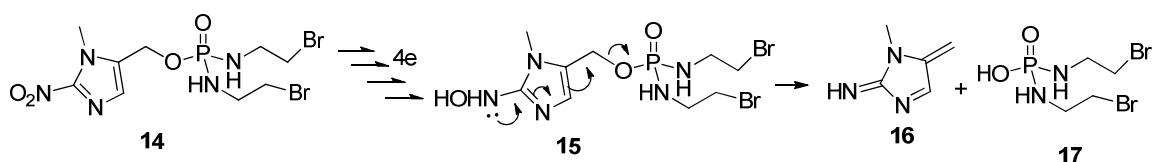
The increased electron density on **12** works toward the formation of alkylating aziridine **13** (Scheme 1.12).<sup>39</sup>



**Scheme 1.12.** Nitrophenyl-mustard alkylating agents

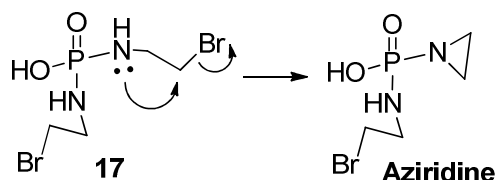
### 1.3.2 Elimination of active agent through nitroaromatic reduction

The electronic properties of a molecule can undergo a major shift when a pendent nitro group is reduced to the respective hydroxylamine and to the amine group in hypoxia mediated by cellular reductases. The increase of electron density on hydroxylamine nitrogen has been employed release an active agent. The active drug is attached to a suitable nitro aromatic group in its prodrug form.<sup>40</sup> The activity of the agent is diminished or masked due to the ligation with the nitro aromatic group. The structural difference of conjugate **14**, nitroimidazole-phosphoramidate to the active agent **17**, a phosphoramidate, may cause the reduced effect of drug.<sup>41</sup> Once the nitro group on **14** is reduced in hypoxia, to the hydroxylamine group bearing **15**, the enhanced electron density on nitrogen of hydroxylamine will eject the active agent **17**, which is a good leaving group.<sup>42</sup> This electron movement will trigger covalent bond scission, which releases the active drug **17** from the pro-drug complex (Scheme 1.13) while forming imine methide **16**.<sup>43</sup>



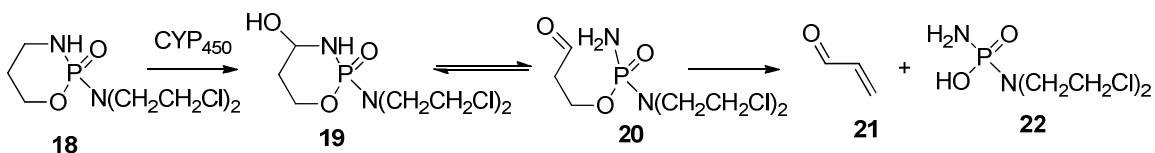
**Scheme 1.13.** Hydroxylamine releases the active drug

The phosphoramidate **17** can form aziridine, which acts as an electrophile that can alkylate cellular nucleophiles (Scheme 1.14).



**Scheme 1.14.** Phosphoramidate forms azide upon elimination of leaving group

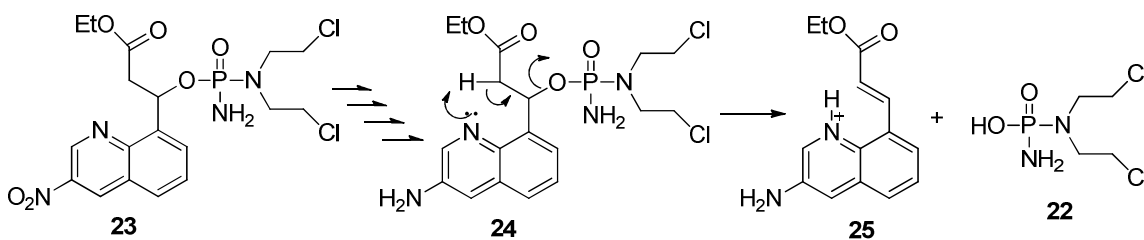
There are number of nitroaromatic-prodrugs designed to carry phosphoramidate toxins, structurally and functionally similar to phosphoramidate, such as **18** to cells. The parent cyclophosphamide drug **18** has been widely used anti-cancer agent with excellent toxicity toward various tumor types.<sup>44</sup> Although the positive results were encouraging, the parent cyclophosphamide showed lethal side effect, occurred due to release of acrolein **21** along the CYP<sub>450</sub>-mediated metabolic pathway via forming intermediates **19** and **20** (Scheme 1.15).<sup>45</sup>



**Scheme 1.15.** Cyclophosphamide **18** metabolism by CYP<sub>450</sub>

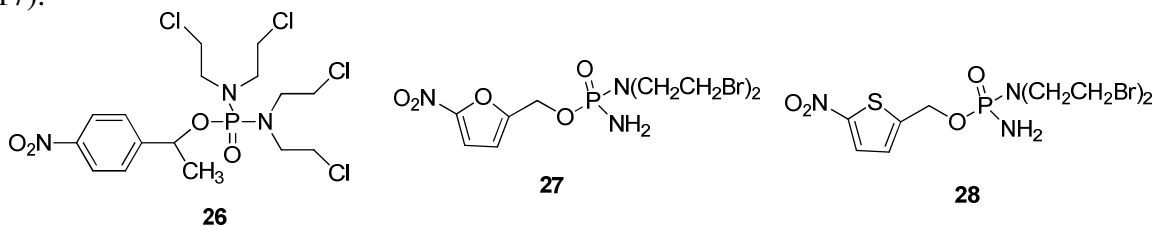
Delivering phosphoramidate, **22**, selectively to tumor is considered important in order to avoid such toxicity reported with **18**.<sup>46</sup> The nitroquinoline-phosphoramidate mustard **23** was developed as a pro-drug to test the ejection of phosphoramidate toxin **22**. Upon the reduction of the nitro group on quinoline, the electron rich quinoline nitrogen on **24** triggers beta elimination of **22** leaving **25** as a metabolite. Tenfold increase of cytotoxicity was observed in hypoxia and evidence for alkylation occurred by

phosphoramidate confirmed the expected release of phosphoramidate **22** upon nitro reduction (Scheme 1.16).<sup>40</sup>



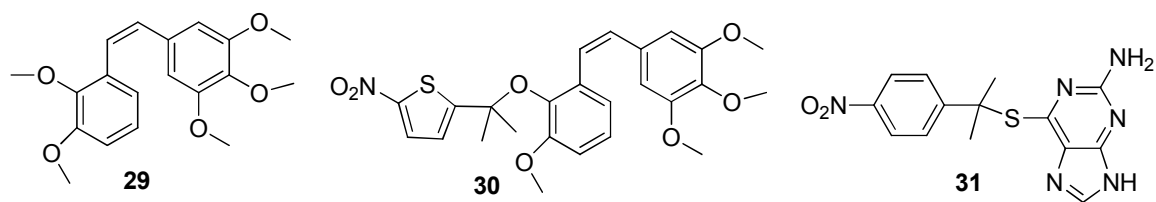
**Scheme 1.16.** Nitroquinoline-phosphoramidate prodrug release

Other nitro-aromatics nitrobenzyl, nitrofuryl and nitrothienyl have been used as bio-reducible triggers for conjugation with phosphoramidates. These prodrugs, constructed from tagging phosphoramidate with nitroaromatics have shown encouraging results; low cytotoxicity but enhanced tumor selectivity. Compound **24** generated DNA interstrand cross links in hypoxic HT-29 cells, with a selectivity ratio of 90.<sup>47</sup> Nitrophenyl **26**, nitrofuryl **27** and nitrothienyl **28** derivatives show low toxicity in aerobic assays (Scheme 1.17).<sup>48</sup>



**Scheme 1.17.** Nitrophenyl, Nitrofuryl and nitrothienyl phosphoramidate conjugates

In addition to the phosphoramidate mustards, various anti-cancer agents are conjugated to nitroaromatics. Combrestatin, **29** and its nitrothienyl couple **30**, and nitrophenyl-mercaptopurine prodrug **31** have shown effective release of agent upon bioreduction (Scheme 1.18).<sup>49</sup>

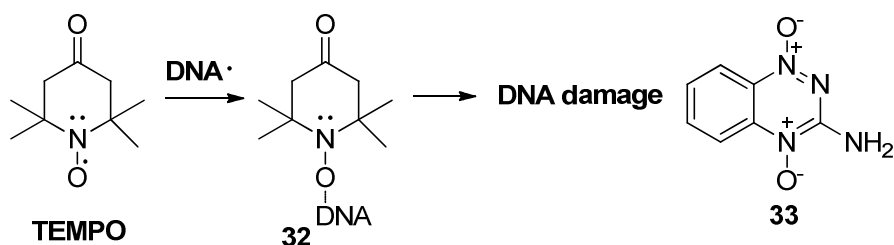


**Scheme 1.18.** Nitrothienyl and nitrophenyl dimethyl prodrugs

The importance of nitroaromatic reduction in tumor therapy and prodrug designing is well established in medicinal chemistry and bioorganic chemistry. In the coming chapters, interesting metabolic and fluorescence studies on 6-nitroquinoline reduction will be discussed. Moreover, the oxygen sensitivity of 6-nitroquinoline reduction, under two enzymatic reducing systems will be presented. Several novel findings related to the 6-nitroquinoline reduction will add complexity to enzyme mediated nitroaromatic reduction in hypoxia.

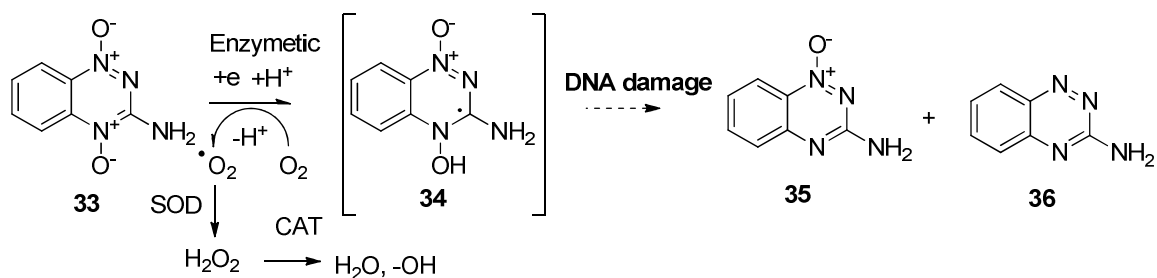
#### 1.4. *N*-oxides

Investigations carried out to develop radio sensitizing agents tested nitroxyl radical TEMPO. It has been discovered that TEMPO connects with the DNA radical, which is formed by radiolysis under hypoxia to produce DNA adduct **32**.<sup>18</sup> In search for backups to *N*-oxide radiosensitizing agents, Brown and coworkers tested tirapazamine (TPZ), *N*-oxide **33** as an oxygen mimetic agent in radiolysis of cells. They found that **33** was toxic as a single agent and the cytotoxicity was 200 fold higher for hypoxic cells.<sup>50</sup> The anti-cancer properties shown by **33** in the absence of  $\gamma$  radiation was stirred interest and the mechanism for the anti-tumor activity of **33** has been subjected further for research (Scheme 1.19).<sup>51</sup>



**Scheme 1.19.** *N*-oxide radiosensitizing agents

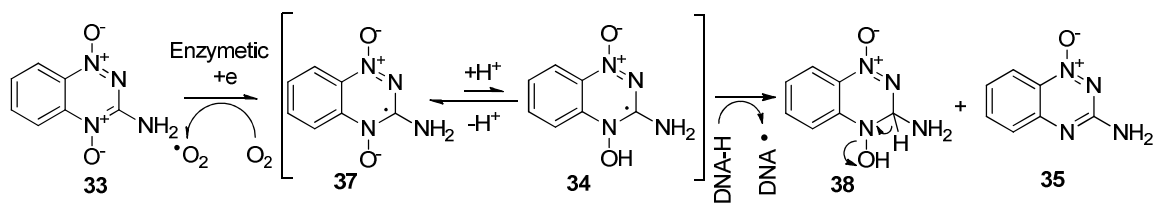
TPZ is believed to be activated by enzyme systems such as cytochrome P450 and cytochrome P450 reductase, xanthine and xanthine oxidase, aldehyde oxidase and nitric oxide synthase in cells.<sup>52</sup> The activation produces a TPZ radical which back oxidizes to the parent TPZ by oxygen under aerobic conditions to produce superoxide radical.<sup>23, 50, 53</sup> The superoxide radical disproportionate to yield hydrogen peroxide by super oxide dismutase (SOD) and hydrogen peroxide is converted to water and hydroxide ion by catalase (CAT).<sup>23</sup> Unless the superoxide radical is handled consecutively by SOD and CAT, radical-mediated oxidative damage may occur to biomolecules.<sup>23</sup> Under hypoxia, the TPZ radical **34** persists and produces an oxidizing radical which cause DNA damage.<sup>51, 54</sup> The in vivo enzymatic reduction process produces metabolites **35**, the major metabolite and **36** (Scheme 1.20).<sup>55</sup>



**Scheme 1.20.** Enzyme mediated reduction of **33** in hypoxia

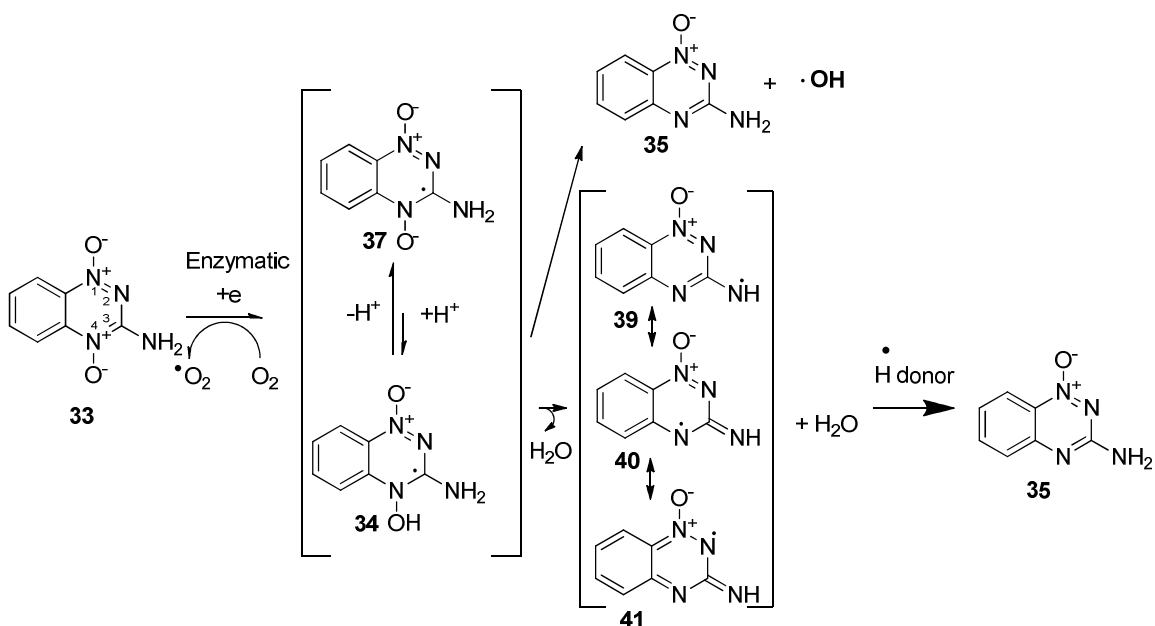
The DNA damage resulted by TPZ in hypoxia is believed to cause cytotoxicity in tumors.<sup>56</sup> The mechanism of TPZ-mediated DNA damage is not properly understood.<sup>57</sup> There are three mechanisms proposed to describe the nature of the DNA damaging species.<sup>58</sup>

The neutral benzotriazine dioxide radical **34**, formed from **37** upon enzymatic reduction of **33** has been proposed by Brown's group as the oxidizing species which causes the DNA damage.<sup>59</sup> In this proposal, a proton on DNA is abstracted by **34** to form **38**. A dehydration event proceeds via **38** to release water and **35** (Scheme 1.21).<sup>60</sup>



**Scheme 1.21.** Enzyme mediated reduction of **33** in hypoxia abstract proton from DNA, followed by dehydration releases **35** as the major metabolite

Alternatively, a homolytic bond scission of N-OH bond in neutral benzotriazine dioxide radical **34** can form a hydroxyl radical and the major metabolite **35** (Scheme 1.22 upper arm).<sup>61</sup> The hydroxyl radical, released from **34** is capable of performing oxidative damage on DNA.<sup>62</sup> Oxidative DNA damage occurs in tumor cells can initiate a cascade of events which result in cytotoxicity.<sup>63</sup> Denny and co-workers suggest a mechanism based on dehydration that might occur on the neutral benzotriazine di-oxide radical **34** forms a benzotriazinyl 1-oxide radical (structures **39**, **40** and **41**) which is responsible for the DNA damage (Scheme 1.22 lower arm).<sup>64</sup>



**Scheme 1.22.** The enzyme mediated reduction of 33 in hypoxia may produce hydroxyl radical or benzotriazine radicals 39, 40 or 41 as the oxidizing species

Research carried out by our group support the mechanism involving hydroxyl radical mediated DNA damage.<sup>65</sup>

## 1.5. Summary

Nitroaromatic compounds have become a prominent drug class in medicinal chemistry research.<sup>66</sup> The nitroaromatic reduction that occurs in low oxygen concentrations is mediated by reductive enzymes and has become an attractive concept in bioreductive prodrug therapy.<sup>58</sup> Nitroaromatic reduction reactions are complex due to the presence of various intermediates and byproducts.<sup>67</sup> The work presented in this thesis describes the use of small molecule 6-nitroquinoline as a fluorescent probe that can detect hypoxia.<sup>68</sup> A rich metabolic study is accompanying the fluorescent results in coming chapters. In addition the lead *N*-oxide tirapazamine, which has been in phase trials I, II and III for clinical therapy over a decade and its analogs were used to study the DNA-

damaging mechanism of *N*-oxides.<sup>69</sup> The chemical basis for the DNA damage, caused by **33** depends on the reduction mechanism of these di-oxide.<sup>65</sup> The chemical nature of the DNA-damaging species has become an interesting topic in research. In the current thesis, a mechanistic study is presented analyze the reduction mechanism and the chemical nature of the oxidizing species.

### References:

1. Brown, J. M., The hypoxic cell: A target for selective cancer therapy. *Cancer Res.* 1999, 59, 5863-5870.
2. Patel, S. A.; Simon, M. C., Biology of hypoxia-inducible factor-2alpha in development and disease. *Cell Death & Diff* 2008, 15 (4), 628-34.
3. Denny, W. A., The role of hypoxia-activated prodrugs in cancer therapy. *The Lancet Oncol.* 2000, 1, 25-29.
4. Harris, A. L., Hypoxia - a key regulatory factor in tumour growth. *Nat. Rev. Cancer* 2002, 2, 38-47.
5. Alper, T.; Howard-Flanders, P., Role of oxygen in modifying the radiosensitivity of *E. coli* B. *Nature* 1956, 178 (4540), 978-9.
6. Vaupel, P.; Kelleher, D. K.; Thews, O., Modulation of tumor oxygenation. *Int. J. Radiat. Oncol. Biol. Phys.* 1998, 42 (4), 843-848.
7. von Sonntag, C.; Hagen, U.; Schon-Bopp, A.; Schulte-Frohlinde, D., Radiation-induced strand breaks in DNA: chemical and enzymatic analysis of end groups and mechanistic aspects. *Adv. Radiat. Biol.* 1981, 9, 109-142.
8. Pogozelski, W. K.; Tullius, T. D., Oxidative strand scission of nucleic acids: routes initiated by hydrogen atom abstraction from the sugar moiety. *Chem. Rev.* 1998, 98, 1089-1107.



9. Pogożelski, W. K.; McNeese, T. J.; Tullius, T. D., What species is responsible for strand scission in the reaction of  $[\text{Fe}(\text{II})\text{EDTA}]^{2-}$  and  $\text{H}_2\text{O}_2$  with DNA? *J. Am. Chem. Soc.* 1995, *117*, 6428-6433.
10. Burrows, C. J.; Muller, J. G., Oxidative nucleobase modifications leading to strand scission. *Chem. Rev.* 1998, *98*, 1109-1151.
11. Murugesan, N.; Xu, C.; Ehrenfeld, G. M.; Sugiyama, H.; Kilkuskie, R. E.; Rodriguez, L. O.; Chang, L. H.; Hecht, S. M., Analysis of products formed during bleomycin-mediated DNA degradation. *Biochemistry* 1985, *24* (21), 5735-44.
12. Giese, B.; Beyrich-Graf, X.; Erdmann, P.; Petretta, M.; Schwitter, U., The chemistry of single-stranded 4'-DNA radicals: influence of the radical precursor on anaerobic and aerobic strand cleavage. *Chem. Biol.* 1995, *2*, 367-375.
13. Greenberg, M. M., Investigating nucleic acid damage processes via independent generation of reactive intermediates. *Chem. Res. Toxicol.* 1998, *11* (11), 1235-1248.
14. Debatin, K., Activation of apoptosis pathways by anticancer treatment. *Toxicol Lett* 2000, *112-113*, 41-8.
15. Hockel, M.; Vaupel, P., Biological consequences of tumor hypoxia. *Semin Oncol* 2001, *28*, 36-41.
16. Bump, E. A.; Brown, J. M., Role of glutathione in the radiation response of mammalian cells in vitro and in vivo. *Pharmac. Ther.* 1990, *47*, 117-136.
17. (a) Wilson, W. R., Tumour hypoxia: challenges for cancer chemotherapy. In *The Search For New Anticancer Drugs*, Waring, M. J.; Ponder, B. A. J., Eds. Kluwer Academic: Lancaster, 1992; (b) Brown, J. M., SR4233 (Tirapazamine): a new anticancer drug exploiting hypoxia in solid tumours. *Br. J. Cancer* 1993, *67*, 1163-1170.
18. Hohman, W. F.; Palcic, B.; Skarsgard, L. D., The effect of nitroimidazole and nitroxyl radiosensitizers on the post-irradiation synthesis of DNA. *Int. J. Radiat. Biol. Relat. Stud. Phys., Chem. Med.* 1976, *30*, 247-61.
19. Amphlett, C. B.; Adams, G. E.; Michael, B. D., Pulse radiolysis studies of deaerated aqueous salicylate solutions. *Advan. Chem. Ser.* 1968, *81*, 231-50.

20. Jagannadham, V.; Steenken, S., Reactivity of N1-heteroatom-substituted alkyl radicals with nitrobenzenes in aqueous solution: an entropy controlled electron transfer/addition mechanism. *J. Am. Chem. Soc.* 1988, *110*, 2188-92.
21. Kappen, L. S.; Lee, T. R.; Yang, C.-c.; Goldberg, I. H. I., Oxygen transfer from the nitro group of a nitroaromatic radiosensitizer to a DNA sugar damage product. *Biochemistry* 1989, *28*, 4540-4542.
22. Hall, E. J.; Roizin-Towle, L.; Attix, F. H., Radiobiological studies with cyclotron-produced neutrons currently used for radiotherapy. *Int J Radiat Oncol Biol Phys* 1975, *1*, 33-40.
23. Butler, J.; Hoey, B. M., DNA and Free Radicals. In *Redox cycling drugs and DNA damage*, Halliwell, B.; Aruoma, O. I., Eds. Ellis Horwood: New York, NY, 1993; pp 243-273.
24. Feller, D. R.; Morita, M.; Gillette, J. R., Reduction of heterocyclic nitro compounds in the rat liver. *Proc. Soc. Exp. Biol. Med.* 1971, *137*, 433-7.
25. (a) Miller, J. A., Carcinogenesis by chemicals: an overview--G. H. A. Clowes memorial lecture. *Cancer Res* 1970, *30* (Copyright (C) 2012 U.S. National Library of Medicine.), 559-76; (b) McClelland, R. A.; Fuller, J. R.; Seaman, N. E.; Rauth, A. M.; Battistella, R., 2-Hydroxylaminoimidazoles--unstable intermediates in the reduction of 2-nitroimidazoles. *Biochem Pharmacol* 1984, *33*, 303-9.
26. McClelland, R. A.; Panicucci, R.; Rauth, A. M., Products of the reductions of 2-nitroimidazoles. *J. Am. Chem. Soc.* 1987, *109*, 4308-4314.
27. Denny, W. A.; Wilson, W. R., Considerations for the design of nitrophenyl mustards as agents with selective toxicity for hypoxic tumor cells. *J. Med. Chem.* 1986, *29* (6), 879-887.
28. (a) Walton, M. I.; Wolf, C. R.; Workman, P., Molecular enzymology of the reductive bioactivation of hypoxic cell cytotoxins. *Int. J. Radiat. Oncol. Biol. Phys.* 1989, *16*, 983-986; (b) Wilson, W. R.; Anderson, R. F.; Denny, W. A., Hypoxia-selective antitumor agents. 1. Relationships between structure, redox properties and hypoxia-selective cytotoxicity for 4-substituted derivatives of nitracrine. *J. Med. Chem.* 1989, *32*, 23-30.

29. (a) Gutierrez, P. L., The metabolism of quinone-containing alkylating agents: free radical production and measurement. *Front Biosci* 2000, 5, D629-38; (b) Belcourt, M. F.; Hodnick, W. F.; Rockwell, S.; Sartorelli, A. C., Exploring the mechanistic aspects of mitomycin antibiotic bioactivation in Chinese hamster ovary cells overexpressing NADPH:cytochrome C (P-450) reductase and DT-diaphorase. *Adv Enzyme Regul* 1998, 38, 111-33; (c) Volpato, M.; Abou-Zeid, N.; Tanner, R. W.; Glassbrook, L. T.; Taylor, J.; Stratford, I.; Loadman, P. M.; Jaffar, M.; Phillips, R. M., Chemical synthesis and biological evaluation of a NAD(P)H:quinone oxidoreductase-1-targeted tripartite quinone drug delivery system. *Mol. Cancer Ther.* 2007, 6, 3122-3130.
30. Sykes, B. M.; Atwell, G. J.; Hogg, A.; Wilson, W. R.; O'Connor, C. J.; Denny, W. A., N-Substituted 2-(2,6-Dinitrophenylamino)propanamides: Novel Prodrugs That Release a Primary Amine via Nitroreduction and Intramolecular Cyclization. *J. Med. Chem.* 1999, 42, 346-355.
31. Moselen, J. W.; Hay, M. P.; Denny, W. A.; Wilson, W. R., N-[2-(2-Methyl-5-nitroimidazolyl)ethyl]-4-(2-nitroimidazolyl)butanamide (NSC 639862), a bisnitroimidazole with enhanced selectivity as a bioreductive drug. *Cancer Res.* 1995, 55, 574-80.
32. Knox, R. J.; Friedlos, F.; Marchbank, T.; Roberts, J. J., Bioactivation of CB 1954: reaction of the active 4-hydroxylamino derivative with thioesters to form the ultimate DNA-DNA interstrand crosslinking species. *Biochem. Pharmacol.* 1991, 42, 1691-7.
33. Stratford, I. J.; O'Neill, P.; Sheldon, P. W.; Silver, A. R. J.; Walling, J. M.; Adams, G. E., RSU 1069, a nitroimidazole containing an aziridine group. Bioreduction greatly increases cytotoxicity under hypoxic conditions. *Biochem. Pharmacol.* 1986, 35, 105-9.
34. Binger, M.; Workman, P., Pharmacokinetic contribution to the improved therapeutic selectivity of a novel bromoethylamino prodrug (RB 6145) of the mixed-function hypoxic cell sensitizer/cytotoxin N1-(1-aziridinomethyl)-2-nitro-1H-imidazole-1-ethanol (RSU 1069). *Cancer Chemother. Pharmacol.* 1991, 29, 37-47.
35. Wilson, W. R.; Denny, W. A.; Twigden, S. J.; Baguley, B. C.; Probert, J. C., Selective toxicity of nitracrine to hypoxic mammalian cells. *Br. J. Cancer* 1984, 49, 215-23.
36. Knox, R. J.; Burke, P. J.; Chen, S.; Kerr, D. J., CB 1954: From the Walker tumor to NQO2 and VDEPT. *Curr. Pharm. Des.* 2003, 9, 2091-2104.

37. (a) Helsby, N. A.; Wheeler, S. J.; Pruijn, F. B.; Palmer, B. D.; Yang, S.; Denny, W. A.; Wilson, W. R., Effect of Nitroreduction on the Alkylating Reactivity and Cytotoxicity of the 2,4-Dinitrobenzamide-5-aziridine CB 1954 and the Corresponding Nitrogen Mustard SN 23862: Distinct Mechanisms of Bioreductive Activation. *Chem. Res. Toxicol.* 2003, *16*, 469-478; (b) Palmer, B. D.; Wilson, W. R.; Atwell, G. J.; Schultz, D.; Xu, X. Z.; Denny, W. A., Hypoxia-Selective Antitumor Agents. 9. Structure-Activity Relationships for Hypoxia-Selective Cytotoxicity among Analogs of 5-[N,N-Bis(2-chloroethyl)amino]-2,4-dinitrobenzamide. *J. Med. Chem.* 1994, *37*, 2175-84; (c) Palmer, B. D.; Wilson, W. R.; Anderson, R. F.; Boyd, M.; Denny, W. A., Hypoxia-Selective Antitumor Agents. 14. Synthesis and Hypoxic Cell Cytotoxicity of Regioisomers of the Hypoxia-Selective Cytotoxin 5-[N,N-Bis(2-chloroethyl)amino]-2,4-dinitrobenzamide. *J. Med. Chem.* 1996, *39*, 2518-2528.
38. Helsby, N. A.; Ferry, D. M.; Patterson, A. V.; Pullen, S. M.; Wilson, W. R., 2-Amino metabolites are key mediators of CB 1954 and SN 23862 bystander effects in nitroreductase GDEPT. *Br. J. Cancer* 2004, *90*, 1084-1092.
39. Patterson, A. V.; Ferry, D. M.; Edmunds, S. J.; Gu, Y.; Singleton, R. S.; Patel, K. B.; Pullen, S. M.; Hicks, K. O.; Syddall, S. P.; Atwell, G. J.; Yang, S.; Denny, W. A.; Wilson, W. R., Mechanism of action and preclinical antitumor activity of the novel hypoxia-activated DNA cross-linking agent PR-104. *Clin. Cancer Res.* 2007, *13* (13), 3922-3932.
40. Firestone, A.; Mulcahy, R. T.; Borch, R. F., Nitro heterocycle reduction as a paradigm for intramolecular catalysis of drug delivery to hypoxic cells. *J. Med. Chem.* 1991, *34*, 2933-5.
41. Duan, J.-X.; Jiao, H.; Kaizerman, J.; Stanton, T.; Evans, J. W.; Lan, L.; Lorente, G.; Banica, M.; Jung, D.; Wang, J.; Ma, H.; Li, X.; Yang, Z.; Hoffman, R. M.; Ammons, W. S.; Hart, C. P.; Matteucci, M., Potent and highly selective hypoxia-activated achiral phosphoramidate mustards as anticancer drugs. *J. Med. Chem.* 2008, *51*, 2412-2420.
42. Hay, M. P.; Sykes, B. M.; Denny, W. A.; Wilson, W. R., A 2-nitroimidazole carbamate prodrug of 5-amino-1-(chloromethyl)-3-[(5,6,7-trimethoxyindol-2-yl)carbonyl]-1,2-dihydro-3H-ben[E]indole (amino-seco-CBI-TMI) for use with ADEPT and GDEPT. *Bioorg. Med. Chem. Lett.* 1999, *9*, 2237-2242.
43. Hay, M. P.; Wilson, W. R.; Denny, W. A., Design, synthesis and evaluation of imidazolylmethyl carbamate prodrugs of alkylating agents. *Tetrahedron* 2000, *56*, 645-657.

44. Borch, R. F.; Canute, G. W., Synthesis and antitumor properties of activated cyclophosphamide analogs. *J. Med. Chem.* 1991, *34*, 3044-52.
45. Li, F.; Patterson, A. D.; Hoefler, C. C.; Krausz, K. W.; Gonzalez, F. J.; Idle, J. R., Comparative metabolism of cyclophosphamide and ifosfamide in the mouse using UPLC-ESI-QTOFMS-based metabolomics. *Biochem. Pharmacol.* 2010, *80*, 1063-1074.
46. Borch, R. F.; Liu, J.; Schmidt, J. P.; Marakovitz, J. T.; Joswig, C.; Gipp, J. J.; Mulcahy, R. T., Synthesis and evaluation of nitroheterocyclic phosphoramidates as hypoxia-selective alkylating agents. *J. Med. Chem.* 2000, *43*, 2258-2265.
47. Mulcahy, R. T.; Gipp, J. J.; Schmidt, J. P.; Joswig, C.; Borch, R. F., Nitrobenzyl Phosphorodiamidates as Potential Hypoxia-Selective Alkylating Agents. *J. Med. Chem.* 1994, *37*, 1610-15.
48. Borch, R. F.; Liu, J.; Joswig, C.; Baggs, R. B.; Dexter, D. L.; Mangold, G. L., Antitumor Activity and Toxicity of Novel Nitroheterocyclic Phosphoramidates. *J. Med. Chem.* 2001, *44*, 74-77.
49. Thomson, P.; Naylor, M. A.; Stratford, M. R. L.; Lewis, G.; Hill, S.; Patel, K. B.; Wardman, P.; Davis, P. D., Hypoxia-driven elimination of thiopurines from their nitrobenzyl prodrugs. *Bioorg. Med. Chem. Lett.* 2007, *17*, 4320-4322.
50. Zeman, E. M.; Brown, J. M.; Lemmon, M. J.; Hirst, V. K.; Lee, W. W., SR-4233: a new bioreductive agent with high selective toxicity for hypoxic mammalian cells. *Int J Radiat Oncol Biol Phys* 1986, *12*, 1239-42.
51. Brown, J. M., SR 4233 (tirapazamine): a new anticancer drug exploiting hypoxia in solid tumors. *Br. J. Cancer* 1993, *67*, 1163-70.
52. Denny, W. A., Prodrug strategies in cancer therapy. *Eur. J. Med. Chem.* 2001, *36*, 577-595.
53. Fitzsimmons, S. A.; Lewis, A. D.; Riley, R. J.; Workman, P., Reduction of 3-amino-1,2,4-benzotriazine-1,4,-di-N-oxide to a DNA-damaging species: a direct role for NADPH:cytochrome P450 oxidoreductase. *Carcinogenesis* 1994, *15* (8), 1503-1510.

54. Lloyd, R. V.; Duling, D. R.; Rummyantseva, G. V.; Mason, R. P.; Bridson, P. K., Microsomal reduction of 3-amino-1,2,4-benzotriazine 1,4-dioxide to a free radical. *Mol. Pharmacol.* 1991, *40*, 440-445.
55. Costa, A. K.; Baker, M. A.; Brown, J. M.; Trudell, J. R., In vitro hepatotoxicity of SR 4233 (3-amino-1,2,4-benzotriazine-1,4-dioxide), a hypoxic cytotoxin and potential antitumor agent. *Cancer Res* 1989, *49*, 925-9.
56. McKeown, S. R.; Cowen, R. L.; Williams, K. J., Bioreductive drugs: from concept to clinic. *Clin Oncol (R Coll Radiol)* 2007, *19*, 427-42.
57. Von, P. J.; Von, R. R.; Gatzemeier, U.; Boyer, M.; Elisson, L. O.; Clark, P.; Talbot, D.; Rey, A.; Butler, T. W.; Hirsh, V.; Olver, I.; Bergman, B.; Ayoub, J.; Richardson, G.; Dunlop, D.; Arcenas, A.; Vescio, R.; Viallet, J.; Treat, J., Tirapazamine plus cisplatin versus cisplatin in advanced non-small-cell lung cancer: a report of the international CATAPULT I study group. *J. Clin. Oncol.* 2000, *18*, 1351-1359.
58. Chen, Y.; Hu, L., Design of anticancer prodrugs for reductive activation. *Med. Res. Rev.* 2009, *29* (1), 29-64.
59. Baker, M. A.; Zeman, E. M.; Hirst, V. K.; Brown, J. M., Metabolism of SR 4233 by Chinese hamster ovary cells: basis of selective hypoxic cytotoxicity. *Cancer Res.* 1988, *48*, 5947-52.
60. Laderoute, K. L.; Wardman, P.; Rauth, M., Molecular mechanisms for the hypoxia-dependent activation of 3-amino-1,2,4-benzotriazine 1,4-dioxide (SR4233). *Biochem. Pharmacol.* 1988, *37* (8), 1487-1495.
61. Daniels, J. S.; Gates, K. S., DNA Cleavage by the Antitumor Agent 3-Amino-1,2,4-benzotriazine 1,4-Dioxide (SR4233): Evidence for Involvement of Hydroxyl Radical. *J. Am. Chem. Soc.* 1996, *118* (14), 3380-3385.
62. Daniels, J. S.; Gates, K. S.; Tronche, C.; Greenberg, M. M., Direct evidence for bimodal DNA damage induced by tirapazamine. *Chem. Res. Toxicol.* 1998, *11* (11), 1254-1257.
63. Chowdhury, G.; Junnutula, V.; Daniels, J. S.; Greenberg, M. M.; Gates, K. S., DNA strand damage analysis provides evidence that the tumor cell-specific cytotoxin

tirapazamine produces hydroxyl radical and acts as a surrogate for O<sub>2</sub>. *J. Am. Chem. Soc.* 2007, *129*, 12870-12877.

64. (a) Shinde, S. S.; Anderson, R. F.; Hay, M. P.; Gamage, S. A.; Denny, W. A., Oxidation of 2-Deoxyribose by Benzotriazinyl Radicals of Antitumor 3-Amino-1,2,4-benzotriazine 1,4-Dioxides. *J. Am. Chem. Soc.* 2004, *126* (25), 7865-7874; (b) Anderson, R. F.; Shinde, S. S.; Hay, M. P.; Gamage, S. A.; Denny, W. A., Radical properties governing the hypoxia-selective cytotoxicity of antitumor 3-amino-1,2,4-benzotriazine 1,4-dioxides. *Org. Biomol. Chem.* 2005, *3* (11), 2167-2174.

65. Junnotula, V.; Sarkar, U.; Sinha, S.; Gates, K. S., Initiation of DNA strand cleavage by 1,2,4-benzotriazine 1,4-dioxides: mechanistic insight from studies of 3-methyl-1,2,4-benzotriazine 1,4-dioxide. *J. Am. Chem. Soc.* 2009, *131*, 1015-1024.

66. Boelsterli, U. A.; Ho, H. K.; Zhou, S.; Leow, K. Y., Bioactivation and hepatotoxicity of nitroaromatic drugs. *Curr. Drug Metab.* 2006, *7*, 715-727.

67. (a) Rooseboom, M.; Commandeur, J. N. M.; Vermeulen, N. P. E., Enzyme-catalyzed activation of anticancer prodrugs. *Pharm. Rev.* 2004, *56*, 53-102; (b) Fitzsimmons, S. A.; Workman, P. A.; Grever, M.; Paull, K.; Camalier, R.; Lewis, A. D., Reductase enzyme expression across the National Cancer Institute tumor cell line panel: correlation with sensitivity to mitomycin C and E09. *J. Natl. Cancer Inst.* 1996, *88*, 259-269.

68. Rajapakse, A.; Gates, K. S., Hypoxia-Selective, Enzymatic Conversion of 6-Nitroquinoline into a Fluorescent Helicene: Pyrido[3,2-f]quinolino[6,5-c]cinnoline 3-Oxide. *J. Org. Chem.* 2012, *77*, 3531-3537.

69. Hay, M. P.; Pchalek, K.; Pruijn, F. B.; Hicks, K. O.; Siim, B. G.; Anderson, M. M.; Shinde, S. S.; Denny, W. A.; Wilson, W. R., Hypoxia-selective 3-alkyl 1,2,4-benzotriazine 1,4-dioxides: the influences of hydrogen bond donors on extravascular transport and antitumor activity. *J. Med. Chem.* 2007, *50* (26), 6654-6664.

## Chapter 2

### **Hypoxia-selective, enzymatic conversion of 6-nitroquinoline into a fluorescent helicene: pyrido[3,2-f]quinolino[6,5-c]cinnoline 3-oxide**

#### **2.1 Hypoxia as a parameter to be determined qualitatively and quantitatively.**

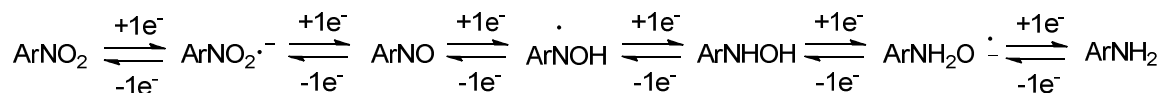
Hypoxia or low oxygen concentrations exist in disease conditions such as ischemia, stroke, inflammation and solid tumors, and in normal human physiology.<sup>1</sup> Transient regions of hypoxia, reportedly present in stem tissues may have an effect on controlling cell division and differentiation during hematopoiesis and embryogenesis.<sup>2</sup>

Oxygen concentration in a normal healthy cell is within a range of 20 to 90  $\mu\text{M}$  (14–65 mm Hg).<sup>3</sup> Any concentration below 20  $\mu\text{M}$  is considered hypoxia.<sup>4</sup> Efforts were made to quantify hypoxia using an oxy probe, radiochemical imaging and immunohistochemical staining methods.<sup>5</sup> Practical and technical difficulties limit accuracy and applicability of these techniques.<sup>6</sup> Hence, there is a demand for a noninvasive tool which can qualitatively and quantitatively characterize tumor hypoxia in biological conditions. Fluorescent probes can be designed to light up inside the hypoxic tumor under physiological conditions, and the fluorescence outcome can be used as a parameter that can be measured and relate to the oxygen concentration of tumors.<sup>7</sup>



## 2.2 Fluorescent probes to detect hypoxia

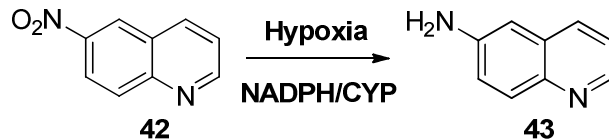
Several approaches have been used to deliver a fluorescent agent into the tumor setting to mark hypoxic tissues. One method is to use nitro-aromatic non-fluorescent compound which converts to a fluorescent amino metabolite under hypoxic conditions.<sup>7-8</sup> Enzyme mediated cellular reduction of nitroaromatics, under low oxygen levels, has been reported and developed as a concept in biochemical research. The reduction process consists of consecutive addition of six electrons, in a stepwise manner to produce the final reduced product, the respective arylamine.<sup>9</sup> The hypoxia selectivity arises within the first reduction step where the nitro radical anion back-oxidizes to the parent nitro compound in the presence of oxygen.<sup>9d, e, 10</sup> The first electron addition step is oxygen sensitive and the remaining one electron addition steps may be oxygen sensitive. Nitroso compound would next be converted to hydroxylamine intermediate by adding two electrons and in the final two electrons addition produces the amino product. (Scheme 2.1).<sup>11</sup>



**Scheme 2.1.** Enzymatic reduction profile of nitroaromatic compound

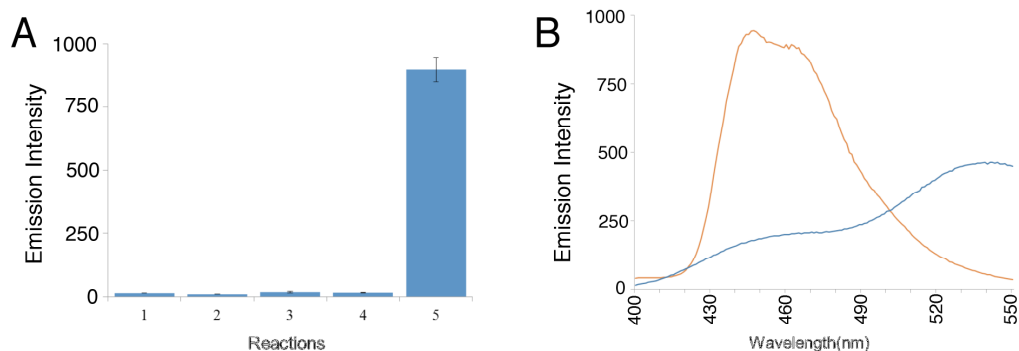
## 2.3 Reduction of 42 to obtain 43 under anaerobic conditions

Non-fluorescent nitroaromatic compound 6-nitroquinoline **42** was used as a small molecule nitroaromatic probe to detect hypoxia. The compound **42** may be reduced under low oxygen levels and under bio-reductive conditions to produce fluorescent metabolite, 6-aminoquinoline (**43**, Scheme 2.2)



**Scheme 2.2.** Hypoxic metabolism of **42** is expected to form fluorescent **43**

The amino compound **43** is a known fluorescent molecule and the reduction of **42** to **43** step yields a good Stokes shift of 205 nm.<sup>12</sup> The probe **42** is non-fluorescent in aqueous sodium phosphate buffer at pH 7.4 (Figure 1A, column 1).<sup>11</sup> The enzyme NADPH:cytochrome P450 reductase, a known reductase that reduces nitrocompounds in cells is used as the reducing enzyme with assistance of the substrate NADPH to reduce **42** under hypoxia.<sup>9c, 13</sup> The hypoxic reduction reaction forms fluorescence with an impressive 63-fold increase at 445 nm, indicating conversion of the non-fluorescent **42** to a fluorescent metabolite (Figure 1A, column 5). The enzymatic reduction of **42** under aerobic conditions produced no fluorescence (Figure 1A, column 4). Similarly, when non fluorescent electron acceptor benzotriazine 1,2,4-di-oxide was used in aerobic and anaerobic enzymatic reduction reactions, very low fluorescence was observed (Figure 1A, columns 2 and 3). Careful inspection of the shape of the fluorescent curve in Figure 1, column 5 showed that the fluorescence emission curve does not resemble the fluorescence curve of authentic **43**. The fluorescence emission curve of **43** is broader at 445 nm and 530 nm regions (Figure 1B blue line) and, instead consists of a pair of emission maxima at 440 and 460 nm. The unexpected fluorescence, yielded in the hypoxic metabolism of **42**, was explored to identify and characterize the fluorescent metabolite.

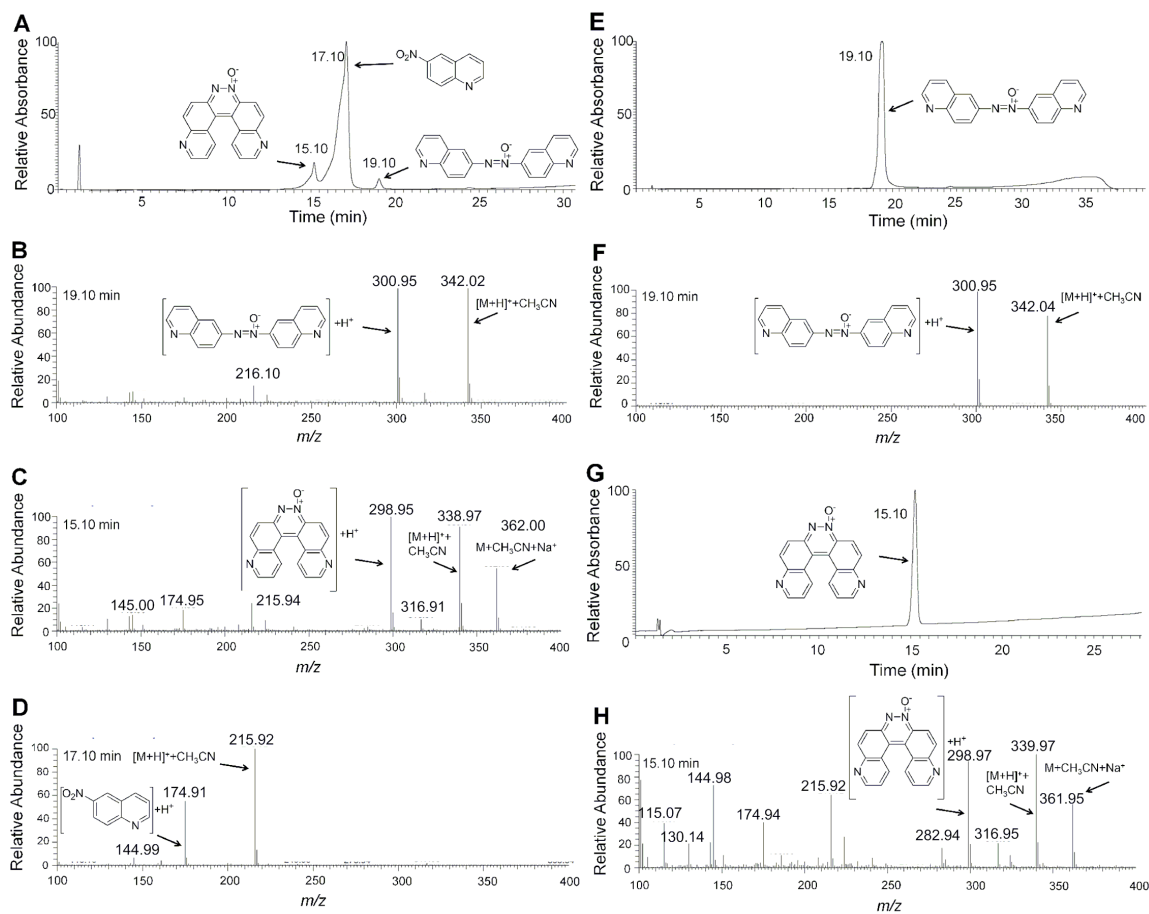


**Figure 2.1.** Enzymatic conversion of **42** into a fluorescent product under hypoxic conditions. A. Fluorescence emission at 445 nm ( $\lambda_{ex}$  307 nm) for: (1) a control sample of compound **42** alone (0.8 mM), (2) a control reaction composed of NADPH:cytochrome P450 reductase (1.1 U/mL), NADPH (2.4 mM), and a non-fluorescent electron acceptor 1,2,4-benzotriazine 1,4-dioxide (6.4 mM) under aerobic conditions, (3) a control reaction composed of NADPH:cytochrome P450 reductase, NADPH, and a non-fluorescent electron acceptor 1,2,4-benzotriazine 1,4-dioxide (6.4 mM) under anaerobic conditions, (4) compound **42** (0.8 mM) + NADPH:cytochrome P450 reductase and NADPH under aerobic conditions, (5) compound **42** (0.8 mM) + cytochrome P450 reductase and NADPH anaerobic. Reactions were incubated for 18 h in sodium phosphate buffer at (12 mM, pH 7.4) at 24 °C, then diluted with aerobic sodium phosphate buffer (12 mM, pH 7.4) and the fluorescence measured ( $\lambda_{ex}$  307 nm,  $\lambda_{em}$  445 nm). It is important to note that NADPH exhibits fluorescence with an emission maximum at 445 nm. However, control experiments showed that any NADPH left unconsumed at the end of the anaerobic reactions described here is ultimately converted to the non-fluorescent NADP<sup>+</sup> product by enzyme-driven redox cycling of the electron accepting organic substrate upon opening the reaction vessel to air and dilution with aerobic buffer prior to fluorescence measurements. B. Fluorescence spectrum of the reaction mixture generated in the anaerobic metabolism of **42** by NADPH:cytochrome P450 reductase as described for reaction 5 above (orange line, with emission maxima at 440 and 450 nm) and fluorescence spectrum of 6-aminoquinoline (**43**, 50  $\mu$ M,  $\lambda_{ex}$  340 nm, in sodium phosphate buffer, 10 mM, pH 7.4).<sup>11</sup>

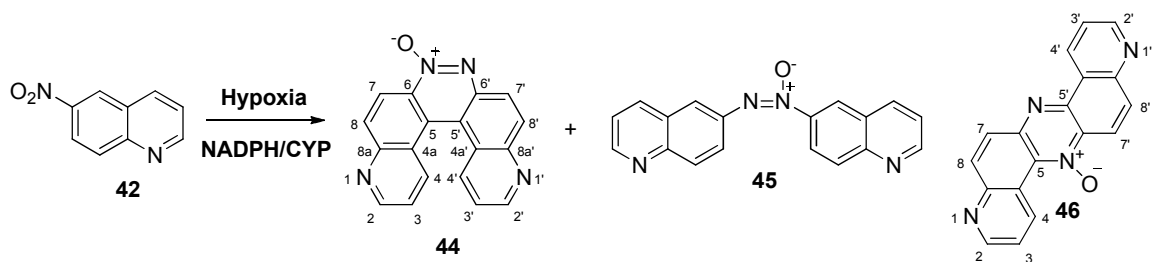
## 2.4 Identification of products arising from the anaerobic reaction

The anaerobic reaction mixture of metabolism of **42**, mediated by NADPH:cytochrome P450 reductase was analyzed using LC/MS. Two major products were identified in addition to the remaining starting material **42** (Figure 2.2 A). Confirming the analysis of the fluorescence spectrum of the anaerobic reaction mixture, **43**, the product expected by the original six electron reduction process was not observed in the LC/MS analysis. Under the same LC/MS conditions **43** appears at approximately 4.5 min (Figure S1). One of the products, eluting at 19.4 min in the UV trace has m/z

value of 301 (Figure 2.2 B). The  $[M+H]^+$  ion of 6,6'-azoxyquinoline would have a mass-to-charge ratio of 301 (**45**, Scheme 2.2). Formation of **45** under relevant conditions is expected to be produced, based on precedents which suggest condensation of intermediates 6-nitrosoquinoline and 6-hydroxylaminoquinoline that are formed along the reduction path.<sup>14</sup> An authentic sample of **45**, synthesized from reducing **42** by hydrazine hydrate in the presence of Raney nickel gave similar LC/MS spectra with a peak at 19.4 min (Figures 2.2 E and F).<sup>15</sup> Compound **45** is non-fluorescent under the applied conditions in the solution. Hence the fluorescence should arise from the product appearing at 15 min in the LC trace. There is evidence that complex dimmers such as **44** could be fluorescent.<sup>16</sup> The mass-to-charge ratio of the new product was 299 (Figure 2.2 C). A simple, quinoline dimer such as azoxy or azo does not have a  $m/z$  of 299, rather a more complex quinoline-based bi aryl compound such as pyrido[3,2-*f*]quinolino[6,5-*c*]cinnoline 3-oxide (**44**, Scheme 2.3) or dipyrdo[3,2-*a*:3',2'-*h*]phenazine 7-oxide (**46**, Scheme 2.3) does have the observed  $m/z$  value.



**Figure 2.2.** LC/MS analysis of the reaction mixture generated by anaerobic metabolism of **42** (0.8 mM) by cytochrome p450 reductase (1.1 U/mL) and NADPH (6.4 mM). The enzymatic reduction of **42** was carried out as described in the experimental section and the legend of Figure 2.1. The reaction was dried and products dissolved in methanol. The mixture was eluted with a gradient of 99% A (water containing 0.1% acetic acid) and 1% B (acetonitrile containing 0.1% acetic acid) followed by linear increase to 90% B over 30 min. The elution was continued at 90% B for 3 min and then B was decreased to 1% over next 8 min. A flow rate of 0.35 mL/min was used and the metabolites were detected at 254 nm. Mass spectra were obtained using electrospray ionization in the positive ion mode. Panel A: HPLC of the anaerobic reaction mixture monitoring absorbance at 254 nm. Panel B: LC/MS spectrum of the product eluting at 19.1 min. Panel C: LC/MS spectrum of the product eluting at 15.1 min. Panel D: LC/MS spectrum for of the product eluting at 17.1 min. Panel E: HPLC retention time of authentic **45** monitoring absorbance at 254 nm. Panel F: LC/MS spectrum of authentic **45**. Panel G: HPLC retention time of authentic **44** monitoring absorbance at 254 nm. Panel H: LC/MS spectrum of authentic **44**.



**Scheme 2.3.** Metabolites formed by the reduction of **42** with NADPH/CYP450R

According to precedents, helicenes are structurally similar to **44**, and are fluorescent.<sup>16</sup> Hence, the enzymatic reduction of **42**, under above condition might be producing **44**. The two structures **44** and **46** have same molecular formula. Huisgen proposed that compound **44** is formed in a reaction when **42** is reduced by sodium methoxide.<sup>17</sup> Farrar claimed that Huisgen was obtaining compound **46**, not **44**.<sup>18</sup> Moreover, Farrar carried out reduction of **42**, with alkaline glucose as suggested by Galbraith *et al* to produce **45**. Farrar claimed that alkaline glucose mediated reduction of **42** actually produces **44** not **45**.<sup>18</sup>

## 2.4 Synthesis and structural characterization of **44**

Galbraith's alkaline glucose reduction of **42** has been successfully used as the chemical method to synthesize **44**.<sup>19</sup> The thin layer chromatographic (TLC) properties of the product of enzymatic reduction of **42** are compared with that of the product, obtained by the chemical synthesis. The blue fluorescent product showed similar migration with different solvent systems on TLC, suggesting two different reactions produce the same chemical product. Hence, we separated the suspected product from the chemical synthesis by preparative TLC and carried out full spectroscopic characterization (see materials and methods). The molecular formula obtained from a high-resolution mass

spectrometric analysis of product, formed by alkaline glucose reduction of **42**, matches with structures **44** or **46**. Presence of 18 different  $^{13}\text{C}$  resonances suggested that the dimer is not symmetric, but rather contains a complex asymmetric structure. The  $^1\text{H}$  NMR analysis showed ten hydrogen resonances; aryl-aryl bridge between two quinoline molecules might be present in the structure. The 5 proton of **46** was expected to be downfielded to  $\geq 9.3$  ppm due to its proximity to the *N*-oxide oxygen (We used a quinolone based numbering system in the section).<sup>20</sup> In the product, a resonance at 9.3 ppm is absent. The fluorescence of enzymatic metabolite and NMR properties are supportive of **44** as the possible structure for the metabolite. Moreover, COSY and TOCSY spectra analysis allowed assigning resonances for 4 and 4' protons for structure **44**. NOE experiment results showed a correlation between 4 and 4' protons that arises due to close proximity between two protons. The NOE correlation between 4 and 4' can be only present in **44**. In **46**, the protons 4 and 4' are unable to produce NOE resonance. Ultimately, the actual structure obtained from alkaline glucose reduction of **42** shows the distance between protons 4 and 4' is 2.5 Å (Figure 4).

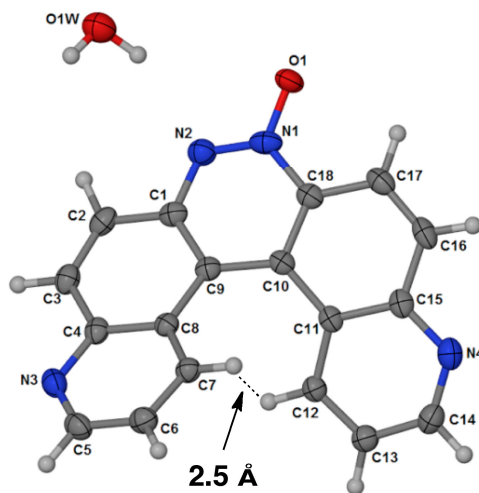
The NMR data obtained from the enzymatically synthesized **44** was compared with the NMRs of chemically synthesized **44**. The  $^1\text{H}$  NMR resonances and peak shifts obtained from the enzymatic reaction matched with that obtained from the glucose reduction. NOE spectrum of the enzymatic product shows a correlation between 4 and 4' protons, similar to the NOE result obtained from the glucose reduction. This observation confirms that product **44** is the metabolite produced in the anaerobic enzymatic reaction. The complete NMR analysis including TOCSY, COSY, HMQC, and HMBC data were consistent with the azoxy-helicene **44** (Table 1).

position	$\delta_C$	$\delta_H$ (J in Hz)	COSY	TOCSY	HMBC <sup>a</sup>	NOE
2'	153.4	9.15 1H, d (4.5)	3'	3', 4'	4', 8a'	3'
2	151.5	9.05 1H, m	3	3, 4	4, 8a	3
3'	120.5	7.46 1H, dd (9.0, 4.5)	2', 4'	2', 4'	4a'	2', 4'
3	120.7	7.41 1H, dd (9.0, 4.5)	2, 4	2, 4	4a	2, 4
4'	136.0	8.87 1H, d (9.0)	3'	3', 2'	2', 8a'	4
4	134.8	8.67 1H, d (9.0)	3	3, 2	2, 8a	4'
5'	128.0					
5	114.2					
4'a	123.4					
4a	123.5					
7'	121.8	9.05 1H, m	8'	8'	8a', 5'	8'
7	127.4	8.23 1H, d (9.0)	8	8	8a, 5	8
8'	133.4	8.43 1H, d (9.0)	7'	7'	6', 4a'	7'
8	134.3	8.41 1H, d (9.0)	7	7	6, 4a	7
6'	137.1					
6	144.1					
8'a	149.7					
8a	148.5					

**Table 1.** NMR Data (CDCl<sub>3</sub>) for compound **44**<sup>a</sup>HMBC correlations are from the proton to the stated carbon(s).



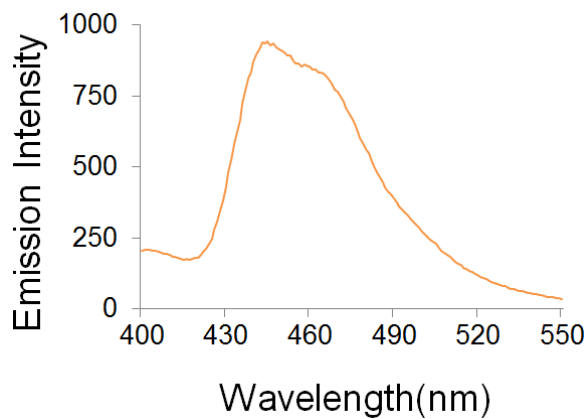
The ultimate confirmation of the structure **44** was carried out by X-ray crystallographic analysis (Figure 2.3).<sup>21</sup>



**Figure 2.3.** In **44**, the 4 and 4'-hydrogens (see numbering system in Scheme 2.2) are close in space<sup>11</sup>

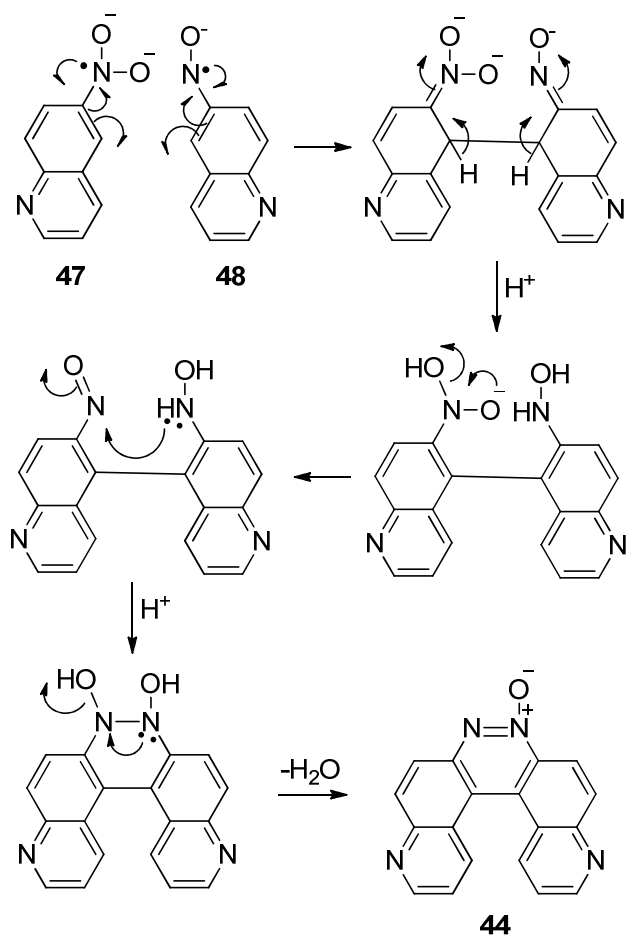
In summary, the spectroscopic and crystallographic characterization of **44** arising from the alkaline glucose reduction is consistent with Farrar's claim; **44** produced in the alkaline glucose reduction of **42**. More importantly **44**, produced by alkaline glucose method used as an authentic compound for comparison with the enzymatically produced **44**. LC/MS properties of **44**, produced under chemical and enzymatic methods showed matching retention times and  $m/z$  results (Figure 2.2). The  $^1\text{H}$  NMR analysis of the enzyme product resembles the authentic compound **44**, made by the glucose reduction reaction. In addition, NOE experiment clearly shows the close distance between 4 and 4' protons of enzymatically-generated **44**. The fluorescence spectrum of **44**, obtained from the glucose reduction (Figure 2.4) resembles the fluorescence spectrum obtained from the

enzymatic reaction (Figure 2B). Close analysis of the spectra shows the similarity of emission maxima at 440 and 460 nm of both curves (Figure 2.1 and 2.4).



**Figure 2.4.** Fluorescence spectrum of authentic **45** (50  $\mu$ M,  $\lambda_{\text{exc}}$  307 nm) in sodium phosphate buffer (12 mM, pH 7.4).

The azoxy functional group is known to be reduced to the corresponding azo group by NADPH:cytochrome P450 reductase.<sup>22</sup> In this particular reaction compound **45** is not reduced to an azo product.



**Scheme 2.4.** Mechanism for the formation of **44** under anaerobic conditions

## 2.5 Conclusion

In conclusion, intermediate hydroxylamino or amino product were not observed in NADPH:cytochrome P450 reductase mediated reduction of **42** under hypoxic conditions. The azoxy compound **45** and the bi aryl bonded dimer **44** were formed under reductive conditions. The mechanism for the formation of **44** in the enzymatic reaction is

complex. A possible pathway can be initiated when a nitroaryl radical **47** and a nitrosoaryl radical **48** are condensed to form a bi aryl bond to connect two quinolone groups and then tautomerization occurs toward an intramolecular condensation between hydroxylamine and nitroso moieties to produce **44** (Scheme 5).

Nitro aryl compounds are good candidates to selectively label hypoxic cells using fluorescence under bio-reductive conditions.<sup>8a, 23</sup> Many probes have been synthesized but the products resulting from the bioreduction have not been characterized.<sup>7a, 23a, 24</sup> Our work underlines the importance of characterization of complex metabolites that can arise in these reduction reactions of nitro-aromatic probes.

## 2.6 Experimental

**Materials and methods.** Materials were purchased from following sources: NADPH, cytochrome p450 reductase, sodium phosphate, DMF, glucose, Raney nickel slurry in water, silica gel (0.04-0.063 mm pore size) for column chromatography, and silica gel plates for thin layer chromatography from Sigma chemical company (St. Louis, MO); 6-nitroquinoline, 6-aminoquinoline, and hydrazine hydrate from Alfa-Aesar (Ward Hill, MA); ethyl acetate, hexane, dichloromethane, methanol, ethanol, HPLC acetonitrile and HPLC water from Fischer; Deuterated NMR solvents were from Cambridge Isotope Laboratories (Andover, MA). The compound 1,2,4-benzotriazine-1,4-di-N-oxide was synthesized according literature methods.<sup>1</sup> High resolution mass spectrometry (HRMS) analyses were performed at the mass spectroscopy facility of the University of Illinois Champaign-Urbana and low resolution mass spectroscopic analyses were carried out at

the University of Missouri-Columbia.  $^1\text{H}$  and  $^{13}\text{C}$  NMR experiments and were done on a Bruker Avance DRX300 with 5 mm broadband probe and Bruker Avance DRX500 with CPTCI probe using deuterated NMR solvents methanol ( $\text{CD}_3\text{OD}$ ) and chloroform( $\text{CDCl}_3$ ) at the University of Missouri-Columbia. The reference peaks were set to 3.31 ppm and 49.00 ppm for deuterated methanol and 7.26 ppm and 77.00 ppm for deuterated chloroform from tetramethylsilane for the  $^1\text{H}$  and  $^{13}\text{C}$  spectra respectively. The fluorescence spectra were obtained on a Varian Cary Eclipse Fluorescence Spectrophotometer equipped with xenon flash lamp with instrumental slit width settings at 10 nm employing a 10 mm path length quartz cuvette.

#### **Procedure for hypoxic metabolism.**

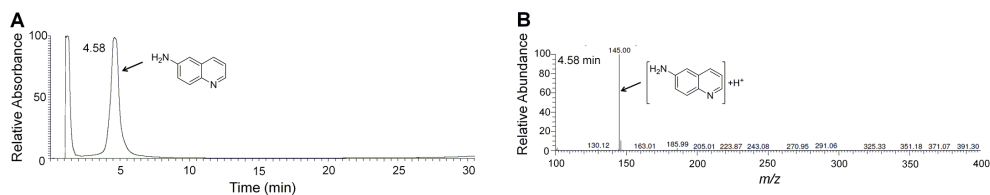
In a typical enzymatic reaction, **42** ( 4  $\mu\text{L}$  from 50 mM in DMF, final concentration 0.8 mM) or non-fluorescent electron acceptor (24  $\mu\text{L}$  from 50 mM in 15 % DMF water, final concentration 6.4 mM), was mixed with NADPH (20-160  $\mu\text{L}$  of 10 mM, final concentration 0.8 mM-6.4 mM), cytochrome p450 reductase (2  $\mu\text{L}$  from 140 U/mL, final concentration 1.1 U/mL), sodium phosphate buffer (6  $\mu\text{L}$  from 50 mM, final concentration 12 mM, pH 7.4) and HPLC water to obtain the final solution (0.25mL, less than 2% DMF) at room temperature ( $24^\circ\text{C}$ ). For anaerobic reactions, all reagents except NADPH and cytochrome p450 reductase were de-gassed in glass tubes by three freeze pump thaw cycles. The glass tubes were broke open inside an argon purged glove bag and bubbled with argon for five minutes. Solid NADPH was dissolved in HPLC water to make stock solution inside the glove bag and cytochrome p450 reductase was used as is from the original sample from the supplier. Upon mixing, the containers were wrapped with aluminum foil to prevent exposure to light.

### **Procedure for Fluorescence experiment**

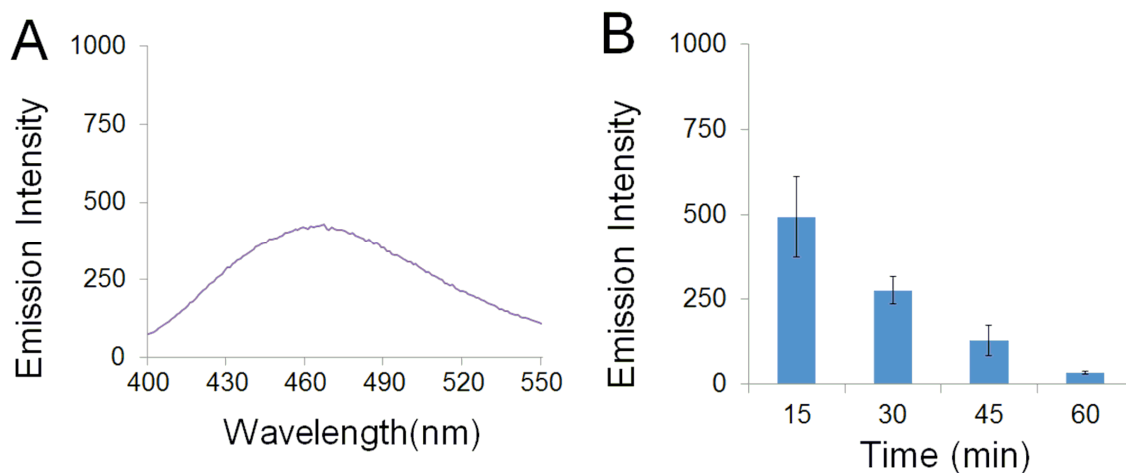
Upon completion of incubation reaction solution was diluted up to 1 mL with sodium phosphate buffer (50 mM, pH 7.4) in HPLC water, and then was added to the cuvette. In anaerobic experiments, upon completion the reaction mixtures were taken out of glove bag and kept 1 h under atmospheric conditions prior to the dilutions.

### **Procedure for LC/MS analysis.**

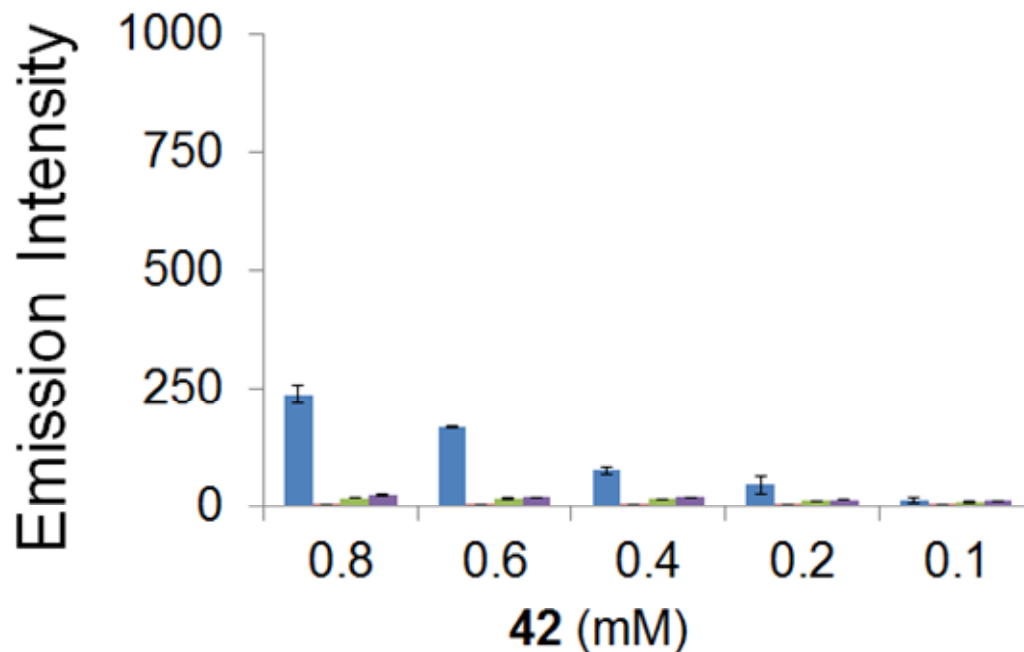
In vitro enzymatic metabolism of **42** was carried out as described above, and the resulting products were extracted into ethyl acetate and dried using brine followed by roto vap evaporation of ethyl acetate. The solid was re-dissolved in methanol and analyzed by LC/MS in the positive ion mode. Separation of metabolites was carried using a C18 reverse phase Phenomenex Luna column (5  $\mu$ m particle size, 100 Å pore size, 150 mm length, 2.00 mm i.d.) and a ThermoSeparations liquid chromatograph (TSP4000), the metabolites were detected by their UV-absorbance at 254 nm. The elution started with a gradient of A, 99% HPLC water (0.1% acetic acid) and B acetonitrile (0.1% acetic acid) followed by a linear increase to 90 % B over the course of 30 min. The elution was continued at 90% B for 3 min and decreased to 1% over the next 8 min. A flow rate of 0.35 mL/min was used. The LC/ESI-MS analyses were carried out in the positive ion mode on a Finnigan TSQ 7000 triple quadrupole instrument using a 250 kV needle voltage and at a capillary temperature of 250 °C.



**Figure S1.** LC/MS analysis of **43**. (A) UV chromatogram of **43**, (B) LC/MS analysis of the product eluting at 4.6 min in the chromatogram.



**Figure S2.** (A) Fluorescence spectrum of NADPH (50  $\mu$ M,  $\lambda_{ex}$  307 nm, in sodium phosphate buffer, 10 mM, pH 7.4). It is noteworthy that the shape of the fluorescence emission peaks of NADPH and **44** are distinct. (B) NADPH fluorescence diminishes over the course of 1 h when the reactions are exposed to aerobic conditions. Reactions contained **42** (0.8 mM), NADPH:cytochrome P450 reductase (1.1 U/mL), and NADPH (3 mM) in sodium phosphate buffer, 10 mM, pH 7.4 ( $\lambda_{ex}$  307 nm,  $\lambda_{em}$  460 nm). Reactions described here were incubated quenched with aerobic buffer and incubated for approximately 1 h before fluorescence analysis. Thus, the control experiment provides evidence that fluorescence detected in the metabolism of **42** is not due to residual NADPH.



**Figure S3.** Fluorescence emission at 445 nm ( $\lambda_{ex}$  307 nm) for reactions: compound **42** (0.1-0.8 mM) + NADPH:cytochrome P450 reductase (1.1 U/mL), NADPH (0.1-0.8 mM) under anaerobic (blue) and aerobic (red), and a non-fluorescent electron acceptor 1-methyl-2-nitro-5-carbethoxyimidazole (0.1-0.8 mM) + NADPH:cytochrome P450 reductase (1.1 U/mL), NADPH (0.1-0.8 mM) under anaerobic (green) and aerobic (purple). Reactions were incubated for 18 h in sodium phosphate buffer at (12 mM, pH 7.4) at 24 °C, then diluted with aerobic sodium phosphate buffer (12 mM, pH 7.4) and the fluorescence measured ( $\lambda_{ex}$  307 nm,  $\lambda_{em}$  445 nm). It is important to note that NADPH exhibits fluorescence with an emission maximum at 445 nm. However, control experiments showed that any NADPH left unconsumed at the end of the anaerobic reactions described here is ultimately converted to the non-fluorescent NADP<sup>+</sup> product by enzyme-driven redox cycling of the electron accepting organic substrate upon opening the reaction vessel to air and dilution with aerobic buffer prior to fluorescence measurements.



**Synthesis of 1,2-di(quinolin-6-yl)diazene oxide (45).** We employed a variation on the literature procedure of Boge *et al.*<sup>2</sup> To a solution of compound **42** (0.5 g, 2.87 mmol) in a mixture of EtOH:CH<sub>2</sub>Cl<sub>2</sub> (1:1, 20 mL) at 0 °C in an ice/salt bath was added Raney nickel slurry (0.5 mL, active catalyst in water, Sigma-Aldrich cat. number 221678). To this mixture, hydrazine hydrate (1.5 mL, 30 mmol) portions were added over the course of 3 h with stirring until **42** was consumed (TLC) and the resulting mixture stirred overnight. The solid was removed by filtration and the resulting solution dried by extraction with brine and then over sodium sulfate. The compound was purified by column chromatography on silica gel eluted with ethyl acetate in the first column separation and second column chromatography separation on silica gel was done with MeOH:CH<sub>2</sub>Cl<sub>2</sub> (99:1) to obtain **45**, a yellow solid, in pure form (100 mg, R<sub>f</sub> value = 0.25 in 4% MeOH in CH<sub>2</sub>Cl<sub>2</sub>) <sup>1</sup>H NMR (CDCl<sub>3</sub>, 300 MHz): δ ppm 9.14 (d, J = 2.5 Hz, 1H), δ 9.00 (dd, J = 4.5 Hz, J = 1.5 Hz, 1H), δ 8.93 (dd, J = 4.5 Hz, J = 1.5 Hz, 1H), δ 8.82 (d, J = 2.5 Hz, 1H), δ 8.67 (d, J = 9.0 Hz, 1H), δ 8.31 (dd, J = 9.0 Hz, J = 1.5 Hz, 1H), δ 8.21 (m, 4H), δ 7.49 (dd, J = 8.5 Hz, J = 4.5 Hz, 1H), 7.42 (dd, J = 8.5 Hz, J = 4.5 Hz, 1H), 1.23 grease. <sup>13</sup>C NMR (CDCl<sub>3</sub>, 75.5 MHz): δ 152.86, 151.97, 149.64, 148.72, 146.01, 141.93, 137.88, 137.76, 130.95, 130.32, 129.32, 128.46, 127.73, 123.76, 123.40, 122.68, 122.64, 122.09; HRMS (ESI, [M+H]<sup>+</sup>) m/z calcd for C<sub>18</sub>H<sub>13</sub>N<sub>4</sub>O 301.1089, found 301.1080. <sup>2</sup>Boge, N.; Kruger, S.; Schroder, M.; Meier, C.; *Synthesis* **2007**, *24*, 3907-3914.

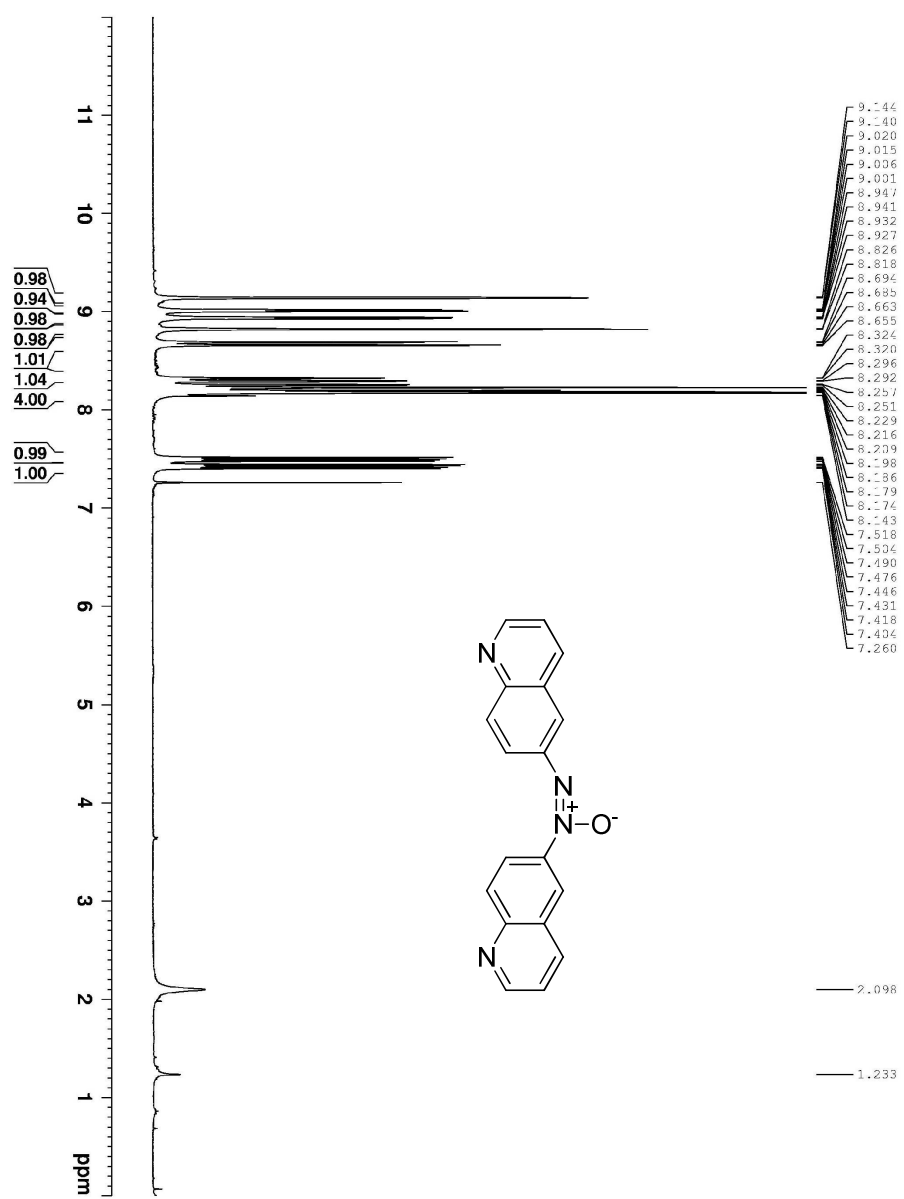


Figure S3.  $^1\text{H}$  NMR of **45** ( $\text{CDCl}_3$ , 300 MHz)

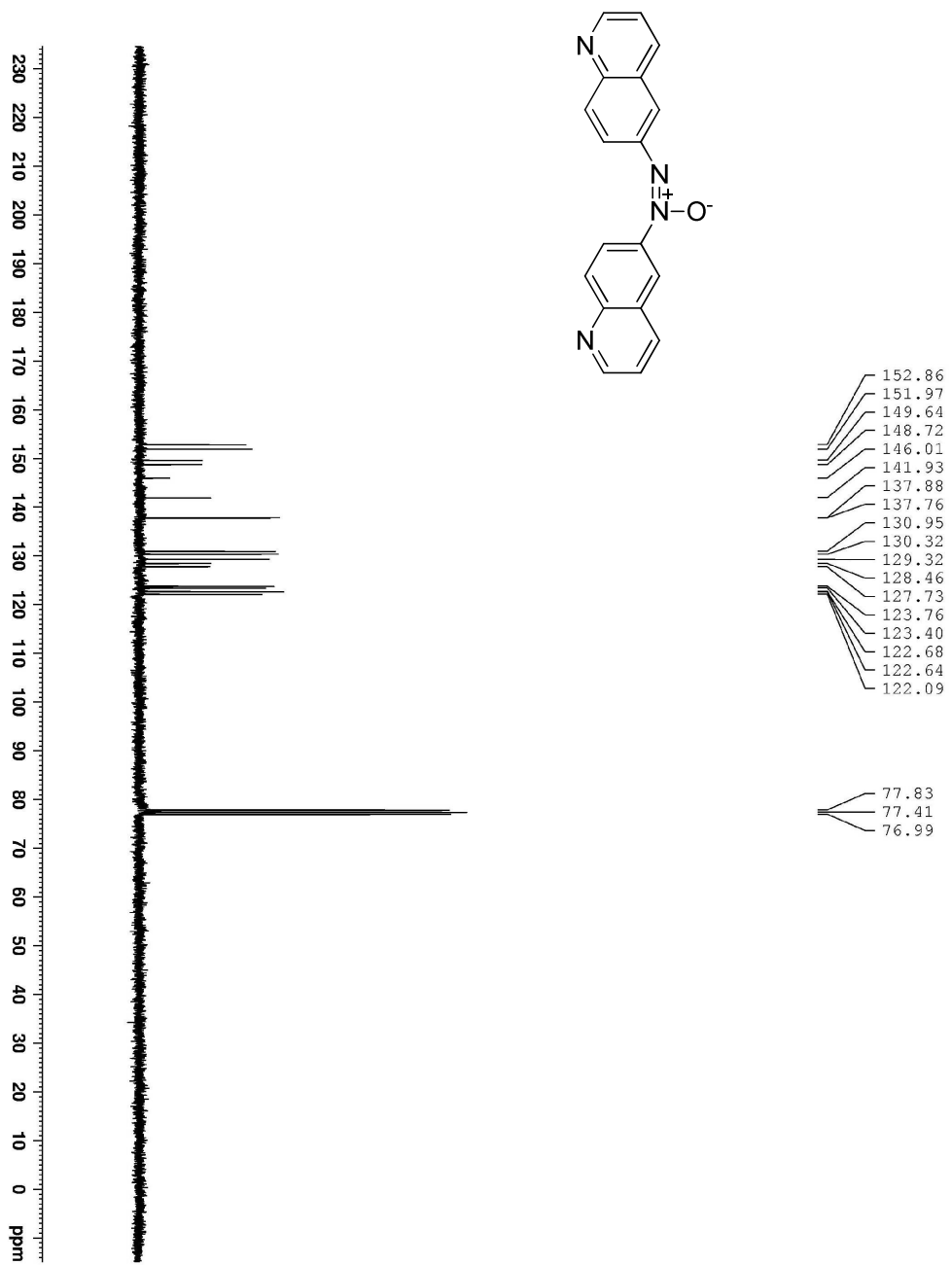


Figure S4.  $^{13}\text{C}$  NMR of 45 ( $\text{CDCl}_3$ , 75.5 MHz)

**Preparation of pyrido[3,2-*f*]quinolino[6,5-*c*]cinnoline 3-oxide (44) via alkaline glucose reduction of 42.**<sup>3</sup> A solution of **42** (1.0 g, 5.61 mmol) in NaOH (20% aqueous solution, 10 mL) and was heated to 90 °C with stirring. To this solution, D-(+) glucose (1.3 g, 7.21 mmol) was added over 30 min and stirred for 1 h. The mixture was extracted with EtOAc (20 mL) and the combined organic extracts washed with brine and dried over magnesium sulfate. The mixture separated by column chromatography on silica gel and eluted with ethyl acetate and MeOH (99:1) to obtain the helicene **44**, a yellow solid (300 mg, 18% yield). <sup>1</sup>H NMR (CDCl<sub>3</sub>, 500 MHz,): δ 9.15 (d, J = 4.5 Hz, 1H), 9.05 (m, 2H), 8.87 (d, J = 9.0 Hz, 1H), 8.67 (d, J = 9.0 Hz, 1H), 8.44 (d, J = 9.0 Hz, 1H), 8.40 (d, J = 9.0 Hz, 1H), 8.23 (d, J = 9.0 Hz, 1H), 7.46 (dd, J = 9.0 Hz, J = 4.5 Hz, 1H), 7.41 (dd, J = 9.0 Hz, J = 4.5 Hz, 1H). <sup>13</sup>C-NMR (CDCl<sub>3</sub>, 125.8 MHz,): δ 153.35, 151.47, 149.71, 148.53, 144.08, 137.09, 136.02, 134.79, 134.28, 133.41, 128.00, 127.45, 123.52, 123.34, 121.75, 120.56, 120.46, 114.21; HRMS (ESI, [M+H]<sup>+</sup>) *m/z* calcd C<sub>18</sub>H<sub>11</sub>N<sub>4</sub>O calculated mass 299.0933; actual mass 299.0934 Crystals for X-ray analysis were obtained by dissolving the pure compound in minimum amount of warm MeOH, followed by slow evaporation (3 d) in a 2 mL vial.

<sup>3</sup>Galbraith, H. W.; Degering, E. F.; Hitch, E. F. *J. Am. Chem. Soc.* **1951**, 73:1323

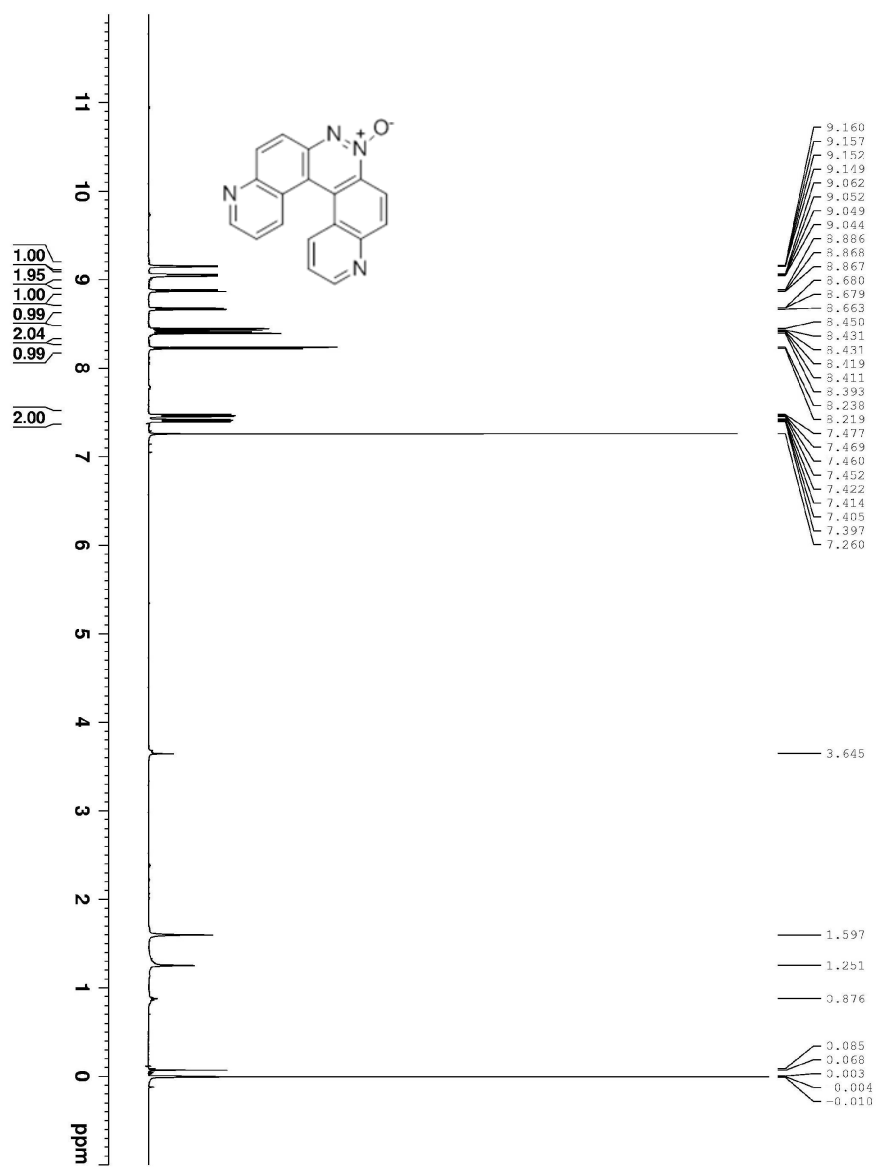


Figure S5.  $^1\text{H}$  NMR of **44** ( $\text{CDCl}_3$ , 500 MHz)

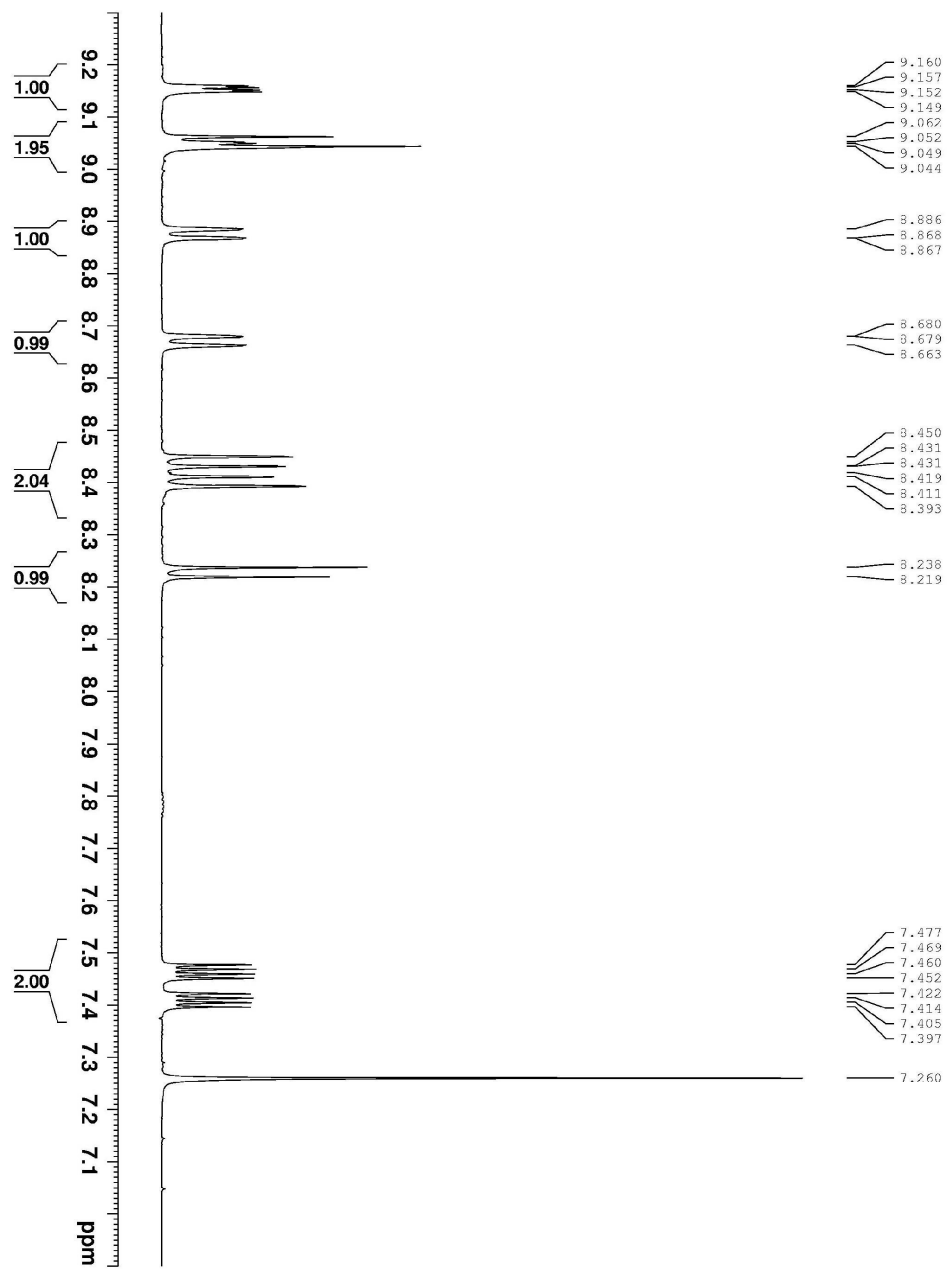


Figure S6. <sup>1</sup>H NMR of **44** aromatic region (CDCl<sub>3</sub>, 500 MHz)

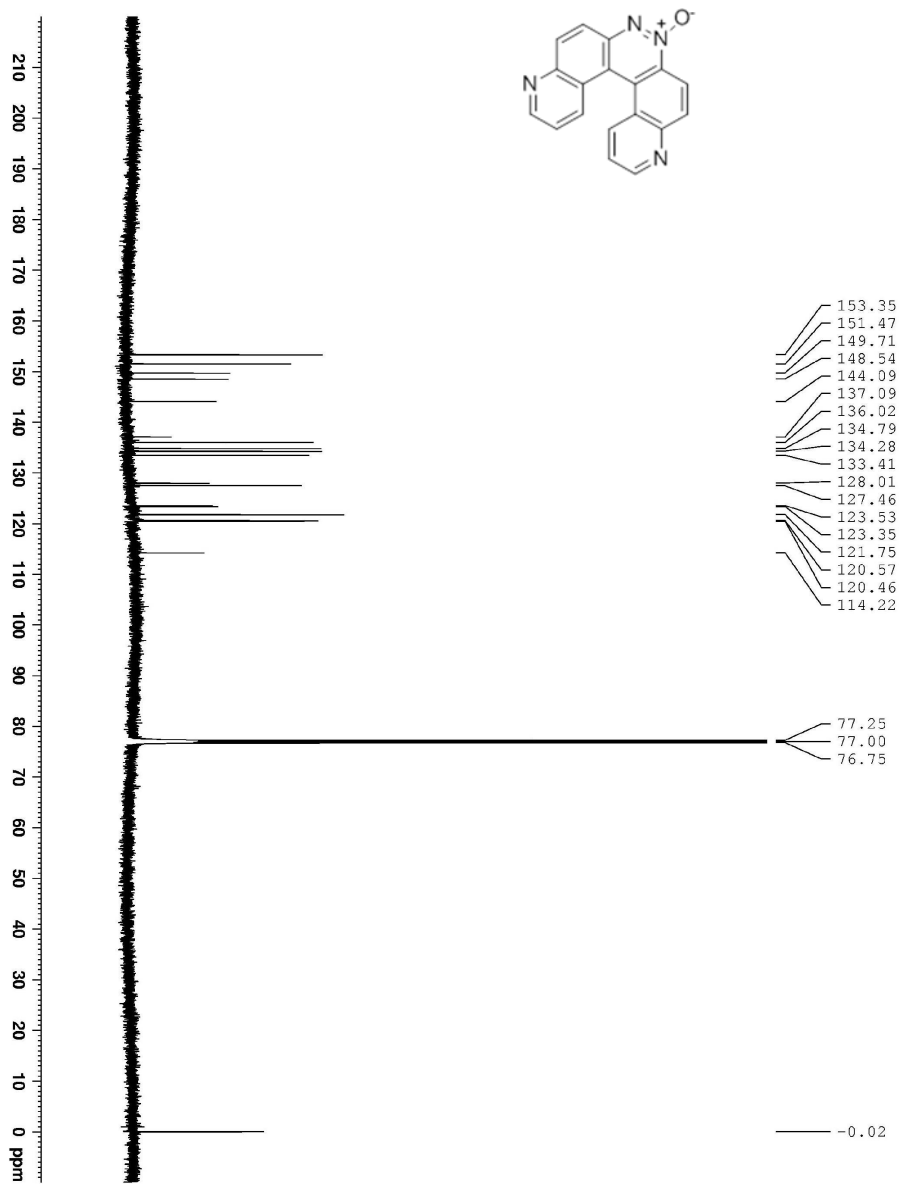
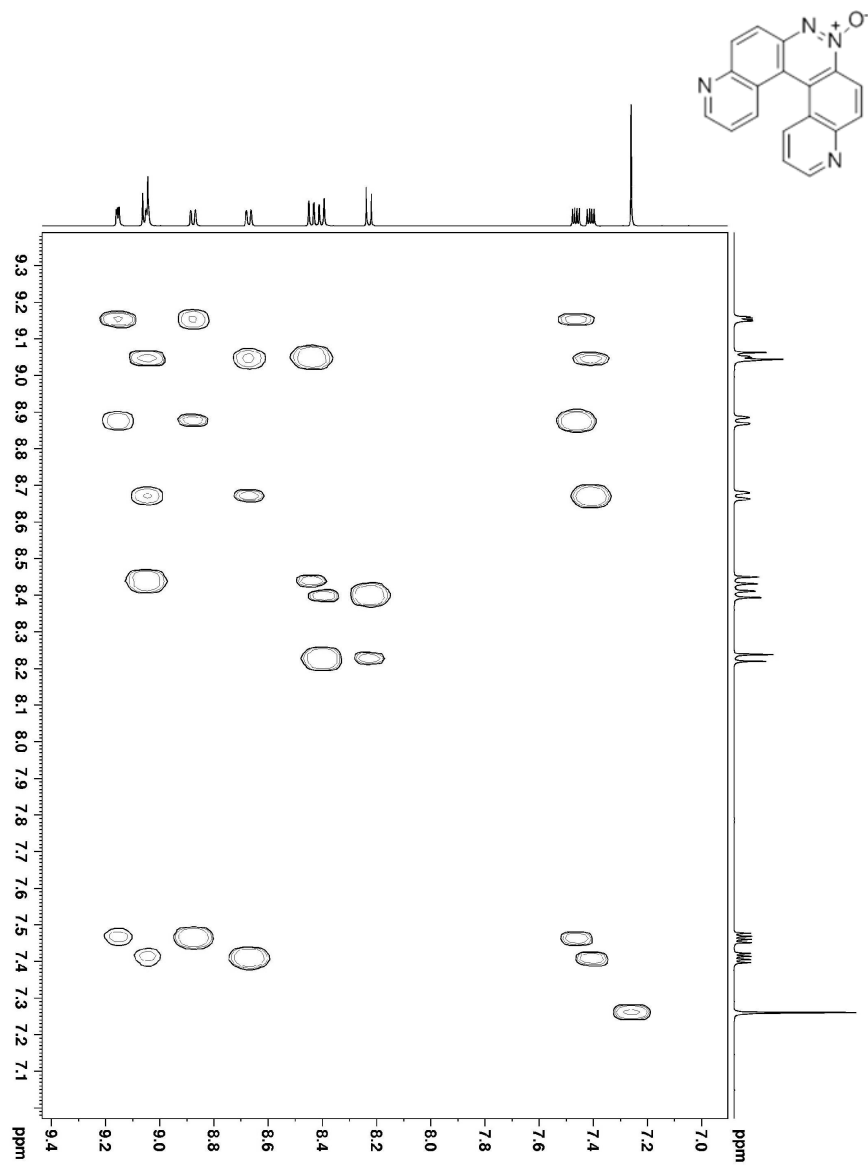
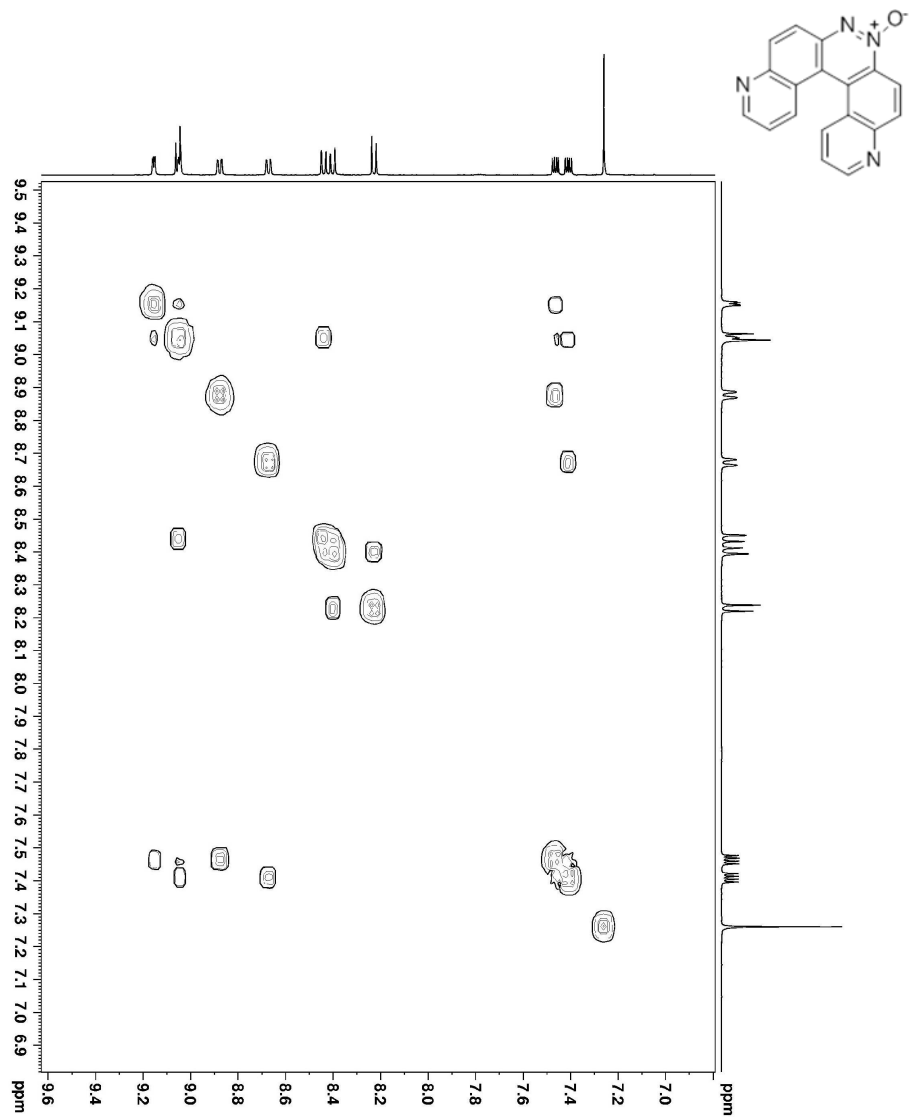


Figure S6.  $^{13}\text{C}$  NMR of **44** (CDCl<sub>3</sub>, 125.77 MHz)

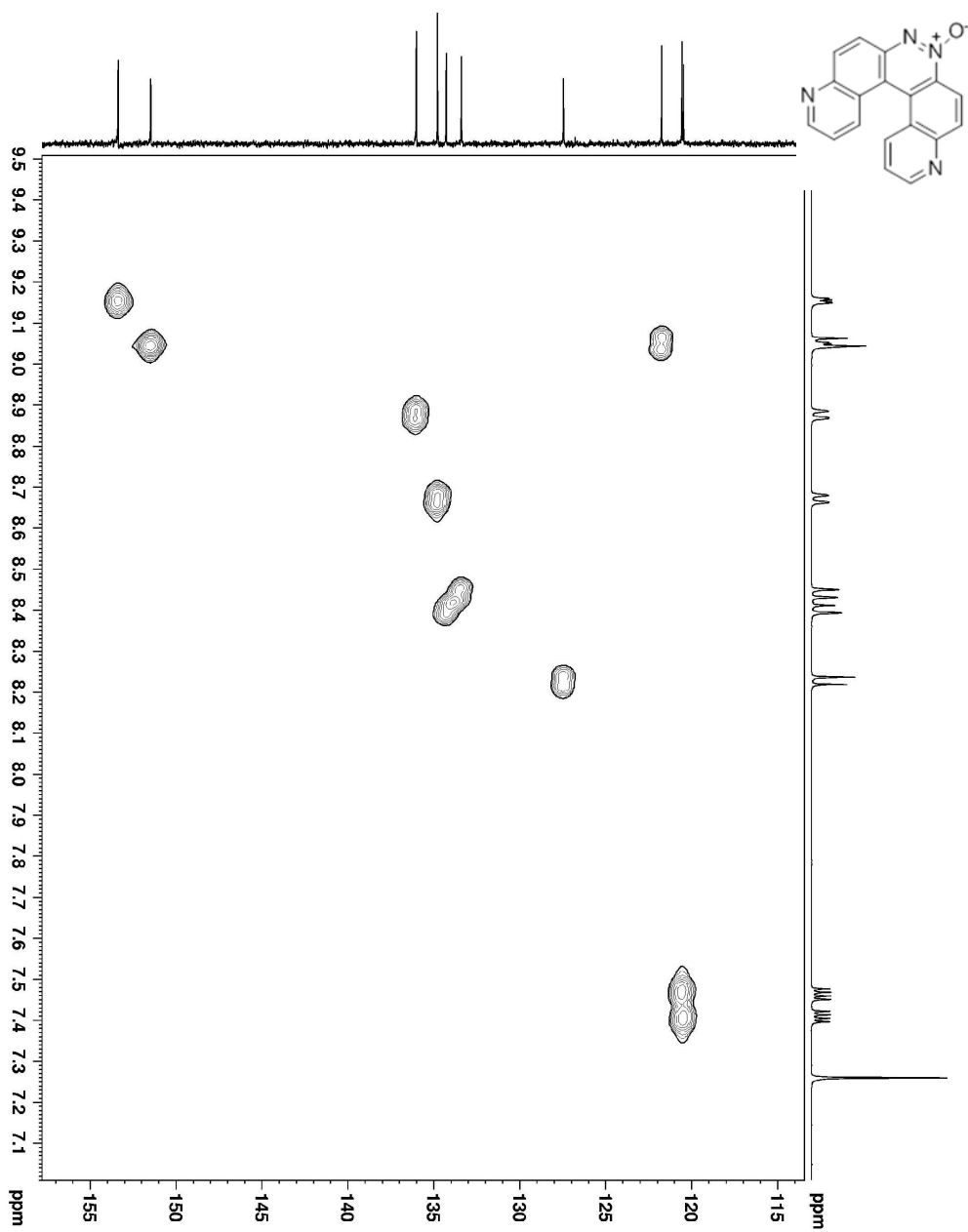


**Figure S7.**  $^1\text{H}$ - $^1\text{H}$  TOCSY of **44** ( $\text{CDCl}_3$ , 500 MHz)

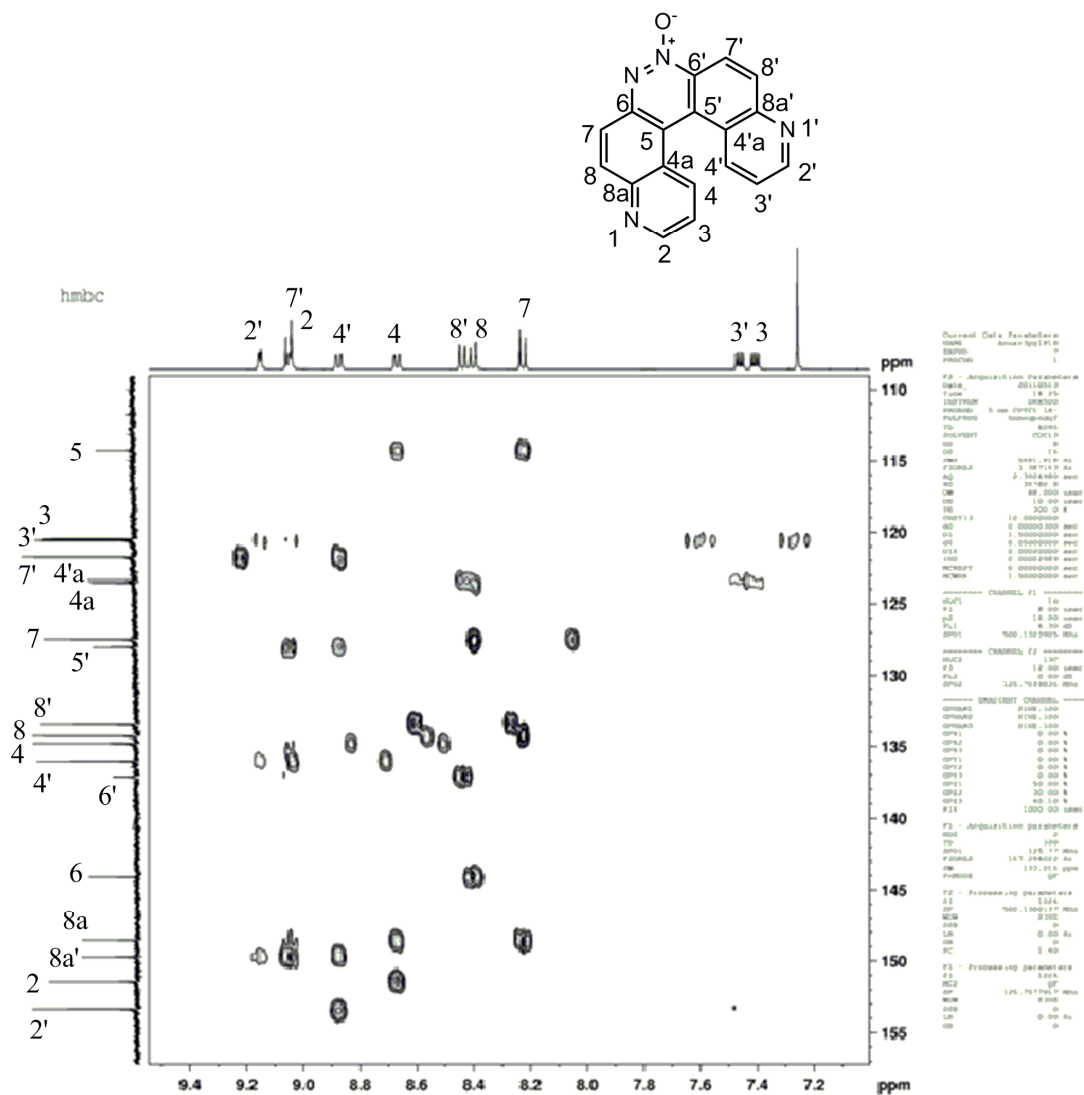




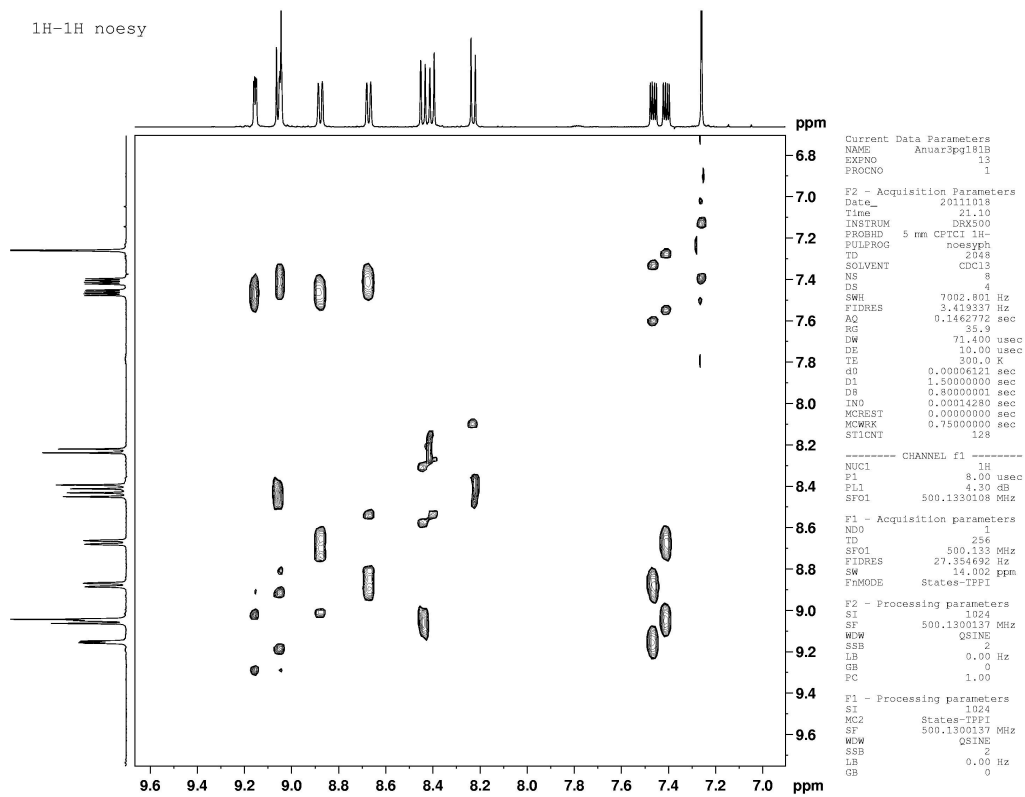
**Figure S8.**  $^1\text{H}$ - $^1\text{H}$  COSY of **44** ( $\text{CDCl}_3$ , 500 MHz)



**Figure S9.**  $^1\text{H}$ - $^{13}\text{C}$  HMQC of **44** ( $\text{CDCl}_3$ , 500 and 125.77 MHz):



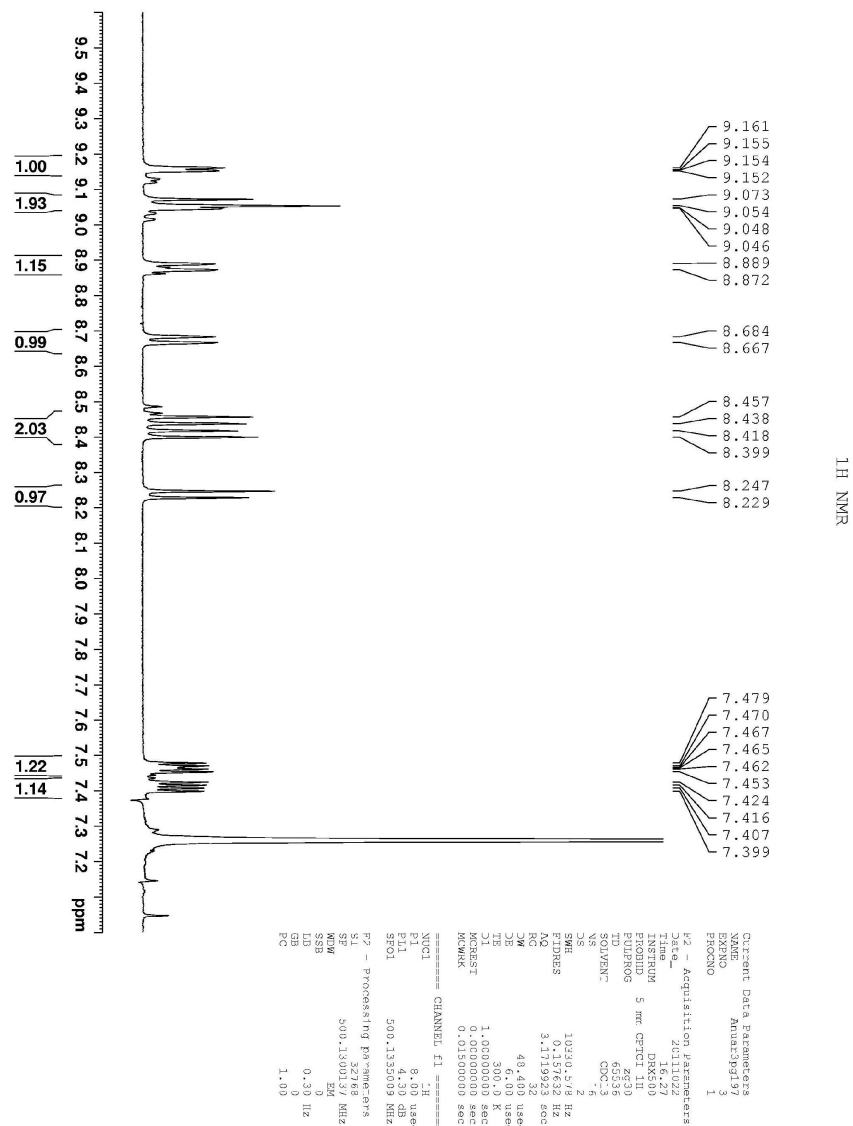
**Figure S10.**  $^1\text{H}$ - $^{13}\text{C}$  HMBC of **44** ( $\text{CDCl}_3$ , 500 and 125.77 MHz):



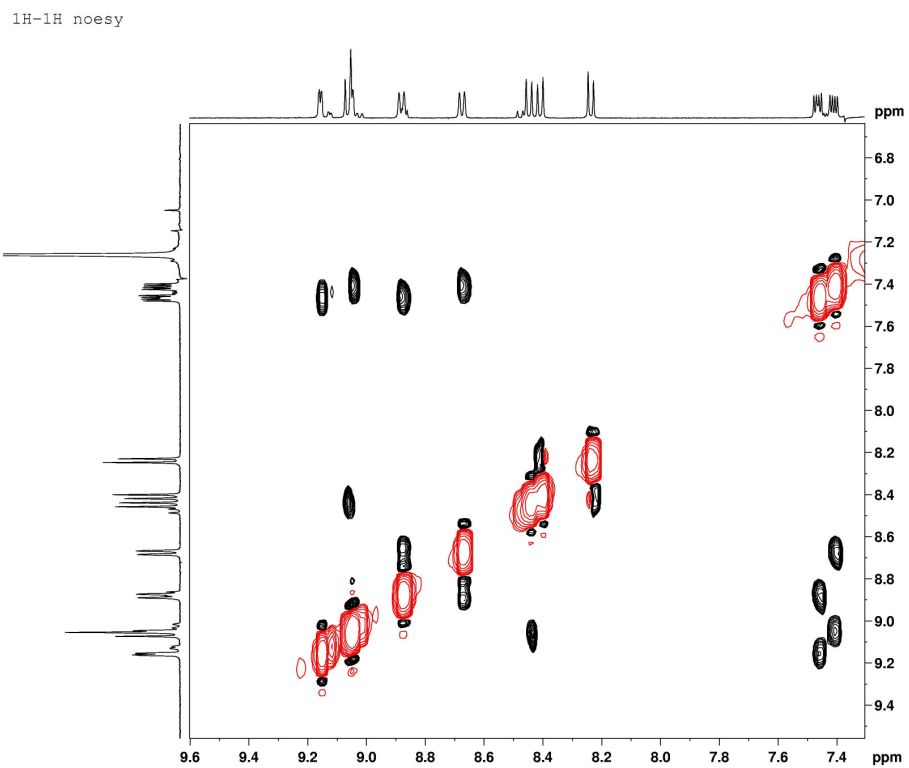
**Figure S11.**  $^1\text{H}$ - $^1\text{H}$  NOESY of **44** ( $\text{CDCl}_3$ , 500 MHz):

**Enzymatic generation of pyrido[3,2-*f*]quinolino[6,5-*c*]cinnoline 3-oxide (44)**

Compound **42** (50 mM, in 0.2 mL DMF) was mixed with sodium phosphate buffer (0.3 mL, 10 mM, pH 7.4) and water (12.0 mL) in an argon-purged glove bag and the solution purged with argon (20 min). To this mixture was added NADPH (25 mg, 0.033 mmol) and NADPH:cytochrome P450 reductase (0.03 mL of a 0.35 U/mL solution). The resulting mixture was stirred inside the argon-filled glove bag for 18 h. The reaction was then extracted with ethyl acetate (20 mL), the combined organic extract washed with brine and dried with magnesium sulfate. Column chromatography on silica gel eluted with ethyl acetate and MeOH (99:1), followed by preparative TLC eluted with ethyl acetate and MeOH (99:1) gave **4** (five reactions combined to yield 0.300 mg, 2% yield). The <sup>1</sup>H-NMR and LC/MS properties of this material matched that of authentic **44** prepared as described above.



**Figure S12.**  $^1\text{H}$  NMR of **44** ( $\text{CDCl}_3$ , 500 MHz), obtained from NADPH and NADPH:cytochrome P450 reductase mediated synthesis



**Figure S13.**  $^1\text{H}$ - $^1\text{H}$  NOESY of **44** ( $\text{CDCl}_3$ , 500 MHz), obtained from NADPH and NADPH:cytochrome P450 reductase mediated synthesis

## References for chapter 2

1. (a) Cejudo-Martin, P.; Johnson, R. S., A new notch in the HIF belt: how hypoxia impacts differentiation. *Cell* **2005**, *9*, 575-576; (b) Parmar, K.; Mauch, P.; Vergillo, J.; Sackstein, R.; Down, J. D., Distribution of hematopoietic stem cells in the bone marrow according to regional hypoxia. *Proc. Nat. Acad. Sci. USA* **2007**, *104*, 5431-5
2. Simon, M. C.; Keith, B., The role of oxygen availability in embryonic development and stem cell function. *Nat. Rev. Mol. Cell Biol.* **2008**, *9*, 285-296.
3. Brown, J. M., The hypoxic cell: a target for selective cancer therapy-eighteenth Bruce F. Cain memorial award lecture. *Cancer Res.* **1999**, *59* (Copyright (C) 2012 American Chemical Society (ACS). All Rights Reserved.), 5863-5870.
4. Harris, A. L., Hypoxia - a key regulatory factor in tumour growth. *Nat. Rev. Cancer* **2002**, *2*, 38-47.
5. (a) Evans, S. M.; Kachur, A. V.; Shiue, C.-Y.; Hustinx, R.; Jenkins, W. T.; Shive, G. G.; Karp, J. S.; Alavi, A.; Lord, E. M.; Dolbier, W. R.; Koch, C. J., Noninvasive detection of tumor hypoxia using the 2-nitroimidazole [18F]EF1. *J. Nucl. Med.* **2000**, *41*, 327-336; (b) Koch, C. J., Measurements of absolute oxygen levels in cells and tissues using oxygen sensors and 2-nitroimidazole EF5. *Methods Enzymol.* **2002**, *352*, 3-31.
6. Nordmark, M.; Loncaster, J.; Aquino-Parsons, C.; Chou, S.-C.; Ladekarl, M.; Havsteen, H.; Lindegaard, J. C.; Davidson, S. E.; Varia, M.; West, C.; Hunter, R.; Overgaard, J.; Raleigh, J. A., Measurements of hypoxia using pimonidazole and polarographic oxygen-sensitive electrodes in human cervix carcinomas. *Radiother. Oncol.* **2003**, *67*, 35-44.
7. (a) Dai, M.; Zhu, W.; Xu, Y.; Qian, X.; Liu, Y.; Xiao, Y.; You, Y., Versatile nitro-fluorophore as highly effective sensor for hypoxic tumor cells: design, imaging, and evaluation. *J. Fluoresc.* **2008**, *18* (2), 591-597; (b) Stratford, M. R. L.; Clarke, E. D.; Hodgkiss, R. J.; Middleton, R. W.; Wardman, P., Nitroaryl compounds as potential fluorescent probes for hypoxia. II. Identification and properties of reductive metabolites. *Int. J. Radiat. Oncol. Biol. Phys.* **1984**, *10*, 1353-1356.



8. (a) Wardman, P.; Clarke, E. D.; Hodgkiss, R. J.; Middleton, R. W.; Parrick, J.; Stratford, M. R. L., Nitroaryl compounds as potential fluorescent probes for hypoxia. I. Chemical criteria and constraints. *Int. J. Radiat. Oncol. Biol. Phys.* **1984**, *10*, 1347-1351; (b) Zhu, W.; Dai, M.; Xu, Y.; Qian, X., Novel nitroheterocyclic hypoxic markers for solid tumor: synthesis and biological evaluation. *Bioorg. Med. Chem. Lett.* **2008**, *16*, 3255-3260.
9. (a) Wardman, P.; Dennis, M. F.; Everett, S. A.; Patel, K. B.; Stratford, M. R. L.; Tracy, M., Radicals from one-electron reduction of nitro compounds, aromatic N-oxides and quinones: the kinetic basis for hypoxia-selective, bioreductive drugs. *Biochem. Soc. Trans* **1995**, *61*, 171-194; (b) Fitzsimmons, S. A.; Workman, P. A.; Grever, M.; Paull, K.; Camalier, R.; Lewis, A. D., Reductase enzyme expression across the National Cancer Institute tumor cell line panel: correlation with sensitivity to mitomycin C and E09. *J. Natl. Cancer Inst.* **1996**, *88*, 259-269; (c) Rooseboom, M.; Commandeur, J. N. M.; Vermeulen, N. P. E., Enzyme-catalyzed activation of anticancer prodrugs. *Pharm. Rev.* **2004**, *56*, 53-102; (d) Wilson, W. R.; Anderson, R. F.; Denny, W. A., Hypoxia-selective antitumor agents. 1. Relationships between structure, redox properties and hypoxia-selective cytotoxicity for 4-substituted derivatives of nitracrine. *J. Med. Chem.* **1989**, *32*, 23-30; (e) Denny, W. A.; Wilson, W. R., Considerations for the design of nitrophenyl mustards as agents with selective toxicity for hypoxic tumor cells. *J. Med. Chem.* **1986**, *29* (6), 879-887.
10. Chen, Y.; Hu, L., Design of anticancer prodrugs for reductive activation. *Med. Res. Rev.* **2009**, *29* (1), 29-64.
11. Rajapakse, A.; Gates, K. S., Hypoxia-Selective, Enzymatic Conversion of 6-Nitroquinoline into a Fluorescent Helicene: Pyrido[3,2-f]quinolino[6,5-c]cinnoline 3-Oxide. *J. Org. Chem.* **2012**, *77*, 3531-3537.
12. (a) Danieli, E.; Shabat, D., Molecular probe for enzymatic activity with dual output. *Bioorg. Med. Chem.* **2007**, *15*, 7318-7324; (b) Tanaka, F.; Thayumanavan, R.; Barbas, C. F., Fluorescent detection of carbon-carbon bond formation. *J. Am. Chem. Soc.* **2003**, *125*, 8523-8528; (c) Brynes, P. J.; Bevilacqua, P.; Green, A., 6-Aminoquinoline as a fluorogenic leaving group in peptide cleavage reactions: a new fluorogenic substrate for chymotrypsin. *Anal. Biochem.* **1981**, *116*, 408-413; (d) Huang, W.; Hicks, S. N.; Sondek, J.; Zhang, Q., A fluorogenic, small molecule reporter for mammalian phospholipase C isozymes. *ACS Chem Biol.* **2011**, *6* (3), 223-228.
13. (a) Smith, G. C. M.; Tew, D. G.; Wolf, C. R., Dissection of NADPH-cytochrome P450 oxidoreductase into distinct

functional domains. *Proc. Nat. Acad. Sci. USA* **1994**, *91* (Aug), 8710-8714; (b) Walton, M. I.; Wolf, C. R.; Workman, P., Molecular enzymology of the reductive bioactivation of hypoxic cell cytotoxins. *Int. J. Radiat. Oncol. Biol. Phys.* **1989**, *16*, 983-986; (c) Wen, B.; Coe, K. J.; Rademacher, P.; Fitch, W. L.; Monshouwer, M.; Nelson, S. D., Comparison of in vitro bioactivation of flutamide and its cyano analogue: evidence for reductive activation by human NADPH:cytochrome P450 reductase. *Chem. Res. Toxicol.* **2008**, *21* (12), 2393-2406; (d) Solano, B.; Junnotula, V.; Marin, A.; Villar, R.; Burguete, A.; Vicente, E.; Perez-Silanes, S.; Monge, A.; Dutta, S.; Sarkar, U.; Gates, K. S., Synthesis and biological evaluation of new 2-arylcarbonyl-3-trifluoromethylquinoxaline 1,4-dioxide derivatives and their reduced analogues. *J. Med. Chem.* **2007**, *50* (22), 5485-5492.

14. (a) Pizzolatti, M. G.; Yunes, R. A., Azoxybenzene formation from nitrosobenzene and phenylhydroxylamine. A unified view of the catalysis and mechanisms of the reactions. *J. Chem. Soc. Perkin 2* **1990**, 759-764; (b) Agrawal, A.; Tratnyek, P. G., Reduction of nitroaromatic compounds by zero-valent iron metal. *Env. Sci. Technol.* **1996**, *30* (1), 153-160.

15. (a) Fletcher, T. L.; Namkung, M. J., Derivatives of fluorene. IV. Raney nickel-hydrazine hydrate reduction of various mono- and dinitrofluorene derivatives; some new 9-substituted fluorenes. *J. Org. Chem.* **1958**, *23*, 680-683; (b) Furst, A.; Moore, R. E., Reductions with hydrazine hydrate catalyzed by Raney nickel. II. Aromatic nitro compounds to intermediate products. *J. Am. Chem. Soc.* **1957**, *79*, 5492-5493.

16. (a) Holt, P. F.; Went, C. W., Polycyclic cinnoline derivatives. Part XIII. The cyclisation of azo-compounds and the ultraviolet absorption of benzo[g]naphtho[1,2-c]cinnoline. *J. Chem. Soc.* **1963**, 4099-4102; (b) Morrison, D. J.; Trefz, T. K.; Piers, W. E.; McDonald, R.; Parvez, M., 7:8,9:10-Dibenzo-1,2,3,4-tetrafluorotriphenylene: synthesis, structure, and photophysical properties of a novel [5]helicene. *J. Org. Chem.* **2005**, *70*, 5309-5312.

17. Huisgen, R., Beiträge und deutungsversuche zur reaktionsweise aromatischer bicylen. *Liebigs Ann.* **1948**, *559* (2), 101-152.

18. Farrar, W. V., Polycyclic reduction products of 6-nitroquinoline. *J. Chem. Soc.* **1965**, 799-800.

19. Galbraith, H. W.; Degering, E. F.; Hitch, E. F., The reduction of aromatic nitro compounds with glucose. *J. Am. Chem. Soc.* **1951**, *73*, 1323-1324.

20. Silva, R. S. F.; de Amorim, M. B.; Pinto, M. d. C. F. R.; Emery, F. S.; Goulart, M. O. F.; Pinto, A. V., Chemoselective oxidation of benzophenazines by m-CPBA: N-oxidation vs. oxidative cleavage. *J. Braz. Chem. Soc.* **2007**, *18* (4), 759-764.
21. Rajapakse, A.; Barnes, C. L.; Gates, K. S., Synthesis and Crystal Structure of the Azoxydichinyl Helicene, Pyrido[3,2-f]quinolino[6,5-c]cinnoline 5-Oxide Monohydrate. *J. Chem. Crystallog.* **2011**,
22. (a) Fuchs, T.; Chowdhary, G.; Barnes, C. L.; Gates, K. S., 3-Amino-1,2,4-benzotriazine 4-Oxide: Characterization of a New Metabolite Arising From Bioreductive Processing of the Antitumor Agent 3-Amino-1,2,4-benzotriazine 1,4-Dioxide (Tirapazamine). *J. Org. Chem.* **2001**, *66*, 107-114; (b) Fitzsimmons, S. A.; Lewis, A. D.; Riley, R. J.; Workman, P., Reduction of 3-amino-1,2,4-benzotriazine-1,4,-di-N-oxide to a DNA-damaging species: a direct role for NADPH:cytochrome P450 oxidoreductase. *Carcinogenesis* **1994**, *15* (8), 1503-1510.
23. (a) Duan, J.-X.; Jiao, H.; Kaizerman, J.; Stanton, T.; Evans, J. W.; Lan, L.; Lorente, G.; Banica, M.; Jung, D.; Wang, J.; Ma, H.; Li, X.; Yang, Z.; Hoffman, R. M.; Ammons, W. S.; Hart, C. P.; Matteucci, M., Potent and highly selective hypoxia-activated achiral phosphoramidate mustards as anticancer drugs. *J. Med. Chem.* **2008**, *51*, 2412-2420; (b) Patterson, A. V.; Ferry, D. M.; Edmunds, S. J.; Gu, Y.; Singleton, R. S.; Patel, K. B.; Pullen, S. M.; Hicks, K. O.; Syddall, S. P.; Atwell, G. J.; Yang, S.; Denny, W. A.; Wilson, W. R., Mechanism of action and preclinical antitumor activity of the novel hypoxia-activated DNA cross-linking agent PR-104. *Clin. Cancer Res.* **2007**, *13* (13), 3922-3932.
24. Mulcahy, R. T.; Gipp, J. J.; Schmidt, J. P.; Joswig, C.; Borch, R. F., Nitrobenzyl Phosphorodiamidates as Potential Hypoxia-Selective Alkylating Agents. *J. Med. Chem.* **1994**, *37*, 1610-15.

## **Chapter 3**

### **Hypoxia-selective enzymatic conversion of 6-nitroquinoline to the fluorescent product, 6-aminoquinoline**

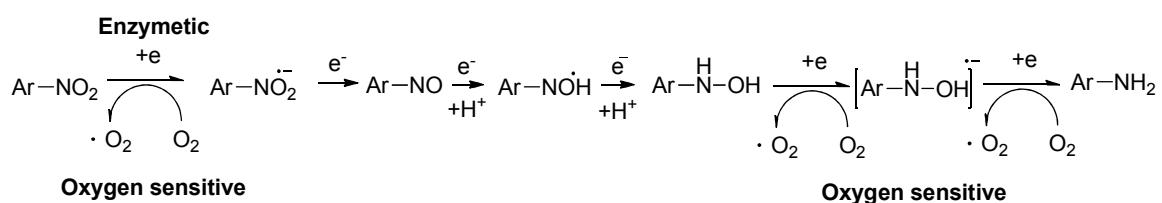
#### **3.1 Hypoxia is an attractive target to develop fluorescent probes**

Studies carried out on tumor physiology suggested that solid tumors contain low oxygenated areas (hypoxic regions).<sup>1</sup> Irregular vascularization, present inside tumors causes hypoxic conditions.<sup>2</sup> Further research, conducted on hypoxia over decades had established the importance of hypoxia in tumor biology.<sup>3</sup> Hypoxia selects for malignant phenotypes, which are unable to undergo apoptosis and result in poor prognosis.<sup>4</sup> Moreover, hypoxic regions contain cancer stem cells which can differentiate and cause metastases.<sup>5</sup> Hence, hypoxic regions are considered as targets of interest in tumor biology. Fluorescent based probing agents may be useful to mark low oxygenated regions.<sup>6</sup> Organic compound which can produce fluorescent response, selectively within tumor, may select as a candidate fluorescent probe for detecting hypoxic tumors.

#### **3.2 Fluorescent Probes to Detect Hypoxia**

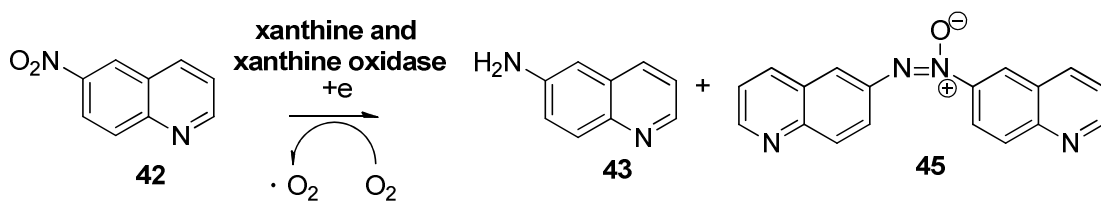
Nitroaryl groups can undergo enzyme mediated reduction in hypoxia.<sup>7</sup> The final product of the reduction process is hydroxyl amine and/or amine.<sup>8</sup> Under normal oxygenated conditions, single electron reduced nitro radical gets back oxidized to nitro group.<sup>9</sup> Hence the first reduction step is oxygen sensitive.<sup>7d, 10</sup> This sensitivity has been exploited by nitroaromatic prodrugs to spare normal oxygenated cells.<sup>11</sup> Nitro-based

anticancer prodrugs are selectively toxic to low-oxygenated tumors and that may be due to the oxygen-sensitive reduction of nitro group.<sup>12</sup> These prodrugs have been further tested for their oxygen sensitivity and enzymatic activation in hypoxia.<sup>11</sup> Nitro-based agents which are used to mark hypoxic regions in radio imaging and immunohistochemical staining techniques.<sup>13</sup> Along with these methods, nitro-based fluorescent probes would provide an attractive mean to visualize low oxygenated regions.<sup>6a, b, 14</sup> In the designing step, a non-fluorescent nitroaromatic compound can be selected as a fluorescent probe when the respective amino compound is fluorescent. In addition, these probes should be substrates for cellular reductases, which can supply electrons to nitro-amine reduction (Scheme 3.1).



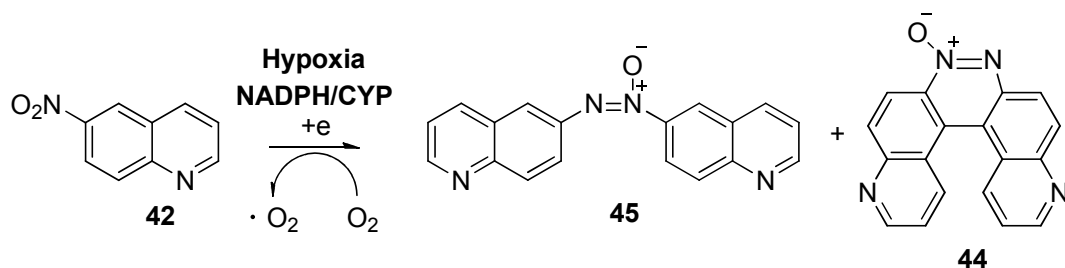
**Scheme 3.1.** Enzymatic reduction steps of a typical nitroaromatic compound

Based on this strategy, non-fluorescent 6-nitroquinoline (**42**) is tested as a nitroaryl fluorescent probe to detect hypoxia.<sup>15</sup> In addition, a metabolic study is carried out to identify fluorescent and non-fluorescent metabolites. Under hypoxia, a reductive metabolism of **42** can be reduced to 6-aminoquinoline (**43**, Scheme 3.2), which is a known fluorophore used in biochemical assays.<sup>16</sup> The production of non-fluorescent dimer 6,6'-azoxyquinoline **45** also can be anticipated (Scheme 3.2). Moreover, 205 nm stokes shift can be obtained by the reduction assay.<sup>16d</sup>



**Scheme 3.2.** Hypoxic metabolism of **42** forms fluorescent **43**

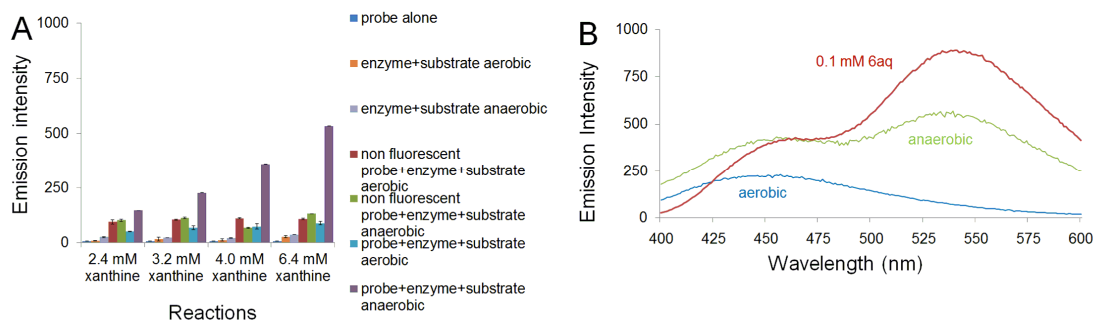
Similar hypoxic metabolism of **42** by NADPH:cytochrome P450 reductase (CYP450R) produced **45** and fluorescent helicene, pyrido[3,2-*f*]quinolino[6,5-*c*]cinnoline 3-oxide (**44**, chapter 1 scheme 3.3).<sup>15</sup> The anticipated fluorescent product **43** was not produced by the reducing system CYP450R (Scheme 3.2). Alternatively, another enzymatic reducing system xanthine and xanthine oxidase may be used to test metabolism of **42** in hypoxia.



**Scheme 3.3.** CYP450R mediates conversion of **42** into fluorescent metabolites

Xanthine and xanthine oxidase system is known to reductively activate bio reducible compounds and conduct one electron reduction under hypoxic conditions.<sup>17</sup> Accordingly, hypoxic conditions were applied to solutions, by conducting three cycles of freeze-pump-thawing.<sup>18</sup> The deoxygenated reaction solutions, **42** and reducing system were mixed inside an argon purged glove bag. The compound **42** is non-fluorescent in solutions. Anaerobic incubation of **42** with xanthine and xanthine oxidase produced 12-

fold fluorescence increase at 530 nm (Figure 3.1A, purple column). When xanthine concentration is increased, emission at 530 nm is increased.



**Figure 3.1** Enzymatic conversions of **42** to a fluorescent product selectively under hypoxic conditions. **A.** Fluorescence emission at 530 nm ( $\lambda_{\text{ex}}$  340 nm). Each set of assays depicted in the bar graph consists of (from left to right): a control sample of compound **42** alone (0.8 mM) ■, a control reaction composed of xanthine oxidase (2.4 U/mL) and xanthine (2.4 mM, 3.2 mM, 4.0 mM and 6.4 mM) under aerobic conditions ■, a control reaction composed of xanthine oxidase (2.4 U/mL) and xanthine (2.4 mM, 3.2 mM, 4.0 mM and 6.4 mM) under anaerobic conditions ■, a control reaction composed of xanthine oxidase (2.4 U/mL), xanthine (2.4 mM, 3.2 mM, 4.0 mM and 6.4 mM) and the non-fluorescent electron acceptor, 1,2,4-benzotriazine 1,4-dioxide, (6.4 mM) under aerobic conditions ■, a control reaction composed of xanthine oxidase (2.4 U/mL), xanthine (2.4 mM, 3.2 mM, 4.0 mM and 6.4 mM) and the non-fluorescent electron acceptor, 1,2,4-benzotriazine 1,4-dioxide, (6.4 mM) under anaerobic conditions ■, a reaction composed of xanthine oxidase (2.4 U/mL), xanthine (2.4 mM, 3.2 mM, 4.0 mM and 6.4 mM) and **42** under aerobic conditions ■, a reaction composed of xanthine oxidase (2.4 U/mL), xanthine (2.4 mM, 3.2 mM, 4.0 mM and 6.4 mM) and **42** under anaerobic conditions ■. Reactions were incubated for 18 h in sodium phosphate buffer at (12 mM, pH 7.4) at 24 °C, diluted with aerobic sodium phosphate buffer (12 mM, pH 7.4), and the fluorescence measured ( $\lambda_{\text{ex}}$  340 nm,  $\lambda_{\text{em}}$  530 nm). **B.** Fluorescence spectra of reaction mixtures generated in the aerobic and anaerobic metabolism of **42** by xanthine oxidase (2.4 U/mL) and xanthine (6.4 mM) carried out as described in the Experimental Section and fluorescence spectrum of 6-aminoquinoline (**43**, 0.1 mM,  $\lambda_{\text{ex}}$  340 nm, in sodium phosphate buffer, 10 mM, pH 7.4).

When the fluorescent emission of anaerobic **42** reduction by xanthine and xanthine oxidase is inspected, the shape of the fluorescent curve is clear different from that of **44**, which is generated by the metabolism of **42** by NADPH:cytochrome P450 reductase.<sup>15</sup> The fluorescence curve of **44** contains two distinct emission maxima, at 440 and 460 nm. The shape of the curve, obtained from xanthine oxidase mediated

metabolism of **42** resembles fluorescence spectrum of **43** (Figure 3.1B, green and red curves). The fluorescence intensity of aerobic reaction, containing **42**, at 530 nm region, is low relative to the corresponding anaerobic reaction (Figure 3.10, E). When non fluorescent electron acceptor benzotriazine 1,2,4-di-oxide is incubated with xanthine and xanthine oxidase under aerobic and anaerobic conditions, low fluorescence intensity is detected at 530 nm region (Figure 3A, columns red and green).<sup>15</sup> Xanthine and xanthine oxidase produced fluorescence, in low intensities under aerobic and anaerobic conditions may be due to the decomposition of cofactor of xanthine oxidase (Figure 3.10, C and D).<sup>19</sup>

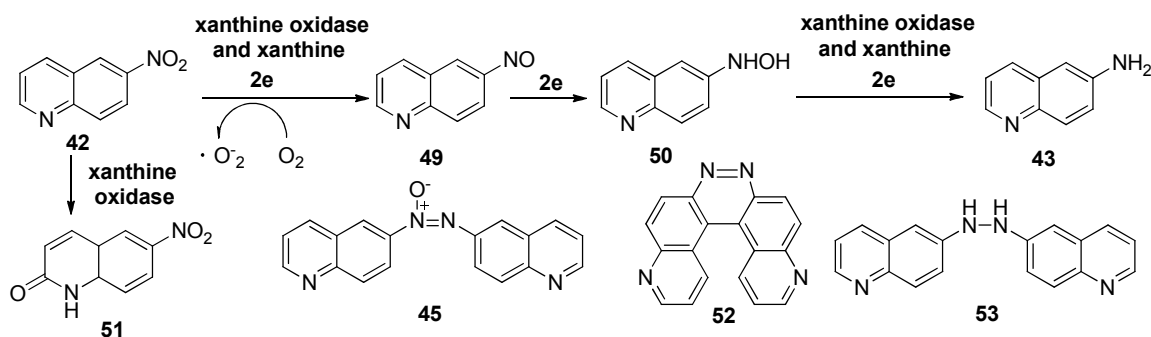
### **3.3 LC/MS analysis of the reaction mixtures generated by hypoxic metabolism of **42** by xanthine/xanthine oxidase**

To identify metabolites, produced in the enzymatic reduction reaction we analyzed reaction mixtures using LC/MS. The complete LC/MS analysis includes results of reaction mixtures and authentic compounds (Figures 3.2 and 3.3). The anaerobic reaction mixture of two equivalents of xanthine shows the presence of **50** (Figure 3.2 panels A, B and E). Compound **50** is fluorescent at 450 nm region (Figure 3.10, A). The contribution of **50** to the fluorescence at 530 nm region is minimal because it is unstable due to condensation with **49** to form **45**. The mass to charge value ( $m/z$ ) of  $M+H$  ion of peak at 3.1 min on HPLC matches with that of authentic **50** (Figure 3.3, A and B). In the same mixture, the  $m/z$  of  $M+H$  ion of peak at 4.5 min on the HPLC (Figure 3.2, F) is the same as that of the authentic **43** (Figure 3.3, C and D), consistent with the fluorescent results (Figure 3.1B, curves green and red). The  $m/z$  of ( $M+H$ ) ion of the eluent at 5.5 min shows 285.1, which is the  $M+H$   $m/z$  value of **53** (Figure 3.2, A and scheme 3.4). In



the same reaction mixture the product eluting at 14.6 min showed  $m/z$  of 190.9 (Figure 3.2, A and G). The authentic LC analysis of **51** is consistent with the product eluting at 14.6 min in Figure 3.2, panel A (Figure 3.3 panels E and F). When **42** is incubated in the presence of xanthine oxidase, formation of **51** is possible as a metabolite along the reduction profile.<sup>15, 20</sup> The product eluting at 16.4 min shows  $m/z$  value of 158.9, which is the  $M+H$  ion of nitroso, **49**. (Figure 3.2, A, B, C and H)

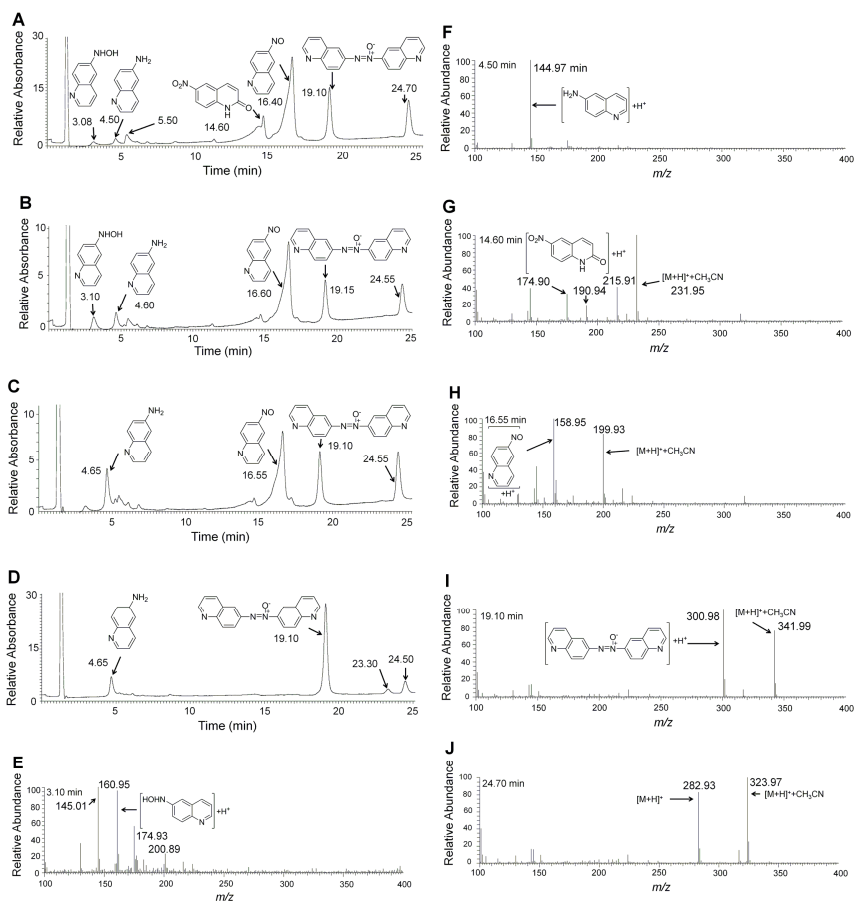
The product eluting at 19.1 min on HPLC showed  $m/z$  of 301.1 as the  $(M+H)$  ion (Figure 3.2 panels A and I). We employed Raney nickel mediated chemical reduction of **42**, with hydrazine hydrate to obtain **45**.<sup>21</sup> The authentic LC analysis of **45** is consistent with the product eluting at 19.1 min (Figure 3.3, I and J). There is no contribution to the fluorescence of anaerobic reactions by **45** (Figure 3.1A, purple column). The product appears at 24.7 min, with  $m/z$  of 282.9 may be an isomer of **52**, which is not formed in these reactions (Figure 3.2, A and J, Figure 3.3, K and L, scheme 3.4).



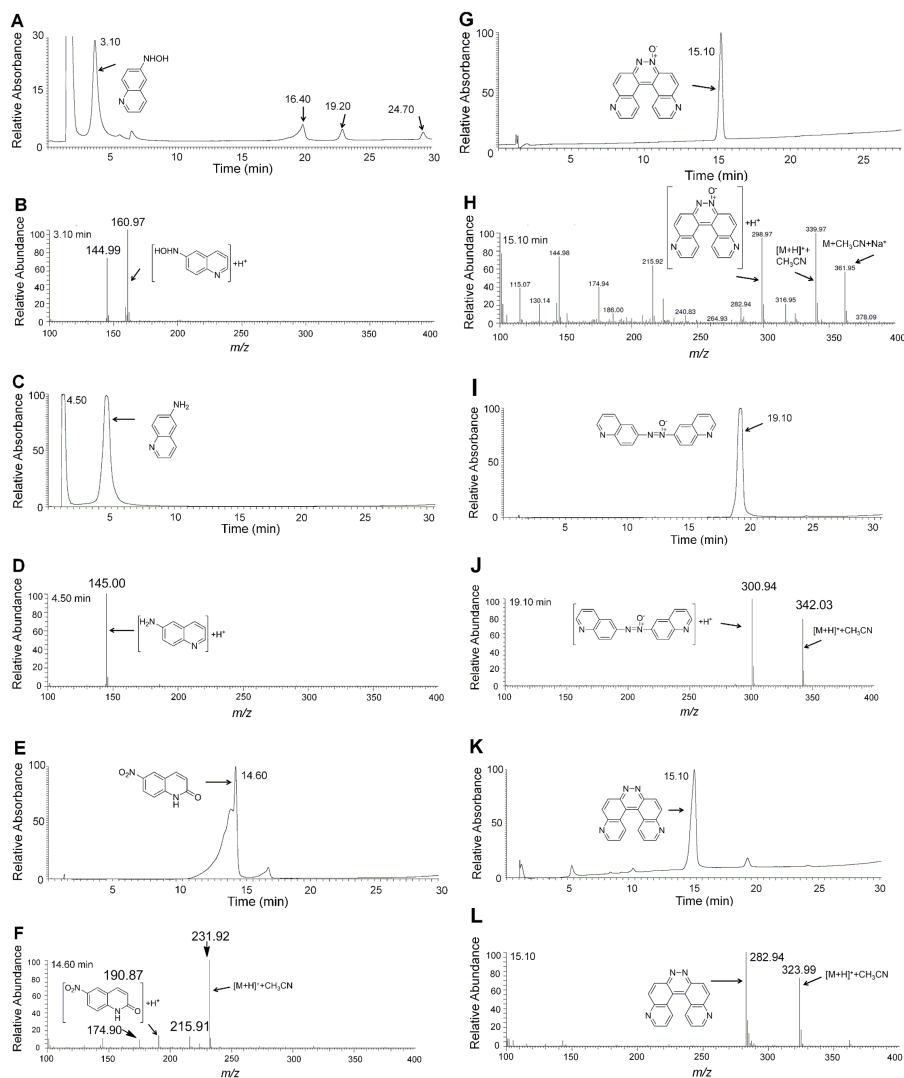
**Scheme 3.4.** Hypoxic metabolism of **42** by xanthine and xanthine oxidase

The reaction mixture containing 2.4 mM xanthine shows diminished amounts of **51** (Figure 3.2, B). Similarly, in 4.0 mM anaerobic xanthine assay, **51** and **50** are not present (Figure 3.2, C). When the xanthine amount is increase to 6.4 mM, under anaerobic conditions, as seen on the HPLC trace only **43**, **45** and an isomer of **52** are

formed (Figure 3.2, D). Fluorescent product **44** is not detected in the current study (Figure 3.3, G and H).



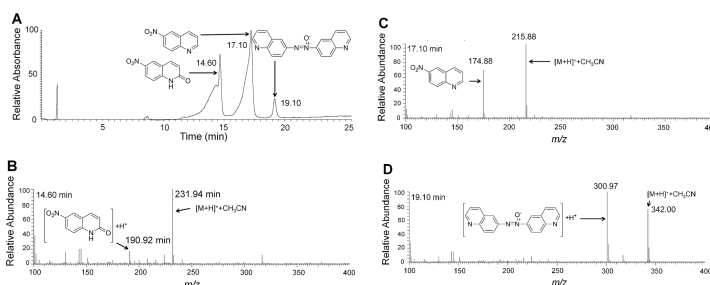
**Figure 3.2.** LC/MS analysis of reaction mixture, generated by anaerobic metabolism of **42**. Compound **42** (0.8 mM), xanthine oxidase (2.4 U/mL) and xanthine were mixed under anaerobic conditions and the reaction was carried out as described in the experimental section. The reaction was dried and products dissolved in methanol. The mixture was eluted with a gradient of 99% A (water containing 0.1% acetic acid) and 1% B (acetonitrile containing 0.1% acetic acid) followed by linear increase to 90% B over 30 min. The elution was continued at 90% B for 3 min and then B was decreased to 1% over next 8 min. A flow rate of 0.35 mL/min was used and the metabolites were detected at 254 nm. Mass spectra were obtained using electrospray ionization in the positive ion mode. Panel A: HPLC trace of the anaerobic reaction mixture with xanthine (1.6 mM) monitoring absorbance at 254 nm. Panel B: HPLC of the anaerobic reaction mixture with xanthine (2.4 mM) monitoring absorbance at 254 nm. Panel C: HPLC trace of the anaerobic reaction mixture with xanthine (4.0 mM) monitoring absorbance at 254 nm. Panel D: HPLC trace of the anaerobic reaction mixture with xanthine (6.4 mM) monitoring absorbance at 254 nm. Panel E: LC/MS spectrum of product eluting at 3.08 min in panels A and B. Panel F: LC/MS spectrum of the product eluting at 4.50 min in panels A, B, C and D. Panel G: LC/MS spectrum for of the product eluting at 14.60 min in panel A. Panel H: LC/MS spectrum for of the product eluting at 16.40 min in panels A, B, and C. Panel I: LC/MS spectrum for of the product eluting at 19.10 min in panels A, B, C and D. Panel J: LC/MS spectrum for of the product eluting at 24.50 min in panels A, B, C and D.



**Figure 3.3.** LC/MS analysis of authentic compounds. The compounds were dissolved in methanol. The mixture was eluted with a gradient of 99% A (water containing 0.1% acetic acid) and 1% B (acetonitrile containing 0.1% acetic acid) followed by linear increase to 90% B over 30 min. The elution was continued at 90% B for 3 min and then B was decreased to 1% over next 8 min. A flow rate of 0.35 mL/min was used and the metabolites were detected at 254 nm. Mass spectra were obtained using electrospray ionization in the positive ion mode. Panel A: HPLC trace of **50** monitoring absorbance at 254 nm. Panel B: LC/MS spectrum of **50**. Panel C: HPLC trace of **43** monitoring at 254 nm. Panel D: LC/MS spectrum of **43** eluting at 4.50 min. Panel E: HPLC trace of **51** monitoring at 254 nm. Panel F: LC/MS spectrum of **51** eluting at 14.60 min. Panel G: HPLC trace of **44** monitoring at 254 nm. Panel H: LC/MS spectrum of **44** eluting at 15.10 min. Panel I: HPLC trace of **45** monitoring at 254 nm. Panel J: LC/MS spectrum of **45**. Panel K: HPLC trace of **52** monitoring at 254 nm. Panel L: LC/MS spectrum of **52**.

### 3.4 LC/MS analysis of the reaction mixtures generated by aerobic metabolism of **42** by xanthine/xanthine oxidase

Starting compound **42** is remaining in the mixture while **51** and **45** appeared as new products under aerobic conditions (Scheme 3.4). None of the compounds are fluorescent.



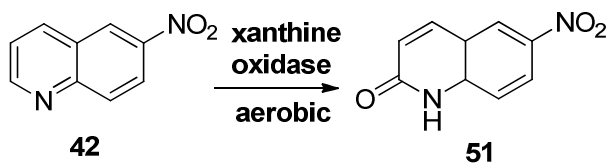
**Figure 3.4** LC/MS analysis of the reaction mixture generated by aerobic metabolism of **42**. Compound **42** (0.8 mM) xanthine oxidase (2.4 U/mL) and xanthine (6.4 mM) were mixed and the reaction was carried out as described in the experimental section. The reaction was dried and products dissolved in methanol. The mixture was eluted with a gradient of 99% A (water containing 0.1% acetic acid) and 1% B (acetonitrile containing 0.1% acetic acid) followed by linear increase to 90% B over 30 min. The elution was continued at 90% B for 3 min and then B was decreased to 1% over next 8 min. A flow rate of 0.35 mL/min was used and the metabolites were detected at 254 nm. Mass spectra were obtained using electrospray ionization in the positive ion mode. Panel A: HPLC of the aerobic reaction mixture monitoring absorbance at 254 nm. Panel B: LC/MS spectrum of the product eluting at 14.60 min. Panel C: LC/MS spectrum of the product eluting at 17.10 min. Panel D: LC/MS spectrum of the product eluting at 19.10 min.

### 3.5 Xanthine oxidase oxidizes aryl carbon, bonded to heteroatom of **42** to produce 6-nitroquinolone **51**

The compound **51** (Figure 3.3, E), was synthesized using xanthine oxidase and **42** as the starting material. There is evidence for oxidation of aromatic carbon, adjacent to nitrogen by enzyme xanthine oxidase.<sup>22</sup> It was clear from the metabolic results of aerobic reaction of **42** by xanthine oxidase that xanthine oxidase does oxidation chemistry on **42**, as a substrate when reduction of **42** is diminished in the presence of oxygen (Figure 3.4,

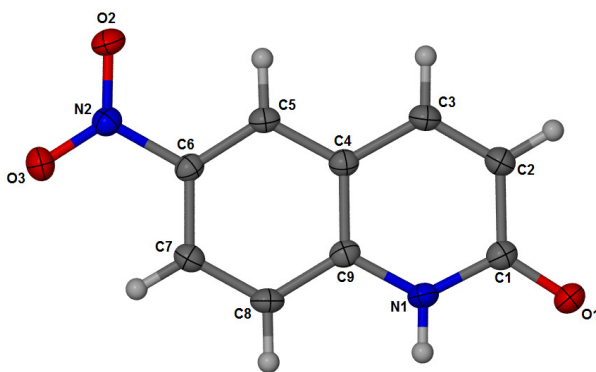
A). Moreover, at lower concentration of xanthine, under hypoxia **51** was produced as a main metabolite.

We speculated that xanthine oxidase should be able to convert **42** to **51** under aerobic conditions and xanthine is not required for the oxidation process. When **42** stirred with xanthine oxidase in aqueous media, **51** was obtained in milligram amounts (Scheme 3.5).



**Scheme 3.5.** Enzymatic generation of **51** by **42** using xanthine oxidase

Chemical characterization of **51** was conducted by NMR, HRMS and crystallography analysis (Figure 3.5 and experimental). Analysis of the  $^1\text{H}$ -NMR spectrum of **51** clearly shows the absence of the resonance for the proton adjacent to the nitrogen of the heterocyclic quinoline ring and a new resonance is seen on  $^{13}\text{C}$  spectrum at 165 ppm diagnostic for the carbonyl carbon of the quinolone system.

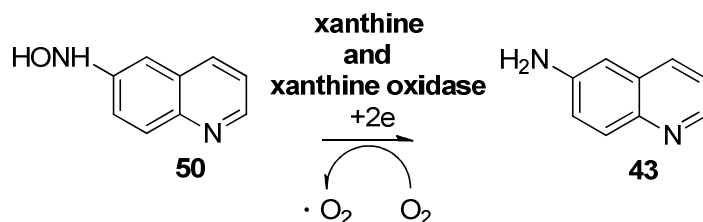


**Figure 3.5.** ORTEP diagram of **51**

When enzymatically synthesized **51** was analyzed on LC/MS (Figure 3.3, E and F), retention time and m/z matched with that which eluted with anaerobic and aerobic reactions (Figures 3.2, A and G, 3.3, E and F and 3.4, A and B).

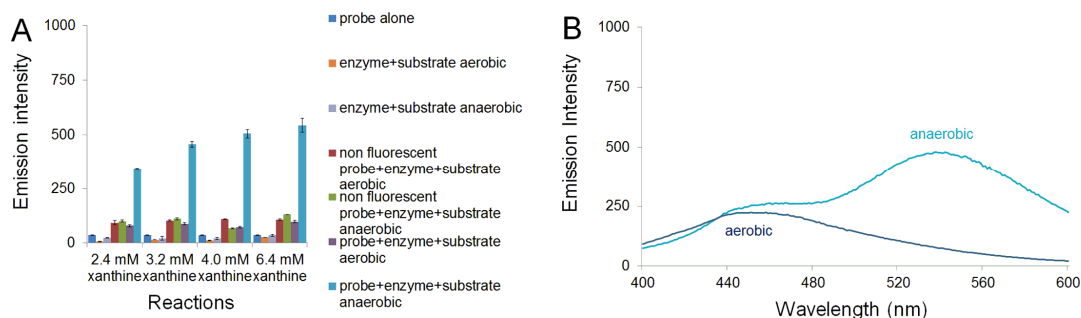
### 3.6 Hypoxia-selective conversion of hydroxylamine **50** to amino **43**

It is well established that enzymatic reduction of nitroaromatics proceeds via intermediates nitroso and hydroxylamine to produce amine product.<sup>7a-c, 10, 23</sup> The final reduction step from intermediate hydroxylamine to amine is not well studied in the current literature.<sup>24</sup> The final reduction step of the reduction profile of **42** is studied using **50** and the reduction of **50** is tested by xanthine and xanthine oxidase system under aerobic and anaerobic conditions. Characterization of enzyme mediated reduction of aromatic hydroxylamine to amine has not been reported (Scheme 3.6).



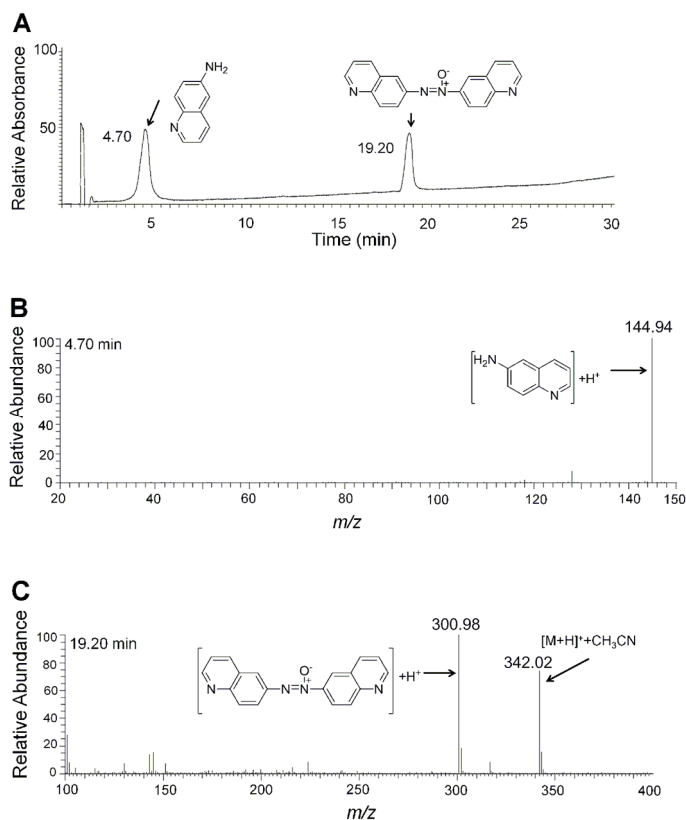
**Scheme 3.6** Enzymatic generation of **43** by xanthine and xanthine oxidase

Hydroxylamine **50** has been chemically synthesized using hydrazine hydrate in the presence of Raney nickel and characterized using NMR, HRMS and crystallographic methods. The LC/MS characterization of **50** shows spontaneous formation of **49** and **45** (Figure 3.3, panels A and B). The hypoxic incubation of **50** with xanthine oxidase and xanthine shows fluorescence growth at 530 nm and the fluorescence increases with xanthine concentration (Figure 3.6 A).



**Figure 3.6.** Enzymatic conversion of **50** to fluorescent **43** under hypoxic conditions. **A.** Fluorescence emission at 530 nm ( $\lambda_{ex}$  340 nm). Each set of assays depicted in the bar graph consists of (from left to right): a control sample of compound **50** alone (0.8 mM) ■, a control reaction composed of xanthine oxidase (2.4 U/mL) and xanthine (2.4 mM, 3.2 mM, 4.0 mM and 6.4 mM) under aerobic ■, a control reaction composed of xanthine oxidase (2.4 U/mL) and xanthine (2.4 mM, 3.2 mM, 4.0 mM and 6.4 mM) under anaerobic conditions ■, a control reaction composed of xanthine oxidase (2.4 U/mL), xanthine (2.4 mM, 3.2 mM, 4.0 mM and 6.4 mM) and the non-fluorescent electron acceptor, 1,2,4-benzotriazine 1,4-dioxide, (6.4 mM) under aerobic conditions ■, a control reaction composed of xanthine oxidase (2.4 U/mL), xanthine (2.4 mM, 3.2 mM, 4.0 mM and 6.4 mM) and the non-fluorescent electron acceptor, 1,2,4-benzotriazine 1,4-dioxide, (6.4 mM) under anaerobic conditions ■, a reaction composed of xanthine oxidase (2.4 U/mL), xanthine (2.4 mM, 3.2 mM, 4.0 mM and 6.4 mM) and **50** under aerobic conditions ■, a reaction composed of xanthine oxidase (2.4 U/mL), xanthine (2.4 mM, 3.2 mM, 4.0 mM and 6.4 mM) and **50** under anaerobic conditions ■. Reactions were incubated for 18 h in sodium phosphate buffer at (12 mM, pH 7.4) at 24 °C, diluted with aerobic sodium phosphate buffer (12 mM, pH 7.4), and the fluorescence was measured ( $\lambda_{ex}$  340 nm,  $\lambda_{em}$  530 nm). **B.** Fluorescence spectra of aerobic and anaerobic reaction mixtures containing **50** (0.8 mM), xanthine oxidase (2.4 U/mL), and xanthine (3.2 mM).

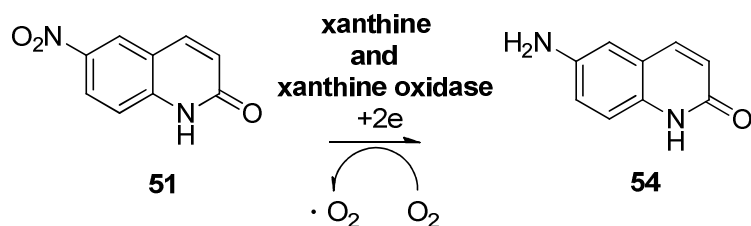
In the aerobic reaction, fluorescence growth is not detected (Figure 3.10 panel F). The shape of the fluorescence curve of the anaerobic reaction is similar to **43** in solution (Figure 3.6 B). The LC/MS analysis of anaerobic reaction shows the presence of **43** and **45**. The evidence shows the oxygen sensitivity of reduction of **50** by xanthine and xanthine oxidase, to form **43** (Figure 3.7).



**Figure 3.7.** LC/MS analysis of the reaction mixture generated by anaerobic metabolism of **50**. Compound **50** (0.8 mM), xanthine oxidase (2.4 U/mL) and xanthine (6.4 mM) were mixed and the reaction was carried out as described in the experimental section. The reaction was dried and products dissolved in methanol. The mixture was eluted with a gradient of 99% A (water containing 0.1% acetic acid) and 1% B (acetonitrile containing 0.1% acetic acid) followed by linear increase to 90% B over 30 min. The elution was continued at 90% B for 3 min and then B was decreased to 1% over next 8 min. A flow rate of 0.35 mL/min was used and the metabolites were detected at 254 nm. Mass spectra were obtained using electrospray ionization in the positive ion mode. Panel A: HPLC trace of the anaerobic reaction mixture monitoring absorbance at 254 nm. Panel B: LC/MS spectrum of the product eluting at 4.70 min. Panel C: LC/MS spectrum of the product eluting at 19.20 min.

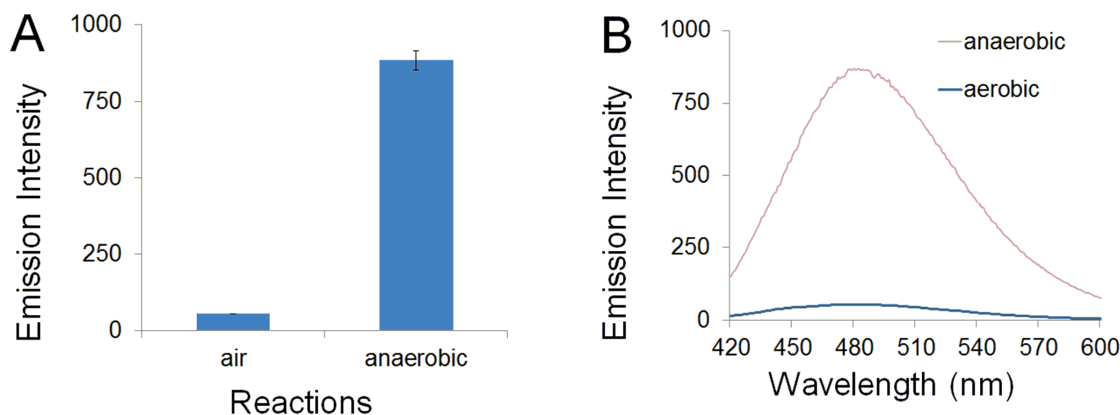


### 3.7 Hypoxia-selective conversion of 6-nitroquinolone **51** to 6-aminoquinolone **54**



**Scheme 3.7.** Enzymatic generation of **54** from **51** by xanthine and xanthine oxidase is hypoxia selective

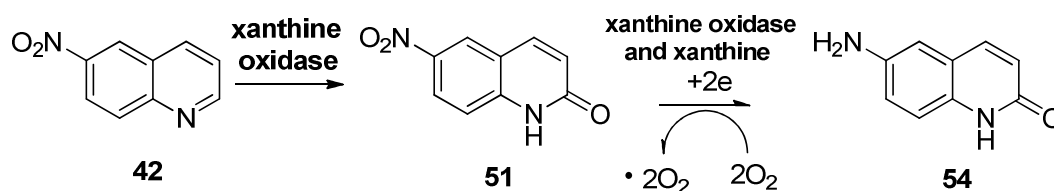
We speculated that the 6-aminoquinolone **54** may be fluorescent. The compound **54** was chemically synthesized by reducing **51** on palladium/charcoal hydrogenation to obtain the fluorescent spectrum (Figure 3.10 panel B). Then, hypoxia selective reduction of **51** by xanthine and xanthine oxidase system is tested. The anaerobic reaction produced expected fluorescence of **54** (Scheme 3.7). A Sixteen fold increase of fluorescence is obtained against the aerobic reaction (Figure 3.8).



**Figure 3.8.** Enzymatic conversions of **51** to **54** under hypoxic conditions. A. Fluorescence emission at 485 nm ( $\lambda_{\text{ex}}$  390 nm) for **51** (0.8 mM) + xanthine oxidase (2.4 U/mL) and xanthine (3.2 mM) under aerobic conditions, **51** (0.8 mM) + xanthine oxidase (2.4 U/mL) and xanthine (3.2 mM) under anaerobic conditions, Reactions were incubated for 18 h in sodium phosphate buffer at (12 mM, pH 7.4) at 24 °C, then diluted with aerobic sodium phosphate buffer (12 mM, pH 7.4) and the fluorescence measured ( $\lambda_{\text{ex}}$  390 nm,  $\lambda_{\text{em}}$  485 nm). B. Fluorescence spectra (in sodium phosphate buffer, 10 mM, pH 7.4) of the reaction mixture generated in the aerobic metabolism of **51** by xanthine oxidase (2.4 U/mL) and xanthine (3.2 mM) (pink,  $\lambda_{\text{em}}$  485 nm) and fluorescence spectrum (in sodium phosphate buffer, 10 mM, pH 7.4) of the reaction mixture generated in the anaerobic metabolism of **51** by xanthine oxidase (2.4 U/mL) and xanthine (3.2 mM) (blue)  $\lambda_{\text{em}}$  485 nm.

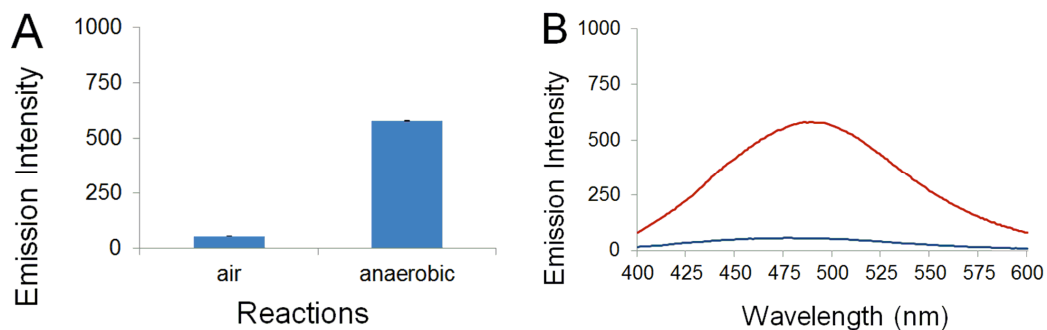
### 3.8 Enzymatic conversion of **42** to 6-nitroquinolone **51** followed by hypoxia-selective conversion to 6-aminoquinolone **54**

LC/MS analysis of anaerobic and aerobic metabolism of **42** reveals that under low concentrations of xanthine, **42** was oxidized to form **51** and that oxidation can dominate over reduction of nitro under low oxygen levels. Upon forming **51**, xanthine oxidase can perform nitro reduction on **51**, under hypoxia to produce **54** in the same reaction mixture (Scheme 3.8).



Scheme 3.8 Enzymatic generation of **51** from **42** and production of **54** from **51**

In the assay we used 0.5 molar equivalent of xanthine, 0.4 mM, with **42** and xanthine oxidase and carried out the normal enzymatic reactions under anaerobic and aerobic conditions. In the fluorescence assays a ten-fold increase of fluorescence was obtained against the aerobic reaction mixture (Figure 3.9).



**Figure 3.9** Enzymatic conversion of **42** to **51** and reduction to **54** in hypoxia. A. Fluorescence emission at 485 nm ( $\lambda_{ex}$  390 nm) for **1** (0.8 mM) + xanthine oxidase (2.4 U/mL) and xanthine (0.4 mM) under aerobic conditions. Compound **1** (0.8 mM) + xanthine oxidase (2.4 U/mL) and xanthine (0.4 mM) were incubated for 18 h in sodium phosphate buffer at (12 mM, pH 7.4) at 24 °C under hypoxia, then diluted with aerobic sodium phosphate buffer (12 mM, pH 7.4) and the fluorescence measured ( $\lambda_{ex}$  390 nm,  $\lambda_{em}$  485 nm). B. Fluorescence spectra (in sodium phosphate buffer, 10 mM, pH 7.4) of the reaction mixtures generated in the anaerobic (red) and aerobic (blue) metabolism of **42** by xanthine oxidase (2.4 U/mL) and xanthine (0.4 mM) ( $\lambda_{em}$  at 485 nm)

### 3.9 Conclusions

In the current work, we provide evidence for the hypoxia-selective conversion of 6-nitroquinoline **42** to 6-aminoquinoline **43**, by xanthine/xanthine oxidase enzyme system. The reduction steps are consecutive one electron additions, as seen in scheme 3.1. In addition, condensation occurs between **50** and **49** to produce **45**. The chemical synthesis and complete characterization of **50** facilitates the analysis of the oxygen sensitivity of final reduction step. Fluorescent and LC/MS analysis of reduction of **50** in hypoxia, by xanthine and xanthine oxidase show the presence of fluorescent **43**. This finding is important and striking because the existing evidence in the literature discusses only the oxygen sensitivity of the first reduction step of nitro compounds.<sup>7d, 10, 25</sup> The evidence we provide supports the existence of multiple oxygen sensitive reduction steps over the enzymatic reduction of nitro aromatic compound. In an early work, related to the

reduction of **42** by CYP450R<sup>15</sup>, together with current xanthine and xanthine oxidase-mediated reduction of **42** in hypoxia shows different product profile and metabolism that may occur on a single nitro compound. The comparison reveals that the inability of CYP450R to reduce intermediate **50**, under the conditions we applied, leaving them to condense to form byproducts.

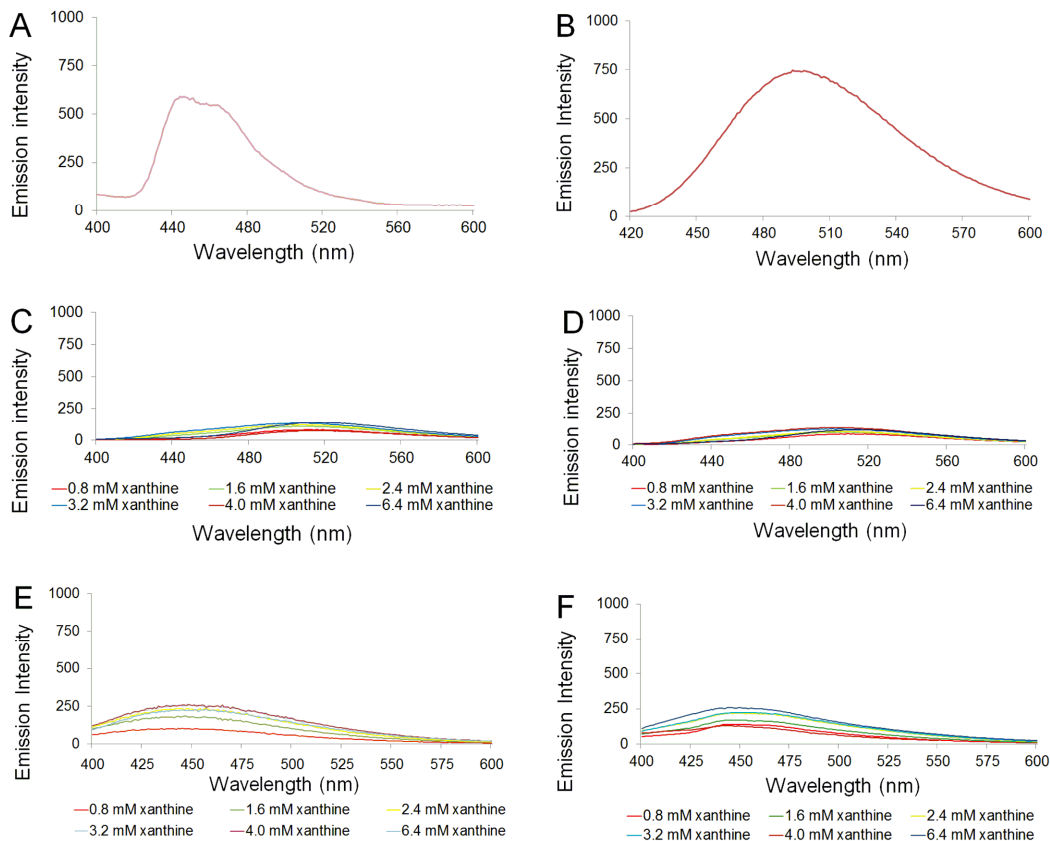
We observed the oxidation of **42** to **51**, conducted by xanthine oxidase (**51**, Scheme 3.4). The ability of xanthine oxidase to oxidize aromatic carbon atoms next to nitrogen is well documented.<sup>22b, 22d</sup> The oxidizing capability of xanthine oxidase is responsible for the transformation of **42** to **51**. The aerobic assays show the oxidation product **51** as a major product. Upon reduction **51** produces fluorescent **54**, which emits at 490 nm (data not shown) under assay conditions. In assays, when xanthine concentration is increased the yield of **51** decreases. Hence, it can be concluded that under anaerobic conditions xanthine/xanthine oxidase system efficiently reduces **42**. The oxidizing ability of xanthine oxidase slows when conditions for reduction is favored.

Reduction of **51**, in a separate experiment by xanthine/xanthine oxidase system, under hypoxia produces fluorescence at 485 nm. The emission parameters of **54** match with the fluorescence obtained from the anaerobic metabolism of **51** (data not shown). The fluorescent enhancement obtained with **51** grants future experiments on **51** as a potential fluorescent probe to detect hypoxia.

Finally, the work we presented shows the ability of **42** to be used as a fluorescent probe that can be activated by one electron reductases, under hypoxia. Chemical characterization of metabolites, produced from enzymatic reduction of nitroaromatic compounds is essential to understand the complexity of nitroaromatic reduction.

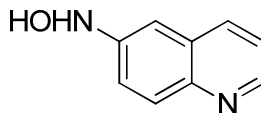
### 3.10 Experimental

**Materials and methods.** Chemicals were purchased from following sources: Sodium phosphate, glucose, NADPH, cytochrome p450 reductase, DMF, Raney nickel slurry in water, silica gel plates for thin layer chromatography and silica gel (0.04-0.063 mm pore size) for column chromatography were obtained from Sigma Aldrich (St. Louis, MO); 6-aminoquinoline, 6-nitroquinoline, and hydrazine hydrate from Alfa-Aesar (Ward Hill, MA). deuterated NMR solvents were from Cambridge Isotope Laboratories (Andover, MA); ethyl acetate, dichloromethane, methanol, hexane, ethanol, HPLC water and HPLC acetonitrile from Fischer; The compound 1,2,4-benzotriazine-1,4-di-N-oxide was made following literature methods.<sup>1</sup> High resolution mass spectrometry (HRMS) analyses were performed at the mass spectroscopy facility of the University of Illinois Champaign-Urbana and low resolution mass spectroscopic analyses were carried out at the University of Missouri-Columbia. <sup>1</sup>H and <sup>13</sup>C NMR experiments and were done on a Bruker Avance DRX300 with 5 mm broadband probe and Bruker Avance DRX500 with CPTCI probe using deuterated NMR solvents methanol (CD<sub>3</sub>OD) and chloroform(CDCl<sub>3</sub>) at the University of Missouri-Columbia. The reference peaks were set to 3.31 ppm and 49.00 ppm for deuterated methanol and 7.26 ppm and 77.00 ppm for deuterated chloroform from tetramethylsilane for the <sup>1</sup>H and <sup>13</sup>C spectra respectively. The fluorescence spectra were obtained on a Varian Cary Eclipse Fluorescence Spectrophotometer equipped with xenon flash lamp with instrumental slit width settings at 10 nm employing a 10 mm path length quartz cuvette.



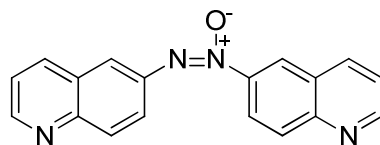
**Figure 3.10.** Fluorescence spectra of control reactions. A: Fluorescence spectrum of **50** (0.03 mM,  $\lambda_{\text{ex}}$  340 nm, in sodium phosphate buffer, 10 mM, pH 7.4). B: Fluorescence spectrum of **54** (0.003 mM,  $\lambda_{\text{ex}}$  390 nm, in sodium phosphate buffer, 10 mM, pH 7.4). C: Fluorescence spectra ( $\lambda_{\text{ex}}$  340 nm, in sodium phosphate buffer, 10 mM, pH 7.4) of control reactions composed of xanthine oxidase (2.4 U/mL), xanthine (2.4 mM, 3.2 mM, 4.0 mM and 6.4 mM) and a non-fluorescent electron acceptor 1,2,4-benzotriazine 1,4-dioxide (6.4 mM) under aerobic conditions (referred to brown bar in figure 3.1, **■**), D: Fluorescence spectra of control reactions composed of xanthine oxidase (2.4 U/mL), xanthine (2.4 mM, 3.2 mM, 4.0 mM and 6.4 mM) and a non-fluorescent electron acceptor 1,2,4-benzotriazine 1,4-dioxide (6.4 mM) under anaerobic conditions (referred to green bar in figure 3.1 A, **■**) E: Fluorescence spectra ( $\lambda_{\text{ex}}$  340 nm, in sodium phosphate buffer, 10 mM, pH 7.4) of reactions composed of xanthine oxidase (2.4 U/mL), xanthine (2.4 mM, 3.2 mM, 4.0 mM and 6.4 mM) and **42** under aerobic conditions (blue bar in figure 3.1 A, **■**), F: Fluorescence spectra ( $\lambda_{\text{ex}}$  340 nm, in sodium phosphate buffer, 10 mM, pH 7.4) of reactions composed of xanthine oxidase (2.4 U/mL), xanthine (2.4 mM, 3.2 mM, 4.0 mM and 6.4 mM) and **50** under aerobic conditions.

### Synthesis of 6-hydroxylaminoquinoline **50**:<sup>1</sup>



6-nitroquinoline (0.5 g, 2.87 mmol) **42** was stirred in 20 mL of EtOH/CH<sub>2</sub>Cl<sub>2</sub> (1:1) at 0°C and 0.5 mL of was Raney nickel slurry (active catalyst in water-sigma 221678) was added. Then, 10 molar eq. of hydrazine hydrate was added drop wise and stirred for 1 hour while purging nitrogen gas. The solid was filtered and the organic mixture was dried using brine and sodium sulfate. The compound **50** was separated by column chromatography using EtOAc and MeOH/ CH<sub>2</sub>Cl<sub>2</sub> solvents. To obtain crystals, the pure product was dissolved in warm EtOAc and was cooled rapidly to isolate yellow crystals. <sup>1</sup>H – NMR (CD<sub>3</sub>OD, 300 MHz): δ 8.53 (d, J = 5.0 Hz, 1H), 8.07 (d, J = 8.0 Hz, 1H), 7.82 (m, 1H), 7.33 (m, 3H). <sup>13</sup>C NMR (CD<sub>3</sub>OD, 300 MHz): δ 151.40, 147.64, 144.76, 136.72, 131.05, 129.15, 122.54, 121.01, 107.68. HRMS (ESI, M+H<sup>+</sup>) *m/z* calcd for C<sub>9</sub>H<sub>9</sub>N<sub>2</sub>O 160.0715, found 160.0707

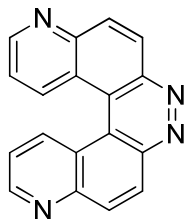
## Synthesis of 1,2-di(quinolin-6-yl)diazene oxide **45**



We employed a variation on the literature procedure of Boge *et al.*<sup>2</sup> To a solution of compound **42** (0.5 g, 2.87 mmol) in a mixture of EtOH:CH<sub>2</sub>Cl<sub>2</sub> (1:1, 20 mL) at 0 °C in an ice/salt bath was added Raney nickel slurry (0.5 mL, active catalyst in water, Sigma-Aldrich cat. number 221678). To this mixture, hydrazine hydrate (1.5 mL, 30 mmol) portions were added over the course of 3 h with stirring until **42** was consumed (TLC) and the resulting mixture stirred overnight. The solid was removed by filtration and the resulting solution dried by extraction with brine and then over sodium sulfate. The compound was purified by column chromatography on silica gel eluted with ethyl acetate in the first column separation and the second column chromatography separation on silica gel was done with MeOH:CH<sub>2</sub>Cl<sub>2</sub> (99:1) to obtain the product, a yellow solid, in pure form (100 mg, R<sub>f</sub> value = 0.25 in 4% MeOH in CH<sub>2</sub>Cl<sub>2</sub>) <sup>1</sup>H NMR (CDCl<sub>3</sub>, 300 MHz): δ ppm 9.14 (d, J = 2.5 Hz, 1H), δ 9.00 (dd, J = 4.5 Hz, J = 1.5 Hz, 1H), δ 8.93 (dd, , J = 4.5 Hz, J = 1.5 Hz, 1H), δ 8.82 (d, J = 2.5 Hz, 1H), δ 8.67 (d, J = 9.0 Hz, 1H), δ 8.31 (dd, J = 9.0 Hz, J = 1.5 Hz, 1H), δ 8.21 (m, 4H), δ 7.49 (dd, J = 8.5 Hz, J = 4.5 Hz, 1H), 7.42 (dd, J = 8.5 Hz, J = 4.5 Hz, 1H), 1.23 grease. <sup>13</sup>C NMR (CDCl<sub>3</sub>, 75.5 MHz): δ 152.86, 151.97, 149.64, 148.72, 146.01, 141.93, 137.88, 137.76, 130.95, 130.32, 129.32, 128.46, 127.73, 123.76, 123.40, 122.68, 122.64, 122.09; HRMS (ESI, [M+H]<sup>+</sup>) m/z calcd for C<sub>18</sub>H<sub>13</sub>N<sub>4</sub>O 301.1089, found 301.1080. <sup>2</sup>Boge, N.; Kruger, S.; Schroder, M.; Meier, C.; *Synthesis* **2007**, 24, 3907-3914.

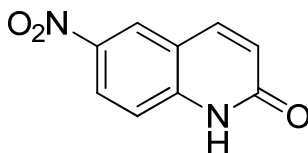


## Synthesis of 52



The compound **44** (0.01 g, 0.0335 mmol) in 70 % EtOH:water (2.5 mL) was added with sodium dithionite( 0.012 g, 0.07 mmol) and was refluxed for 30 min. The reaction mixture was filtered and dried with brine and magnesium sulfate. The crude material was separated by silica gel column chromatography using EtOAc to obtain the product **52**.  $^1\text{H}$  – NMR ( $\text{CDCl}_3$ , 500 MHz):  $\delta$  9.11 (d,  $J = 4.5$  Hz, 2H), 9.01 (d,  $J = 8.0$  Hz, 2H), 8.85 (d,  $J = 9.0$  Hz, 2H), 8.46 (d,  $J = 9.0$  Hz, 2H), 7.43 (dd,  $J = 8.0$  Hz,  $J = 4.5$  Hz, 2H).  $^{13}\text{C}$ -NMR ( $\text{CDCl}_3$ , 125.77 MHz):  $\delta$  152.66, 149.77, 146.06, 136.07, 132.75, 130.81, 123.18, 120.14, 119.28. HRMS (ESI,  $\text{M}+\text{H}^+$ )  $m/z$  calcd  $\text{C}_{18}\text{H}_{11}\text{N}_4$  calculated mass 283.0984; actual mass 283.0982

## Synthesis of 6-nitroquinolone 51

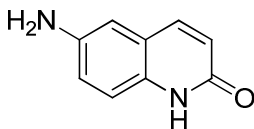


6-nitroquinoline (250 mg, 1.315 mmol) **42** was dissolved in warm DMF (1 mL) and squirted into warm water (300 mL) while stirring vigorously. Then warm sodium phosphate (500 mM, 100 mL, pH 7.4) was added while stirring. Then xanthine oxidase (100  $\mu\text{L}$ , 0.005 U/mL) was added in 12-hour intervals for 3 days. The organic material was extracted to EtOAc and dried using brine and sodium sulfate. The product was

separated by column chromatography using hexane and ethyl acetate to obtain 4 mg of product **51**. The crystals were obtained by dissolving the pure compound in minimum amount of warm ethyl acetate and slow evaporation for 3 days.

$^1\text{H}$  – NMR ( $\text{CD}_3\text{OD}$ , 500 MHz):  $\delta$  8.64 (d,  $J = 2.5$  Hz, 1H), 8.36 (dd,  $J = 9.0$  Hz,  $J = 2.5$  Hz, 1H), 8.09 (d,  $J = 9.0$  Hz, 1H), 7.46 (d,  $J = 9.0$  Hz, 1H), 6.73 (d,  $J = 9.0$  Hz, 1H);  $^{13}\text{C}$ -NMR ( $\text{CD}_3\text{OD}$ , 125.77 MHz)  $\delta$  165.01, 144.11, 144.05, 142.25, 126.28, 125.37, 124.33, 120.63, 117.44 ; HRMS (ESI,  $\text{M}+\text{H}^+$ )  $m/z$  calcd  $\text{C}_9\text{H}_7\text{N}_2\text{O}_3$  calculated mass 191.0457; actual mass 191.0456

#### Synthesis of 6-aminoquinolone **54**



6-nitroquinolone (10 mg, 0.05 mmol) **51** was dissolved in MeOH (10 mL) and was added with Pd on activated carbon (0.5 mg). The hydrogen gas was bubbled for 10 mins. The reaction mixture was filtered and organic material was dried using brine and sodium sulfate. The product was separated by silica gel column chromatography using 1% methanol:ethyl acetate as the mobile solvent system to obtain 2 mg of product **54**.  $^1\text{H}$  – NMR ( $\text{CD}_3\text{OD}$ , 500 MHz,):  $\delta$  7.80 (dd,  $J = 9.0$  Hz,  $J = 3.3$  Hz 1H), 7.16 (d,  $J = 9.0$  Hz, 1H), 7.02 (d,  $J = 9.0$  Hz, 1H), 6.92 (t,  $J = 3.3$ ,  $J = 3.1$  Hz, 1H), 6.54 (dd,  $J = 9.0$  Hz, 3.1 Hz, 1H), 1.28 grease.  $^{13}\text{C}$ -NMR ( $\text{CD}_3\text{OD}$ , 125.77 MHz):  $\delta$  164.59, 144.90, 142.29, 132.46, 122.52, 122.05, 121.45, 117.50, 112.34. HRMS (ESI,  $\text{M}+\text{H}^+$ )  $m/z$  calcd  $\text{C}_9\text{H}_9\text{N}_2\text{O}$  calculated mass 161.0715; actual mass 161.0714

### **Procedure for hypoxic metabolism.**

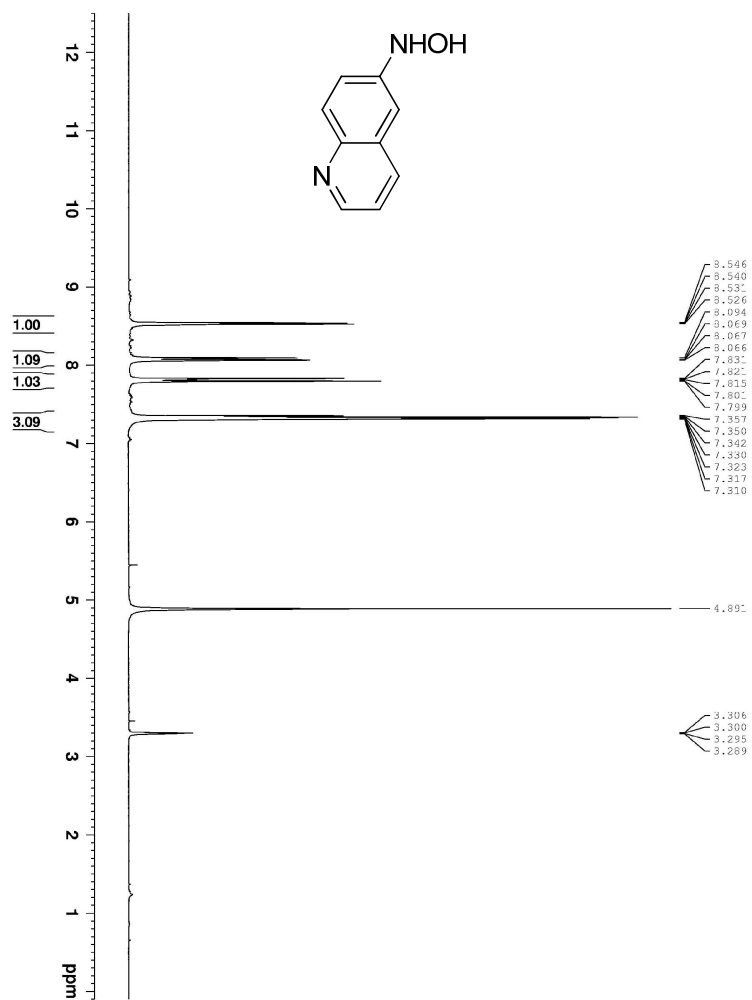
In a typical enzymatic reaction, **42** ( 4  $\mu$ L from 50 mM in DMF, final concentration 0.8 mM), **50**, **51** or non-fluorescent electron acceptor (24  $\mu$ L from 50 mM in 15 % DMF water, final concentration 6.4 mM), was added to xanthine in water(20-160  $\mu$ L of 10 mM, final concentration 0.8 mM-6.4 mM. Then, xanthine oxidase (20  $\mu$ L from 20 U/mL, final concentration 2.4 U/mL), sodium phosphate buffer (6  $\mu$ L from 50 mM, final concentration 12 mM, pH 7.4) and HPLC water were added to xanthine-**42** solution to obtain the final solution (0.25mL, less than 2% DMF) at room temperature (24<sup>0</sup>C). In anaerobic reactions, all reagents except xanthine oxidase were de-gassed in glass tubes by three freeze pump thaw cycles. The glass tubes were broke open inside an argon-purged glove bag and bubbled with argon for five minutes. All reagents were mixed inside the glove bag. Upon mixing, the containers were wrapped with aluminum foil to prevent exposure to light.

### **Procedure for Fluorescence experiment**

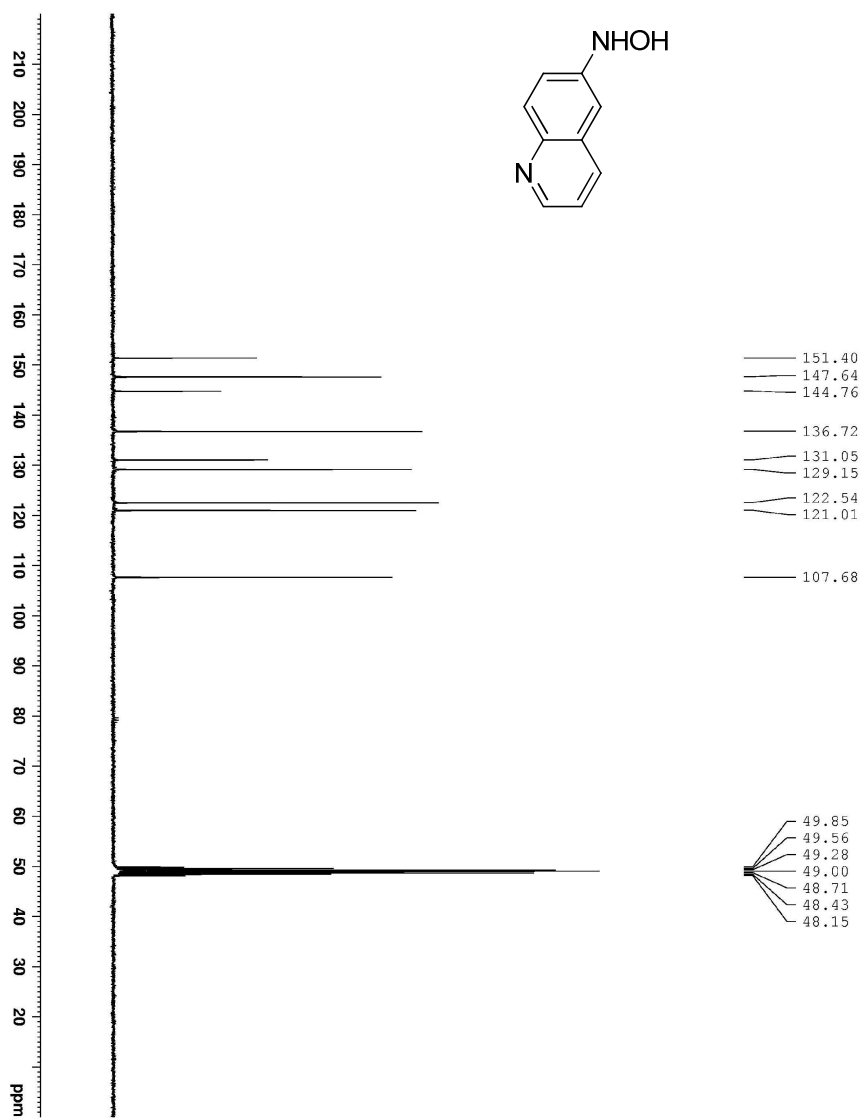
Upon completion of incubation reaction solution was diluted up to 1 mL with sodium phosphate buffer (50 mM, pH 7.4) in HPLC water and then was added to the cuvette. In anaerobic experiments, upon completion the reaction mixtures were taken out of glove bag and kept 1 h under atmospheric conditions prior to the dilutions.

**Procedure for LC/MS analysis.** In vitro enzymatic metabolism of **42** or **50** was carried out as described above and the resulting products were extracted into ethyl acetate and dried using brine followed by roto vap evaporation of ethyl acetate. The solid was re-dissolved in methanol and analyzed by LC/MS in the positive ion mode. Separation of metabolites was carried using a C18 reverse phase Phenomenex Luna column (5  $\mu$ m

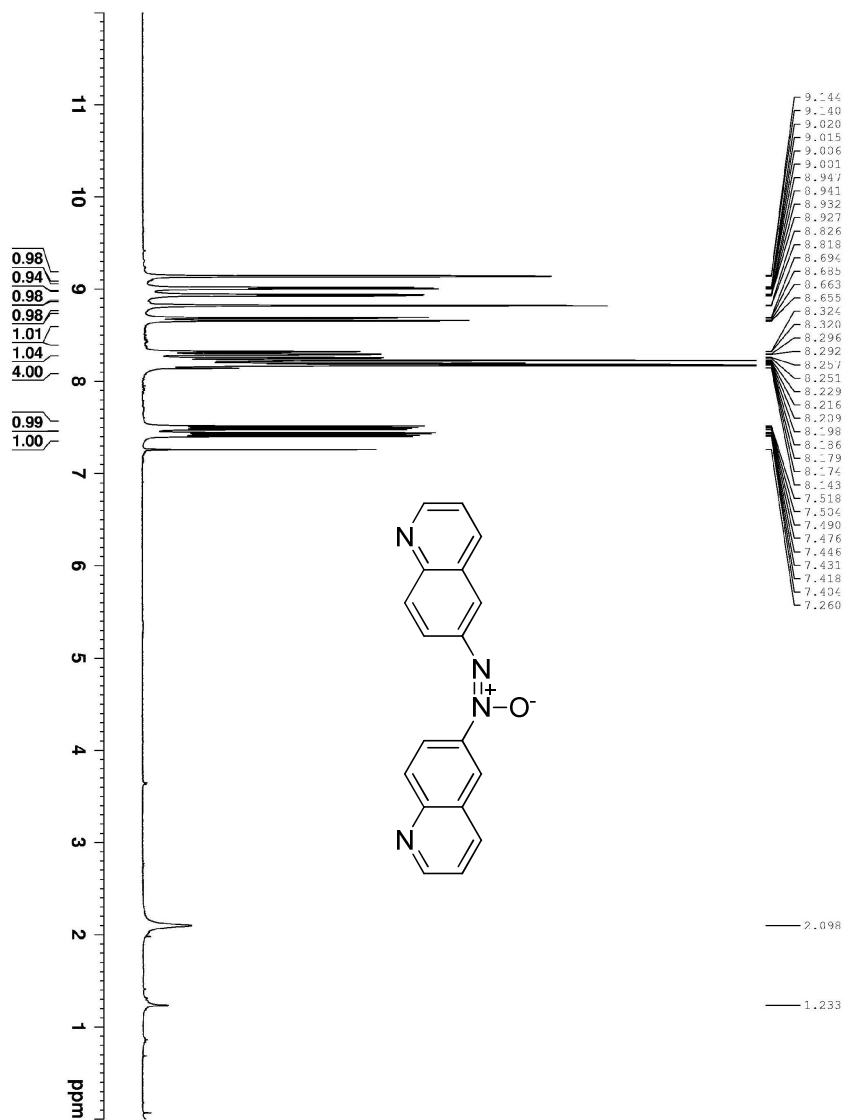
particle size, 100 Å pore size, 150 mm length, 2.00 mm i.d.) and a ThermoSeparations liquid chromatograph (TSP4000) and the metabolites were detected by their UV-absorbance at 254 nm. The elution started with a gradient of A, 99% HPLC water (0.1% acetic acid) and B acetonitrile (0.1% acetic acid) followed by a linear increase to 90 % B over the course of 30 min. The elution was continued at 90% B for 3 min and decreased to 1% over the next 8 min. A flow rate of 0.35 mL/min was used. The LC/ESI-MS analyses were carried out in the positive ion mode on a Finnigan TSQ 7000 triple quadrupole instrument using a 250 kV needle voltage and at a capillary temperature of 250 °C.



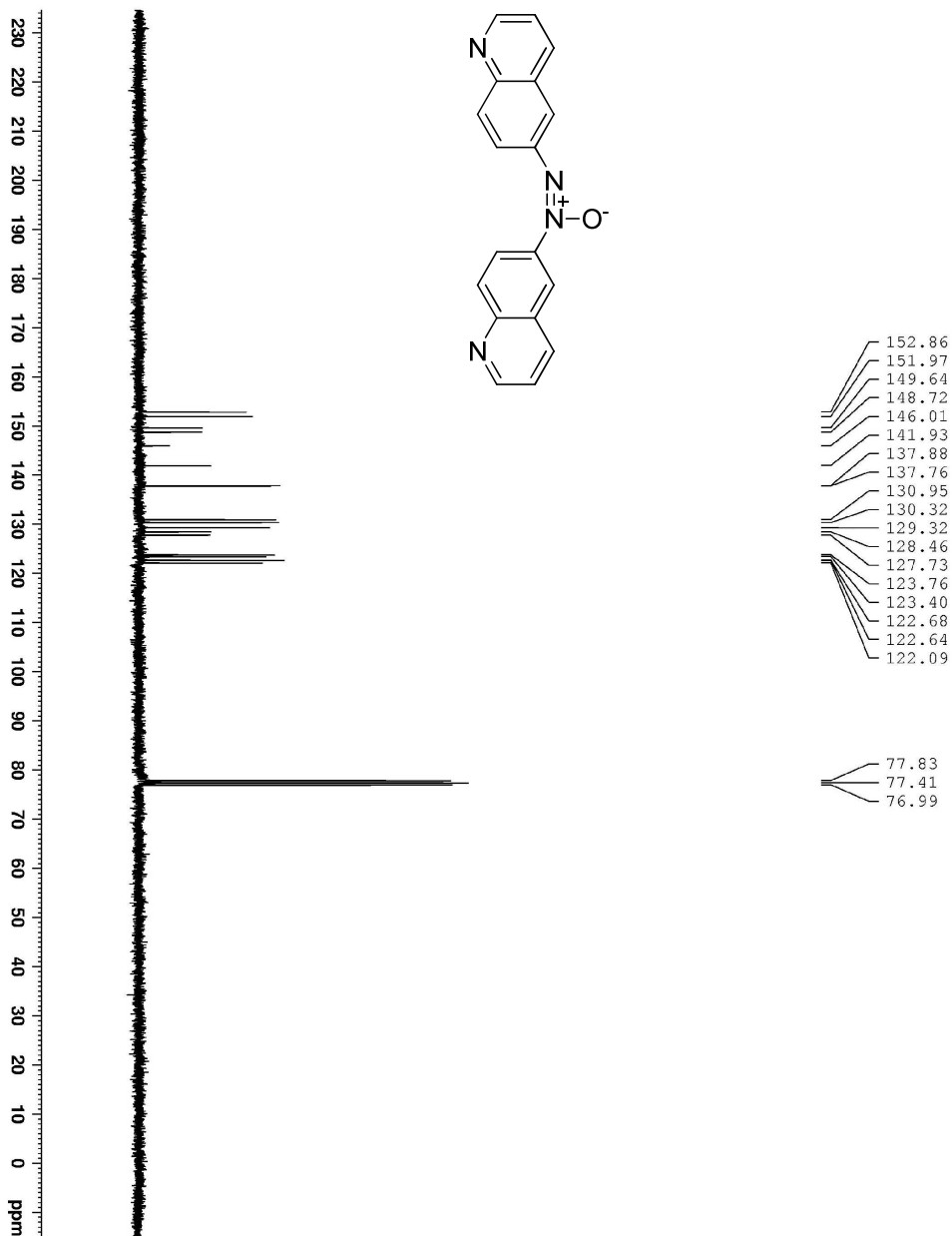
$^1\text{H}$  – NMR of **50** (300 MHz, MeOD)



$^{13}\text{C}$  NMR of **50** (MeOD, 125.77 MHz)

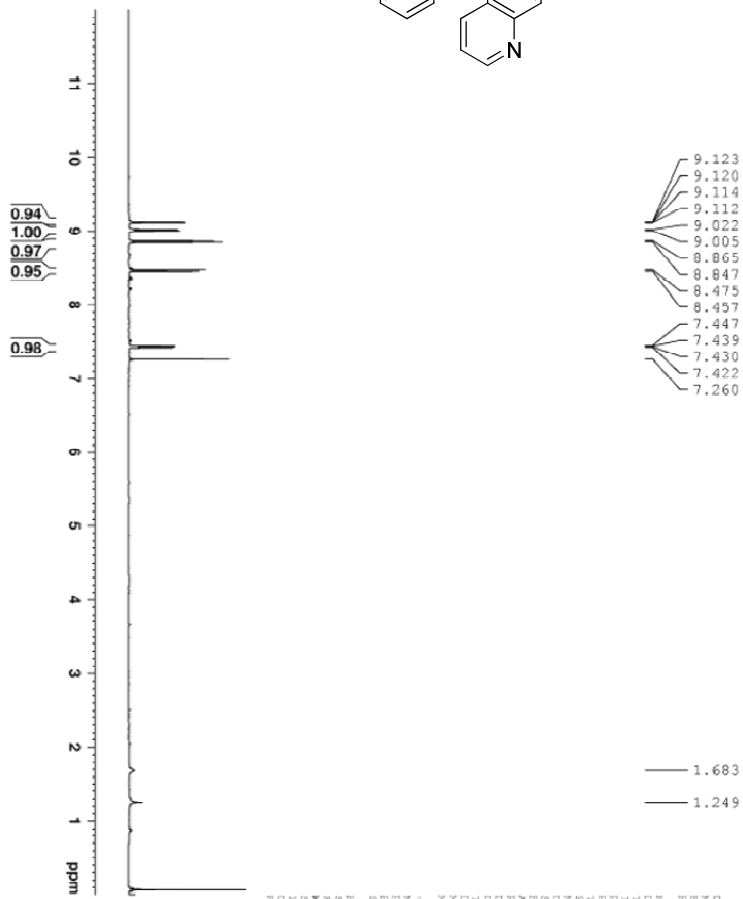
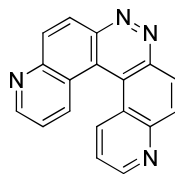


<sup>1</sup>H NMR of **45** (CDCl<sub>3</sub>, 300 MHz)



<sup>13</sup>C NMR of **45** (CDCl<sub>3</sub>, 75.5 MHz)





```

===== CHANNEL f1 =====
NUC1  1H
P1    8.00 uS
P2    4.00 uS
SFO1  500.1335009 MHz

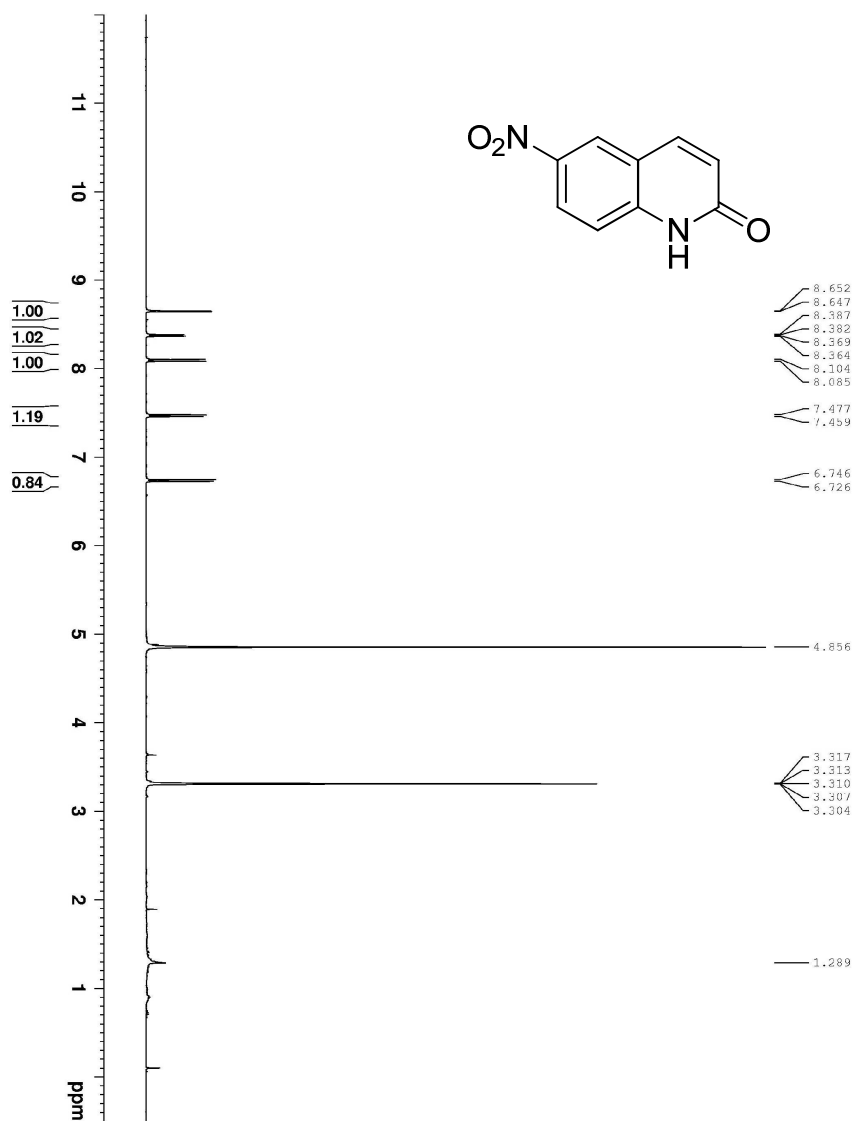
===== Processing parameters =====
SI  - Processing parameters
SF  500.1301351 MHz
RG  32768
AQ  128
RG  128
SI  18
DS  0
PC  1.00

===== Acquisition parameters =====
Date_  20101106
Time  18:58:59
INSTRUM  spect
PROBHD  5 mm CPYCI 1H-
PULPROG  zgpg30
SOLVENT  CDCl3
NS  16
DS  4
AQ  1.0391175 Hz
FIDRES  0.157652 Hz
AQ  3.211922 sec
DE  48.400 uS
DI  6.00 uS
DE  1.0000000 sec
KCMARK  0.0150000 sec
=====
  
```

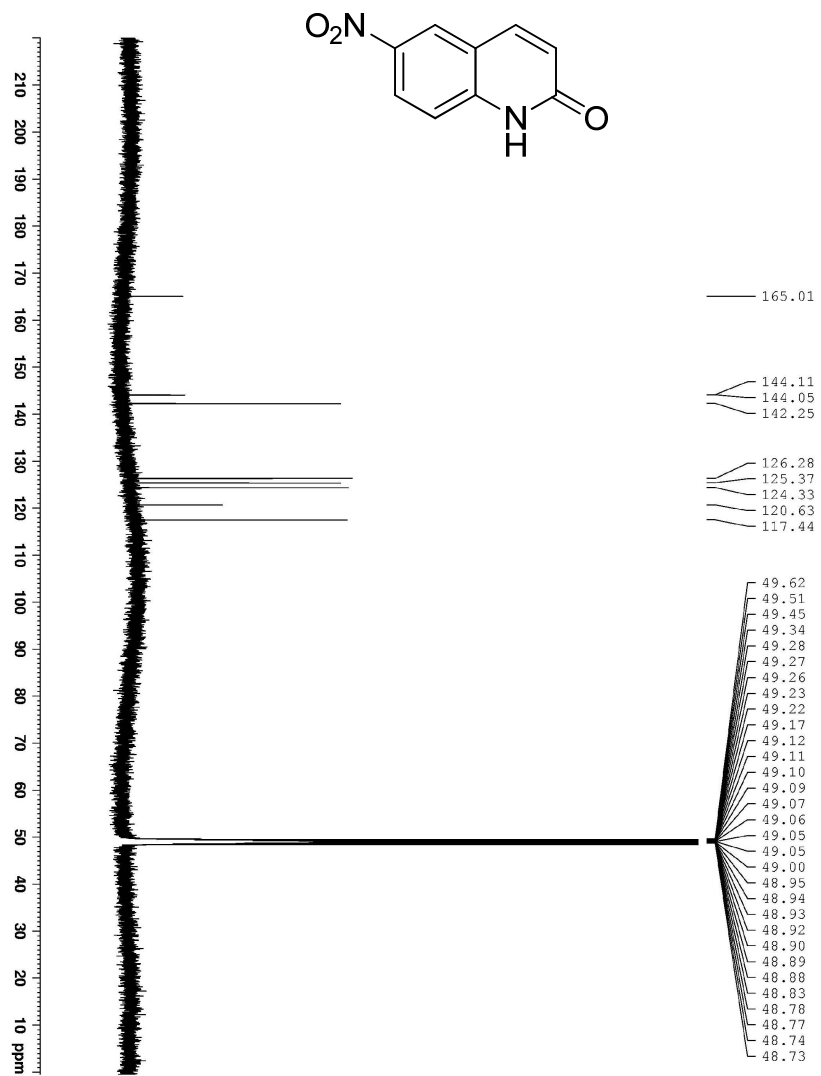
<sup>1</sup>H NMR of **52** (CDCl<sub>3</sub>, 500 MHz)



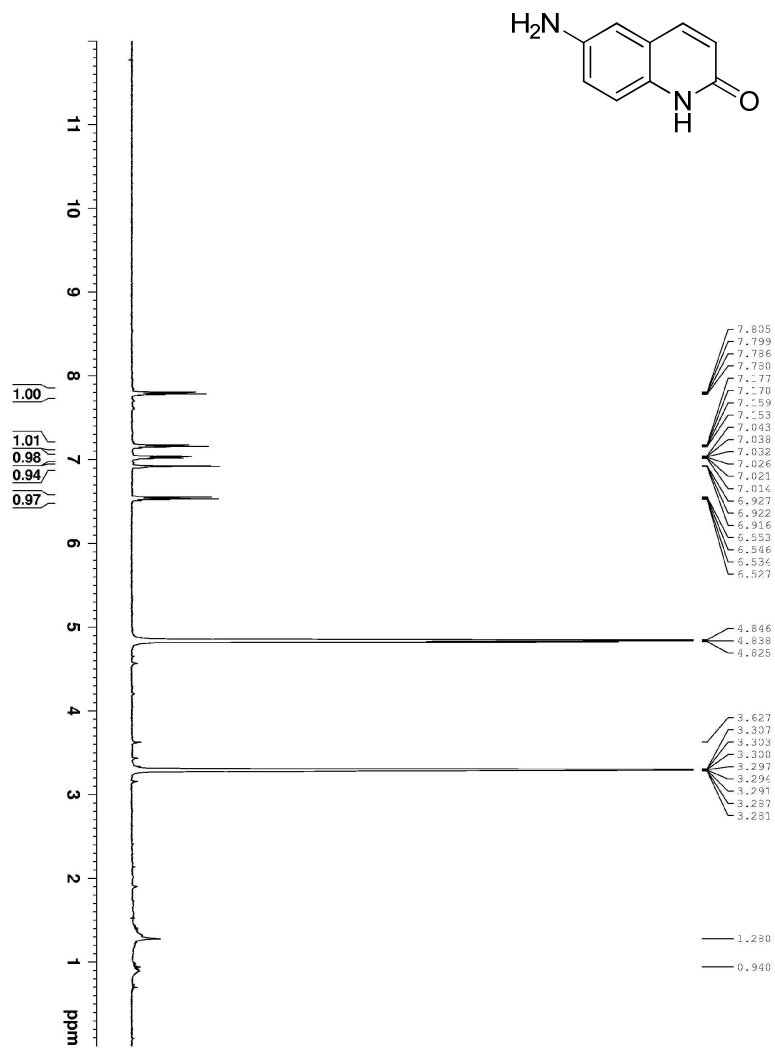
<sup>13</sup>C NMR of **52** (CDCl<sub>3</sub>, 125.77 MHz)



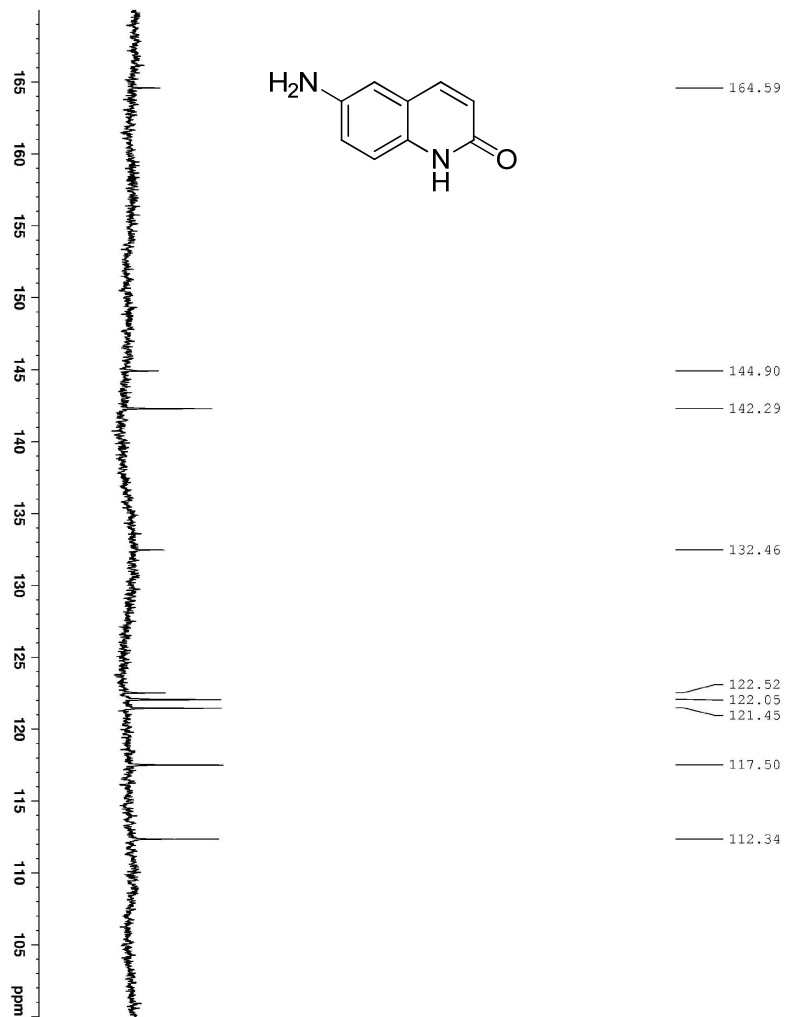
<sup>1</sup>H – NMR of **51** (500 MHz, MeOD)



$^{13}\text{C}$  NMR of **51** (MeOD, 125.77 MHz)



<sup>1</sup>H NMR of **54** (CDCl<sub>3</sub>, 500 MHz)



$^{13}\text{C}$  NMR of **54** (CDCl<sub>3</sub>, 125.77 MHz)

### References of chapter 3

1. Tomlinson, R. H.; Gray, L. H., The histological structure of some human lung cancers and the possible implications for radiotherapy. *Br. J. Cancer* **1955**, *9*, 539-549.
2. (a) Vaupel, P.; Kallinowski, F.; Okunieff, P., Blood flow, oxygen and nutrient supply, and metabolic microenvironment of human tumors: a review. *Cancer Res.* **1989**, *49* (23), 6449-6465; (b) Brown, J. M.; Wilson, W. R., Exploiting tumor hypoxia in cancer treatment. *Nature Rev. Cancer* **2004**, *4* (6), 437-447; (c) Brown, J. M., The hypoxic cell: A target for selective cancer therapy. *Cancer Res.* **1999**, *59*, 5863-5870.
3. Bertout, J. A.; Patel, S. A.; Simon, M. C., The impact of O<sub>2</sub> availability on human cancer. *Nat. Rev. Cancer* **2008**, *8* (Dec ), 967-975.
4. Vaupel, P., Hypoxia and Aggressive tumor phenotype: Implications for therapy and prognosis. *Oncologist* **2008**, *13* (suppl 3), 21-26.
5. (a) Hill, R. P.; Delphine, T. M.-E.; Hedley, D. W., Cancer stem cells, hypoxia and metastasis. *Semin. Radiat. Oncol.* **2009**, *19* (2), 106-111; (b) Vaupel, P.; Mayer, A., Hypoxia in cancer: significance and impact on clinical outcome. *Cancer Metastasis Rev.* **2007**, *26*, 225-239.
6. (a) Wardman, P.; Clarke, E. D.; Hodgkiss, R. J.; Middleton, R. W.; Parrick, J.; Stratford, M. R. L., Nitroaryl compounds as potential fluorescent probes for hypoxia. I. Chemical criteria and constraints. *Int. J. Radiat. Oncol. Biol. Phys.* **1984**, *10*, 1347-1351; (b) Stratford, M. R. L.; Clarke, E. D.; Hodgkiss, R. J.; Middleton, R. W.; Wardman, P., Nitroaryl compounds as potential fluorescent probes for hypoxia. II. Identification and properties of reductive metabolites. *Int. J. Radiat. Oncol. Biol. Phys.* **1984**, *10*, 1353-1356; (c) Weissleder, R.; Tung, C.-H.; Mahmood, U.; Bogdanov, A. J., In vivo imaging of tumors with protease-activated near-infrared fluorescent probes. *Nature Biotechnol.* **1999**, *17*, 375-378.
7. (a) Fitzsimmons, S. A.; Workman, P. A.; Grever, M.; Paull, K.; Camalier, R.; Lewis, A. D., Reductase enzyme expression across the National Cancer Institute tumor cell line panel: correlation with sensitivity to mitomycin C and E09. *J. Natl. Cancer Inst.* **1996**, *88*, 259-269; (b) Wardman, P.; Dennis, M. F.; Everett, S. A.; Patel, K. B.; Stratford, M. R. L.; Tracy, M., Radicals from one-electron reduction of nitro compounds, aromatic N-oxides and quinones: the kinetic basis for hypoxia-selective, bioreductive drugs. *Biochem. Soc. Trans* **1995**, *61*, 171-194; (c) Rooseboom, M.; Commandeur, J. N.

M.; Vermeulen, N. P. E., Enzyme-catalyzed activation of anticancer prodrugs. *Pharm. Rev.* **2004**, *56*, 53-102; (d) Denny, W. A.; Wilson, W. R., Considerations for the design of nitrophenyl mustards as agents with selective toxicity for hypoxic tumor cells. *J. Med. Chem.* **1986**, *29* (6), 879-887.

8. Moselen, J. W.; Hay, M. P.; Denny, W. A.; Wilson, W. R., N-[2-(2-Methyl-5-nitroimidazolyl)ethyl]-4-(2-nitroimidazolyl)butanamide (NSC 639862), a bisnitroimidazole with enhanced selectivity as a bioreductive drug. *Cancer Res.* **1995**, *55*, 574-80.

9. Wardman, P.; Candeis, L. P.; Everett, S. A.; Tracy, M., Radiation chemistry applied to drug design. *Int. J. Radiat. Biol.* **1994**, *65*, 35-41.

10. Wilson, W. R.; Anderson, R. F.; Denny, W. A., Hypoxia-selective antitumor agents. 1. Relationships between structure, redox properties and hypoxia-selective cytotoxicity for 4-substituted derivatives of nitracrine. *J. Med. Chem.* **1989**, *32*, 23-30.

11. Duan, J.-X.; Jiao, H.; Kaizerman, J.; Stanton, T.; Evans, J. W.; Lan, L.; Lorente, G.; Banica, M.; Jung, D.; Wang, J.; Ma, H.; Li, X.; Yang, Z.; Hoffman, R. M.; Ammons, W. S.; Hart, C. P.; Matteucci, M., Potent and highly selective hypoxia-activated achiral phosphoramidate mustards as anticancer drugs. *J. Med. Chem.* **2008**, *51*, 2412-2420.

12. (a) Borch, R. F.; Liu, J.; Schmidt, J. P.; Marakovitz, J. T.; Joswig, C.; Gipp, J. J.; Mulcahy, R. T., Synthesis and evaluation of nitroheterocyclic phosphoramidates as hypoxia-selective alkylating agents. *J. Med. Chem.* **2000**, *43*, 2258-2265; (b) Thomson, P.; Naylor, M. A.; Everett, S. A.; Stratford, M. R. L.; Lewis, G.; Hill, S.; Patel, K. B.; Wardman, P.; Davis, P. D., Synthesis and biological properties of bioreductively targeted nitrothienyl prodrugs of combretastatin A-4. *Mol. Cancer. Ther.* **2006**, *5* (11), 2886-2894; (c) Thomson, P.; Naylor, M. A.; Stratford, M. R. L.; Lewis, G.; Hill, S.; Patal, K. B.; Wardman, P.; Davis, P. D., Hypoxia-driven elimination of thiopurines from their nitrobenzyl prodrugs. *Bioorg. Med. Chem. Lett.* **2007**, *17*, 4320-4322.

13. (a) Evans, B. J.; Doi, J. T.; Musker, W. K., Fluorine-19 NMR study of the reaction of p-fluorobenzenethiol and disulfide with periodate and other selected oxidizing agents. *J. Org. Chem.* **1990**, *55* (8), 2337-2344; (b) Koch, C. J., Measurements of absolute oxygen levels in cells and tissues using oxygen sensors and 2-nitroimidazole EF5. *Methods Enzymol.* **2002**, *352*, 3-31.

14. (a) Dai, M.; Zhu, W.; Xu, Y.; Qian, X.; Liu, Y.; Xiao, Y.; You, Y., Versatile nitro-fluorophore as highly effective sensor for hypoxic tumor cells: design, imaging, and



evaluation. *J. Fluoresc.* **2008**, *18* (2), 591-597; (b) Zhu, W.; Dai, M.; Xu, Y.; Qian, X., Novel nitroheterocyclic hypoxic markers for solid tumor: synthesis and biological evaluation. *Bioorg. Med. Chem. Lett.* **2008**, *16*, 3255-3260.

15. Rajapakse, A.; Gates, K. S., Hypoxia-Selective, Enzymatic Conversion of 6-Nitroquinoline into a Fluorescent Helicene: Pyrido[3,2-f]quinolino[6,5-c]cinnoline 3-Oxide. *J. Org. Chem.* **2012**, *77*, 3531-3537.

16. (a) Brynes, P. J.; Bevilacqua, P.; Green, A., 6-Aminoquinoline as a fluorogenic leaving group in peptide cleavage reactions: a new fluorogenic substrate for chymotrypsin. *Anal. Biochem.* **1981**, *116*, 408-413; (b) Danieli, E.; Shabat, D., Molecular probe for enzymatic activity with dual output. *Bioorg. Med. Chem.* **2007**, *15*, 7318-7324; (c) Tanaka, F.; Thayumanavan, R.; Barbas, C. F., Fluorescent detection of carbon-carbon bond formation. *J. Am. Chem. Soc.* **2003**, *125*, 8523-8528; (d) Huang, W.; Hicks, S. N.; Sondek, J.; Zhang, Q., A fluorogenic, small molecule reporter for mammalian phospholipase C isozymes. *ACS Chem Biol.* **2011**, *6* (3), 223-228.

17. (a) Laderoute, K. L.; Wardman, P.; Rauth, M., Molecular mechanisms for the hypoxia-dependent activation of 3-amino-1,2,4-benzotriazine 1,4-dioxide (SR4233). *Biochem. Pharmacol.* **1988**, *37* (8), 1487-1495; (b) Daniels, J. S.; Gates, K. S., DNA Cleavage by the Antitumor Agent 3-Amino-1,2,4-benzotriazine 1,4-Dioxide (SR4233): Evidence for Involvement of Hydroxyl Radical. *J. Am. Chem. Soc.* **1996**, *118* (14), 3380-3385; (c) Birincioglu, M.; Jaruga, P.; Chowdhury, G.; Rodriguez, H.; Dizdaroglu, M.; Gates, K. S., DNA Base Damage by the Antitumor Agent 3-Amino-1,2,4-benzotriazine 1,4-Dioxide (Tirapazamine). *J. Am. Chem. Soc.* **2003**, *125* (38), 11607-11615; (d) Jones, G. D. D.; Weinfeld, M., Dual action of tirapazamine in the induction of DNA strand breaks. *Cancer Res.* **1996**, *56*, 1584-1590.

18. (a) Chowdhury, G.; Kotandeniya, D.; Barnes, C. L.; Gates, K. S., Enzyme-activated, hypoxia-selective DNA damage by 3-amino-2-quinoxalinecarbonitrile 1,4-dioxido. *Chem. Res. Toxicol.* **2004**, *17* (11), 1399-1405; (b) Junnotula, V.; Rajapakse, A.; Abrillaga, L.; Lopez de Cerain, A.; Solano, B.; Villar, R.; Monge, A.; Gates, K. S., DNA strand cleaving properties and hypoxia-selective cytotoxicity of 7-chloro-2-thienylcarbonyl-3-trifluoromethylquinoxaline 1,4-dioxide. *Bioorg. Med. Chem.* **2010**, *18*, 3125-3132.

19. Claassen, V. P.; Oltmann, L. F.; Van't, R. J.; Brinkman, U. A. T.; Stouthamer, A. H., Purification of molybdenum cofactor and its fluorescent oxidation products. *FEBS Lett.* **1982**, *142*, 133-7.

20. (a) Pizzolatti, M. G.; Yunes, R. A., Azoxybenzene formation from nitrosobenzene and phenylhydroxylamine. A unified view of the catalysis and mechanisms of the reactions. *J. Chem. Soc. Perkin 2* **1990**, 759-764; (b) Agrawal, A.; Tratnyek, P. G., Reduction of nitroaromatic compounds by zero-valent iron metal. *Env. Sci. Technol.* **1996**, *30* (1), 153-160.
21. (a) Furst, A.; Moore, R. E., Reductions with hydrazine hydrate catalyzed by Raney nickel. II. Aromatic nitro compounds to intermediate products. *J. Am. Chem. Soc.* **1957**, *79*, 5492-5493; (b) Fletcher, T. L.; Namkung, M. J., Derivatives of fluorene. IV. Raney nickel-hydrazine hydrate reduction of various mono- and dinitrofluorene derivatives; some new 9-substituted fluorenes. *J. Org. Chem.* **1958**, *23*, 680-683.
22. (a) Krenitsky, T. A.; Neil, S. M.; Elion, G. B.; Hitchings, G. H., A comparison of the specificities of xanthine oxidase and aldehyde oxidase. *Arch. Biochem. Biophys.* **1972**, *150*, 585-599; (b) McCormack, J. J.; Allen, B. A.; Hodnett, C. N., Oxidation of quinazoline and quinoxaline by xanthine oxidase and aldehyde oxidase. *J. Heterocyclic Chem.* **1978**, *15*, 1249-1254; (c) Rastelli, G.; Costantino, L.; Albasini, A., A model of the interaction of substrates and inhibitors with xanthine oxidase. *J. Am. Chem. Soc.* **1997**, *119*, 3007-3016; (d) Ganley, B.; Chowdhury, G.; Bhansali, J.; Daniels, J. S.; Gates, K. S., Redox-activated, hypoxia-selective DNA cleavage by quinoxaline 1,4-di-N-oxide. *Bioorg. Med. Chem.* **2001**, *9*, 2395-2401.
23. (a) Walton, M. I.; Wolf, C. R.; Workman, P., Molecular enzymology of the reductive bioactivation of hypoxic cell cytotoxins. *Int. J. Radiat. Oncol. Biol. Phys.* **1989**, *16*, 983-986; (b) Wen, B.; Coe, K. J.; Rademacher, P.; Fitch, W. L.; Monshouwer, M.; Nelson, S. D., Comparison of in vitro bioactivation of flutamide and its cyano analogue: evidence for reductive activation by human NADPH:cytochrome P450 reductase. *Chem. Res. Toxicol.* **2008**, *21* (12), 2393-2406.
24. Kazanis, S.; McClelland, R. A., Electrophilic intermediate in the reaction of glutathione with nitrosoarenes. *J. Am. Chem. Soc.* **1992**, *114*, 3052-3059.
25. Chen, Y.; Hu, L., Design of anticancer prodrugs for reductive activation. *Med. Res. Rev.* **2009**, *29* (1), 29-64.

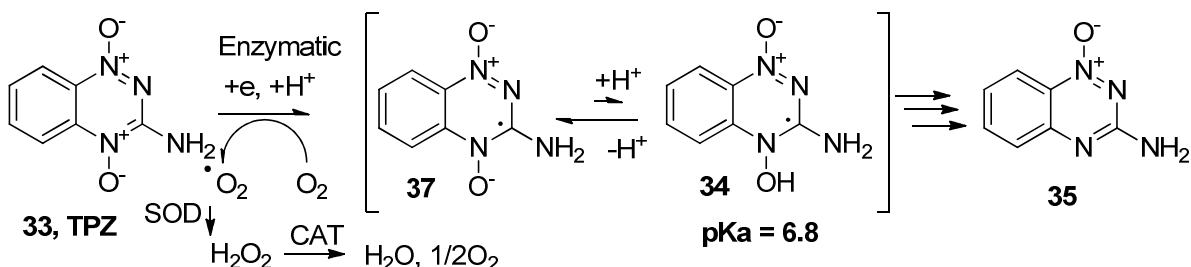
## Chapter 4

### Mechanistic analysis related to the oxidative DNA Damage caused by 1,2,4-benzotriazine-di-oxides, TPZ and analogs of TPZ

#### 4.1 Introduction

Tirapazamine, **33**, (TPZ), 3-amino-1,2,4-benzotriazine 1,4-dioxide is currently in phase I, II and III clinical trials for tumor therapy.<sup>1</sup> TPZ emerged as the lead compound among di *N*-oxide bio-reductive drugs.<sup>2</sup> TPZ causes cytotoxicity to cell, as found in low oxygenated regions (hypoxic) in solid tumors.<sup>3</sup> It is believed that the anti-cancer activity caused by TPZ originates from its ability to cleave DNA under hypoxia.<sup>4</sup> The DNA damage, caused to tumor cells by TPZ arises from the drug radical anion, which is produced by the reduction of TPZ by cellular reductases under low oxygen levels.<sup>5</sup> The enzymatic reduction of TPZ is an oxygen sensitive reaction.<sup>3a, 6</sup> The oxygen sensitivity is due to the oxidation of TPZ radical anion **37**, which is formed by the main forward reduction step, back to the parent TPZ.<sup>7</sup> Molecular oxygen forms superoxide radical in the back oxidation step.<sup>8</sup> The oxidative stress arises due to the superoxide radical formation, in normal oxygenated conditions, but this process is reduced by cellular defense system against reactive oxygen species, which is a collection of enzymes such as glutathione peroxidase, peroxiredoxins, catalase, and superoxide dismutase.<sup>9</sup> In hypoxia TPZ radical anion **37** gets protonated to a drug radical **34**.<sup>10</sup> DNA is the prime target of

the oxidizing species generated following the reduction of TPZ.<sup>11</sup> The neutral drug radical **34** generates a DNA damaging radical species before ultimately producing the major metabolite **35** (Scheme 4.1).<sup>12</sup>



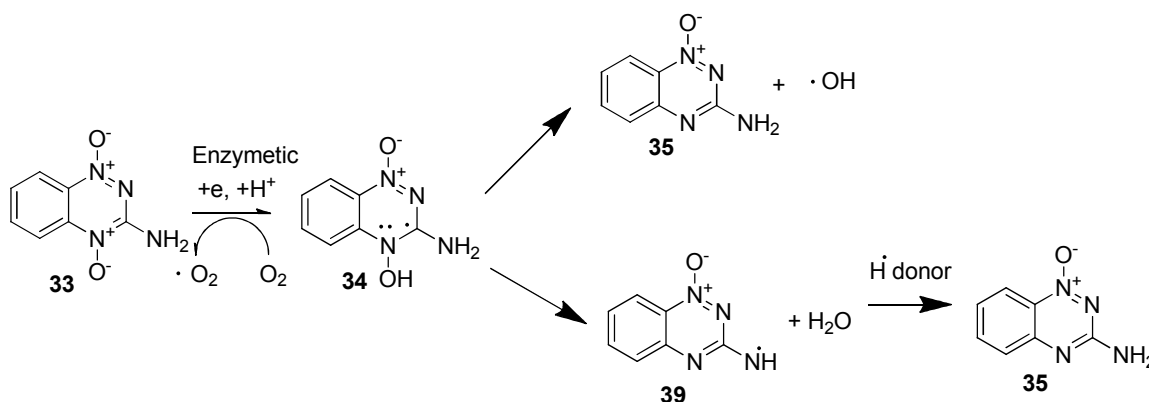
**Scheme 4.1.** Enzymatic reduction of **33** produces DNA damaging radicals and oxidative stress

The oxidative damage to DNA, caused by TPZ is characterized as proton abstraction from deoxyribose sugar backbone and DNA bases.<sup>5b</sup> The oxidative damage to DNA leads to DNA strand breaks.<sup>13</sup> The chemical nature of the DNA damaging species that is emitted during the oxygen sensitive enzymatic reduction of TPZ is not completely characterized.<sup>10, 14</sup>

#### 4.2 Mechanistic evidence for the oxidizing radical formation by TPZ

Research carried out by our group suggests that the activated TPZ produces a radical anion **37** and under low oxygen levels **37** undergoes protonation to produce **34**, followed by a homolytic bond scission on **34** releases hydroxyl radical and produces 1-*N*-oxide metabolite **35**.<sup>4a, 14c, 15</sup> Similar homolytic fragmentation is proposed on Barton's *N*-hydroxypyridinethione esters in literature.<sup>16</sup> Another report on *N*-(alkoxy) pyridinium salts discusses homolytic fragmentation induced by photo-induction.<sup>17</sup> Moreover, radical scavenging experiments and DNA cleavage pattern studies suggest that homolytic fragmentation of di-*N*-oxides such as **34** to produce hydroxyl radical is chemically

plausible.<sup>4a, 14c</sup> Another hypothesis proposed by Denny and co-workers, suggests that **34** undergoes dehydration to form benzotriazinyl radical **38** and they provide evidence for **38** as the species that is responsible for the DNA damage caused by TPZ.<sup>10, 14a, b</sup> Intermediate **34** is, generated radiolytically and has been tested for DNA damage.<sup>18</sup> Similar organic radical formation is reported when hydroxyl radicals are generated by pulse radiolysis in the presence of toluene to produce benzyl radicals.<sup>19</sup>



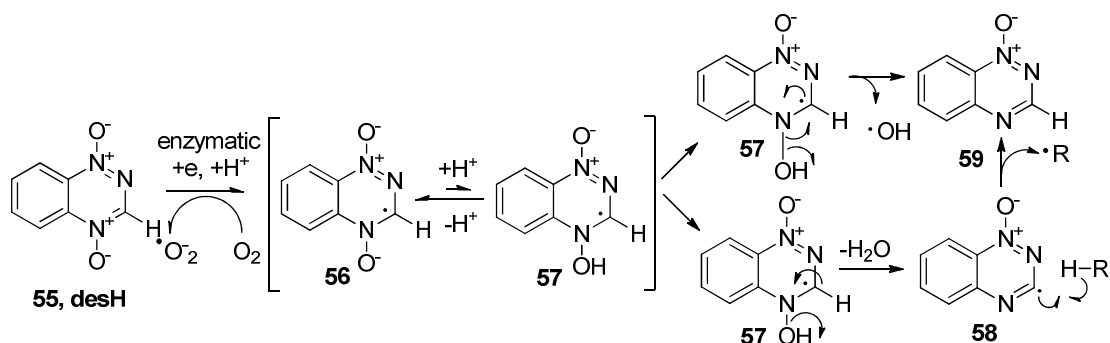
**Scheme 4.2.** Different mechanisms are proposed to explain enzymatic metabolism of **33**

We feel that mechanistic investigation of bio-reductive activation of TPZ under low oxygen concentrations may provide a better understanding on the chemical structure of the DNA damaging species and could be important in designing novel TPZ analogs.

### 4.3 Hypothesis and design of experiments

The benzotriazine 1,4-dioxide analog (desH) **55** may be used to analyze the dehydration mechanism of benzotriazine di-oxides. Metabolic studies of **55** when **55** was enzymatically reduced, in hypoxia may produce **59** as the major metabolite.<sup>20</sup> The enzymatic metabolism of **55** might be similar to that of 1,2,4-benzotriazine 1,4-dioxide drug class; the major metabolite formed is 1,2,4-benzotriazine 1-mono-oxide.<sup>14c</sup> The reduction profile of **55** mirrors the metabolism of 1,2,4-benzotriazine 1,4-dioxide

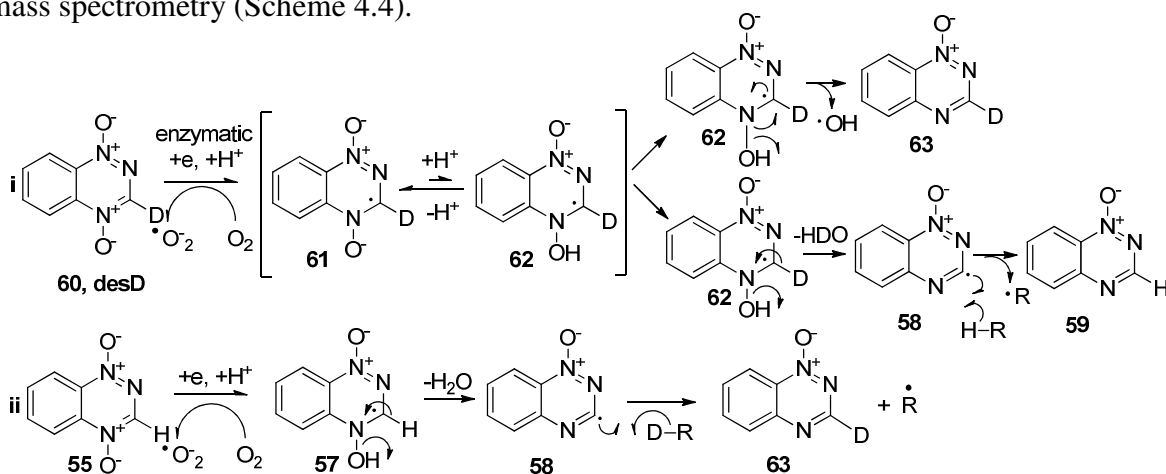
(Scheme 4.3).<sup>20</sup> In the enzyme mediated, one electron reduction of **55**, radical anion **56**, is produced and under normal oxygen concentration, **56** can be oxidized back to **55**.<sup>20</sup> Under hypoxia **56** gets protonated to form the drug radical **57**, which produces the DNA damaging species and the major metabolite **59**.<sup>20b</sup> The dehydration mechanism produces radical **58** by eliminating a water molecule. The radical **58** may abstract a proton from an organic substrate to undergo re-aromatization to form **59** (lower arm). Alternatively, hydroxyl radical mechanism performs homolytic fragmentation on **57** to produce hydroxyl radical and the major metabolite **59**.



**Scheme 4.3.** Enzymatic reduction of **55** under low oxygen concentrations forms major metabolite **59**

In the design, we speculated that deuterated analog of 1,2,4-benzotriazine- 1,4-dioxide **60** (desD) may offer a new approach to analyze the dehydration mechanism. When 1,2,4-benzotriazine- 1,4-dioxide **60** is reductively activated to radical anion **61**, protonation occurs to form neutral radical **62**. The homolytic fragmentation of **63** produces hydroxyl radical and the major metabolite **63**. When the dehydration mechanism occurs on **60**, the neutral drug radical **62** converts to radical **58** and **58** may abstract a deuterium from an organic substrate to produce **63**. Similarly, when **55** is reductively activated under hypoxia, in the presence of a deuterated organic substrate, the

dehydration mechanism might produce radical **58** and, upon deuterium abstraction major metabolite **63**. Accordingly, the loss or incorporation of deuterium/hydrogen can be detected when the isotopic content of the major metabolite 1-oxide is analyzed using mass spectrometry (Scheme 4.4).



**Scheme 4.4.** Isotopic content of major metabolite of **55/60** determines mechanism

#### 4.4 Examine the dehydration mechanism in relation to the release of oxidizing species from 1,2,4-benzotriazine-di-oxide

Various TPZ analogs such as 3-methyl-1,2,4-benzotriazine 1,4-dioxide (Me-TPZ) and 1,2,4-benzotriazine 1,4-dioxide, **55**, have been used in cytotoxicity assays.<sup>21</sup> The anti-cancer activity of these analogs is similar and comparable to that of TPZ. Structurally and functionally similar benzotriazine di-oxide analogs can be used as tools to study the chemical nature of DNA damaging species and mechanism for the formation of DNA damaging species.<sup>14b, c, 22</sup> A study carried out by Raman Junnotula in our group used 3-methyl-1,2,4-benzotriazine 1,4-dioxide (MeTPZ) to investigate the formation of benzotriazinyl radical and explored the dehydration mechanism.<sup>20b</sup> The current chapter describes a similar related mechanistic study. In the beginning, compounds **55** and **60** are

synthesized. The metabolism and DNA damaging properties of **55** and **60** were compared against TPZ for their ability to cause DNA damage under reductive enzyme activated hypoxic conditions.

#### **4.5 Chemical Synthesis of 1,2,4-benzotriazine-1,4-dioxide**

The compound 1,2,4-benzotriazine 1,4-dioxide **55** was obtained by known methods using TPZ as the starting material in the preparation. Briefly, in an argon-purged glove bag two glass vials were added with TPZ in anhydrous DMF and *tert*-butyl nitrite in anhydrous DMF (argon was purged upon preparing stock solutions). Then, the *tert*-butyl nitrite solution was heated to 65<sup>0</sup>C, and to this TPZ in DMF was added slowly over 10 min. Then the mixture was cooled to room temperature. The solution was removed from the glove bag, and DMF was removed using high vacuum. Brownish yellow crude material was used to perform column chromatography, followed by preparative thin layer chromatography separated product **55**. The deuterated analog **60** was prepared using deuterated DMF as the solvent. Synthesis of **55** was followed exactly to prepare and separate **60**. The compound 3-amino 1,2,4-benzotriazine 1-*N* oxide **35** was used as the starting material to prepare 1,2,4-benzotriazine 1-*N* oxides **59** and **63**. Same procedure, which was followed to synthesize **55** was adopted in the preparation of **59**.and **63**, using deuterated DMF as the solvent.

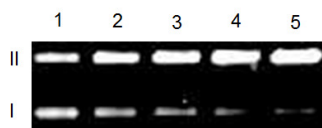
#### **4.6 DNA-damaging properties of 1,2,4-benzotriazine-1,4-dioxide analogs and TPZ**

##### **4.6.1 TPZ analogs perform concentration dependent DNA damage**

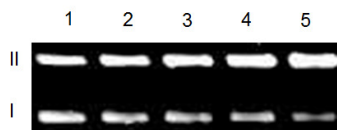
Cytotoxicity caused by TPZ and 1,2,4-benzotriazine-1,4-dioxide **55** are similar.<sup>21a</sup> In TPZ, the cytotoxicity derives from its ability to initiate oxidative damage to cellular



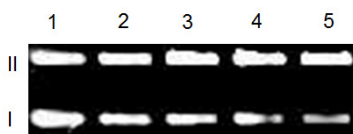
DNA. In the current work, the damage to DNA caused by TPZ was analyzed using plasmid DNA damage based assays. In the plasmid DNA-based assay, the supercoiled form I DNA molecule converts to form II when a hydrogen atom is abstracted from the sugar phosphate backbone. The DNA which is nicked will be converted to form II and intact DNA, the form I, is detected and quantified on agarose gel-based method.<sup>23</sup> Similar DNA-damaging study with **55** and **60** provides a comparative DNA damage study among TPZ drug class. In the anaerobic assays TPZ, **55** or **60** were activated using NADPH:cytochrome P450 reductase and upon activation the oxidative DNA damage would assume on plasmid DNA. Gel pictures obtained upon completion of assays, conducted using **TPZ**, **55** and **60** showed an increase in the amount of form II DNA with the concentration of respective di- *N*-oxide (Figures 4.1, 4.2 and 4.3).



**Figure 4.1:** Cleavage of supercoiled plasmid DNA by **33** (50-250  $\mu\text{M}$ ) in the presence of NADPH:cytochrome P450 reductase as an activating system. All reactions contained DNA (33  $\mu\text{g}/\text{mL}$ , pGL-2 Basic), sodium phosphate buffer (50 mM, pH 7.0), acetonitrile (2.5% v/v), catalase (100  $\mu\text{g}/\text{mL}$ ), superoxide dismutase (10  $\mu\text{g}/\text{mL}$ ), and desferal (1 mM) and were incubated under anaerobic conditions at 24  $^{\circ}\text{C}$  for 6 h, followed by agarose gel electrophoretic analysis. lane 1, **33** (50  $\mu\text{M}$ ) + NADPH (500  $\mu\text{M}$ ) + reductase (33 mU/mL) ( $S = 0.75 \pm 0.04$ ); lane 2, **33** (100  $\mu\text{M}$ ) + NADPH (500  $\mu\text{M}$ ) + reductase (33 mU/mL) ( $S = 1.25 \pm 0.14$ ); lane 3, **33** (150  $\mu\text{M}$ ) + NADPH (500  $\mu\text{M}$ ) + reductase (33 mU/mL) ( $S = 1.74 \pm 0.21$ ); lane 4, **33** (200  $\mu\text{M}$ ) + NADPH (500  $\mu\text{M}$ ) + reductase (33 mU/mL) ( $S = 2.58 \pm 0.14$ ); lane 5, **33** (250  $\mu\text{M}$ ) + NADPH (500  $\mu\text{M}$ ) + reductase (33 mU/mL) ( $S = 3.53 \pm 0.32$ ).The value  $S$  represents the mean number of strand breaks per plasmid molecule and is calculated using the equation  $S = -\ln f_1$ , where  $f_1$  is the fraction of plasmid present as form I.



**Figure 4.2:** Cleavage of supercoiled plasmid DNA by **55** (50-250  $\mu\text{M}$ ) in the presence of NADPH:cytochrome P450 reductase as an activating system. All reactions contained DNA (33  $\mu\text{g}/\text{mL}$ , pGL-2 Basic), sodium phosphate buffer (50 mM, pH 7.0), acetonitrile (2.5% v/v), catalase (100  $\mu\text{g}/\text{mL}$ ), superoxide dismutase (10  $\mu\text{g}/\text{mL}$ ), and desferal (1 mM) and were incubated under anaerobic conditions at 24  $^{\circ}\text{C}$  for 6 h, followed by agarose gel electrophoretic analysis. lane 1, **55** (50  $\mu\text{M}$ ) + NADPH (500  $\mu\text{M}$ ) + reductase (33 mU/mL) ( $S = 0.77 \pm 0.02$ ); lane 2, **55** (100  $\mu\text{M}$ ) + NADPH (500  $\mu\text{M}$ ) + reductase (33 mU/mL) ( $S = 1.10 \pm 0.08$ ); lane 3, **55** (150  $\mu\text{M}$ ) + NADPH (500  $\mu\text{M}$ ) + reductase (33 mU/mL) ( $S = 1.27 \pm 0.07$ ); lane 4, **55** (200  $\mu\text{M}$ ) + NADPH (500  $\mu\text{M}$ ) + reductase (33 mU/mL) ( $S = 1.71 \pm 0.17$ ); lane 5, **55** (250  $\mu\text{M}$ ) + NADPH (500  $\mu\text{M}$ ) + reductase (33 mU/mL) ( $S = 2.19 \pm 0.20$ ).The value  $S$  represents the mean number of strand breaks per plasmid molecule and is calculated using the equation  $S = -\ln f_I$ , where  $f_I$  is the fraction of plasmid present as form I.<sup>24</sup>

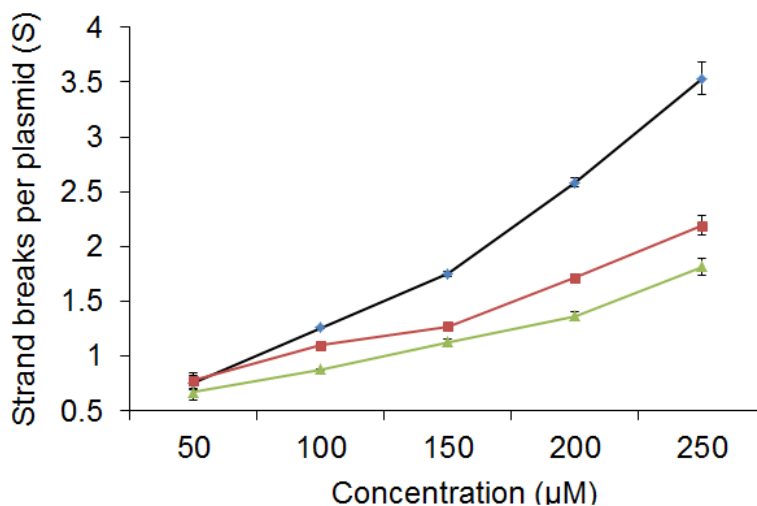


**Figure 4.3:** Cleavage of supercoiled plasmid DNA by **60** (50-250  $\mu\text{M}$ ) in the presence of NADPH:cytochrome P450 reductase as an activating system. All reactions contained DNA (33  $\mu\text{g}/\text{mL}$ , pGL-2 Basic), sodium phosphate buffer (50 mM, pH 7.0), acetonitrile (2.5% v/v), catalase (100  $\mu\text{g}/\text{mL}$ ), superoxide dismutase (10  $\mu\text{g}/\text{mL}$ ), and desferal (1 mM) and were incubated under anaerobic conditions at 24  $^{\circ}\text{C}$  for 6 h, followed by agarose gel electrophoretic analysis. lane 1, **60** (50  $\mu\text{M}$ ) + NADPH (500  $\mu\text{M}$ ) + reductase (33 mU/mL) ( $S = 0.66 \pm 0.04$ ); lane 2, **60** (100  $\mu\text{M}$ ) + NADPH (500  $\mu\text{M}$ ) + reductase (33 mU/mL) ( $S = 0.87 \pm 0.07$ ); lane 3, **60** (150  $\mu\text{M}$ ) + NADPH (500  $\mu\text{M}$ ) + reductase (33 mU/mL) ( $S = 1.12 \pm 0.12$ ); lane 4, **60** (200  $\mu\text{M}$ ) + NADPH (500  $\mu\text{M}$ ) + reductase (33 mU/mL) ( $S = 1.36 \pm 0.03$ ); lane 5, **60** (250  $\mu\text{M}$ ) + NADPH (500  $\mu\text{M}$ ) + reductase (33 mU/mL) ( $S = 1.81 \pm 0.22$ ).The value  $S$  represents the mean number of strand breaks per plasmid molecule and is calculated using the equation  $S = -\ln f_I$ , where  $f_I$  is the fraction of plasmid present as form I.

The amount of nicking can be represented as  $S$  values ( $S = -\ln f_I$ , where  $f_I$  is the fraction of plasmid present as form I) of **TPZ**, **55** and **60**. The  $S$  values of **TPZ**, **55** and **60** show a positive correlation between DNA strand cleavage and respective drug

concentration. As the concentration of drug is increased, under identical enzyme mediated reductive activation, the DNA damage is increased (Figures 4.1, 4.2, 4.3 and 4.4). This behavior is a reported trend among *N*-di-oxides when they are metabolized in the presence of plasmid DNA under reductively activated hypoxic conditions.<sup>25</sup> In addition, control experiments were carried out without the activating enzyme, substrate or drugs to show that the observed DNA damage occurs solely due to the reductively activation of di-*N*-oxides. Reductive activation, under aerobic conditions, of TPZ, **55** or **60** is unable to produce considerable DNA damage compared to anaerobic reactions (Table 1).

#### 4.6.2 DNA damage is decreased by radical scavengers

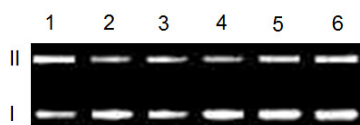


**Figure 4.4.** Comparison of DNA cleavage by reductively activated **33**, **55** and **60** under anaerobic conditions (black line-strand cleavage by **33**, red line-**55** and green line-**60**). Supercoiled plasmid DNA (33 µg/mL, pGL-2 Basic) was incubated with drug (50-250 µM), NADPH (500 µM), cytochrome P450 reductase (33 mU/mL), catalase (100 µg/mL), superoxide dismutase (10 µg/mL), sodium phosphate buffer (50 mM, pH 7.0), acetonitrile (0.5-2.5% v/v), and desferal (1 mM) under anaerobic conditions at room temperature for 6 h, followed by agarose gel electrophoretic analysis. The values, *S*, derived from agarose gel data and represent the mean number of strand breaks per plasmid molecule and were calculated using the equation  $S = -\ln f_i$ , where  $f_i$  is the fraction of plasmid present as form I.<sup>24</sup> Background cleavage in the untreated plasmid was subtracted to allow direct comparison of DNA cleavage yields between different experiments.

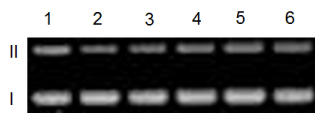
<b>Reaction</b>	<b>% form II</b>	<b>S value</b>
DNA alone	17.4	0.19±0.07
NADPH:cytochrome P450 reductase/NADPH aerobic	14.3	0.15±0.06
NADPH:cytochrome P450 reductase	17.3	0.19±0.02
<b>55</b> alone	16.5	0.18±0.03
<b>55</b> +NADPH:cytochromeP450 reductase/NADPH aerobic	17.0	0.18±0.03
<b>60</b> alone	29.3	0.38±0.70
<b>60</b> +NADPH:cytochromeP450 reductase/NADPH aerobic	25.8	0.29±0.74
<b>55</b> alone	16.5	0.18±0.03
<b>55</b> +NADPH:cytochromeP450 reductase/NADPH aerobic	17.0	0.18±0.03
<b>33</b> alone	11.6	0.19±0.01
<b>33</b> +NADPH:cytochromeP450 reductase/NADPH aerobic	20.7	0.23±0.08

**Table 4.1.** Cleavage of plasmid DNA in control reactions

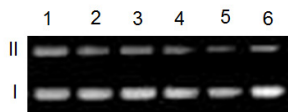
To test the chemical nature of the DNA damaging species, plasmid DNA based damaging assays were carried out in the presence of radical scavenging agents as a reagent in reaction solutions. The DNA damage caused by **33**, under reductive enzyme activity in hypoxia, diminishes in the presence of radical scavenging agents such as methanol, ethanol, *t*-butanol, DMSO and mannitol. Analogous radical scavenging assays were carried out using **55** and **60**. The agarose gels obtained from the radical scavenging assays of **55** and **60** are qualitatively and quantitatively comparable with those obtained with **33** (Figures 4.5, 4.6 and 4.7). The DNA damage caused by reductive activation of **33**, **55** and **60** under hypoxia has been decreased by the addition of radical scavengers. It is well established that the radical scavengers used in the current assay reacts with hydroxyl radicals. Hence, homolytic fragmentation mechanism, which is proposed to explain the formation of hydroxyl radical in the metabolism of **33**, is also plausible to occur when **55** and **60** undergo reductive activation in our assay conditions



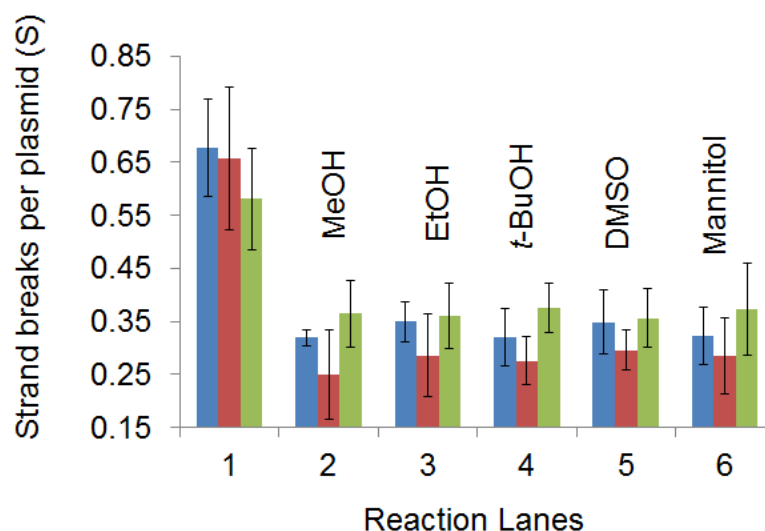
**Figure 4.5.** Cleavage of supercoiled plasmid DNA by **33** (25  $\mu\text{M}$ ) in the presence of NADPH:cytochrome P450 reductase as an activating system is reduced by radical scavengers. All reactions contained DNA (33  $\mu\text{g}/\text{mL}$ , pGL-2 Basic), sodium phosphate buffer (50 mM, pH 7.0), acetonitrile (2.5% v/v), catalase (100  $\mu\text{g}/\text{mL}$ ), superoxide dismutase (10  $\mu\text{g}/\text{mL}$ ), and desferal (1 mM) and were incubated under anaerobic conditions at 24  $^{\circ}\text{C}$  for 4 h, followed by agarose gel electrophoretic analysis. Lane 1, **33** (50  $\mu\text{M}$ ) + NADPH (500  $\mu\text{M}$ ) + reductase (33 mU/mL) ( $S = 0.67 \pm 0.09$ ); lanes 2-6, **33** (50  $\mu\text{M}$ ) + NADPH (500  $\mu\text{M}$ ) + reductase (33 mU/mL) + methanol (500 mM, lane 2) ( $S = 0.32 \pm 0.01$ ); ethanol (500 mM, lane 3) ( $S = 0.35 \pm 0.04$ ); *tert*-butyl alcohol (500 mM, lane 4) ( $S = 0.32 \pm 0.05$ ); DMSO (500 mM, lane 5) ( $S = 0.35 \pm 0.06$ ); mannitol (500 mM, lane 6) ( $S = 0.32 \pm 0.05$ ). The value  $S$  represents the mean number of strand breaks per plasmid molecule and is calculated using the equation  $S = -\ln f_{\text{I}}$ , where  $f_{\text{I}}$  is the fraction of plasmid present as form I.



**Figure 4.6.** Cleavage of supercoiled plasmid DNA by **55** (50  $\mu\text{M}$ ) in the presence of NADPH:cytochrome P450 reductase as an activating system is reduced by radical scavengers. All reactions contained DNA (33  $\mu\text{g}/\text{mL}$ , pGL-2 Basic), sodium phosphate buffer (50 mM, pH 7.0), acetonitrile (2.5% v/v), catalase (100  $\mu\text{g}/\text{mL}$ ), superoxide dismutase (10  $\mu\text{g}/\text{mL}$ ), and desferal (1 mM) and were incubated under anaerobic conditions at 24  $^{\circ}\text{C}$  for 4 h, followed by agarose gel electrophoretic analysis. Lane 1, **55** (50  $\mu\text{M}$ ) + NADPH (500  $\mu\text{M}$ ) + reductase (33 mU/mL) ( $S = 0.66 \pm 0.13$ ); lanes 2-6, **55** (50  $\mu\text{M}$ ) + NADPH (500  $\mu\text{M}$ ) + reductase (33 mU/mL) + methanol (500 mM, lane 2) ( $S = 0.25 \pm 0.08$ ); ethanol (500 mM, lane 3) ( $S = 0.29 \pm 0.08$ ); *tert*-butyl alcohol (500 mM, lane 4) ( $S = 0.27 \pm 0.04$ ); DMSO (500 mM, lane 5) ( $S = 0.30 \pm 0.04$ ); mannitol (500 mM, lane 6) ( $S = 0.28 \pm 0.07$ ). The value  $S$  represents the mean number of strand breaks per plasmid molecule and is calculated using the equation  $S = -\ln f_I$ , where  $f_I$  is the fraction of plasmid present as form I.



**Figure 4.7.** Cleavage of supercoiled plasmid DNA by **60** (50  $\mu\text{M}$ ) in the presence of NADPH:cytochrome P450 reductase as an activating system is reduced by radical scavengers. All reactions contained DNA (33  $\mu\text{g}/\text{mL}$ , pGL-2 Basic), sodium phosphate buffer (50 mM, pH 7.0), acetonitrile (2.5% v/v), catalase (100  $\mu\text{g}/\text{mL}$ ), superoxide dismutase (10  $\mu\text{g}/\text{mL}$ ), and desferal (1 mM) and were incubated under anaerobic conditions at 24  $^{\circ}\text{C}$  for 4 h, followed by agarose gel electrophoretic analysis. Lane 1, **60** (50  $\mu\text{M}$ ) + NADPH (500  $\mu\text{M}$ ) + reductase (33 mU/mL) ( $S = 0.58 \pm 0.10$ ); lanes 2-6, **60** (50  $\mu\text{M}$ ) + NADPH (500  $\mu\text{M}$ ) + reductase (33 mU/mL) + methanol (500 mM, lane 2) ( $S = 0.36 \pm 0.06$ ); ethanol (500 mM, lane 3) ( $S = 0.36 \pm 0.06$ ); *tert*-butyl alcohol (500 mM, lane 4) ( $S = 0.38 \pm 0.05$ ); DMSO (500 mM, lane 5) ( $S = 0.35 \pm 0.06$ ); mannitol (500 mM, lane 6) ( $S = 0.37 \pm 0.09$ ). The value  $S$  represents the mean number of strand breaks per plasmid molecule and is calculated using the equation  $S = -\ln f_I$ , where  $f_I$  is the fraction of plasmid present as form I.



**Figure 4.8.** Comparison of DNA cleavage by reductively activated **33** (blue), **55** (red) or **60** (green) under anaerobic conditions and DNA cleavage is inhibited by radical scavengers. Supercoiled plasmid DNA (33  $\mu\text{g/mL}$ , pGL-2 Basic) was incubated with drug (50 $\mu\text{M}$ ), NADPH (500  $\mu\text{M}$ ), cytochrome P450 reductase (33 mU/mL), catalase (100  $\mu\text{g/mL}$ ), superoxide dismutase (10  $\mu\text{g/mL}$ ), sodium phosphate buffer (50 mM, pH 7.0), acetonitrile (0.5-2.5% v/v), and desferal (1 mM) under anaerobic conditions at room temperature for 4 h, followed by agarose gel electrophoretic analysis. Lane 1, drug (50  $\mu\text{M}$ ) + NADPH (500  $\mu\text{M}$ ) + reductase (33 mU/mL); lanes 2-6, drug (50  $\mu\text{M}$ ) + NADPH (500  $\mu\text{M}$ ) + reductase (33 mU/mL) + methanol (500 mM, lane 2); ethanol (500 mM, lane 3); *tert*-butyl alcohol (500 mM, lane 4); DMSO (500 mM, lane 5); mannitol (500 mM, lane 6); The values, S, derived from agarose gel data and represent the mean number of strand breaks per plasmid molecule and were calculated using the equation  $S = -\ln f_i$ , where  $f_i$  is the fraction of plasmid present as form I. Background cleavage in the untreated plasmid was subtracted to allow direct comparison of DNA cleavage yields between different experiments.

#### 4.7 Examining the chemical mechanism of bioreductive metabolism of **55** and **60**

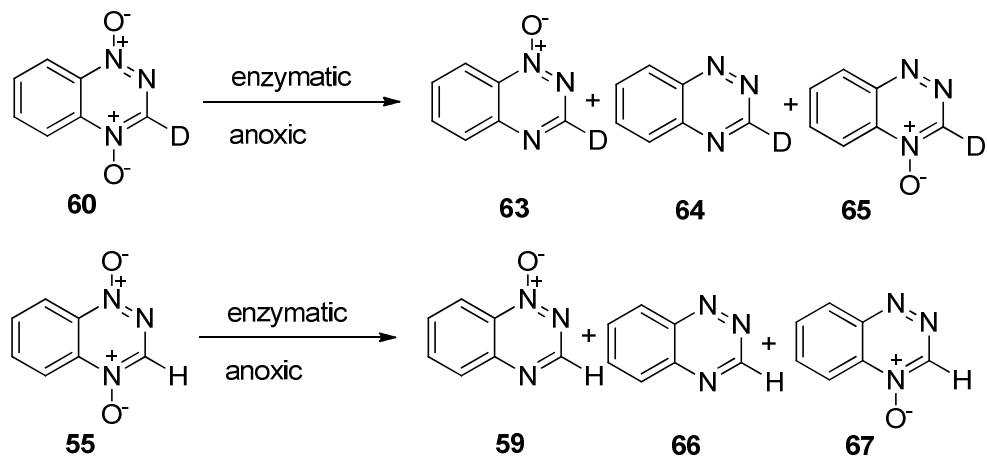
Metabolite identification showed that the reductive activation of drugs under anaerobic conditions produced 1-*N*-oxide. In this way, the metabolism mirrors TPZ.<sup>20</sup> Cytotoxicity assay results of TPZ and **55** show comparable anti-cancer activity. Hence, it can be suggested that TPZ and **55** would follow the same mechanism of DNA damage which forms the oxidizing radical under reductively activated conditions in hypoxia. To

test the DNA damaging mechanism, we designed comparative metabolic experiments with **55** and the isotopically labeled analog of **55**, **60**.

#### **4.8 Metabolic studies of 55 and 60 with organic substrate**

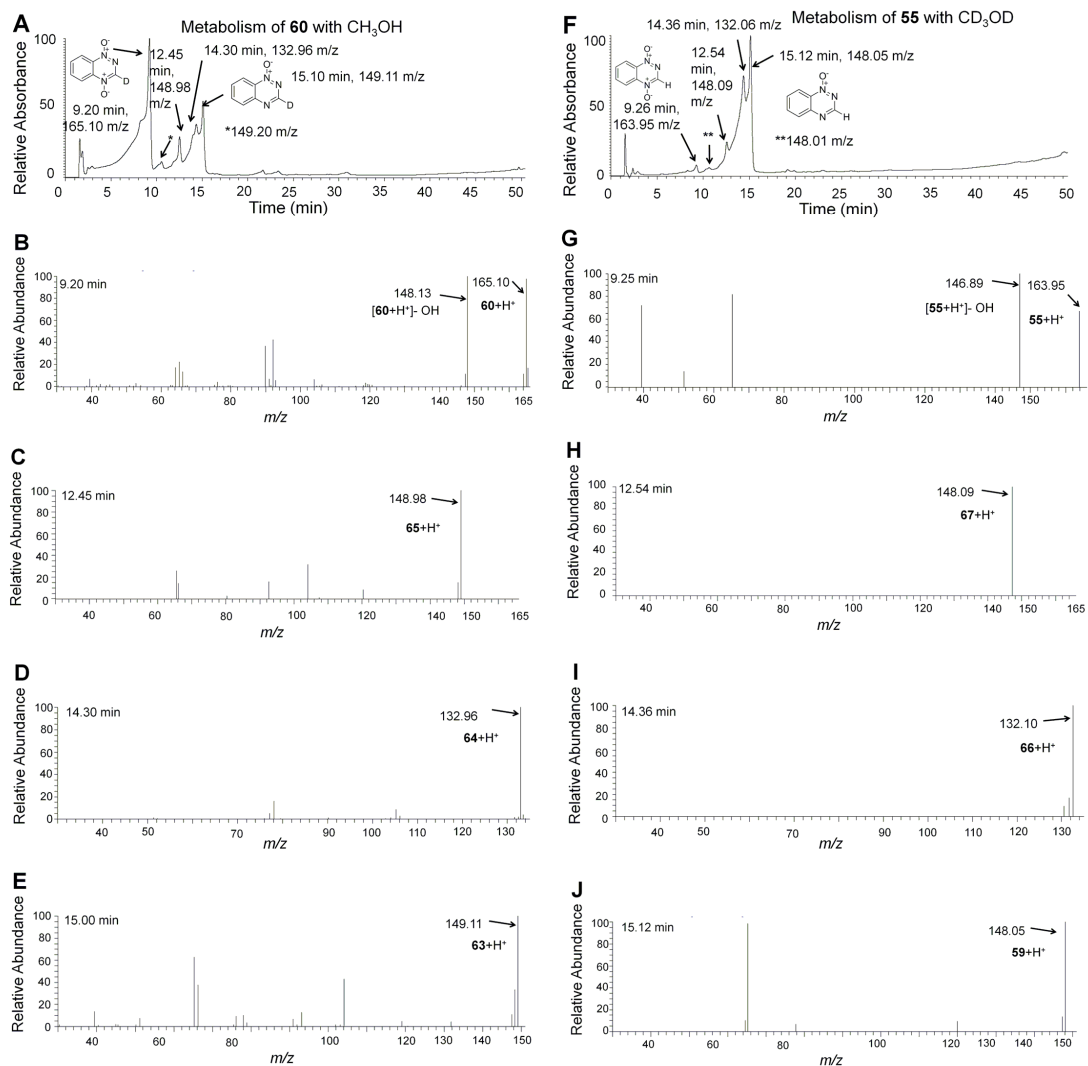
Metabolic studies were carried out to test the metabolism of **60** and **55** by enzymatic reducing system in the presence of an organic substrate. To test the metabolism of **60**, NADPH:cytochrome P450 reductase and NADPH was used as the enzyme system and CH<sub>3</sub>OH was added as the organic substrate. The reaction was carried out under anaerobic conditions in aqueous sodium phosphate buffer at pH 7.4. Upon metabolism the reaction mixture was subjected to be analyzed by LC/MS for the metabolites of **60**. Anaerobic metabolism of **60** produced **63** as the major metabolite with **64** and **65** as minor metabolites. In a metabolic analysis carried out using **55** with CD<sub>3</sub>OD in deuterated water under anaerobic conditions using sodium phosphate buffer at pD 6.6 produced major metabolite **59** and minor metabolites **66** and **67** (Scheme 4.5).





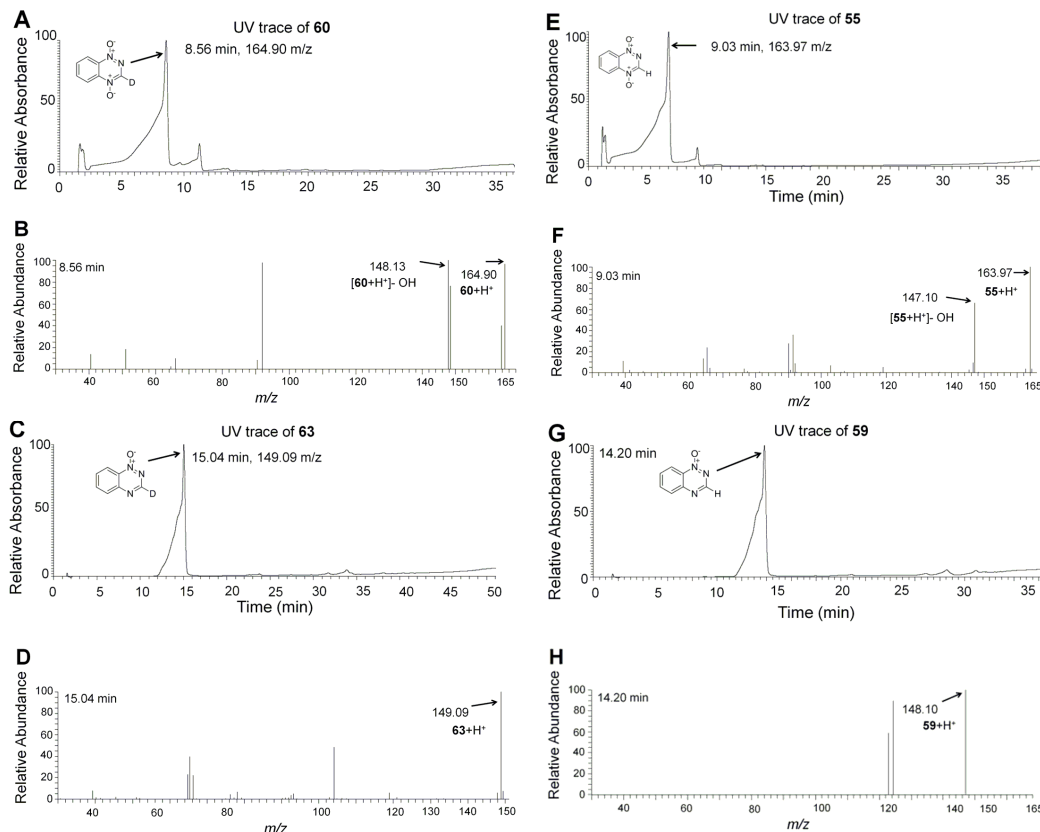
**Scheme 4.5** Enzymatic metabolism of **60** and **55** with organic substrate in anoxia

The complete LC/MS analysis for the metabolism of **60** shows retained deuterium in metabolites **63**, **64** and **65** (Figure 4.9 panels A, C, D and E). Hence benzotriazine radical **58** is unlikely to be formed in the bio-reductive metabolism of **60** (Scheme 4.4). Moreover, in the LC/MS analysis of metabolites **59**, **66** and **67**, derived from metabolism of **55** shows no exchange of deuterium into metabolites (Figure 4.9 panels F, H, I and J). Similar to the metabolism of **60**, compound **55** may not form the benzotriazine radical **58** over the anaerobic bio-reduction process (Scheme 4.4).



**Figure 4.9.** LC/MS analysis of anaerobic metabolism of **55** and **60** (0.5 mM) by cytochrome p450 reductase (0.4 U/mL) and NADPH (0.5 mM). The enzymatic reduction of **55/60** was carried out as described in the experimental section. The reaction was dried and products dissolved in methanol. The mixture was eluted with a gradient of 99% A (water containing 0.1% acetic acid) and 1% B (acetonitrile containing 0.1% acetic acid) followed by linear increase to 90% B over 30 min. The elution was continued at 90% B for 3 min and then B was decreased to 1% over next 8 min. A flow rate of 0.35 mL/min was used and the metabolites were detected at 254 nm. Mass spectra were obtained using electrospray ionization in the positive ion mode. Panel A: HPLC of the anaerobic reaction mixture of **60** monitoring absorbance at 254 nm. Panel B: LC/MS of **60**; eluting at 9.2 min. Panel C: LC/MS of metabolites of **60**; product eluting at 12.45 min. Panel D: LC/MS of metabolites of **60**; product eluting at 14.30 min. Panel E: LC/MS of metabolites of **60**; product eluting at 15.00 min. Panel F: HPLC of the anaerobic reaction mixture of **55** monitoring absorbance at 254 nm. Panel G: LC/MS of **55** eluting at 9.25 min. Panel H: LC/MS of metabolites of **55**; product eluting at 12.54 min. Panel I: LC/MS of metabolites of **55**; product eluting at 14.36 min. Panel J: LC/MS of metabolites of **55**; product eluting at 15.12 min.

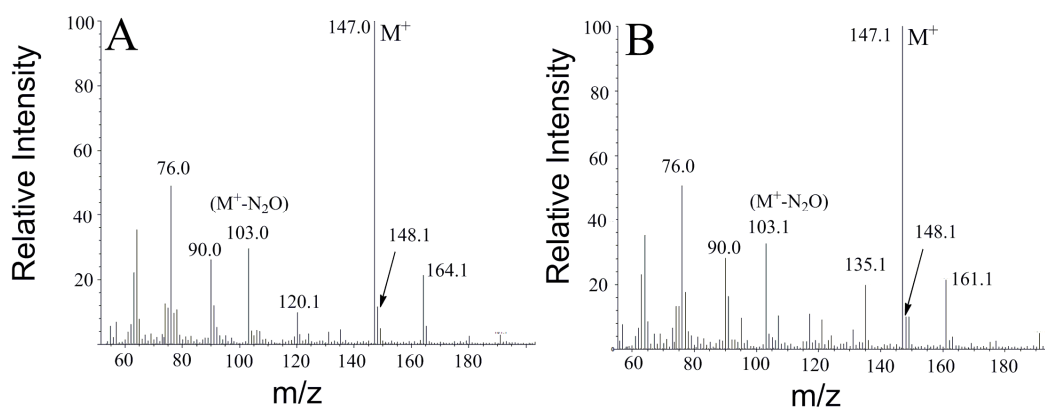
LC/MS analysis of authentic **60**, **63**, **55**, and **59**, using the same LC/MS method, used to analyze anaerobic reaction mixtures of **60** and **55** metabolism shows comparable retention times and mass values with that of LC/MS analysis of **60** and **55** shown in figure 4.11.



**Figure 4.10.** LC/MS analysis of authentic **60**, **63**, **55** and **59**. The products dissolved in methanol. The mixture was eluted with a gradient of 99% A (water containing 0.1% acetic acid) and 1% B (acetonitrile containing 0.1% acetic acid) followed by linear increase to 90% B over 30 min. The elution was continued at 90% B for 3 min and then B was decreased to 1% over next 8 min. A flow rate of 0.35 mL/min was used and the metabolites were detected at 254 nm. Mass spectra were obtained using electrospray ionization in the positive ion mode. Panel A: HPLC of **60** monitoring absorbance at 254 nm. Panel B: LC/MS of **60** eluting at 8.56 min. Panel C: HPLC of **63** monitoring absorbance at 254 nm Panel D: LC/MS of **63** eluting at 15.04 min. Panel E: HPLC of **55** monitoring absorbance at 254 nm. Panel F: LC/MS of **55** eluting at 9.03 min. Panel G: HPLC of **59** monitoring absorbance at 254 nm. Panel H: LC/MS of **59** eluting at 14.20 min.

#### 4.9 Deuterium incorporation into **55**

The dehydration mechanism is further tested using **55** and **60** (Scheme 4.4). In the initial one electron reduction step the di-oxide **55** or **60** will convert to a radical anion and upon protonation, drug radicals **57** and **62** may persist under low oxygen levels. In order to follow the dehydration mechanism, removal of water molecule from **57** and **62** should form radical cation **58** and **58** can abstract hydrogen from an organic substrate (Scheme 4.4). If the dehydration mechanism is plausible, the hydrogen of organic substrate may be abstracted into the major metabolite. HRMS analysis of major metabolite is able to show isotopic content which shows any hydrogen abstraction event (Scheme 4.4). To test the dehydration mechanism, **55** was activated in the presence of CD<sub>3</sub>OD, in D<sub>2</sub>O-sodium phosphate buffer medium at pD 6.6. The major metabolite 1-*N* oxide was separated and HRMS data suggests molecular formula C<sub>7</sub>H<sub>5</sub>N<sub>3</sub>O for the molecular ion peak (M) with m/z of 147.1. Formation of **63**, resulted by dehydration mechanism might have produced a molecular ion peak having m/z of 148.1, which is the M+1 ion in the current assay. The intensity of M+1 ion is 2% higher than that of a control experiment, carried out using **55** in the presence of CH<sub>3</sub>OH in aqueous sodium phosphate buffer at pH 7.4. The 2% difference of m/z of M+1, between **55** in CD<sub>3</sub>OD reaction and **55** in CH<sub>3</sub>OH control may have caused due to the presence of naturally abundant isotopes such as <sup>13</sup>C, <sup>15</sup>N and <sup>2</sup>H or may be occurrence of dehydration mechanism as a minor reaction (Figure 4.11).

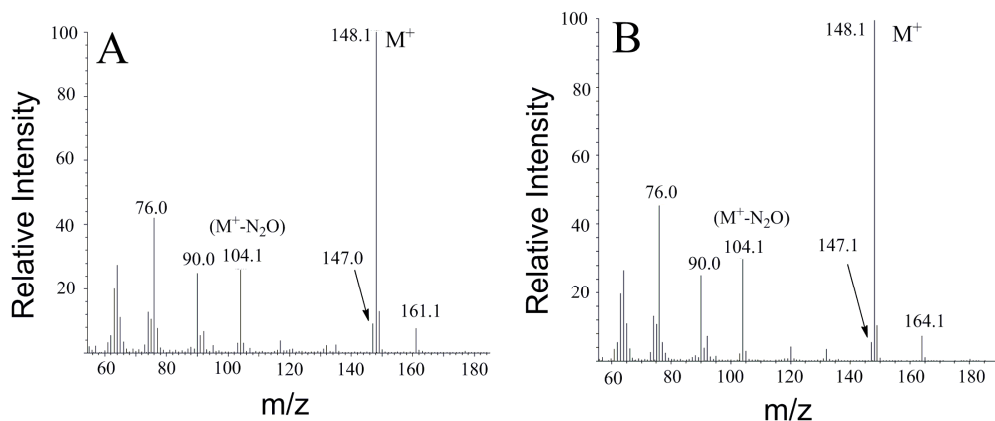


**Figure 4.11.** HRMS of the major metabolite 1-*N*-oxide **59** arising from metabolism of **55** under reductively activated conditions in hypoxia. Briefly **55** (10 mM) was incubated with NADPH (500mM) and NADPH:cytochrome P450 reductase (0.5 U/mL) in argon purged bag with either A) sodium phosphate buffer (30 mM) at pD 6.6 in D<sub>2</sub>O and CD<sub>3</sub>OD (2 mM) were added and incubated over 4 hours. B) sodium phosphate buffer (30 mM) at pH 7.4 in H<sub>2</sub>O and CH<sub>3</sub>OH (2M) were added and incubated over 4 hours. Upon completion reactions A and B were extracted to EtOAc and dried in vacuum. Thin layer chromatography was used to separate the major 1-*N*-oxide metabolite in both A and B. Then corresponding area related to the R<sub>f</sub> value for 1-*N*-oxide was scratched using a metal blade to collect silica. The organic material was extracted to EtOAc from silica and dried in vacuum. The dry organic extract was dissolved in CH<sub>3</sub>CN and directed for HRMS analysis.

#### 4.10 Isotope washout from drug **60**

Metabolism of **60** was carried out under anaerobic reducing conditions in the presence of CH<sub>3</sub>OH in sodium phosphate buffer at pH 7.4 to study the isotopic content of the major metabolite using HRMS. Under dehydration mechanism, deuterium of **60** is removed as water and the major metabolite **59** may form via benzotriazinyl radical **58** (Scheme 4.4). HRMS analysis of molecular ion (M) of the major metabolite shows C<sub>7</sub>H<sub>4</sub>DN<sub>3</sub>O as the molecular formula with m/z of 148.1. Due to dehydration mechanism, if **59** had formed, m/z of the molecular ion should be 147.1 m/z. When the peak intensity of M-1 ion, formed from the reaction **60** with CH<sub>3</sub>OH is compared with the control, **60** with CD<sub>3</sub>OD in D<sub>2</sub>O-sodium phosphate buffer medium at pD 6.6, shows only 3%

increase in the former reaction, **60** with CH<sub>3</sub>OH. This 3% increase might have occurred due to dehydration mechanism, which had occurred as a minor reaction path (Figure 4.12).



**Figure 4.12.** HRMS of the major metabolite 1-*N*-oxide **63** arising from metabolism of **60** under reductively activated conditions in hypoxia. Briefly **60** (10.mM) was incubated with NADPH (500mM) and NADPH:cytochrome P450 reductase (0.5 U/mL) in argon purged bag with either A) sodium phosphate buffer (30mM) at pH 7.4 in H<sub>2</sub>O and CH<sub>3</sub>OH (2 mM) were added and incubated over 4 hours. B) Sodium phosphate buffer (30 mM) at pD 6.6 in D<sub>2</sub>O and CD<sub>3</sub>OD (2 mM) were added and incubated over 4 hours. Upon completion reactions A and B were extracted to EtOAc and dried in vacuum. Thin layer chromatography was used to separate the 1-*N*-oxide in A and B. Then corresponding area related to the R<sub>f</sub> value for 1-*N*-oxide was scratched using a metal blade to collect silica. The organic material was extracted to EtOAc and dried in vacuum. The dry organic extract was dissolved in CH<sub>3</sub>CN and directed for HRMS analysis.

#### 4.11 Isotope replacement analysis and dehydration mechanism

The results of metabolic experiments of **55**, with CD<sub>3</sub>OD and **60** in the presence of CH<sub>3</sub>OH suggest that the dehydration mechanism may occur as a minor path, responsible for enzyme mediated activation of 1,2,4-benzotriazine-1,4-dioxides under hypoxia. Alternatively, hemolysis of N-O bond, which is evident by radical scavenging studies, suggests that hydroxyl radical might be the oxidizing radical formed in the metabolism of **55** and **60**. The homolytic fragmentation over the bio-reductive

metabolism of **55** and **60** is possible to occur as the major metabolic path under hypoxic bio-reductive conditions.

#### 4.12 Conclusion

The work related to this chapter describes the use of 1,2,4-benzotriazine-1,4-dioxide **55** as a mechanistic handle to analyze dehydration mechanism. The dehydration mechanism is proposed to explain the chemical structure of the oxidizing radical, released by these *N* oxide drugs in hypoxia under reductive activation.<sup>10, 12, 26</sup> The drug 1,2,4-benzotriazine-1,4-dioxide may have formed benzotriazinyl radical as a minor oxidizing radical via dehydration mechanism.<sup>10</sup> In our study we showed that drugs **55** and **60** produce DNA cleavage, comparable to the DNA damage caused by **33**. In addition, the radical scavenging experiments with **33**, **55** and **60** showed reduced DNA damage and diminished DNA damage suggest the involvement of hydroxyl radical as the major DNA damaging process.<sup>4a, 14c</sup>

The results of the experiments, carried out to test deuterium incorporation to **55** in the presence of CD<sub>3</sub>OD and deuterium release from **60**, in the presence of CH<sub>3</sub>OH were not consistent with the dehydration mechanism as the major mechanism in the enzymatic metabolism of 1,2,4-benzotriazine-1,4-dioxide.

Finally, based on various experiment results related to mechanistic studies on *N*-di-oxides, it can be concluded that the one electron reduction of 1,2,4-benzotriazine-1,4-dioxide produces hydroxyl radical as the oxidizing species which might be the major source that carries out DNA cleavage.

## 4.13 Experimental

**4.12.1 Materials.** Materials were of the highest purity available and were obtained from following sources: cytochrome P450 reductase, NADPH, sodium phosphate, mannitol, DMSO desferal, , catalase, and superoxide dismutase (SOD) from Sigma Chemical Co. (St. Louis, MO); agarose from Seakem; HPLC grade solvents (acetonitrile, methanol, ethanol, tert-butyl alcohol, ethyl acetate, hexane, and acetic acid) from Fischer (Pittsburgh, PA); ethidium bromide from Roche Molecular Biochemicals (Indianapolis, IN). Standard protocol was used to prepare plasmid DNA pGL2BASIC.<sup>27</sup> Published methods in literature were followed to prepare TPZ **1** and other N-oxides.<sup>20a, 28</sup>

### 4.12.2 Synthesis of 1,2,4-benzotriazine-1,4-bioxide **55**

Argon was purged into dry DMF for 5 min inside an argon filled glove bag. Then TPZ (115mg, 0.644 mmol) was dissolved in (2 mL) DMF. To another degassed DMF sample (2 mL) *tert*-butyl nitrite (0.25 ml, 2.05 mmol) was added and heated to 65<sup>0</sup>C inside the glove bag. To this solution, TPZ was added and heated for 10 min at 65<sup>0</sup>C with stirring. Upon completion reaction time the reaction mixture was cooled to room temperature and DMF was removed by vacuum. Then column chromatography (1:1 EtOAc/hexane) was performed to obtain (40 mg, 34 %). Deuterated DMF was used in the preparation of 3 position deuterated 1,2,4-benzotriazine-1,4-dioxide. R<sub>f</sub> of is 0.50 (100% EtOAc): <sup>1</sup>H NMR (Acetone, 500 MHz,): δ 9.04 (s, 1H), 8.42 (dd, 2H), 8.15 (m, 1H), 8.03 (m, 1H). <sup>13</sup>C-NMR (Acetone, 125.8 MHz,): δ 142.73, 141.01, 136.50, 136.01, 133.54, 122.20, 120.19; HRMS (ES<sup>+</sup>, [M+H]) *m/z* calcd C<sub>7</sub>H<sub>6</sub>N<sub>3</sub>O<sub>2</sub> calculated mass 164.0460; actual mass 164.0453.



#### 4.12.3 Synthesis of 3 position deuterated 1,2,4-benzotriazine-1,4-dioxide 60

The procedure used to synthesize **55** was followed to prepare **60**. In synthesis, deuterated DMF was used instead of DMF.

$^1\text{H}$  NMR (Acetone, 500 MHz):  $\delta$  8.42 (dd, 2H), 8.15 (m, 1H), 8.03 (m, 1H).  $^{13}\text{C}$ -NMR (Acetone, 125.8 MHz):  $\delta$  142.47 (t,  $J = 32.7$  Hz), 141.02, 136.52, 136.02, 133.54, 122.20, 120.18; HRMS ( $\text{ES}^+$ ,  $[\text{M}+\text{H}]$ )  $m/z$  calcd  $\text{C}_7\text{H}_5\text{DN}_3\text{O}_2$  calculated mass 165.0523; actual mass 165.0515.

#### 4.12.4 Synthesis of 1,2,4-benzotriazine-1-oxide 59

Anhydrous DMF was bubbled with argon for 5 min inside a argon filled glove bag. Then **35** (365mg, 2.2 mmol) was dissolved in (3 mL) DMF. To another DMF sample (3 mL) *tert*-butyl nitrite (1.07 ml, 8.8 mmol) was added and heated to  $65^\circ\text{C}$  inside the glove bag. To this solution TPZ was added and heated for 10 min at  $65^\circ\text{C}$  with stirring. Upon completion reaction time the reaction mixture was cooled to room temperature and DMF was removed by vacuum. Then column chromatography (1:1 EtOAc/hexane) was performed to obtain (77 mg, 34 %).  $R_f = 0.50$  (100% EtOAc)

$^1\text{H}$  NMR (Acetone, 300 MHz):  $\delta$  ppm 9.05 (s, 1H),  $\delta$  8.42 (d,  $J = 8.5$  Hz, 1H),  $\delta$  8.11 (m, 2H),  $\delta$  7.91 (m, 1H)  $^{13}\text{C}$  NMR (Acetone, 75.5 MHz):  $\delta$  155.02, 148.32, 136.66, 131.99, 130.05, 120.63; HRMS ( $\text{ES}^+$ ,  $[\text{M}+\text{H}]$ )  $m/z$  calcd  $\text{C}_7\text{H}_6\text{N}_3\text{O}$  calculated mass 148.0511; actual mass 148.0517.

#### 4.12.5 Synthesis of 1,2,4-benzotriazine-3-deuterium-1-oxide **63**

The synthetic method used to prepare **59** was exactly followed to synthesized **63** and deuterated DMF was used instead of DMF.  $^1\text{H}$  NMR (Acetone, 300 MHz):  $\delta$  ppm 8.40 (d,  $J = 8.5$  Hz, 1H), 8.08 (m, 2H), 7.88 (m, 1H)  $^{13}\text{C}$  NMR (Acetone, 75.5 MHz):  $\delta$  154.72 (t,  $J = 32.7$  Hz), 148.34, 136.66, 131.99, 130.06, 120.64; HRMS ( $\text{ES}^+$ ,  $[\text{M}+\text{H}]$ )  $m/z$  calcd  $\text{C}_7\text{H}_5\text{DN}_3\text{O}$  calculated mass 149.0574; actual mass 149.0579.

#### 4.12.6 DNA damage assays

In normal anaerobic DNA cleaving assay, the drug TPZ, **55** or **61** (5-25  $\mu\text{M}$ ) was incubated with supercoiled plasmid DNA (33  $\mu\text{g}/\text{mL}$ , pGL-2 Basic), NADPH (500  $\mu\text{M}$ ), cytochrome P450 reductase (33  $\text{mU}/\text{mL}$ ), catalase (100  $\mu\text{g}/\text{mL}$ ), superoxide dismutase (10  $\mu\text{g}/\text{mL}$ ), sodium phosphate buffer (50  $\text{mM}$ , pH 7.0), acetonitrile (0.5-2.5% v/v), and desferal (1  $\text{mM}$ ) under anaerobic conditions at 25  $^\circ\text{C}$  for 4 h. Three freeze-pump-thaw cycles were performed on all solutions except enzymes, NADPH, and DNA. To prepare reaction mixtures deoxygenated water was used in an argon-filled glove bag and cytochrome P450 reductase was added as the last reagent to start the reaction. Then the reaction containers were kept in the argon purged glove bag upon wrapped in aluminum

foil to prevent exposure to light. The reactions were quenched by addition of 5  $\mu$ L of 50% glycerol loading buffer and were loaded onto a 0.9% agarose gel and electrophoresed for approximately 2.0 h at 85 V in 1x TAE buffer. Upon completion of electrophoretic separation, the gels were removed and soaked in an aqueous ethidium bromide (0.3 $\mu$ g/mL) solution for staining for 4 h. To visualize DNA UV-transillumination was performed on gels and DNA band quantification was performed using quantity one imaging system. The values reported are not corrected for differential staining of form I and form II DNA by ethidium bromide.

The radical scavenging DNA damage assays were performed following the above typical procedure. The radical scavenging reagents methanol, ethanol, *tert*-butyl alcohol, DMSO, or mannitol (500 mM) were added in addition to the other reagents prior to the addition of cytochrome P450 reductase. All aerobic reactions were carried out using non de oxygenated solutions under normal atmospheric conditions.

#### **4.12.7 Metabolic studies related to drugs**

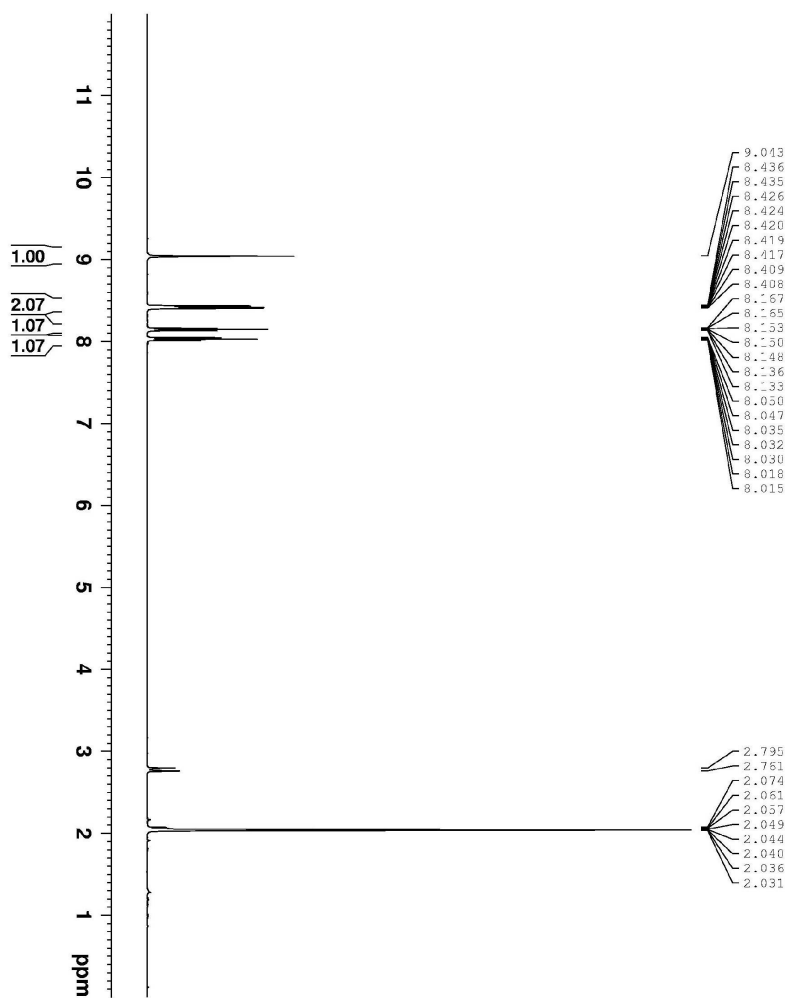
In a typical metabolic assay, all solutions except cytochrome P450 reductase (330 mU/mL), catalase (100  $\mu$ g/mL) were degassed by three cycles of freeze-pump-thaw cycles. The *N* di-oxide ( $\mu$ M) was mixed with desferal (1 mM) in sodium phosphate buffer (pH 7, 50 mM), NADPH (500  $\mu$ M), catalase (100  $\mu$ g/mL), and superoxide dismutase (10  $\mu$ g/mL) followed by the addition of cytochrome P450 reductase (330 mU/mL). Upon 4 hr incubation under argon at 25  $^{\circ}$ C, the organic was extracted to EtOAc (0.5 mL) twice and dried using roto vap. Then the dry reaction mixture was dissolved in 0.5 mL MeOH and was analyzed by LC employing a C18 reverse phase Rainin Microsorb-MV column (5

$\mu\text{m}$  particle size, 100 Å pore size, 25 cm length, 4.6 mm i.d.) eluted with gradient starting at 50% A (0.5% acetic acid in water) and 50% B (acetonitrile) followed by linear increase to 80% B from 0 min to 40 min. A flow rate of 0.6 mL/min was used and the products were monitored by their UV-absorbance at 254 nm. LC/ESI-MS experiments were carried out on a Finnigan TSQ 7000 triple quadrupole instrument interfaced to a ThermoSeparations liquid chromatograph (TSP4000). Positive ion electrospray was used as the means of ionization. The heated inlet capillary temperature was 250 °C and electrospray needle voltage was 4.5 kV. Nitrogen sheath gas was supplied at 80 psi and the LC/ESI-MS analysis was done in the positive ion mode.

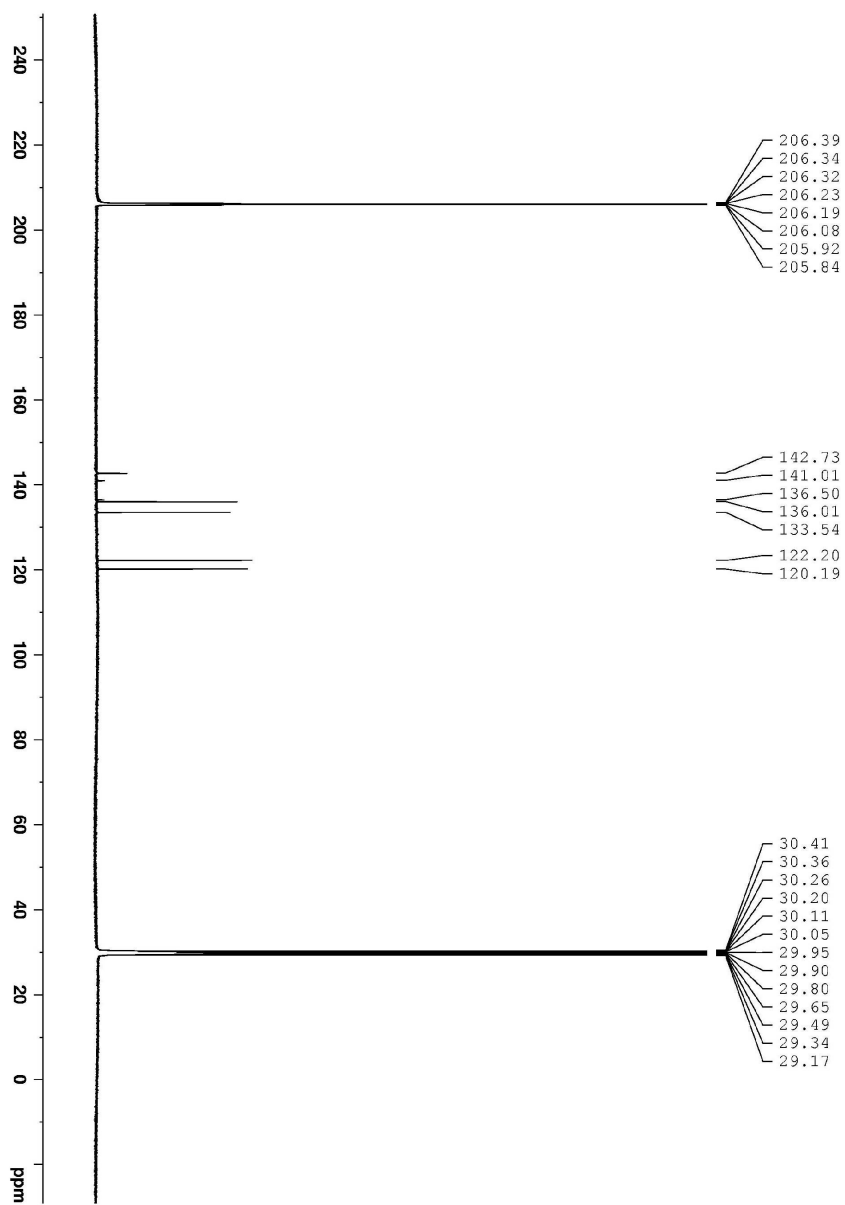
#### **4.12.8 HRMS studies related to drugs**

In a typical metabolic assay, all solutions except cytochrome P450 reductase (330 mU/mL), catalase (100  $\mu\text{g}/\text{mL}$ ) were degassed by three cycles of freeze-pump-thaw cycles. The N di-oxide ( $\mu\text{M}$ ) was mixed with desferal (1 mM) in sodium phosphate buffer (pH 7, 50 mM) and NADPH (500  $\mu\text{M}$ ) followed by the addition of cytochrome P450 reductase (330 mU/mL). Upon 4 hr incubation under argon at 25 °C, the organic was extracted to EtOAc (0.5 mL) twice and dried using roto vap. Then the dry reaction mixture was dissolved in 0.5 mL  $\text{CH}_3\text{CN}$  and used to spot on TLC plates. The preparative TLC was run using (1:1 EtOAc/hexane) as the solvent system. The major metabolite mono N oxide was co-spotted when preparation TLC was run. Upon completion the TLC plates were dried in air and the area correspond to 1-N-oxide co-migration was scratched using a metal blade. The dry silica was re-dissolved in EtOAc and EtOAc was removed

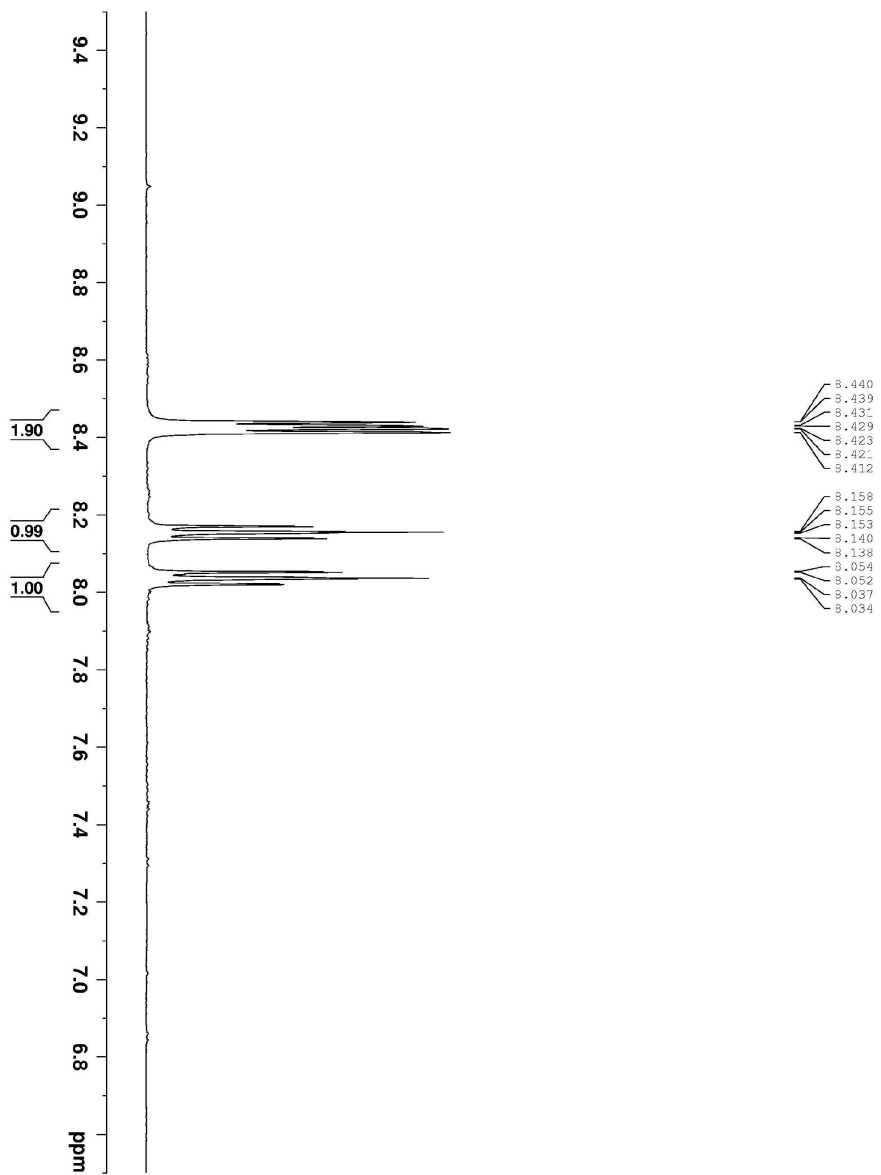
to a glass vial. The EtOAc was dried under roto-vap, protected from light and kept in the freezer. The dry samples were sent for HRMS analysis.



<sup>1</sup>H NMR of **55** (Acetone, 500 MHz)

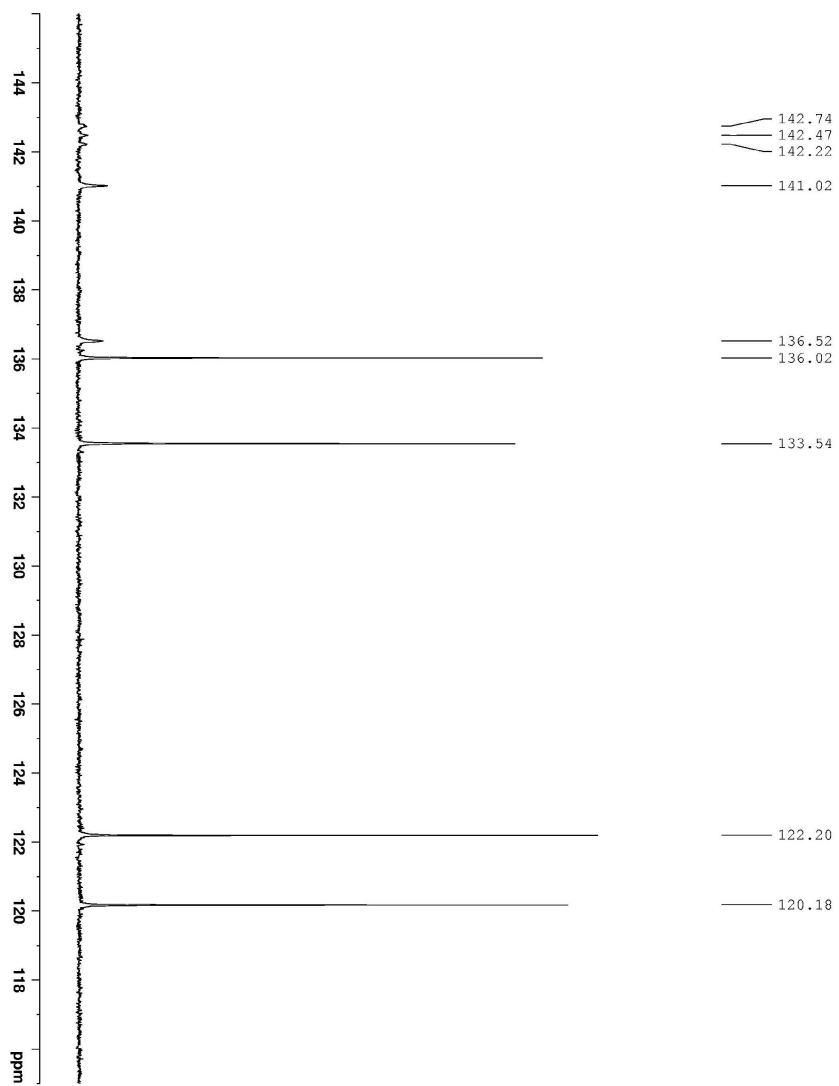


$^{13}\text{C}$  NMR of **55** (Acetone, 125.77 MHz)

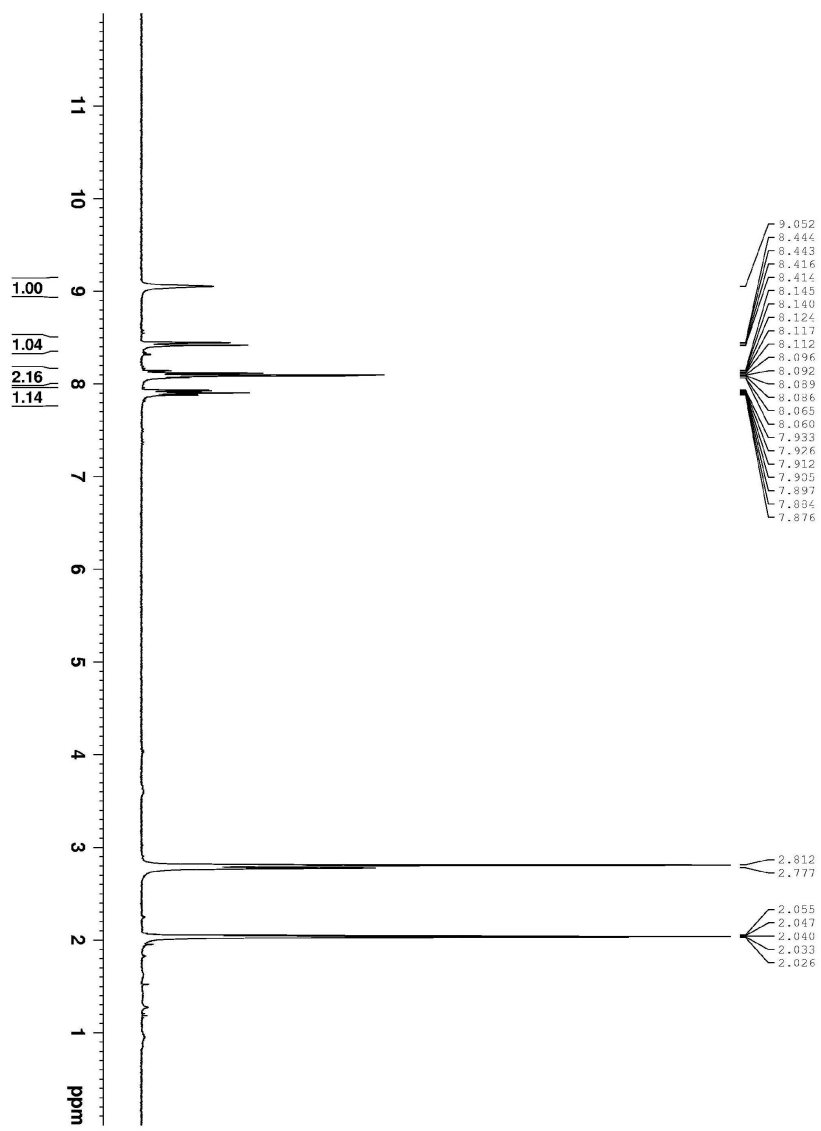


$^1\text{H}$  NMR of **60** (Acetone, 500 MHz)

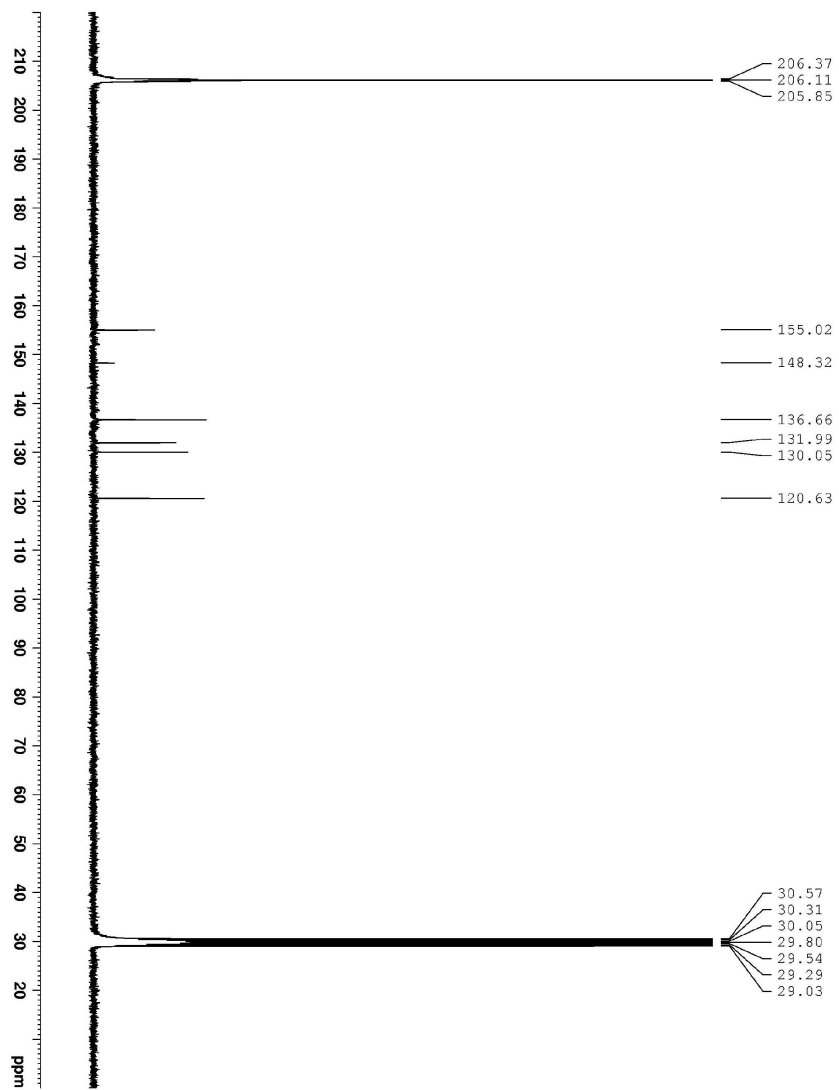




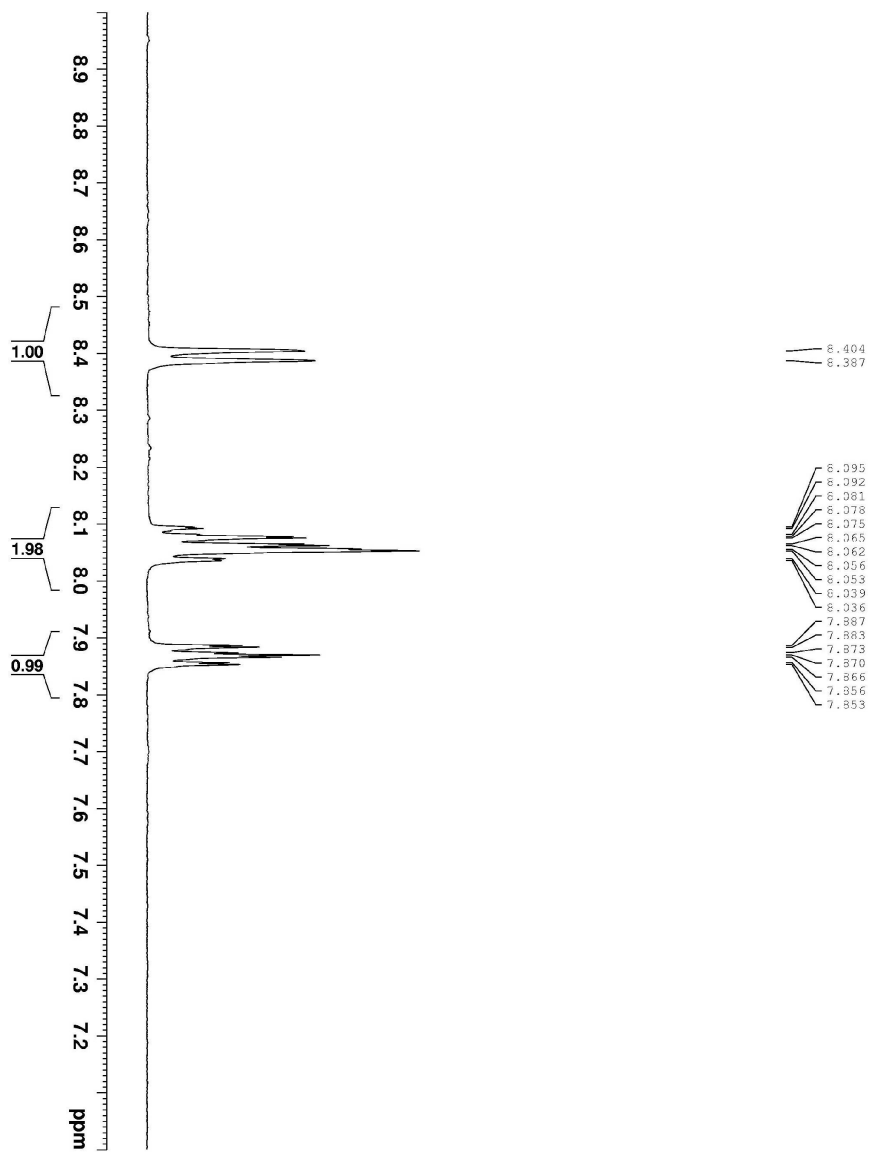
$^{13}\text{C}$  NMR of **60** (Acetone, 125.77 MHz)



<sup>1</sup>H NMR of **59** (Acetone, 300 MHz)

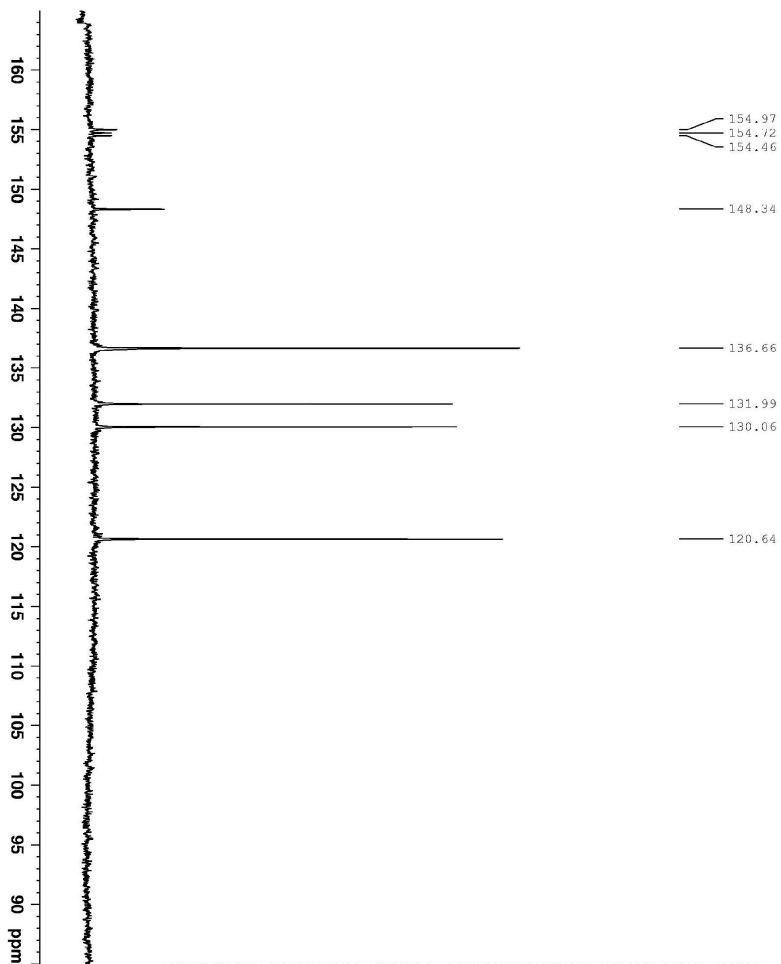


$^{13}\text{C}$  NMR of **59** (Acetone, 75 MHz)



$^1\text{H}$  NMR of **63** (Acetone, 500 MHz)

13C NMR



```

Current Data Parameters
NAME      Annar7P144
EXPNO     1
PROCNO    1
F2 - Acquisition Parameters
Date_     20111130
Time     11:36
INSTRUM   5 mm CPYCI 1H-
PROBHD    DQNP00
PULPROG   zgpg30
TD        27224
SOLVENT   Acetone
NS         15059
DS         4
SWH        35211.270 Hz
FIDRES    0.442568 Hz
AQ         1.044708 sec
RG         400
AQ         4.000000 sec
DM         -4.200 usec
DE         35.00 usec
DI         8
D1         2.00000000 sec
DELTA     0.03000000 sec
DELTAR    0.03000000 sec
PC        0.01000000 sec
===== CHANNEL F1 13C =====
NUC1       13C
P1         12.00 usec
PL1        0.30 dB
SFO1       125.7716224 MHz
===== CHANNEL F2 13C =====
CH2PRG2   waltz16
NUC2       13C
P2         80.00 usec
PL2        5.00 dB
SFO2       500.1320005 MHz
===== Processing parameters =====
SI         32768
SF         125.7572604 MHz
WDW        EM
SSB        0
GB         3.00 Hz
PC         1.00
  
```

<sup>13</sup>C NMR of **63** (Acetone, 125.77 MHz)

## References for chapter 4

- (a) Gattineau, M.; Rixe, O.; Le, C. T., Tirapazamine with cisplatin and vinorelbine in patients with advanced non-small-cell lung cancer: A phase I/II study. *Clin. Lung Cancer* **2005**, *6*, 293-298; (b) Le, Q.-T. X.; Moon, J.; Redman, M.; Williamson, S. K.; Lara, P. N., Jr.; Goldberg, Z.; Gaspar, L. E.; Crowley, J. J.; Moore, D. F., Jr.; Gandara, D. R., Phase II study of tirapazamine cisplatin, and etoposide and concurrent thoracic radiotherapy for limited-stage small-cell lung cancer: SWOG 0222. *J. Clin. Oncol.* **2009**, *27*, 3014-3019; (c) Le, Q.-T.; Fisher, R.; Oliner, K. S.; Young, R. J.; Cao, H.; Kong, C.; Graves, E.; Hicks, R. J.; McArthur, G. A.; Peters, L.; O'Sullivan, B.; Giaccia, A.; Rischin, D., Prognostic and Predictive Significance of Plasma HGF and IL-8 in a Phase III Trial of Chemoradiation with or without Tirapazamine in Locoregionally Advanced Head and Neck Cancer. *Clin. Cancer Res.* **2012**, *18*, 1798-1807; (d) Rischin, D.; Peters, L. J.; O'Sullivan, B.; Giralt, J.; Fisher, R.; Yuen, K.; Trotti, A.; Bernier, J.; Bourhis, J.; Ringash, J.; Henke, M.; Kenny, L., Tirapazamine, cisplatin, and radiation versus cisplatin and radiation for advanced squamous cell carcinoma of the head and neck (TROG 02.02, HeadSTART): a phase III trial of the trans-tasman radiation oncology group. *J. Clin. Oncol.* **2010**, *28* (18), 2989-2995.
- (a) McKeown, S. R.; Cowen, R. L.; Williams, K. J., Bioreductive drugs: from concept to clinic. *Clin Oncol (R Coll Radiol)* **2007**, *19*, 427-42; (b) Sarkar, U.; Glaser, R.; Parsons, Z. D.; Barnes, C. L.; Gates, K. S., Synthesis, Crystal Structure, and Rotational Energy Profile of 3-Cyclopropyl-1,2,4-benzotriazine 1,4-Di-N-oxide. *J. Chem. Crystallogr.* **2010**, *40*, 624-629.
- (a) Zeman, E. M.; Brown, J. M.; Lemmon, M. J.; Hirst, V. K.; Lee, W. W., SR-4233: a new bioreductive agent with high selective toxicity for hypoxic mammalian cells. *Int J Radiat Oncol Biol Phys* **1986**, *12*, 1239-42; (b) Laderoute, K. L.; Wardman, P.; Rauth, M., Molecular mechanisms for the hypoxia-dependent activation of 3-amino-1,2,4-benzotriazine 1,4-dioxide (SR4233). *Biochem. Pharmacol.* **1988**, *37* (8), 1487-1495; (c) Tocher, J. H.; Virk, N. S.; Edwards, D. I., Electrochemical properties as a function of pH for benzotriazine di-N-oxides. *Free Rad. Res. Commun.* **1990**, *10* (4-5), 295-302.
- (a) Daniels, J. S.; Gates, K. S., DNA Cleavage by the Antitumor Agent 3-Amino-1,2,4-benzotriazine 1,4-Dioxide (SR4233): Evidence for Involvement of Hydroxyl Radical. *J. Am. Chem. Soc.* **1996**, *118* (14), 3380-3385; (b) Birincioglu, M.; Jaruga, P.; Chowdhury, G.; Rodriguez, H.; Dizdaroglu, M.; Gates, K. S., DNA Base Damage by the Antitumor Agent 3-Amino-1,2,4-benzotriazine 1,4-Dioxide (Tirapazamine). *J. Am. Chem. Soc.* **2003**, *125* (38), 11607-11615.

5. (a) Wardman, P.; Priyadarsini, K. I.; Dennis, M. F.; Everett, S. A.; Naylor, M. A.; Patel, K. B.; Stratford, I. J.; Stratford, M. R. L.; Tracy, M., Chemical properties which control selectivity and efficacy of aromatic N-oxide bioreductive drugs. *Br. J. Cancer* **1996**, *74*, S70-S74; (b) Biedermann, K. A.; Wang, J.; Graham, R. P., SR 4233 cytotoxicity and metabolism in DNA repair-competent and DNA repair-deficient cell lines. *Br. J. Cancer* **1991**, *63*, 358-362.
6. Tocher, J. H.; Edwards, D. I., Electrochemical studies of tirapazamine: generation of the one-electron reduction product. *Free Radical Res.* **1994**, *21*, 277-83.
7. Brown, J. M., SR 4233 (tirapazamine): a new anticancer drug exploiting hypoxia in solid tumors. *Br. J. Cancer* **1993**, *67*, 1163-70.
8. Butler, J.; Hoey, B. M., DNA and Free Radicals. In *Redox cycling drugs and DNA damage*, Halliwell, B.; Aruoma, O. I., Eds. Ellis Horwood: New York, NY, 1993; pp 243-273.
9. (a) Sies, H., Biochemistry of Oxidative Stress. *Angew. Chem. Int. Ed. Eng.* **1986**, *25*, 1058-1071; (b) Brown, J. M.; Wilson, W. R., Exploiting tumor hypoxia in cancer treatment. *Nat. Rev. Cancer* **2004**, *4*, 437-447; (c) Finkel, T.; Holbrook, N. J., Oxidants, oxidative stress and the biology of ageing. *Nature* **2000**, *408* (Nov 9), 239-247; (d) Wood, Z. A.; Poole, L. B.; Karplus, P. A., Peroxiredoxin evolution and the regulation of hydrogen peroxide signaling. *Science* **2003**, *300* (5619), 650-653.
10. Anderson, R. F.; Shinde, S. S.; Hay, M. P.; Gamage, S. A.; Denny, W. A., Activation of 3-Amino-1,2,4-benzotriazine 1,4-Dioxide Antitumor Agents to Oxidizing Species Following Their One-Electron Reduction. *J. Am. Chem. Soc.* **2003**, *125*, 748-756.
11. (a) Wang, J.; Biedermann, K. A.; Wolf, C. R.; Brown, J. M., Metabolism of the bioreductive cytotoxin SR 4233 by tumor cells: Enzymic studies. *Br. J. Cancer* **1993**, *67*, 321-5; (b) Siim, B. G.; Van, Z. P. L.; Brown, J. M., Tirapazamine-induced DNA damage measured using the comet assay correlates with cytotoxicity towards hypoxic tumor cells in vitro. *Br. J. Cancer* **1996**, *73*, 952-960; (c) Cahill, A.; White, I. N., Reductive metabolism of 3-amino-1,2,4-benzotriazine-1,4-dioxide (SR 4233) and the induction of unscheduled DNA synthesis in rat and human derived cell lines. *Carcinogenesis* **1990**, *11*, 1407-11.
12. Baker, M. A.; Zeman, E. M.; Hirst, V. K.; Brown, J. M., Metabolism of SR 4233 by Chinese hamster ovary cells: basis of selective hypoxic cytotoxicity. *Cancer Res.* **1988**, *48*, 5947-52.

13. (a) Fitzsimmons, S. A.; Lewis, A. D.; Riley, R. J.; Workman, P., Reduction of 3-amino-1,2,4-benzotriazine-1,4,-di-N-oxide to a DNA-damaging species: a direct role for NADPH:cytochrome P450 oxidoreductase. *Carcinogenesis* **1994**, *15* (8), 1503-1510; (b) Jones, G. D. D.; Weinfeld, M., Dual action of tirapazamine in the induction of DNA strand breaks. *Cancer Res.* **1996**, *56*, 1584-1590.
14. (a) Shinde, S. S.; Hay, M. P.; Patterson, A. V.; Denny, W. A.; Anderson, R. F., Spin trapping of radicals other than the hydroxyl radical upon reduction of the anticancer agent tirapazamine by cytochrome P450 reductase. *J. Am. Chem. Soc.* **2009**, *131* (40), 14220-14221; (b) Shinde, S. S.; Maroz, A.; Hay, M. P.; Patterson, A. V.; Denny, W. A.; Anderson, R. F., Characterization of Radicals Formed Following Enzymatic Reduction of 3-Substituted Analogues of the Hypoxia-Selective Cytotoxin 3-Amino-1,2,4-Benzotriazine 1,4-Dioxide (Tirapazamine). *J. Am. Chem. Soc.* **2010**, *132* (8), 2591-2599; (c) Junnotula, V.; Sarkar, U.; Sinha, S.; Gates, K. S., Initiation of DNA strand cleavage by 1,2,4-benzotriazine 1,4-dioxides: mechanistic insight from studies of 3-methyl-1,2,4-benzotriazine 1,4-dioxide. *J. Am. Chem. Soc.* **2009**, *131*, 1015-1024.
15. Chowdhury, G.; Junnotula, V.; Daniels, J. S.; Greenberg, M. M.; Gates, K. S., DNA strand damage analysis provides evidence that the tumor cell-specific cytotoxin tirapazamine produces hydroxyl radical and acts as a surrogate for O<sub>2</sub>. *J. Am. Chem. Soc.* **2007**, *129*, 12870-12877.
16. (a) Barton, D. H. R.; Crich, D.; Motherwell, W. B., The invention of new radical chain reactions. Part VIII. Radical chemistry of thiohydroxamic esters; a new method for the generation of carbon radicals from carboxylic acids. *Tetrahedron* **1985**, *41* (19), 3901-3924; (b) Barton, D. H. R.; Jasberenyi, J. C.; Morrell, A. I., pyridinethione generation of hydroxyl radical. *Tetrahedron Lett.* **1991**, *32*, 311-314; (c) Adam, W.; Ballmaier, D.; Epe, B.; Grimm, G. N.; Saha-Moller, C. R., N-Hydroxypyridinethiones as photochemical hydroxyl radical sources for oxidative DNA damage. *Angew. Chem. Int. Ed. Eng.* **1995**, *34* (19), 2156-2158.
17. (a) Wölfle, I.; Lodays, J.; Sauerwein, B.; Schuster, G. B., Photoinduced electron transfer reactions: Nitrogen-oxygen bond cleavage in reduced N-(aryloxy)pyridinium and N,N'-dialkoxy-4,4'-bipyridinium salts. *J. Am. Chem. Soc.* **1992**, *114*, 9304-9309; (b) Aveline, B. M.; Kochevar, I. E.; Redmond, R. W., N-Hydroxypyridine-2(1H)-thione: Not a selective generator of hydroxyl radicals in aqueous solution. *J. Am. Chem. Soc.* **1996**, *118*, 289-290.
18. Shinde, S. S.; Anderson, R. F.; Hay, M. P.; Gamage, S. A.; Denny, W. A., Oxidation of 2-Deoxyribose by Benzotriazinyl Radicals of Antitumor 3-Amino-1,2,4-benzotriazine 1,4-Dioxides. *J. Am. Chem. Soc.* **2004**, *126* (25), 7865-7874.



19. Christensen, H. C.; Sehested, K.; Hart, E. J., Formation of benzyl radicals by pulse radiolysis of toluene in aqueous solutions. *J. Phys. Chem.* **1973**, *77* (8), 983-987.
20. (a) Fuchs, T. E. Bioorganic chemistry of DNA-damaging heterocyclic n-oxides. 2003; (b) Junnotula, V. Chemical mechanisms underlying the medicinal activity of metabolically-activated N-oxide antitumor agents. 2008.
21. (a) Kelson, A. B.; McNamara, J. P.; Pandey, A.; Ryan, K. J.; Dorie, M. J.; McAfee, P. A.; Menke, D. R.; Brown, J. M.; Tracy, M., 1,2,4-Benzotriazine 1,4-dioxides. An important class of hypoxic cytotoxins with antitumor activity. *Anticancer Drug Des* **1998**, *13*, 575-92; (b) Zeman, E. M.; Baker, M. A.; Lemmon, M. J.; Pearson, C. I.; Adams, J. A.; Brown, J. M.; Lee, W. W.; Tracy, M., Structure-activity relationships for benzotriazine di-N-oxides. *Int. J. Radiat. Oncol., Biol., Phys.* **1989**, *16*, 977-81.
22. Shinde, S. S.; Hay, M. P.; Patterson, A. V.; Denny, W. A.; Anderson, R. F., Spin Trapping of Radicals Other Than the B7OH Radical upon Reduction of the Anticancer Agent Tirapazamine by Cytochrome P450 Reductase. *J. Am. Chem. Soc.* **2009**, *131*, 14220-14221.
23. (a) Mitra, K.; Kim, W.; Daniels, J. S.; Gates, K. S., Oxidative DNA cleavage by the antitumor antibiotic leinamycin and simple 1,2-dithiolan-3-one 1-oxides: Evidence for thiol-dependent conversion of molecular oxygen to DNA-cleaving oxygen radicals mediated by polysulfides. *J. Am. Chem. Soc.* **1997**, *119*, 11691-11692; (b) Ganley, B.; Chowdhury, G.; Bhansali, J.; Daniels, J. S.; Gates, K. S., Redox-activated, hypoxia-selective DNA cleavage by quinoxaline 1,4-di-N-oxide. *Bioorg. Med. Chem.* **2001**, *9*, 2395-2401.
24. Hertzberg, R. P.; Dervan, P. B., Cleavage of DNA with methidiumpropyl-EDTA-Iron(II): Reaction conditions and product analyses. *Biochemistry* **1984**, *23*, 3934-3945.
25. (a) Chowdhury, G.; Kotandeniya, D.; Barnes, C. L.; Gates, K. S., Enzyme-activated, hypoxia-selective DNA damage by 3-amino-2-quinoxalinecarbonitrile 1,4-di-N-oxide. *Chem. Res. Toxicol.* **2004**, *17* (11), 1399-1405; (b) Junnotula, V.; Rajapakse, A.; Abrillaga, L.; Lopez de Cerain, A.; Solano, B.; Villar, R.; Monge, A.; Gates, K. S., DNA strand cleaving properties and hypoxia-selective cytotoxicity of 7-chloro-2-thienylcarbonyl-3-trifluoromethylquinoxaline 1,4-dioxide. *Bioorg. Med. Chem.* **2010**, *18*, 3125-3132.

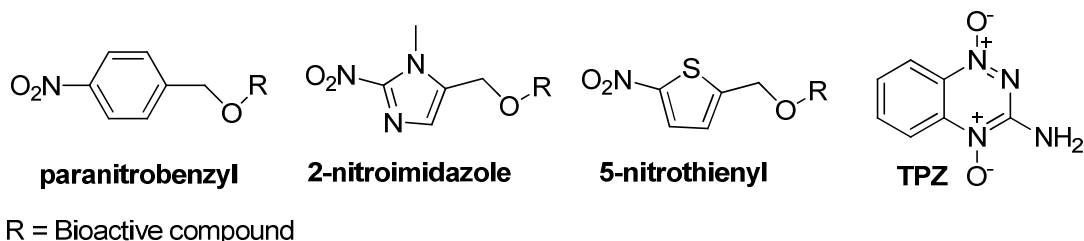
26. Laderoute, K.; Rauth, A. M., Identification of two major reduction products of the hypoxic cell toxin 3-amino-1,2,4-benzotriazine-1,4-dioxide. *Biochem. Pharmacol.* **1986**, *35*, 3417-3420.
  
27. Sambrook, J.; Fritsch, E. F.; Maniatis, T., *Molecular Cloning: A Lab Manual*. Cold Spring Harbor Press: Cold Spring Harbor, NY, 1989.
  
28. Daniels, J. S.; Gates, K. S.; Tronche, C.; Greenberg, M. M., Direct evidence for bimodal DNA damage induced by tirapazamine. *Chem. Res. Toxicol.* **1998**, *11* (11), 1254-1257.

## Chapter 5

### Synthesis of bioreductively activated nitroaromatic triggers

#### 5.1. Qualitative and quantitative determination of hypoxia

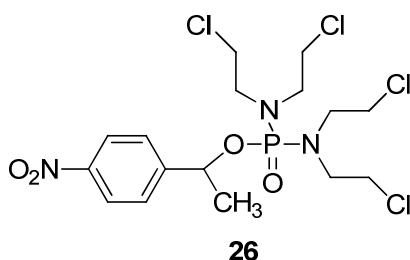
Chapters 1, 2 and 3 described the importance of hypoxia or low oxygen concentration to tumor physiology and tumor therapy. Detection and quantification of oxygen levels is emerging as an important tool in the treatment of tumors.<sup>1</sup> Various methods of characterization for tumor hypoxia have been introduced to the research community.<sup>2</sup> As discussed in previous chapters, there is a demand for suitable fluorescent probes to detect hypoxia.<sup>3</sup> A complete description of small molecule fluorescent probe, which can detect hypoxia, was included in chapters 2 and 3. In a similar approach, a compound which can undergo hypoxia selective enzymatic bioreduction and maintain oxygen sensitive reduction may be coupled to a fluorophore, to construct fluorescent probes to detect hypoxia.<sup>4</sup> Nitroaromatic compounds such as para nitrobenzyl, 2-nitroimidazole and 5-nitrothienyl groups and tirapazamine might be used as a bioreductive aromatic compound which can undergo oxygen-sensitive reduction and release the fluorescent molecule (Scheme 5.1).



**Scheme 5.1.** Bioreducible moieties can be used as oxygen sensors

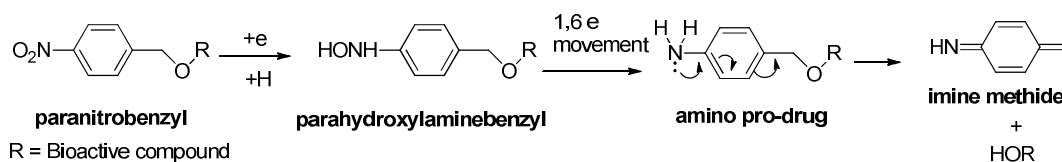
## 5.2 Goal: Constructing suitable nitroaromatic fluorescent probe for hypoxia

Current research on bio-reductive pro-drugs suggests that oxygen sensitive bio-reducible species such as nitro-benzyl, 2-nitroimidazole and 5-nitrothienyl groups, when appended to cytotoxic agents to mask the drug activity, show encouraging selective drug delivery toward low oxygenated tumors. In order to test the performance of nitro-phenyl group as an oxygen sensor, Borche and coworkers attached phosphoramidite toxin to produce series of prodrugs (Scheme 5.2).<sup>5</sup> Following the same design strategy, fluorophores can be attached to nitroaromatic groups using suitable coupling reactions.



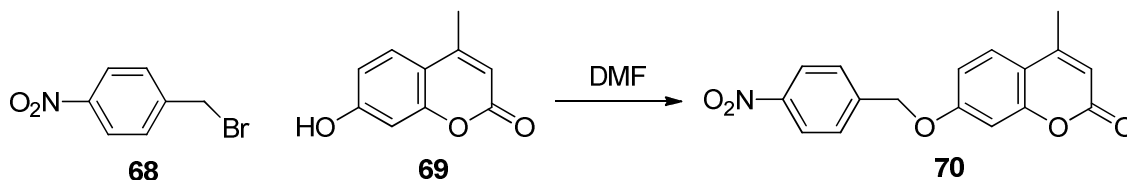
**Scheme 5.2.** Nitrophenyl benzyl phosphoramidite prodrugs

The in vitro cytotoxicity studies with **26** suggest that nitrophenyl may be a suitable bioreducible moiety which can be reduced enzymatically in hypoxia. The reduction process produces electron rich hydroxylamine or amine compounds which can ultimately release the active compound and imine methide upon 1-6 elimination (Scheme 5.3).



**Scheme 5.3.** 1,6-elimination of active drug species

Such a prodrug, with a fluorophore, was made using nitrophenyl benzyl bromide **68**, over a nucleophilic displacement reaction with 7-hydroxyl-4-methyl coumarin **69**, a known fluorophore which possess a better Stokes shift and quantum yield, to produce nitrophenyl-coumarin compound **70** (Scheme 5.3).<sup>6</sup>



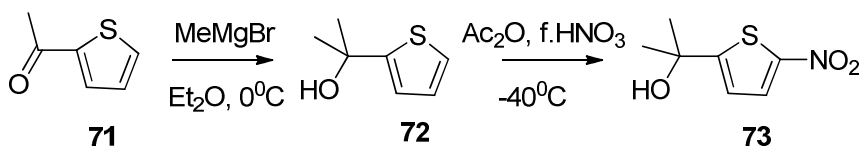
**Scheme 5.4.** Synthesis of **70**

Bioreductive in vitro assays were carried out using **70**, with NADPH:cytochrome p450 reductase;NADPH and xanthine:xanthine oxidase reducing systems. The poor release of **69** is comparable to low amount of release of thiopurine, which was attached to nitrobenzyl in the pro-drug form.<sup>7</sup> While concluding that nitrophenyl group is not compatible for enzymatic reducing systems NADPH:cytochrome p450 reductase;NADPH and xanthine:xanthine oxidase, however we set out to construct other nitroaromatic bioreducible groups 5-nitrothienyl and 2-nitroimidazole.

### 5.3 Synthesis of 5-nitrothienyl moiety, 2-(5-Nitrothien-2-yl) propan-2-ol (**73**)

Nitrothiophenes are bioreducible nitroaromatic group, which can be reduced by cellular reductases under low oxygen levels.<sup>8</sup> In addition, methyl groups on the benzylic carbon facilitates effective drug release from the probe.<sup>9</sup> Hence, Nitrothienyl 2-(5-Nitrothien-2-yl) propan-2-ol **73** was prepared as a nitroaromatic trigger candidate. Methyl magnesium bromide was added to 2-acetylthiophene **71**, in ethyl ether to afford thiophene alcohol **72**. Compound **72** was separated by column chromatography. Nitration

on the 5 carbon of **72** was done using acetic anhydride: Nitric acid nitration mixture. To a cold solution of **72** in acetic anhydride, fuming nitric acid was added while mixing at  $-70^{\circ}\text{C}$ .<sup>10</sup> Upon neutralizing, using sodium bicarbonate, the product 2-(5-nitrothien-2-yl)propan-2-ol (**73**) was separated and purified using column chromatography (Scheme 5.5).

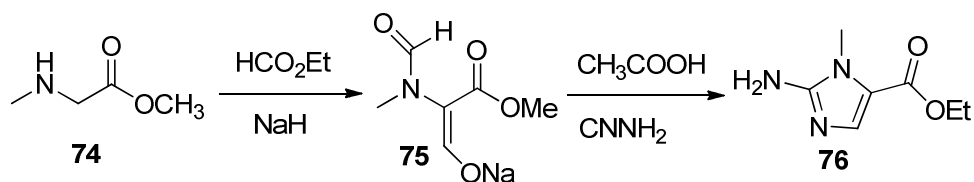


**Scheme 5.5.** Synthesis of 2-(5-nitrothien-2-yl)propan-2-ol **73**

#### 5.4 Synthesis of 1-methyl-2-nitro-5-hydroxymethyl imidazole **79**

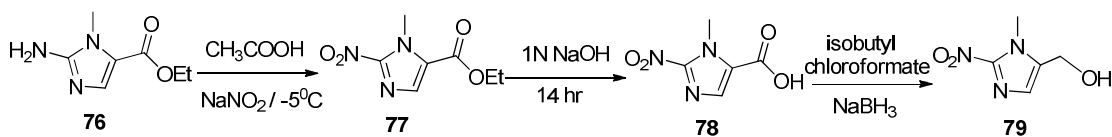
The compound 2-nitro-1-methyl imidazole group has been used as a component of bio-reductive prodrugs.<sup>2a, 4a, 11</sup> The amino compound 1-methyl-2-amino-imidazole may be used as the starting compound to reach the desired nitro imidazole group. In the synthesis, published by Bellani and Lancini was modified in the preparation of 1-methyl-2-amino-5-carbomethoxyimidazole **76**.<sup>12</sup> Briefly, Ethyl formate was added to ethyl sarcocine ester (**74**) powder and the mixture was cooled below  $0^{\circ}\text{C}$ . Then NaH was added gradually and stirred for 14 hrs. Then, trituration using hexane produced a thick liquid and was separated from hexane. The residue was mixed with ethanol and HCl, followed by heating at  $100^{\circ}\text{C}$  with vigorous stirring for 1 hr. Then the reaction was cooled and added with cyanamide, 10% acetic acid and sodium acetate and heated at  $90^{\circ}\text{C}$  for 90 min. Then the reaction was cooled and the pH adjusted to 1 using HCl. The solvent was removed by rotary evaporation below  $45^{\circ}\text{C}$  until the volume had reduced to one fifth of the initial volume. Then the pH was raised to 8-9 using  $\text{KHCO}_3$ . Ethyl acetate was used to separate

organic layer and the extract was dried with MgSO<sub>4</sub>. Compound **76** was isolated by column chromatography (Scheme 5.5).



**Scheme 5.6.** Synthesis of **76** from sarcosine ethyl ester **74**

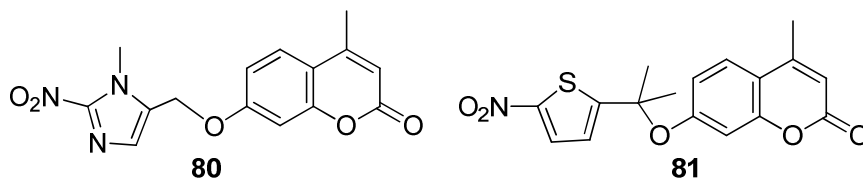
The nitration of **76** afforded the nitro imidazole compound 1-methyl-2-nitro-5-carbomethoxyimidazole **77**. In the synthesis, the compound **79** was added to acetic acid and the acetic acid/**79** mixture was added to a sodium nitrite solution, which is at 0°C, drop wise while stirring. Overnight stirring at room temperature was followed by extraction of the organic material into methylene chloride. The methylene chloride layer was dried over MgSO<sub>4</sub>. Compound **77** was separated using column chromatography.<sup>13</sup> The ester bond of **77** was hydrolyzed using 1N NaOH to obtain **78**. The carboxylic group of **78** was reduced using NaBH<sub>3</sub> and isoformyl chloroformate.<sup>14</sup> The resulting solution was extracted with THF and the dry organic material was column chromatographed to obtain **79** (Scheme 5.7).



**Scheme 5.7.** Synthesis of 1-methyl-2-nitro-5-hydroxymethyl imidazole **79**

## 5.5 Synthesis of 80 and 81

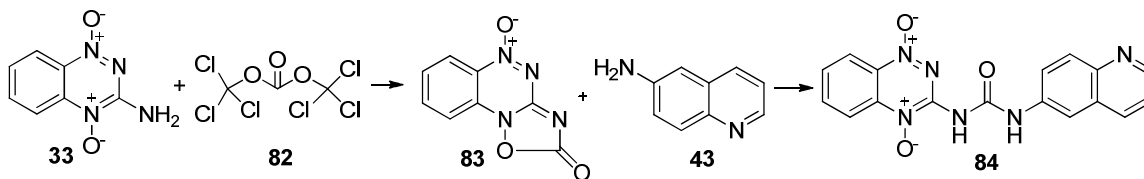
Prodrugs **80** and **81** may be made employing Mitsunobu coupling reactions. The nitroaromatics **73** and **79** were reacted with the coumarin fluorophore **69** under Mitsunobu conditions. The attempts to make compounds **80** and **81** were not successful (Scheme 5.8).



**Scheme 5.8.** Fluorescent probes **83** and **84**.

## 5.7 Synthesis of 3-acetylquinoline-1,2,4-benzotriazine 1,4-dioxide **84**

In an separate effort to prepare a probe for hypoxia was done by coupling 3-amino-1,2,4-benzotriazine 1,4-dioxide (TPZ), **33** with 6-aminoquinoline **43**, a known fluorophore. TPZ was reacted with triphosgene **82** to produce intermediate **83** and then, **43** was added in situ to obtain **84** (Scheme 5.9).<sup>15</sup>



**Scheme 5.9.** Synthesis of **84** using triphosgene **82**, **33** and **43**



## 5.8 Experimental

### 5.7.1 Synthesis of paranitrophenyl-4-methyl-coumarin ether (70)

To a slurry of NaH (148 mg, 6.16 mmol) in dry DMF (10 mL), at 0°C was added with **69** (542.6 mg, 3.08 mmol), in dry DMF. Then **68** (1000 mg, 4.6 mmol) was added to the mixture and was stirred at 0°C for 12 h. Upon disappearance of **69** on TLC, the mixture was extracted to EtOAc, dried with brine and column chromatographed to obtain the ether **70** (214 mg, R<sub>f</sub> value = 0.5 in 50% hexane in EtOAc). <sup>1</sup>H NMR (CDCl<sub>3</sub>, 500 MHz): δ ppm 8.27 (d, J = 8.5 Hz, 2H), 7.62 (d, J = 8.5 Hz, 2H), 7.53 (d, J = 8.5 Hz, 1H), 6.94 (d, J = 8.5 Hz, 1H), 6.87 (s, 1H), 6.16 (s, 1H), 5.24 (s, 1H), 2.40 (s, 1H). <sup>13</sup>C NMR (CDCl<sub>3</sub>, 125.5 MHz): δ 160.9, 155.2, 152.3, 143.1, 127.7, 125.8, 123.9, 114.3, 112.7, 112.5, 101.9, 69.0, 18.7. LRMS (ESI, [M+H]<sup>+</sup>) m/z calcd for C<sub>17</sub>H<sub>14</sub>N<sub>1</sub>O<sub>5</sub> 312.09 calculated, found 311.95.

### 5.7.2 Synthesis of 2-thien-2-yl-propan-2-ol (72)

Compound **71**, 2-acetylthiophene (18 mL, 143 mmol) was dissolved in 300 mL Et<sub>2</sub>O at 0°C and stirred. Then nitrogen was purged. Methyl magnesium bromide (65 mL from 3M in Et<sub>2</sub>O solution) was added via a syringe. Then the reaction mixture was stirred at room temperature for 4 hr. The reaction mixture was extracted into CH<sub>2</sub>Cl<sub>2</sub> and dried with brine and MgSO<sub>4</sub>. Column chromatography afforded **72** (4.39 g, R<sub>f</sub>value = 0.4 in 100% CH<sub>2</sub>Cl<sub>2</sub>). <sup>1</sup>H NMR (CDCl<sub>3</sub>, 300 MHz): δ ppm 7.17 (d, J = 4.5 Hz, 1H), 6.93 (m, 2H), 1.66 (m, 6H). <sup>13</sup>C NMR (CDCl<sub>3</sub>, 75.5 MHz): δ 154.7, 126.9, 124.1, 122.3, 71.6, 32.5. HRMS (ESI, [M+H]<sup>+</sup>) m/z calcd for C<sub>7</sub>H<sub>10</sub>OS 142.0445 calculated, found 142.0452.

### 5.7.3 Synthesis of 2-Thien-2-yl-Propan-2-ol (73)

The thienyl alcohol 2-thien-2-yl-Propan-2-ol **72** (2 g, 10.6 mmol) was dissolved in 30 mL acetic acid and cooled to  $-70^{\circ}\text{C}$  using MeOH dry ice slurry. While stirring, fuming  $\text{HNO}_3$  (0.7 mL, 11.6 mmol) was gradually added with vigorous stirring and reaction was run for 2 hr. Then another hour stirring was done at  $-40^{\circ}\text{C}$ . Temperature was raised to  $0^{\circ}\text{C}$  and stirred for another 1 hr. Then water/ice 200 g was added and EtOAc (100 mL) was used to extract organic material. The EtOAc layer was dried using  $\text{Na}_2\text{SO}_4$ . Column chromatography performed to separate **73** (310 mg,  $R_f$  value = 0.2 with 20% EtOAc in hexane)  $^1\text{H}$  NMR ( $\text{CDCl}_3$ , 300 MHz):  $\delta$  ppm 7.78 (d,  $J = 4.5$  Hz, 1H), 6.86 (d,  $J = 4.5$  Hz, 1H), 1.66 (m, 6H).  $^{13}\text{C}$  NMR ( $\text{CDCl}_3$ , 75.5 MHz):  $\delta$  163.6, 128.8, 121.2, 71.8, 31.9. HRMS (ESI,  $[\text{M}+\text{H}]^+$ )  $m/z$  calcd for  $\text{C}_7\text{H}_9\text{O}_3\text{NS}$  187.0303 calculated, found 187.0299.

### 5.7.4 Synthesis of 1-methyl-2-amino-5-carbethoxyimidazole (76)

Ethyl formate (62.5 mL) was added to sarcosine methylester hydrochloride **74** (10 g, 71 mmol) in a 500 mL r.b. and chilled at  $0^{\circ}\text{C}$ . Sodium hydride (60% oil suspension, 6.58 g, 0.1645 mmol) was added slowly over 2 h and stirred for 14 h to produce **75**.<sup>12a</sup> Then, trituration was done twice using 50 ml of hexane to obtain light brown slurry. The brown slurry was added to a new 500 mL r.b. and added with 50 mL EtOH and 8 mL of conc. HCl. The mixture was stirred at  $90^{\circ}\text{C}$  for 1 hr. Then the mixture was cooled to room temperature and filtered. To the filtrate, 10 mL of 10% aqueous HOAc, sodium acetate (10.73g, 0.13 mmol) and  $\text{CH}_3\text{CN}$  (5.5 g, 0.13 mmol) were added and stirred for 90 min. The pH was raised to 8-9 using  $\text{KHCO}_3$  and the organic material was extracted to

EtOAc. Ethyl acetate layer was dried using brine and concentrated. The dry organic mixture was column chromatographed to obtain **76** (1 g,  $R_f$  value = 0.31 with 2% MeOH in EtOAc in hexane)  $^1\text{H}$  NMR (DMSO, 500 MHz):  $\delta$  ppm 7.26 (s, 1H), 6.15 (s, 2H), 4.14 (q,  $J$ = 7.0 Hz, 2H), 3.50 (s, 3H), 1.210 (t,  $J$ = 7.0 Hz, 3H).  $^{13}\text{C}$  NMR (DMSO, 125.5 MHz):  $\delta$  159.0, 154.3, 136.1, 116.86, 58.9, 30.2, 14.4. HRMS (ESI,  $[\text{M}+\text{H}]^+$ )  $m/z$  calcd for  $\text{C}_7\text{H}_{12}\text{O}_2\text{N}_3$  170.0930 calculated, found 170.0929.

### 5.7.5 Synthesis of 1-methyl-2-nitro-5-carbethoxyimidazole (**77**)

Water (20 ml) was added with  $\text{NaNO}_2$  (3g) and the solution was cooled below  $-5^\circ\text{C}$ . Then, 1.5 g of **76** in acetic acid was added drop wise to sodium nitrite solution while maintaining the temperature below  $0^\circ\text{C}$ . Upon completion of the reaction, ethyl acetate was used to extract organic products. The EtOAc layer was dried using  $\text{MgSO}_4$ . Compound **77** was separated by silica gel chromatography (0.6 g,  $R_f$  value = 0.5 in 100%  $\text{CH}_2\text{Cl}_2$ ).  $^1\text{H}$  NMR ( $\text{CDCl}_3$ , 500 MHz):  $\delta$  ppm 7.73 (s, 1H), 4.38 (m, 5H), 1.40 (s, 3H).  $^{13}\text{C}$  NMR ( $\text{CDCl}_3$ , 125.5 MHz):  $\delta$  159.0, 136.5, 134.64, 126.6, 61.8, 35.3, 14.1. HRMS (ESI,  $[\text{M}+\text{H}]^+$ )  $m/z$  calcd for  $\text{C}_7\text{H}_{10}\text{O}_4\text{N}_3$  200.0671 calculated, found 200.0669.

### 5.7.6 Synthesis of 1-methyl-2-nitro-5-carboxylimidazole (**78**)

In 10 mL of 1N NaOH compound **77** (0.6 g, 3.015 mmol) was dissolved and the mixture was stirred overnight. The pH was adjusted to 1 using conc. HCl. Then the product **78** was extracted to EtOAc and ethyl acetate layer was dried using  $\text{MgSO}_4$  (0.6 g,  $R_f$  value = 0.2 in 100% EtOAc).  $^1\text{H}$  NMR (DMSO, 500 MHz):  $\delta$  ppm 7.71 (s, 1H), 7.56

(s, acidic H), 4.17 (s, 3H).  $^{13}\text{C}$  NMR (DMSO, 125.5 MHz):  $\delta$  160.71, 147.8, 134.1, 127.3, 35.4. LRMS (ESI,  $[\text{M}+\text{H}]^+$ )  $m/z$  calcd for  $\text{C}_5\text{H}_6\text{O}_4\text{N}_3$  172.03 calculated, found 172.11.

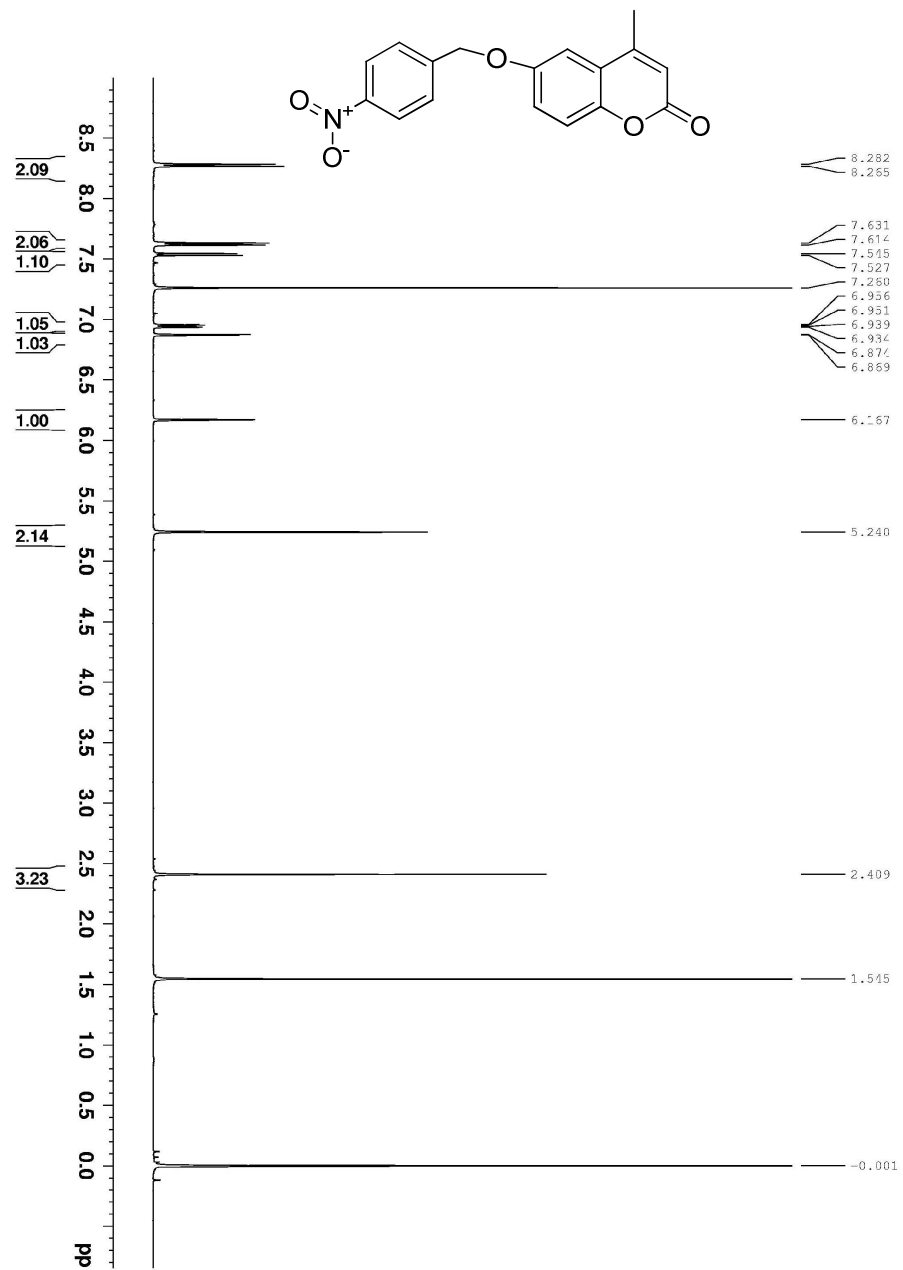
### 5.7.7 Synthesis of 1-methyl-2-nitro-5-hydroxymethylimidazole (79)

A mixture of **78** (70 mg, 0.41 mmol) and triethylamine (0.318 mL, 0.649 mmol) in anhydrous THF (1 mL) was cooled in dry acetonitrile bath ( $-20^\circ\text{C}$ ). Isobutyl chloroformate (100  $\mu\text{L}$ , 7.7 mmol) was added dropwise, over 10 min. Then the reaction was stirred over 1 h. Then sodium borohydride (81 mg) was added to the reaction mixture. Then water was added drop wise over a period of 1h and the temperature was kept below  $0^\circ\text{C}$ . The products were extracted to ethyl acetate and dried with brine. Column chromatography separated pure **14** (30 mg,  $R_f$  value = 0.28 in 100% EtOAc)  $^1\text{H}$  NMR (MeOD, 500 MHz):  $\delta$  ppm 7.08 (s, 1H), 4.84 (s, 1H), 4.65 (s, 2H), 4.02 (s, 3H).  $^{13}\text{C}$  NMR (MeOD, 125.5 MHz):  $\delta$  147.4, 139.5, 127.6, 54.7, 34.9, HRMS (ESI,  $[\text{M}+\text{H}]^+$ )  $m/z$  calcd for  $\text{C}_5\text{H}_8\text{O}_3\text{N}_3$  158.0566 calculated, found 158.0575.

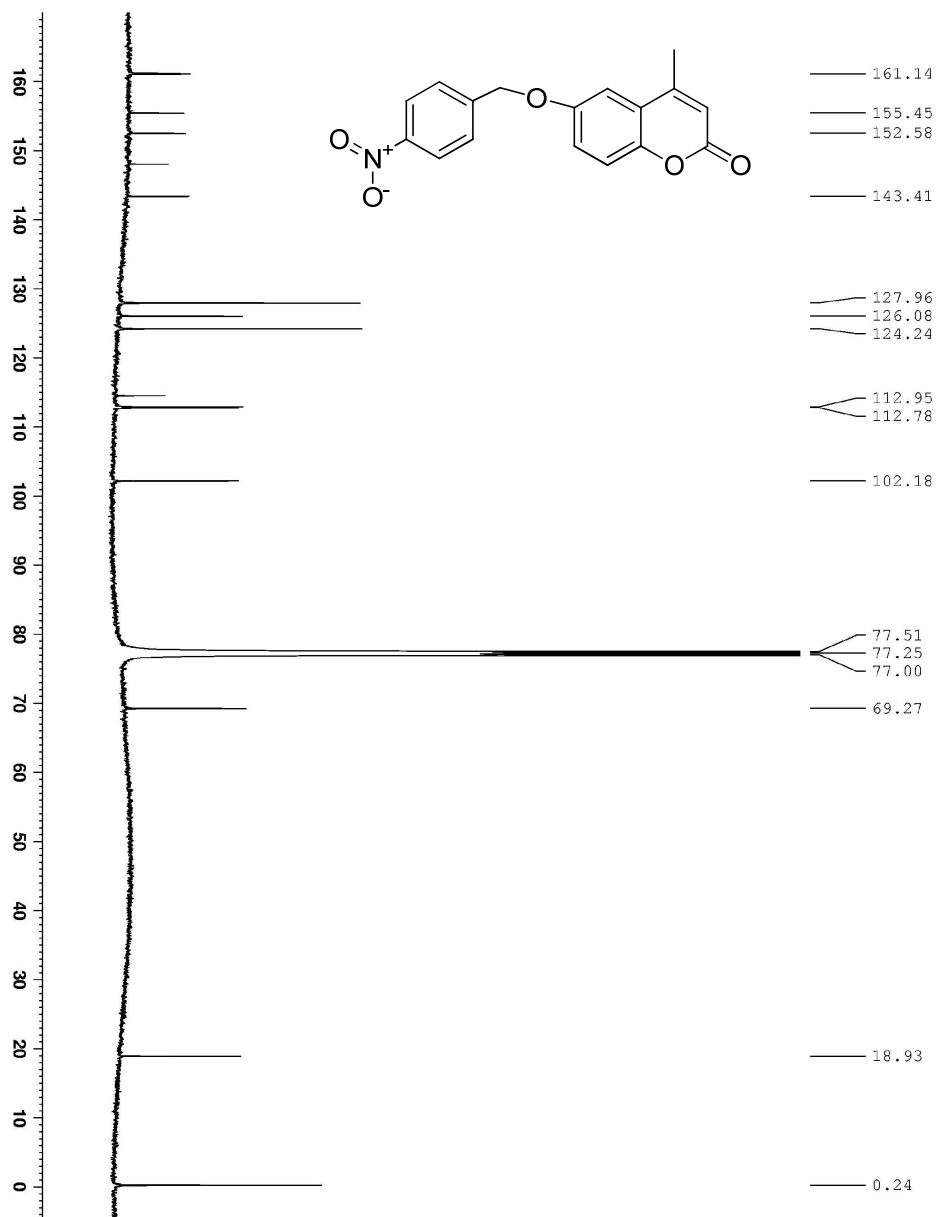
### 5.7.7 Synthesis of 3-acetylquinoline-1,2,4-benzotriazine 1,4-dioxide **84**

The compound **33** (0.15 g, 0.85 mmol) was dissolved in dry toluene (2.5 mL) and the mixture was stirred and heated to  $90^\circ\text{C}$ . Then triphosgene **82** (0.086 g, 0.29 mmol) was added to the TPZ mixture and the reaction was stirred for 5-10 min. Another batch of **82** (0.086 g, 0.29 mmol) was added and then the reaction was cooled to obtain crude **83**.<sup>15</sup> To the crude **83**, **43** (0.15 g, 0.763 mmol) in 2.5 mL DMF was added and stirred at room temperature for 10 min. The yellow solid product **84** was separated (0.02 g,  $R_f$  value = 0.1 in 2% MeOH in EtOAc).  $^1\text{H}$  NMR (DMSO, 500 MHz):  $\delta$  ppm 10.45 (s, 1H), 10.30 (s,

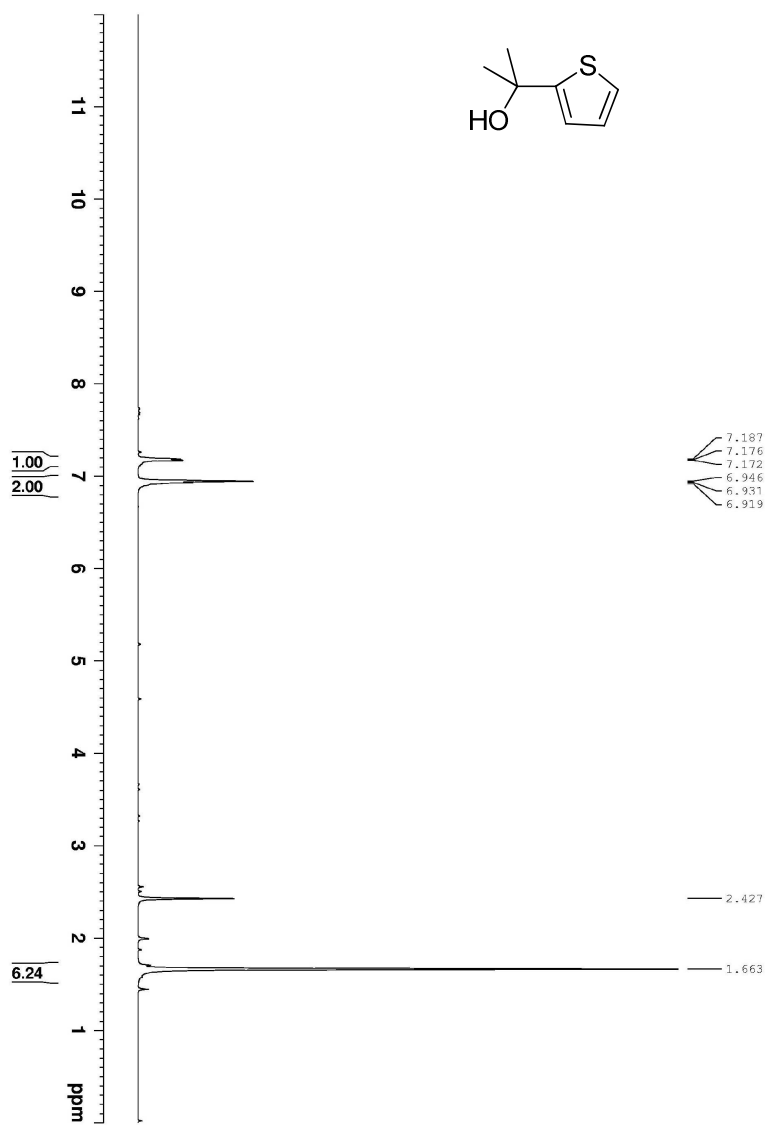
1H), 8.79 (s, 1H), 8.30 (m, 4H), 8.05 (m, 2H), 7.78 (m, 2H), 7.51 (d, J = 7.0 Hz, 1H). <sup>13</sup>C  
NMR (DMSO, 500 MHz): δ 148.7, 148.3, 145.9, 138.0, 136.6, 135.8, 132.5, 129.7,  
128.5, 122.9, 121.9, 121.1, 118.0, 114.0, HRMS (ESI [M+H]<sup>+</sup>) m/z calcd for C<sub>17</sub>H<sub>13</sub>N<sub>6</sub>O<sub>3</sub>  
349.1049 calculated, found 349.1057.



<sup>1</sup>H NMR of **70** (CDCl<sub>3</sub>, 500 MHz)

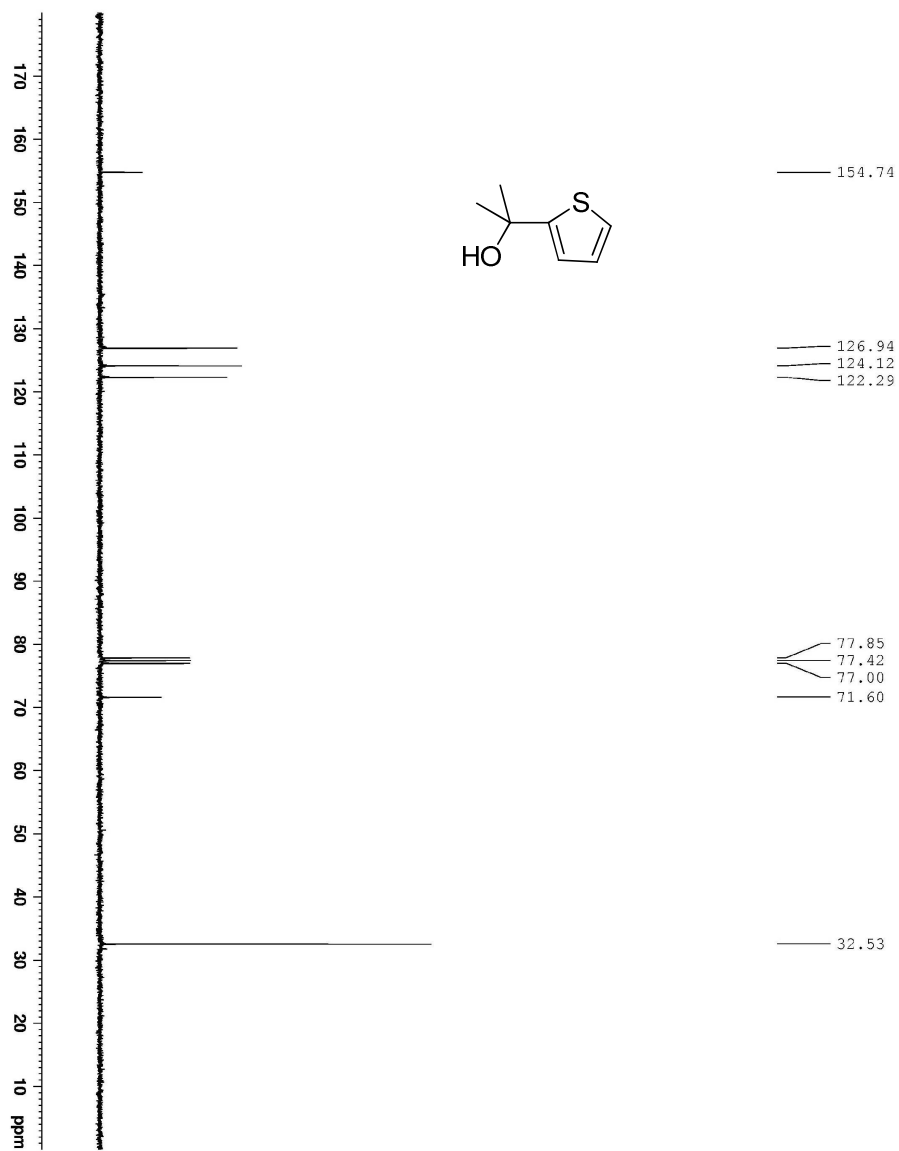


$^{13}\text{C}$  NMR of **70** ( $\text{CDCl}_3$ , 125.5 MHz)

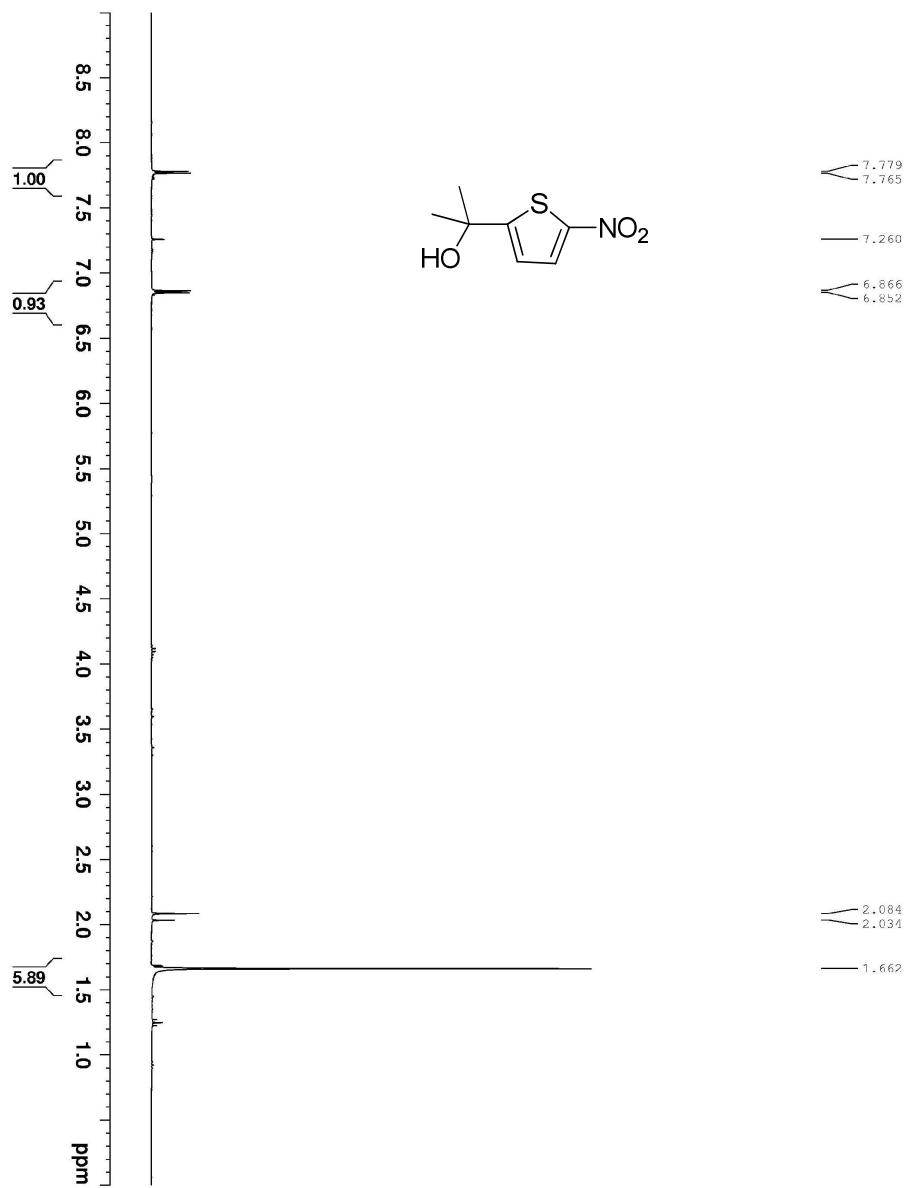


$^1\text{H}$  NMR of **72** (CDCl<sub>3</sub>, 300 MHz)

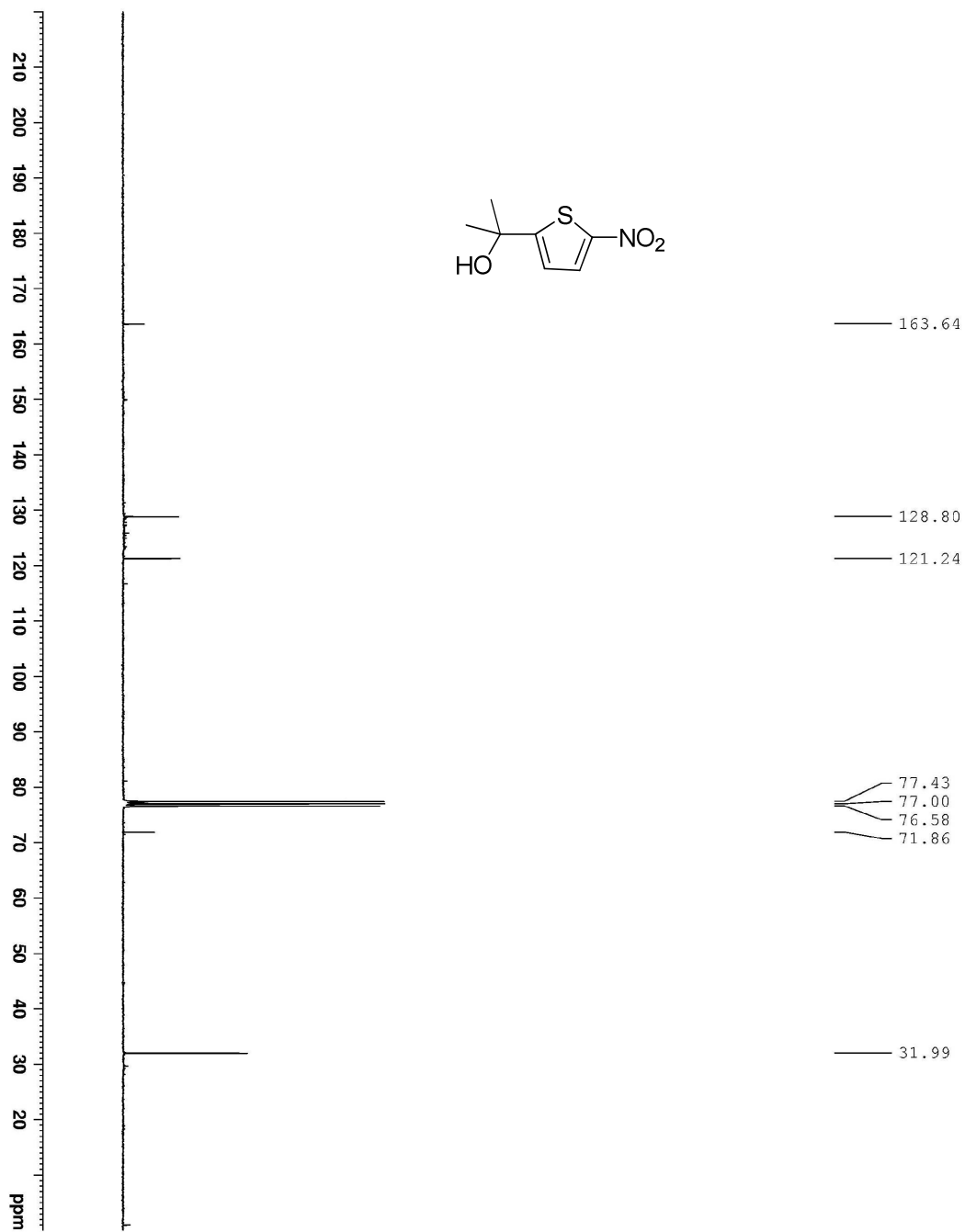




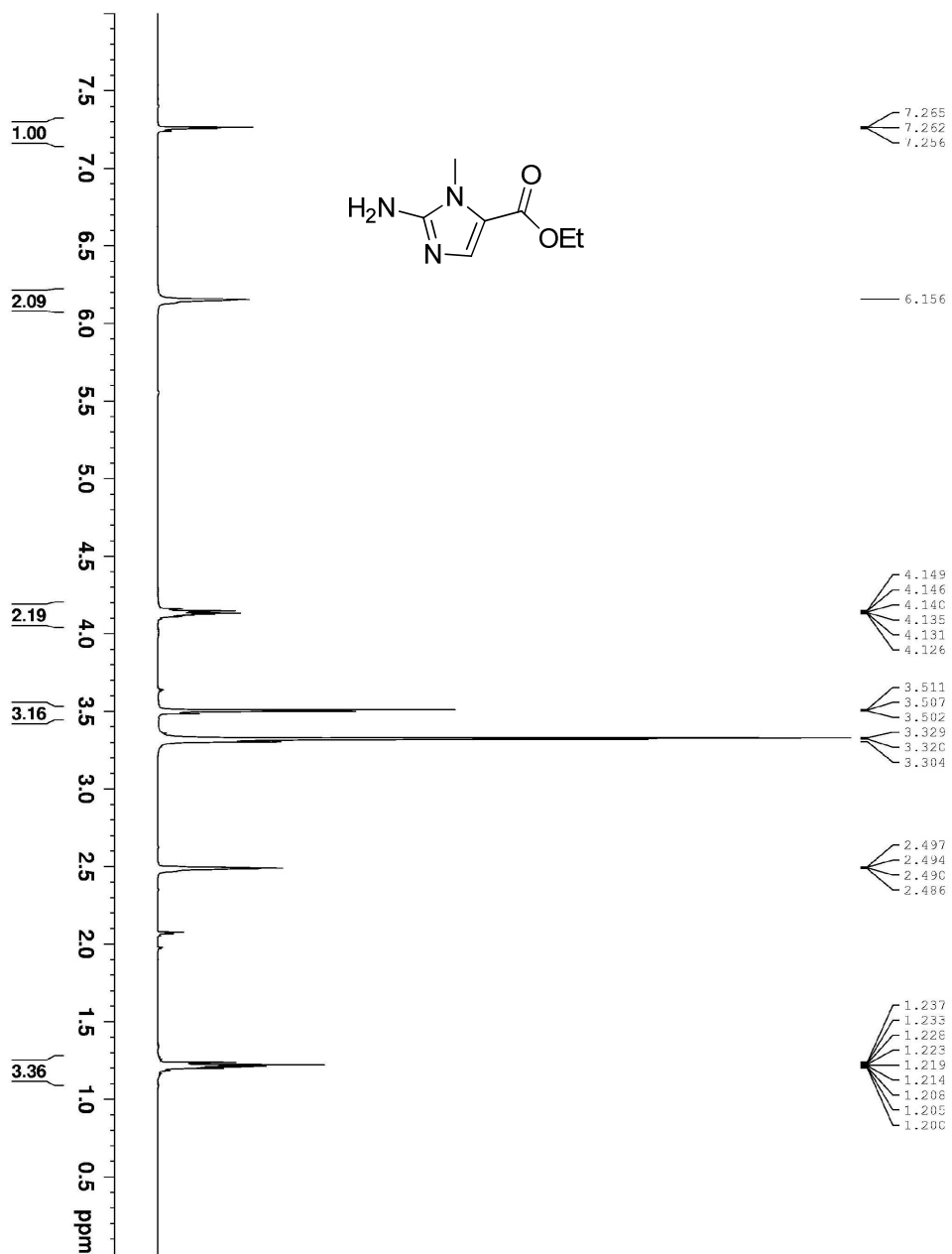
$^{13}\text{C}$  NMR of **72** ( $\text{CDCl}_3$ , 75.5 MHz)



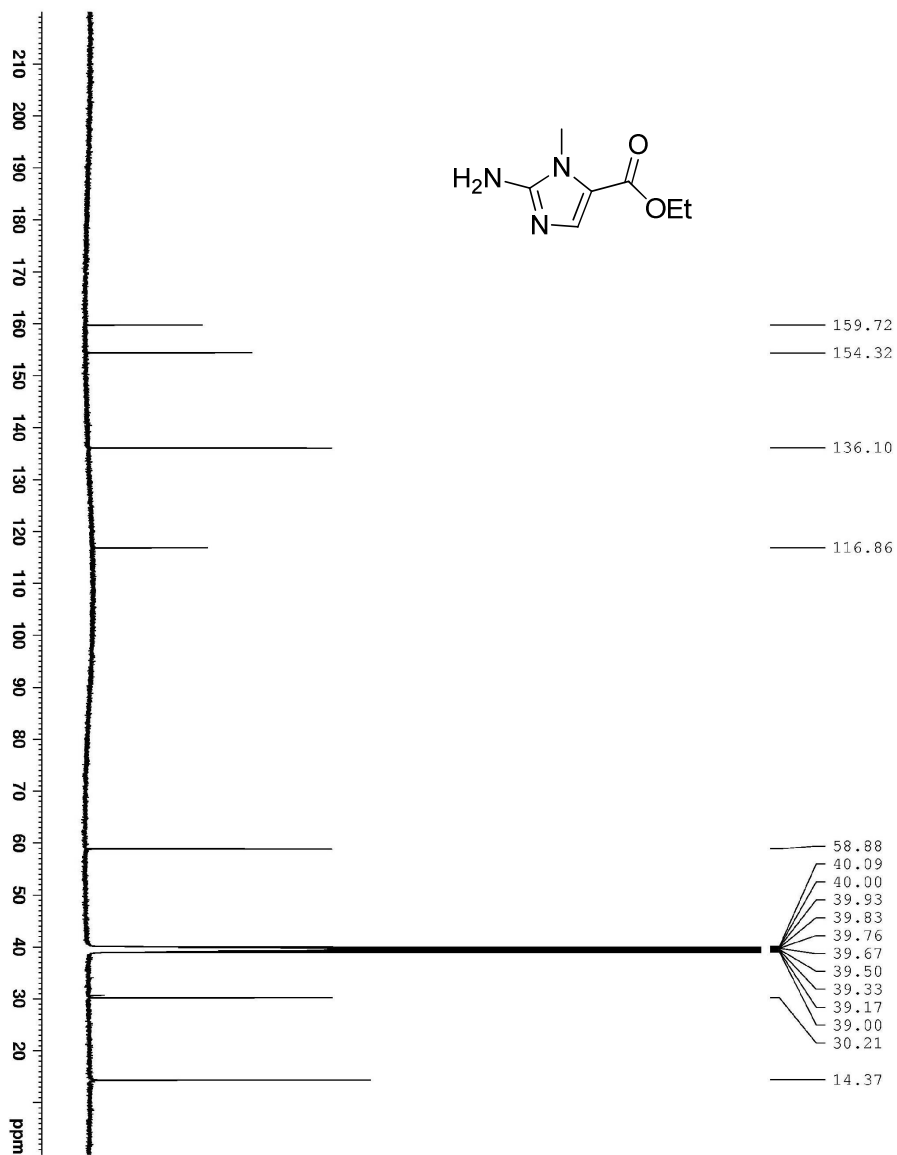
$^1\text{H NMR}$  of **73** (CDCl<sub>3</sub>, 300 MHz)



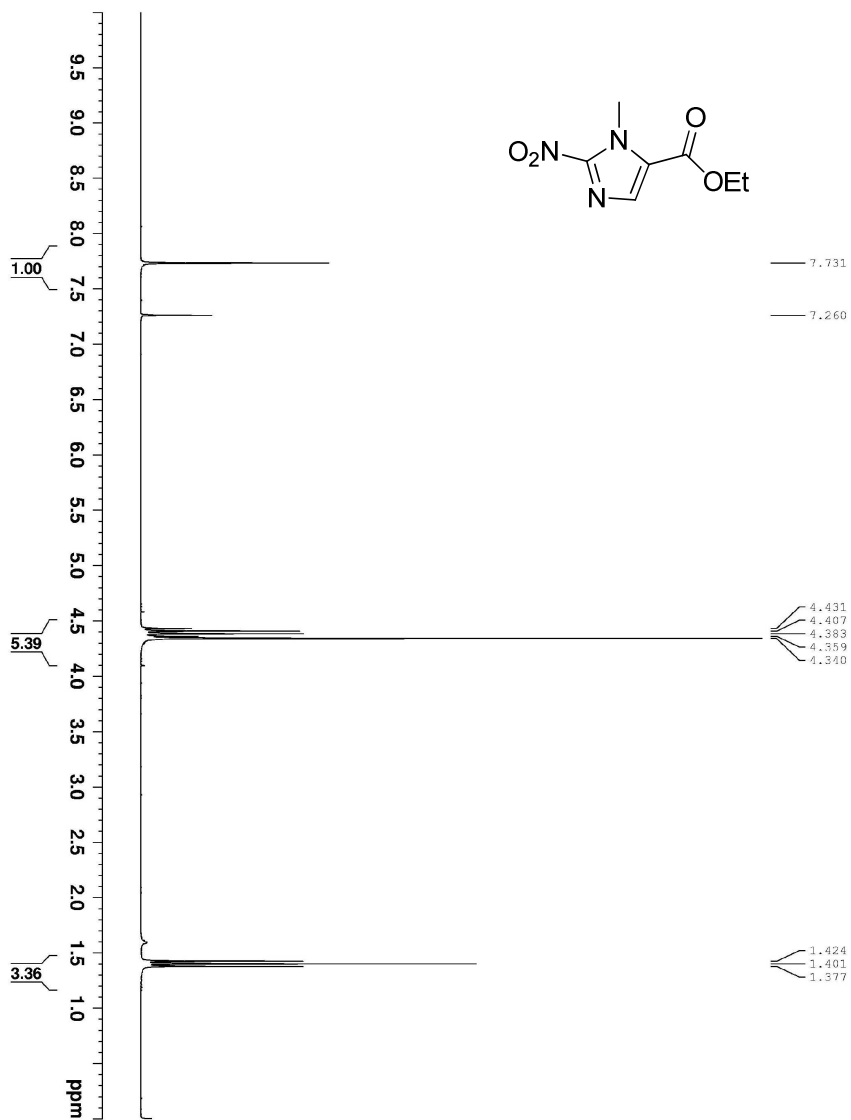
$^{13}\text{C}$  NMR of **73** (CDCl<sub>3</sub>, 75.5 MHz)



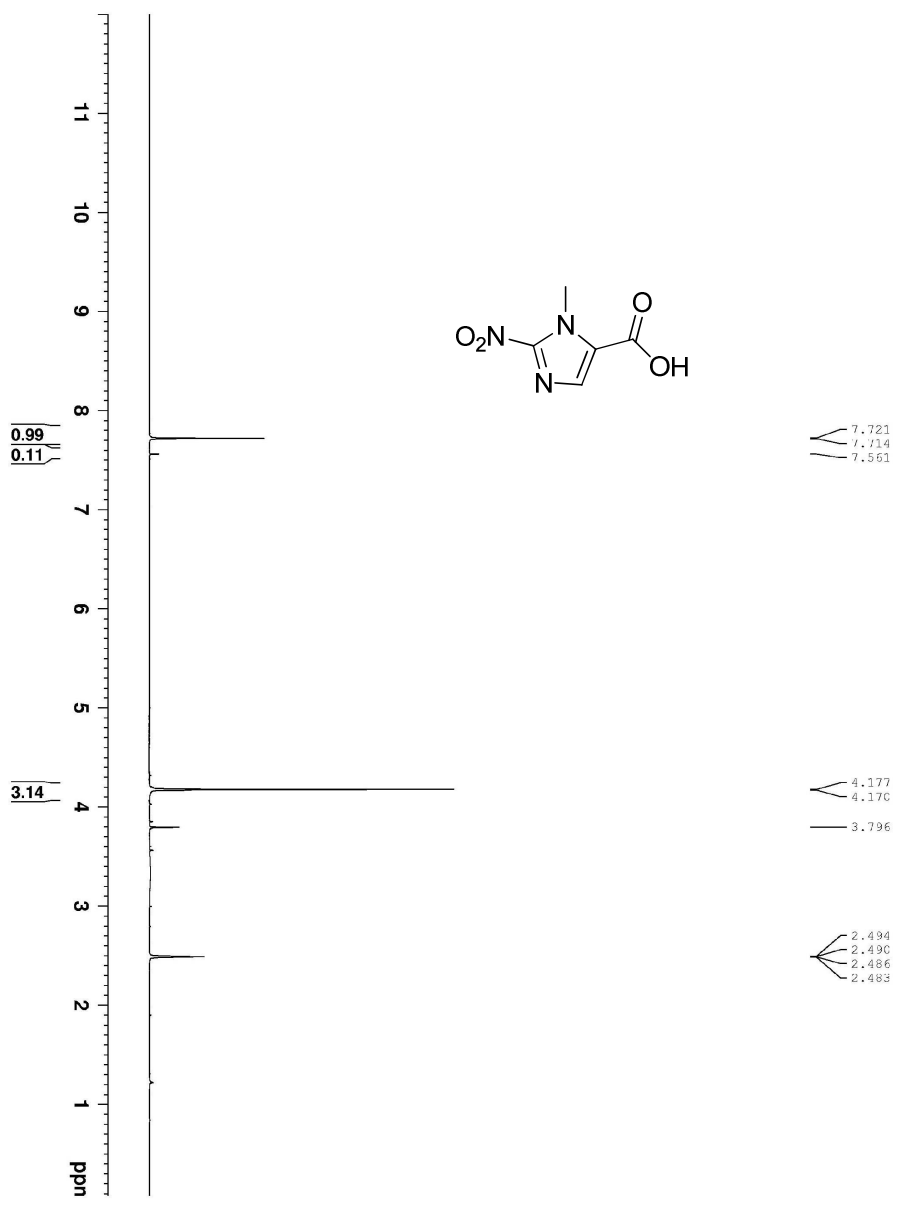
<sup>1</sup>H NMR of 76 (DMSO, 500 MHz)



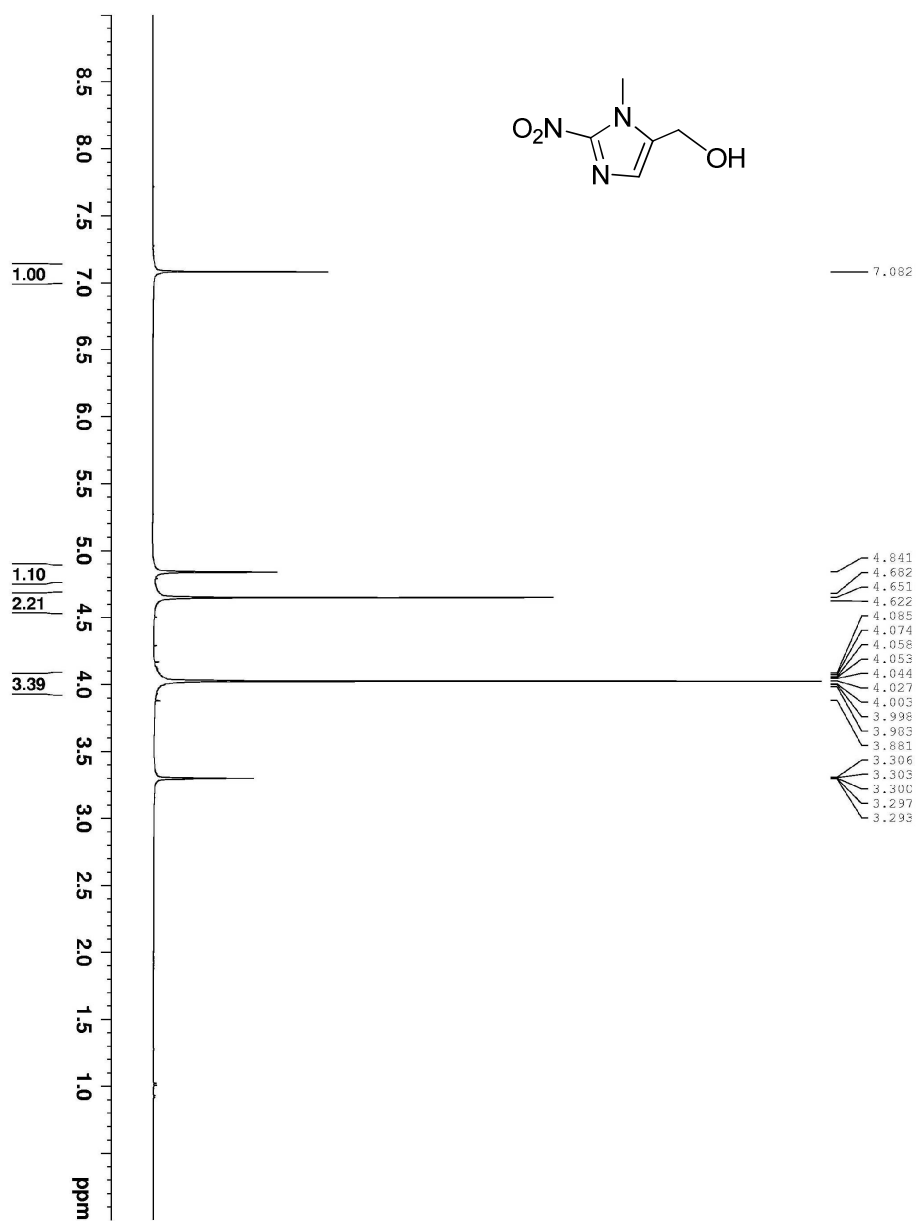
$^{13}\text{C}$  NMR of **76** (DMSO, 125.5 MHz)



$^1\text{H}$  NMR of **77** ( $\text{CDCl}_3$ , 500 MHz)

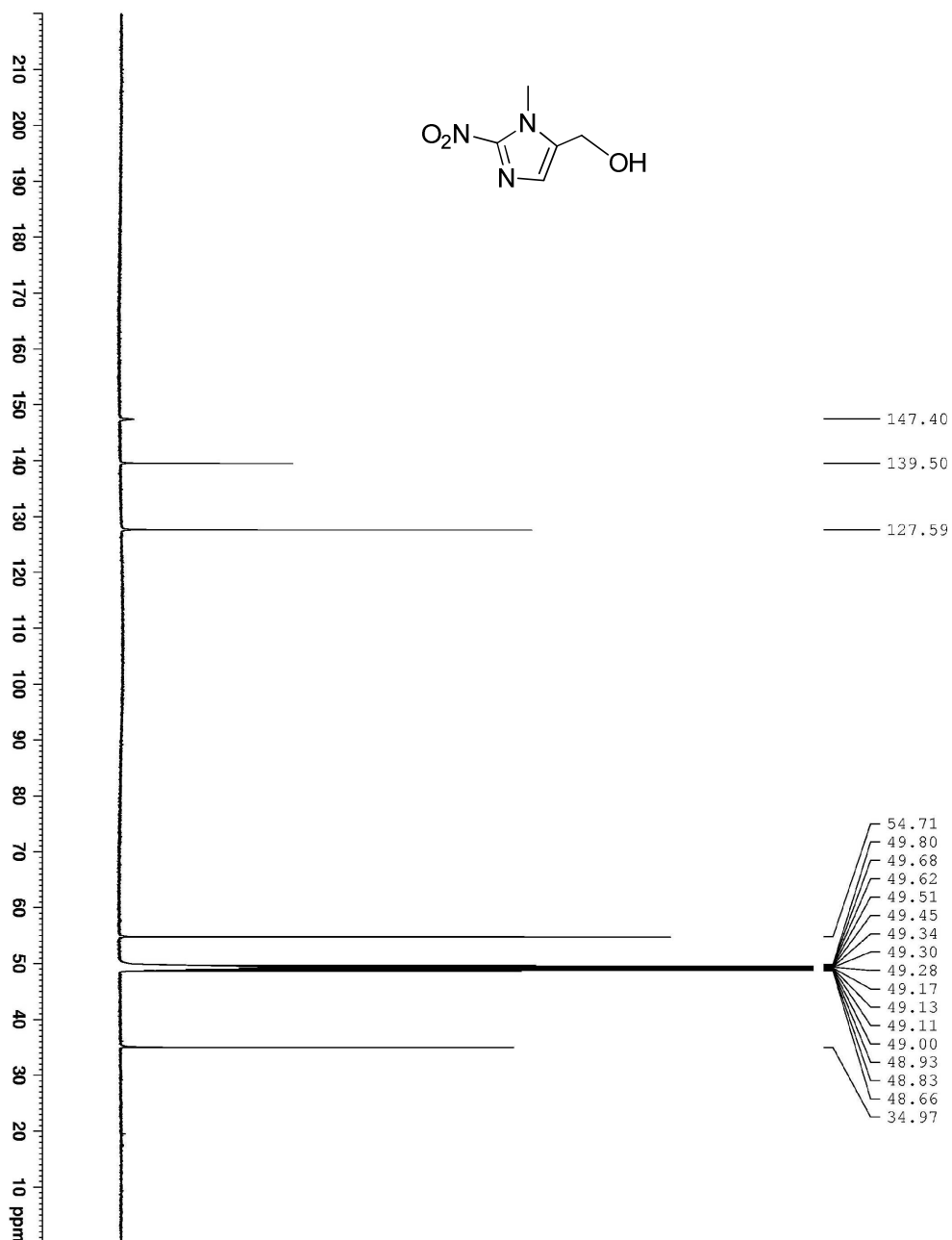


<sup>1</sup>H NMR of 78 (DMSO, 500 MHz)

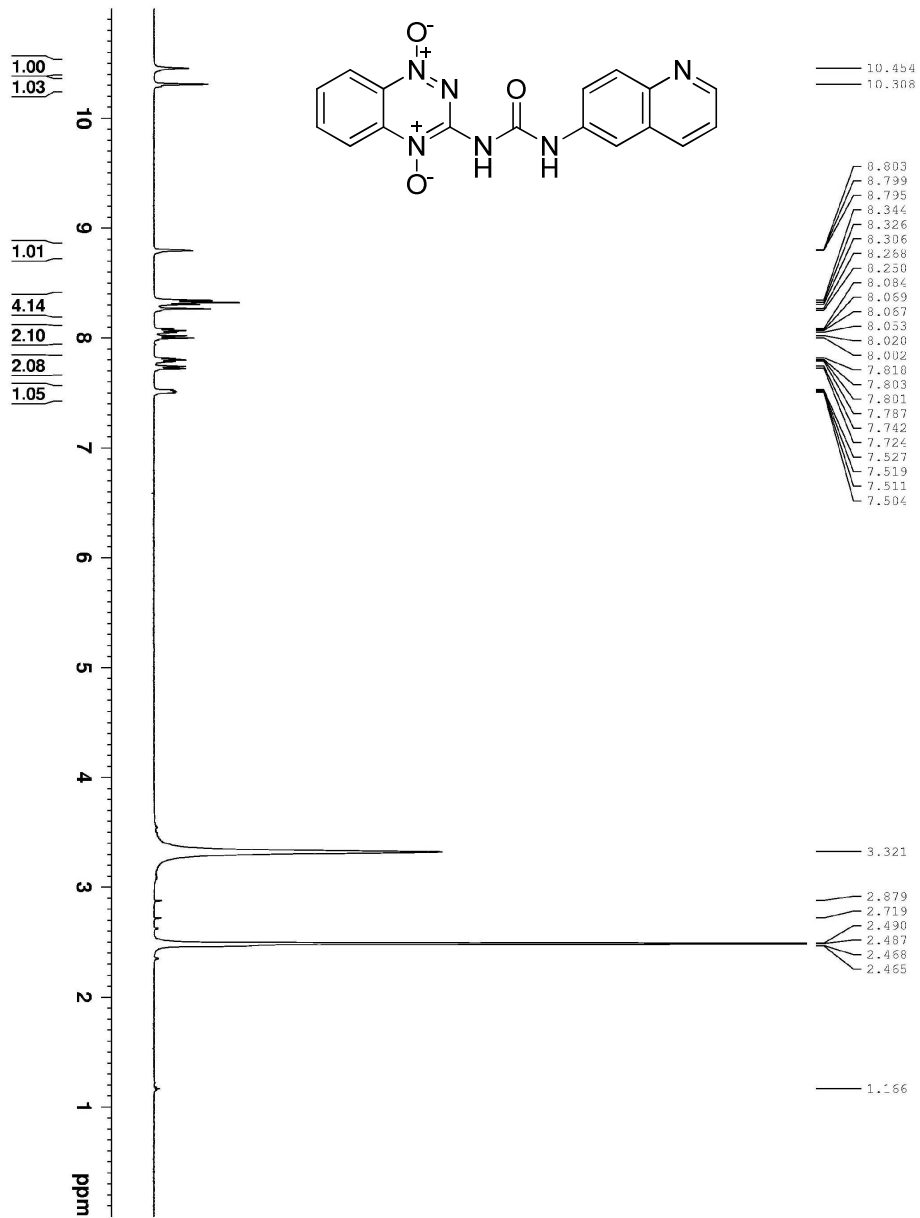


$^1\text{H}$  NMR of **79** (MeOD, 500 MHz)

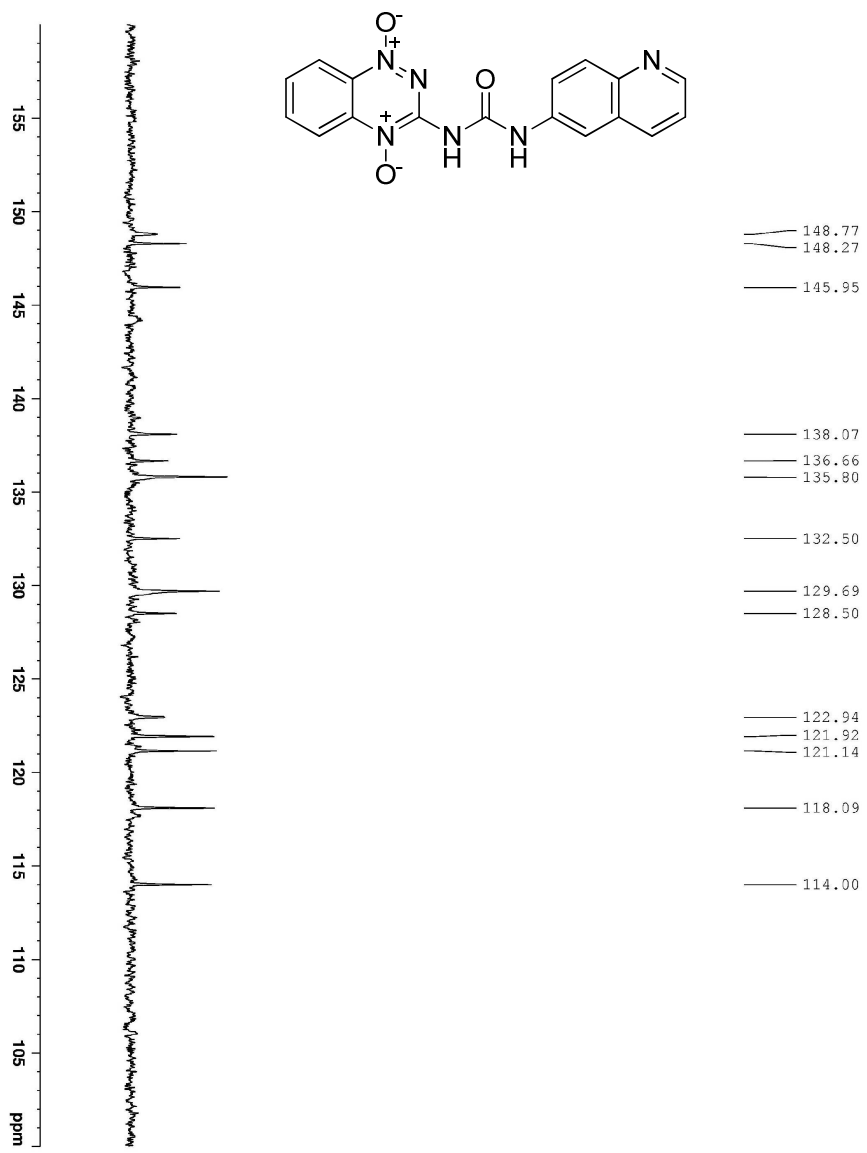




$^{13}\text{C}$  NMR of **79** (MeOD, 500 MHz)



<sup>1</sup>H NMR of **84** (MeOD, 500 MHz)



<sup>13</sup>C NMR of **84** (MeOD, 125.7 MHz)

## References for chapter 5

1. Hay, M. P.; Pchalek, K.; Pruijn, F. B.; Hicks, K. O.; Siim, B. G.; Anderson, M. M.; Shinde, S. S.; Denny, W. A.; Wilson, W. R., Hypoxia-selective 3-alkyl 1,2,4-benzotriazine 1,4-dioxides: the influences of hydrogen bond donors on extravascular transport and antitumor activity. *J. Med. Chem.* **2007**, *50* (26), 6654-6664.
2. (a) Koch, C. J., Measurements of absolute oxygen levels in cells and tissues using oxygen sensors and 2-nitroimidazole EF5. *Methods Enzymol.* **2002**, *352*, 3-31; (b) Nordmark, M.; Loncaster, J.; Aquino-Parsons, C.; Chou, S.-C.; Ladekarl, M.; Havsteen, H.; Lindegaard, J. C.; Davidson, S. E.; Varia, M.; West, C.; Hunter, R.; Overgaard, J.; Raleigh, J. A., Measurements of hypoxia using pimonidazole and polarographic oxygen-sensitive electrodes in human cervix carcinomas. *Radiother. Oncol.* **2003**, *67*, 35-44; (c) Ueda, M.; Kudo, T.; Mutou, Y.; Umeda, I. O.; Miyano, A.; Ogawa, K.; Ono, M.; Fujii, H.; Kizaka-Kondoh, S.; Hiraoka, M.; Saji, H., Evaluation of [<sup>125</sup>I]IPOS as a molecular imaging probe for hypoxia-inducible factor-1-active regions in a tumor: comparison among single-photon emission computed tomography/X-ray computed tomography imaging, autoradiography, and immunohistochemistry. *Cancer Sci.* **2011**, *102* (Copyright (C) 2012 American Chemical Society (ACS). All Rights Reserved.), 2090-2096.
3. Dai, M.; Zhu, W.; Xu, Y.; Qian, X.; Liu, Y.; Xiao, Y.; You, Y., Versatile nitro-fluorophore as highly effective sensor for hypoxic tumor cells: design, imaging, and evaluation. *J. Fluoresc.* **2008**, *18* (2), 591-597.
4. (a) Okuda, K.; Okabe, Y.; Kadonosono, T.; Ueno, T.; Youssif, B. G. M.; Kizaka-Kondoh, S.; Nagasawa, H., 2-Nitroimidazole-Tricarbocyanine Conjugate as a Near-Infrared Fluorescent Probe for in Vivo Imaging of Tumor Hypoxia. *Bioconjugate Chem.* **2012**, *23* (Copyright (C) 2012 American Chemical Society (ACS). All Rights Reserved.), 324-329; (b) Youssif, B. G. M.; Okuda, K.; Kadonosono, T.; Abdel, R. S. O. I.; Hayallah, A. A. M.; Hussein, M. A.; Kizaka-Kondoh, S.; Nagasawa, H., Development of a hypoxia-selective near-infrared fluorescent probe for non-invasive tumor imaging. *Chem. Pharm. Bull.* **2012**, *60* (Copyright (C) 2012 American Chemical Society (ACS). All Rights Reserved.), 402-407.
5. Borch, R. F.; Liu, J.; Schmidt, J. P.; Marakovitz, J. T.; Joswig, C.; Gipp, J. J.; Mulcahy, R. T., Synthesis and evaluation of nitroheterocyclic phosphoramidates as hypoxia-selective alkylating agents. *J. Med. Chem.* **2000**, *43*, 2258-2265.

6. Sun, W. C.; Gee, K. R.; Haugland, R. P., Synthesis of novel fluorinated coumarins: excellent UV-light excitable fluorescent dyes. *Bioorg Med Chem Lett* **1998**, *8* (Copyright (C) 2012 U.S. National Library of Medicine.), 3107-10.
7. Thomson, P.; Naylor, M. A.; Stratford, M. R. L.; Lewis, G.; Hill, S.; Patal, K. B.; Wardman, P.; Davis, P. D., Hypoxia-driven elimination of thiopurines from their nitrobenzyl prodrugs. *Bioorg. Med. Chem. Lett.* **2007**, *17*, 4320-4322.
8. (a) Threadgill, M. D.; Webb, P.; O'Neill, P.; Naylor, M. A.; Stephens, M. A.; Stratford, I. J.; Cole, S.; Adams, G. E.; Fielden, E. M., Synthesis of a series of nitrothiophenes with basic or electrophilic substituents and evaluation as radiosensitizers and as bioreductively activated cytotoxins. *J. Med. Chem.* **1991**, *34* (Copyright (C) 2012 American Chemical Society (ACS). All Rights Reserved.), 2112-20; (b) Firestone, A.; Mulcahy, R. T.; Borch, R. F., Nitro heterocycle reduction as a paradigm for intramolecular catalysis of drug delivery to hypoxic cells. *J. Med. Chem.* **1991**, *34* (Copyright (C) 2012 American Chemical Society (ACS). All Rights Reserved.), 2933-5.
9. Naylor, M. A.; Thomson, P., Recent advances in bioreductive drug targeting. *Mini-Rev. Med. Chem.* **2001**, *1* (Copyright (C) 2012 American Chemical Society (ACS). All Rights Reserved.), 17-29.
10. Thomson, P.; Naylor, M. A.; Everett, S. A.; Stratford, M. R. L.; Lewis, G.; Hill, S.; Patel, K. B.; Wardman, P.; Davis, P. D., Synthesis and biological properties of bioreductively targeted nitrothienyl prodrugs of combretastatin A-4. *Mol. Cancer. Ther.* **2006**, *5* (11), 2886-2894.
11. Hay, M. P.; Sykes, B. M.; Denny, W. A.; Wilson, W. R., A 2-nitroimidazole carbamate prodrug of 5-amino-1-(chloromethyl)-3-[(5,6,7-trimethoxyindol-2-yl)carbonyl]-1,2-dihydro-3H-ben[E]indole (amino-seco-CBI-TMI) for use with ADEPT and GDEPT. *Bioorg. Med. Chem. Lett.* **1999**, *9*, 2237-2242.
12. (a) Lancini, G. C.; Lazzari, E.; Arioli, V.; Bellani, P., Synthesis and relationship between structure and activity of 2-nitroimidazole derivatives. *J. Med. Chem.* **1969**, *12* (Copyright (C) 2012 American Chemical Society (ACS). All Rights Reserved.), 775-80; (b) Cavalleri, B.; Ballotta, R.; Arioli, V.; Lancini, G., New 5-substituted 1-alkyl-2-nitroimidazoles. *J. Med. Chem.* **1973**, *16* (Copyright (C) 2012 American Chemical Society (ACS). All Rights Reserved.), 557-60.
13. Parveen, I.; Naughton, D. P.; Whish, W. J. D.; Threadgill, M. D., 2-Nitroimidazol-5-ylmethyl as a potential bioreductively activated prodrug system:

reductively triggered release of the PARP inhibitor 5-bromoisoquinolinone. *Bioorg. Med. Chem. Lett.* **1999**, *9* (Copyright (C) 2012 American Chemical Society (ACS). All Rights Reserved.), 2031-2036.

14. Everett, S. A.; Naylor, M. A.; Patel, K. B.; Stratford, M. R. L.; Wardman, P., Bioreductively-activated prodrugs for targeting hypoxic tissues: elimination of aspirin from 2-nitroimidazole derivatives. *Bioorg. Med. Chem. Lett.* **1999**, *9*, 1267-1272.

15. Posakony, J. J.; Pratt, R. C.; Rettig, S. J.; James, B. R.; Skov, K. A., Porphyrins incorporating heterocyclic N-oxides: (oxidopyridyl)porphyrins, porphyrin-N-oxides, and a tirapazamine-porphyrin conjugate. *Can. J. Chem.* **1999**, *77* (Copyright (C) 2012 American Chemical Society (ACS). All Rights Reserved.), 182-198.

## VITA

Anuruddha Rajapakse, the second son among three sons of Raja Rajapaksa and Sunethra Dias Weerasinghe was born July 2, 1979, in Colombo, Sri Lanka. He received primary education from St' John's College, Nugegoda and completed his secondary education at Asoka Vidyalaya, Colombo. He entered University of Peradeniya in Kandy, Sri Lanka and received a chemistry-special degree from the faculty of science. Upon completing bachelors, he entered University of Missouri-Columbia to pursue his PhD in Chemistry. He worked as a graduate student with Dr. Kent S. Gates and received Breckenridge/Lyons outstanding graduate research award from the department of Chemistry in 2012.